Key cell cycle regulators are implicated in both proliferative and direct glia-to-neuron cell fate switches in *C. elegans*

Michele Sammut

Submitted for the degree of

Doctor of Philosophy

Department of Cell and Developmental Biology

Division of Biosciences

University College London

Supervisor: Dr. Richard Poole

November 2020

Declaration

I, Michele Sammut, declare that this thesis was composed by myself in its entirety and that the work described herein is my own, except where otherwise stated. The persons whom conducted or assisted in said work are acknowledged in the text either by name or citation.

Michele Sammut

Abstract

In the vertebrate nervous system, stably differentiated quiescent radial glial cells act as neural progenitors, for the first time we describe the production of neurons from glia outside of vertebrate models. Here we show that two sets of differentiated glial cells are capable of sex-specifically producing neurons in the male *C. elegans*. The two glia-to-neuron switches in cell fate, occur by distinct developmental mechanisms; the amphid socket (AMso) glial cells, undergo asymmetric division to produce the interneurons, the mystery cells of the male (MCMs), while the phasmid socket 1 (PHso1) glial cells directly transdifferentiate into the sensory phasmid neurons D (PHDs). In order to identify genetic factors that regulate the production of the MCMs, we have isolated nine no mystery cell (*nom*) mutants from a GFP-based forward genetic screen, in which the MCMs fail to be specified. Using a novel mapping-by-sequencing method, designed for male specific phenotypes, we find that two mutant alleles *nom-5(drp5)* and *nom-8(drp8)* which block AMso division, map to the *cdk-4* locus on the X chromosome. Genetic analysis by rescue and complementation confirms they are alleles of *cdk-4*. CDK-4 is a key cell cycle regulator and intriguingly, although *cdk-4* is required for all postembryonic cell divisions *cdk-4(drp5)* and *cdk-4(drp8)* present no obvious pleiotropies, hinting that novel cell cycle pathways may be involved in this specific division. The development of the MCMs and PHD share molecular features in common with vertebrate neural development, such as the expression of *hlh-14,* the homologue of the proneural factor ASCL1. Also, analysis of *cki-1,* a commonly used marker of cell cycle quiescence and G1/S regulator, shows that it is strongly expressed in both the AMso and PHso1 throughout their life prior to the production of neurons. A further surprising finding is that S-phase genes are expressed during the direct PHso1-to-PHD transdifferentiation. The role of S-phase genes in a direct transdifferentiation, that may not require DNA synthesis, is unknown. An understanding of fate plasticity is an often overlooked but key component to the processes of neurogenesis from glia, this model promises to deepen our understanding. How the progenitor cells of neurons control their ability to either re-enter or withdraw from the cell cycle and how this decision is integrated with the terminal differentiation process is an outstanding question. To this end we begin to establish the *C. elegans* male as a model in which to study the molecular mechanisms of late-in-development cell fate plasticity at a single cell level.

Statement of impact

Our discovery of these glia-to-neuron cell fate switches in the worm may offer a unique opportunity to study the cellular and developmental mechanisms that allow glia to give rise to neurons outside of the comparatively complex brains of vertebrates. Neural development in the embryo or stem cell niches, involves complex interactions of developmental signals that coordinate cellular proliferation, exit from the cell cycle and neuronal differentiation. The complexity of the microenvironments in which this occurs has hampered research efforts. There has been great progress in the study of cell fate plasticity using induced pluripotent stem cells, where isolating stem cells from their natural environment has allowed for crucial insights to be made, however these studies come with limitations. In these models, disentangling the effects of experimental manipulations on differentiation from confounding effects on the cell cycle is extremely challenging. A developmentally similar model, like that presented here, in which cell fate plasticity can be studied *in vivo* but also at the single cell level and outside of the complex developmental environment of embryogenesis could be an extremely useful addition to the arsenal of tools available for research. *C. elegans* has various advantages, such as an invariant and well described developmental lineage as well as a wealth of genetic tools.

Neurological disorders that involve uncontrolled proliferation and differentiation have proven to be some of the most pernicious problems in medicine today. Dysfunction of neural development can lead to severe outcomes, for example, excess early neurogenesis is implicated in pervasive developmental disorders such as autism, while in adulthood, neurogenesis, neural differentiation and survival are implicated in various neurodegenerative diseases. Diseases of early neuronal development and those associated with old age have become increasingly costly, firstly in terms of human suffering but also, with an aging population, in taxing the demands of healthcare services due to the extended period of time that care is required. A deeper understanding of the basic biological principles of neuronal differentiation will provide new avenues for research into the root causes of neurological disorders, which could hopefully permit early diagnosis and prevention. The main focus of current research for treatments for neurodegeneration has been on cell replacement strategies, which requires a deep understanding of the

mechanisms governing cellular plasticity in order to make the large amounts of cells required *in vitro*. Unfortunately, however, progress has been limited by the inefficiencies of the process and concerns about potential tumorigenicity.

The results presented here provide a framework in which to study the sequence of the genetic and cellular events that lead to the terminal specification of the MCM neurons and highlight parallels in neuronal development from glia across distant taxa. The role DNA replication and cell division play in cellular differentiation is of particular interest and continued study of these glia-to-neuron cell fate switches hold great promise for furthering our understanding of the processes involved. Such an understanding could provide novel theoretical perspectives which may improve the efficiency and address concerns of current cell replacement techniques. For example, insight into the question of how the cell cycle is interlinked with differentiation could be useful for addressing the potential tumorigenicity of cell replacement strategies. Additionally, the identification of novel alleles of *cdk-4*, a key G1-S regulator, could aid in the treatment of cancers. Identification of new targets or novel mechanisms of action help improve the efficacy of CDK-4/6 inhibitors as anti-cancer agents, particularly in understanding mechanisms of resistance to this class of drugs.

In a broader context, it is my hope that this work will encourage use of the male *C. elegans* as a model and spur the search for similar instances in other non-vertebrate organisms, in order to hasten the discovery of the fundamental mechanisms that govern cell fate plasticity. In particular, to learn more about how the cellular biological phenomena of fate plasticity are intertwined with the developmental processes governing the generation of neurons from glia.

Acknowledgements

I would like to thank my supervisor Dr. Poole and my previous supervisor Dr. Arantza Barrios who gave me the opportunity to learn the fundamentals of science in an open and accepting environment that gave me the space to grow as a scientist and as a person. I am grateful for my labmates, in both of their laboratories for supporting me with their enduring friendship and for the vibrant scientific discussion that helped me challenge myself. In addition, I'd like to thank the greater worm community both in London and abroad for showing me the importance of an accessible and friendly scientific community.

Of course, none of this would be possible without the support of my family who helped send me off on this journey and gave me everything I needed to succeed. Lastly, I'd like to thank my partner Sabrina for her profound kindness and infinite patience which gave me the will to persevere.

Table of Contents

Chapter 1 14

1.1 Cellular identity and development in historical context 14

1.2 Cell fate plasticity 19

1.2.1 Discovering the basis of cell fate plasticity 19

1.2.2 Experimental cell fate modification 23

1.2.3 Natural examples of cell fate plasticity in development and regeneration 28

1.3 Cell fate plasticity in the nervous system 35

1.3.1 Early specification and development of the vertebrate nervous system 36

1.3.2 Vertebrate neurons are derived from glia 38

1.4 Cell cycle control and cell fate plasticity 47

1.4.1 An overview of the cell cycle 48

1.4.2 Cell cycle control and cell fate determination 53

1.5 *Caenorhabditis elegans* as a model for neuronal development and cell fate plasticity 59

1.5.1 Introduction to C. elegans 59

1.5.2 C. elegans as a model for cell fate specification and plasticity 71

1.6 Summary 81

1.7 Aims 82

Chapter 2 83

2.1 General worm methods 83

2.1.1 Maintenance 83

2.1.2 Synchronisation and cleaning 83

2.1.3 Storage 84

2.1.4 Recipes 84
2.2 Microscopy and imaging 85
2.2.1 Microscopy 85
2.2.2 Image processing 85
2.3 EMS Mutagenesis and screening 86
2.4 Temperature shift experiments 87
2.5 Integration of fluorescent markers 87
2.6 Mapping 88
2.7 Genotyping by PCR and sequencing 89
2.8 Primers list 90
2.9 Strain list 90
Chapter 3 94
3.1 Overview 94
3.2 Results 95
3.3 Summary 97
Chapter 4 98
4.1 Overview 98
4.2 Forward genetic screen yields nine No MCM mutants 100
4.3 Isolated mutants affect sequential steps of MCM development 103
4.3.1 Characterisation of Class I and Class II mutants 106
4.3.2 Characterisation of Class III and Class IV mutants 108
4.4 PHD development is minimally affected in *nom* mutants 110
4.5 Summary 111
Chapter 5 112
5.1 Overview 112
5.2 *nom-5(drp5*) and *nom-8*(*drp8*) map to the *cdk-4* locus 113

5.2.1 Mapping-by-sequencing of nom-5(drp5) and nom-8(drp8) 113

5.2.2 drp5 and drp8 alter conserved residues predicted to affect the activation loop 119

5.3 Genetic analysis indicates that *nom-5(drp5*) and *nom-8*(*drp8*) are alleles of *cdk-4* 121

5.3.1 The critical period for MCM development in nom-8 animals is in L3 121

5.3.2 cdk-4(drp5) likely acts cell autonomously downstream of fem-3 in the AMso 122

5.3.3 cdk-4(drp5) does not show dominance effects 124

5.3.4 cdk-4(gv3) does not complement the cdk-4(drp5) nom phenotype 124

5.3.5 Wild type cdk-4 rescues the nom phenotype of cdk-4(drp5) and cdk-4(drp8) 125

5.4 *cdk-4(drp5)* and *cdk-4(drp8)* appear to specifically affect AMso division 129

5.4.1 cdk-4(drp5) complements the larval arrest phenotype of cdk-4 null animals 129

5.4.2 cdk-4(drp5) is not defective in most post-embryonic blast cell division 130

5.4.3 A complex behavioural response is unaltered in cdk-4(drp8) mutants 132

5.5 Summary 133

Chapter 6 134

6.1 Overview 134

6.2 AMso division does not depend on *cdk-7* activity 136

6.3 The regulation of cell cycle quiescence is associated with both proliferative and direct glia-to-neuron cell fate switches 138

6.3.1 Hermaphrodite amphid and phasmid sockets are kept in a state of quiescence throughout life 138

6.3.2 In males cki-1 is downregulated in the MCMs after proliferation as well as in the PHso1/PHD after the direct cell fate switch 141

6.4 S-phase markers are expressed at the time of the PHso1-to-PHD transition 144

6.5 Wnt asymmetry pathway markers are expressed early in MCM development 146

6.6 *hlh-14* is transiently expressed in the MCMs and PHD 147

6.7 Summary 149

Chapter 7 151

7.1 General Discussion 151

7.2 The Molecular regulation of MCM development 153

7.3 On the role *drp5* and *drp8* as novel alleles of *cdk-4* 156

7.4 Cell cycle inhibition and key cell fate determinants are coordinated in both proliferative and direct glia-to-neuron cell fate switches 161

7.5 Considering the role of S-phase machinery during direct transdifferentiation in the absence of DNA replication 164

7.6 Concluding remarks 166

Annexe I 167

Annexe II 183

References 215

Index of figures and tables

Figure 1.1 One of Flemming's original illustrations of eukaryotic cell division 14

Figure 1.2 Morgan's model of Mendelian segregation 15

Figure 1.3 Waddington's epigenetic landscape 17

Figure 1.4 The complex system of interactions underlying the epigenetic landscape 18

Figure 1.5 Ectopic eyes can be induced by the targeted expression of a homeotic gene 22

Figure 1.6 Cell fate conversion in lens regeneration 30

Figure 1.7 Diverse types of cell fate plasticity 34

Figure 1.8 Spemann & Mangold organiser transplant 37

Figure 1.9 Various theories about the origin of neurons and glia over time 38

Figure 1.10 Cortical neurons arise via symmetric and asymmetric division of radial glia 39

Figure 1.11 Neuronal morphology and fate markers induced in hepatocytes 40

Figure 1.12 Passive and active roles for pioneer factors endow transcriptional competence 41

Figure 1.13 Astrocytes in the adult brain induced to produce neurons by SOX2 42

Figure 1.14 Glia produce neurons throughout life 44

Figure 1.15 Adult neural stem cell dynamics in the intact and injured brain 45

Figure 1.16 The cell cycle 47

Figure 1.17 The Rao and Johnson cell fusion experiments 49

Figure 1.18 CDK2-CYCA-p27 complex crystal structure with functional domains 51

Figure 1.19 Expression of Hes1 and Ascl1 in quiescent and active neural stem cells 57

Figure 1.20 Lifecycle of *C. elegans* 60

Figure 1.21 Sexual dimorphism and sex determination in *C. elegans* ... 61

Figure 1.22 The structure of the amphid and phasmid sockets..... 67

Figure 1.23 Selected sex dimorphic lineages in *C. elegans*..... 70

Figure 1.24 Terminal selector regulons..... 73

Figure 1.25 Natural transdifferentiation of Y-PDA in *C. elegans* 80

Figure 3.1 Glia derived neurons in *C. elegans* 97

Figure 4.1 The location of the MCMs in the head of the male..... 99

Figure 4.2 Forward genetic screen strategy..... 100

Figure 4.3 The MCMs and the *nom* phenotype..... 101

Figure 4.4 The penetrance of nine mutants isolated from the forward genetic screen..... 102

Figure 4.5 Wild type expression of neuronal and glial markers in the AMso and MCM 103

Figure 4.6 Mutant classes affect sequential steps of MCM development 105

Figure 4.7 Characterisation of mutant classes..... 109

Figure 5.1 A novel scheme for mapping male specific phenotypes 114

Figure 5.2 Both *nom-5(drp5)* and *nom-8(drp8)* map to 13.5Mb on the X chromosome 116

Figure 5.3 The *cdk-4* locus..... 117

Figure 5.4 *drp5* and *drp8* are predicted to alter key residues of CDK-4120

Figure 5.5 The *cdk-4(drp8)* allele blocks MCM development at mid to late L3..... 122

Figure 5.6 Masculinisation of XX AMso allows for genetic analysis of *nom* phenotype in *cdk-4* alleles..... 123

Figure 5.7 *VpIs9* rescues *nom-5(drp5)* 127

Figure 5.8 *nom* phenotype of *cdk-4(drp5)* and *cdk-4(drp8)* is rescued by *ozEx76* 128

Figure 5.9 *cdk-4(drp5)* complements the larval arrest phenotype of *cdk-4* null animals 130

Figure 5.10 The sexual conditioning response is normal in *cdk-4(drp8)* 132

Figure 6.1 The hermaphrodite amphid and phasmid sockets express *cki-1* throughout life 139

Figure 6.2 *cki-1* dynamics in males correlate with neuronal differentiation 142

Figure 6.3 S-phase markers are expressed in the PHso1-to-PHD transition 145

Figure 6.4 Wnt asymmentry pathway effector POP-1/TCF expression in the AMso and MCMs 146

Figure 6.5 Transient expression of hlh-14/ASCL1 in the early MCM and PHD 148

Table 4.1 AMso *drpIs3* expression and AMso division 26°C 107

Table 4.2 Assessment of PHD morphology by *drpIs3* expression 110

Table 5.1 X-linkage of *nom-5* mutation 118

Table 5.2 *vmIs9* rescues *nom-5(drp5)* 126

Table 5.3 Sex-specific post-embryonic blast cell lineage divisions in *drp5* 131

Table 6.1 *cdk-7* does not affect AMso division 137

Chapter 1

Introduction

1.1 Cellular identity and development in historical context

The first living cells were observed by Leeuwenhoek in 1674 and by 1839 Schwann showed that all life is composed of cells. Soon after, these findings were followed by the deduction of Virchow that all cells must come from other cells. These astonishing discoveries underpin some of the most fundamental questions in biology and have been at the heart of every generation of cell biologist since — If all organisms are related and essentially composed of the same structural units, how then do these cellular units come together to produce the enormous diversity and complexity of all life on Earth?

While we have come a very long way in our understanding, some of the most fundamental questions still don't have answers. Intriguingly, the substrate of heredity which had been intractable to philosophers and scientists for centuries was soon described in mechanical detail by the first cytologist. In 1875, Oskar Hertwig used the sea urchin to describe the fertilisation of sperm and egg and for the first time the fusion of their pronuclei. Three years later Walther Flemming, in his study of salamander embryos, described chromosomes and mitosis for the first time (Figure 1.1).

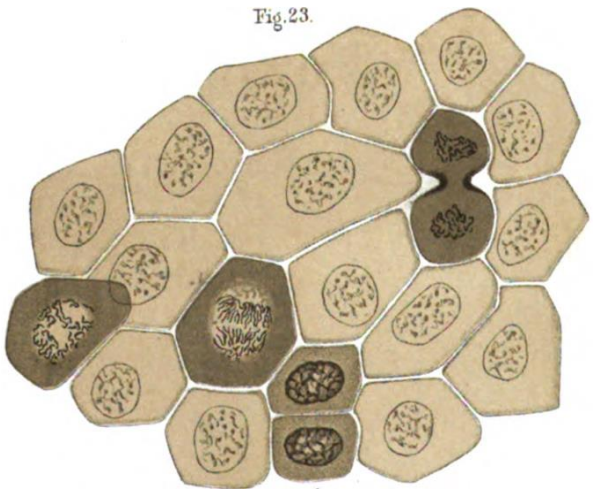

Figure 1.1 One of Flemming's original illustrations of eukaryotic cell division

Illustration of the gill epithelium in a salamander larva fixed with chrome-osmium and hematoxylin stained. The shaded cells show detailed structure of the nucleus and chromosomes in various stages of cell division. From Zellsubstanz, kern und zelltheilung (Flemming, 1882)

Over the next decade, in the laboratory of Hertwig's brother Richard, Theodor Boveri studied early development in the roundworm *Parascaris equorum*, which conveniently only have 2 pairs of chromosomes. He discovered that there are half the number of chromosomes in the gamete lineage compared with the somatic and that fertile egg pronuclei only retain 2 chromosomes until they fuse with the sperm pronuclei to make up the normal somatic complement of four. This was some of the first evidence of a hypothesised reductive meiotic division. More importantly, however, the findings fit neatly with Darwin's 1868 model of evolution, which was conspicuously lacking any mechanism for the process of inheritance, and also with the rediscovery of Mendel's work at the turn of the century. By 1915 Thomas Hunt Morgan, using the fruit fly *Drosophila melanogaster* observed crossing over of chromosomes during meiosis, provided a detailed mechanism of Mendelian heredity and the first genetic map (Figure 1.2). Altogether, this seminal work laid the foundations for the modern disciplines of genetics and developmental biology.

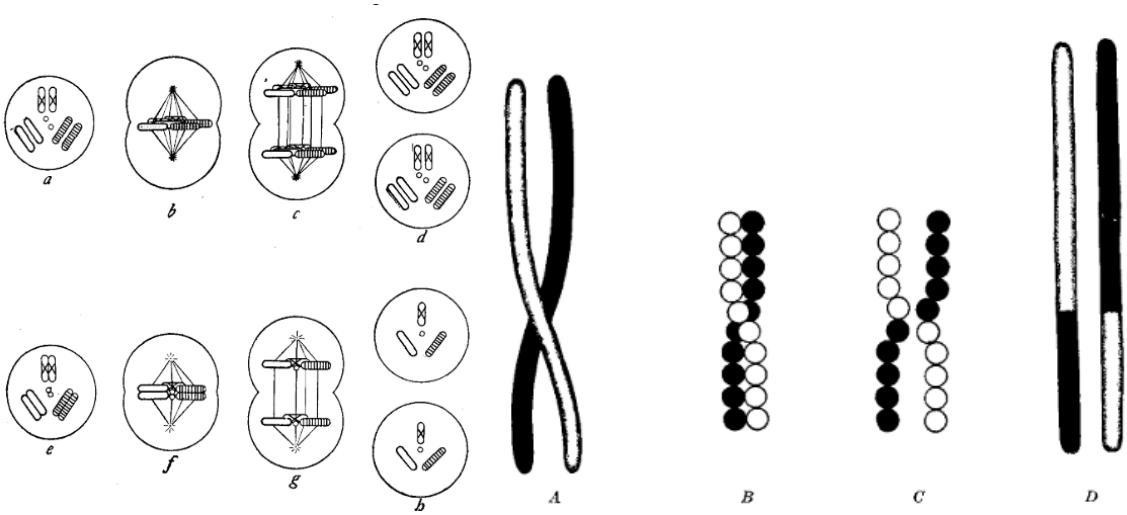

Figure 1.2 Morgan's model of Mendelian segregation

(Left) A representation of how chromosomes are segregated during cell division. (a-d) show four stages in the division of the egg (or of a body cell). Every chromosome divides when the cell divides. (e-h) illustrates the "reduction division" of a germ cell, after the chromosomes have united in pairs. The members of each of the four pairs of chromosomes separate from each other at this division.

(Right) Diagram illustrating crossing over. At the level where the black and white rods cross in (A), they fuse and unite as shown in (D).
From The Mechanism of Mendelian Heredity (Morgan et al., 1915)

Ever since Leeuwenhoek, microscopists catalogued a plethora of cells, seemingly endless in their variety. They focussed on the shapes of cells and realised that there are striking similarities between the cells of analogous tissues in completely different species. The enormous diversity of cell types, counterpoised against the apparent cross species resemblance in structure and function, brought to light the deep complexity concealed in all our organs and tissues. This was made nowhere more evident, than by Ramón y Cajal's 1888 studies of the brain. As it was shown that all cells in an organism come from a single cell which multiplies through division, cell theory demanded a mechanism by which all the different cell types found in the body are formed. Curiously perhaps, the simple question of what differentiates cells from one another proved to be a much harder nut to crack than those of heredity. It is to help answer this question that I chose as the focus of this work, in particular how neuronal cells are specified and how cells can change their differentiation state independently of cell division.

Waddington's epigenetic landscape

The next challenge was to somehow link the phenomena of embryonic development with the underlying mechanisms of genetics. Conrad Waddington, in his studies of genetics and development in flies, chicks and other animals (Lees & Waddington, 1942; Waddington, 1936; Waddington, 1932) became interested in the branching nature of development, viewed in the context of evolution, it was in this light that he first introduced the notion of canalisation. He states that:

"Experimental evidence shows that it may be possible to steer a mass of developing tissue into one of a number of paths but it is difficult to persuade it to differentiate into an intermediate of the two" (Waddington, 1942).

The observation that the wild type phenotype of animals is much more common and regular in nature than the myriad possible mutant phenotypes at first seems paradoxical. However, this may be explained by how natural selection sculpts development through genetic and environmental pressures. Extreme changes in development are likely to be detrimental to survival but slight genetic changes that allow a limited response, even to extreme

environmental changes could be adaptive. Such a scenario would result in selection towards developmental processes becoming resistant to destabilisation i.e. canalised. As a way of reconciling the limited plasticity in development with genetics, Waddington put forward his famous concept of the epigenetic landscape (Figure 1.3).

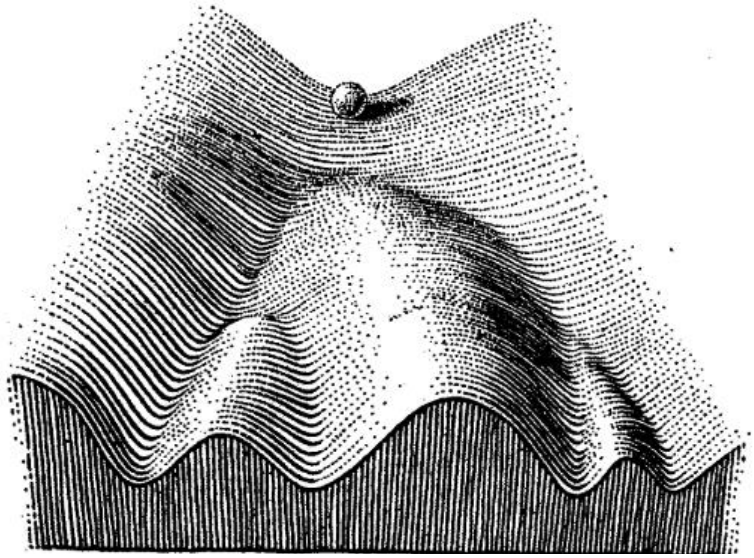

Figure 1.3 Waddington's epigenetic landscape

The path followed by the ball, as it rolls down towards the spectator, corresponds to the developmental history of a particular part of the egg. There is first an alternative, towards the right or the left. Along the former path, a second alternative is offered; along the path to the left, the main. channel continues leftwards, but there is an alternative path which. however, can only be reached over a threshold. From The strategy of the genes (Waddington, 1957)

The tilted three-dimensional landscape represents the developmental space, with the incline representing time, such that, marbles rolling down the valleys demonstrate the canalised path a cell type or tissue can take; from the egg at the top through development, to its final state at the bottom edge. Any one spot on the landscape would correspond to a specific phenotype, so that a peak between two valleys should show an intermediate phenotype. Though, depending on the steepness of the valley edge, an intermediate cell type would be developmentally unstable in this position and tend to 'fall' into one the more stable phenotypes. Switches earlier in development from one path to another should therefore be easier but result in more extreme changes than switches later on in development. Figure 1.4 shows how the landscape itself, with its well-ordered valleys and branchpoints lies above its foundation in the genes. The view of the underside of the landscape which extends like a sheet of fabric

tied down with a complicated network of guy ropes, themselves attached to the ground by pegs. The pegs represent genes and the ropes the complex series of chemical interactions the gene products have that shape the landscape above. This view of development is not without its limitations, chiefly that there are not enough dimensions to accommodate all the known cell types, and that the landscape is static through development, more or less predetermined at the genetic level. We now know that development can be remarkably plastic, but this landscape nevertheless still provides a useful visual metaphor in which to discuss development.

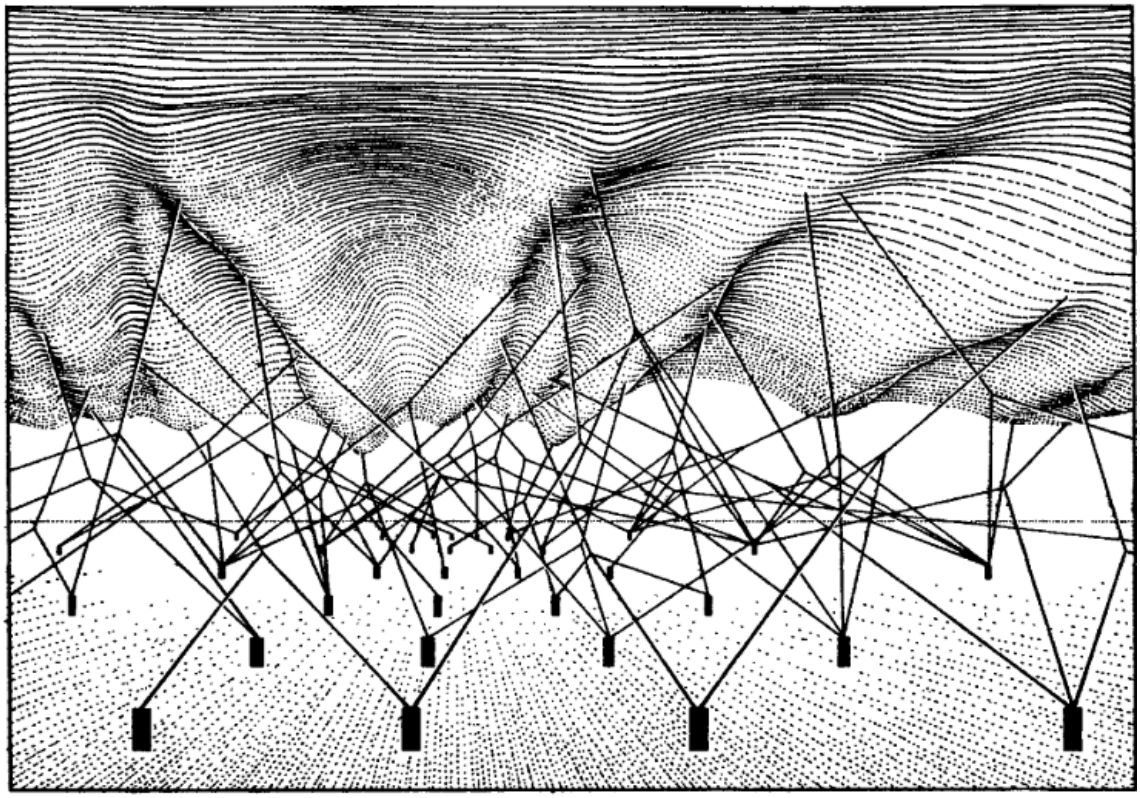

Figure 1.4 The complex system of interactions underlying the epigenetic landscape

The pegs in the ground represent genes; the strings leading from them the chemical tendencies which the genes produce. The modelling of the epigenetic landscape, which slopes down from above one's head towards the distance, is controlled by the pull of these numerous guy-ropes which are ultimately anchored to the genes.
From The strategy of the genes (Waddington, 1957)

1.2 Cell fate plasticity

1.2.1 Discovering the basis of cell fate plasticity

Nuclear transplantation and totipotency

Over the first half of the twentieth century there was considerable debate over how genes become differentially expressed through development. Specifically, if genes are eliminated or get permanently locked away in somatic cells. Briggs & King in 1952 showed that healthy Rana pipens tadpoles could be hatched by transplanting the nucleus of a blastula cell into an enucleated oocyte. This was convincing evidence for the genomic equivalence hypothesis, which states that, all cells in an organism have the same genetic complement through development. While transplantations made at this stage were quite successful, doing so later with cells from all germ layers resulted in abnormal development. These results suggest that, while all cells may have the same genome, their fate becomes more restricted with development. Serial nuclear transfer experiments showed that the restriction of fate was heritable with the nucleus (Di Berardino & King, 1967; King & Briggs, 1956). Later Gurdon replicated these results in Xenopus, and also transplanted somatic intestinal nuclei from feeding tadpoles, which developed into normal tadpoles, although again at a much lower rate than transplanted blastula cells, (Gurdon, 1962). The transplanted nucleus did not alter the fate of the recipient cell to resemble the donor, instead resulting in changes in RNA synthesis were comparable to those seen in the normal developing embryo (Gurdon & Brown, 1965). Later the tadpoles generated from transplanted intestinal nuclei in 1962 developed into fertile adults themselves (Gurdon & Uehlinger, 1966). This conclusively proved that the nuclear material of differentiated cells could produce all the differentiated cell types necessary to produce a fertile adult, but that the potential to do so becomes progressively harder with development.

Similar work in plants showed that whole plants can be grown from single cells. When dissociated carrot cells proliferate enough they begin to form assemblies with differentiated roots and shoots (Steward et al., 1958). More strikingly, single-cell clones of tobacco phloem cells were shown produce differentiated roots, and then shoots, which developed into normal plants

(Vasil, Hildebrandt, & Riker, 1964; Vasil & Vasil, 1972; Vasil & Hildebrandt, 1965). Thus, demonstrating that even intact differentiated cells can be totipotent, capable of recapitulating embryogenesis and producing all the cell types needed throughout the life cycle of the organism. The same proves true for animal cells, the hydra for example, is capable of complete regeneration from isolated epidermal explants containing only two cell types. (Jessen et al., 1973; Lowell & Burnett, 1969). Since all cells belonging to the same organism generally have the same genome, it follows that, it is primarily the differences of the regulation of these genes that produce the vast array of cell types. Britten and Davidson (1969) theorised that transcription is differentially controlled in differing cell types by gene regulatory networks, which during fate specification control events resulting the expression of particular differentiation factors.

Transdetermination

The earliest stages of differentiation are often not observable by differences in morphology, even at the ultrastructural level, however, as cells progress through development the potential fates they can take become more and more limited. When a cell first becomes capable of terminally differentiating into a particular cell type, it is said to be specified, at this stage the terminal fate of the cell may still be altered if it is put in the right environment. When a cell can no longer differentiate into any other fate, other than its terminal fate, it is said to have been determined, even if its terminal phenotype is not yet apparent. This is best described using the model in which it was first defined, the fruit fly imaginal disc. The structures of the adult imago, eyes, legs, wings etc. are present in their primordial form as discs of tissue in the larva, these imaginal discs develop into their adult form during metamorphosis. Genetic mosaic and ablation experiments on fly imaginal disks showed that individual cells within certain regions of each disc are determined to become specific structures in the adult. For example, the more central the region of a leg disc the more distal the portion of the leg its cells differentiate into during metamorphosis.

Determination was originally defined by Hadorn in 1965 as: "a process which initiates a specific pathway of development by singling it out from among various possibilities for which a cellular system is competent".

Imaginal discs can be propagated indefinitely by incubating fragments in the haemolymph of adults, if transplanted into larvae and allowed to develop into adulthood the cells usually differentiate into the adult structures determined by the type of disc. Fragments of discs incubated in adults will proliferate, and when transplanted and allowed to develop, produce multiples of the adult structure already determined by the cells in the region of the original fragment (Hadorn, 1976). Thus, showing that determination can be inherited clonally. The determined fate is remarkably resistant to various experimental perturbations, but occasionally discs develop in an allotypical manner, for example, cultures started from leg discs may start producing parts of antennae or wings. (Schubiger & Hadorn, 1968; Wildermuth, 1970). The process by which one determined cell type is stably converted into another one is termed transdetermination. This change in fate is interpreted to be the result of a change in gene expression from the same set of genetic information available in the mother cell. The first steps towards differentiation are, therefore, not irreversible and given the right circumstances, cells with an established developmental program are capable of going down a different developmental route.

A related phenomenon is that of homeosis, where a normal structure or organ is formed in place of another; for example, eyes or legs forming in the place of antennae (Figure 1.5). This can be caused by injury or the application of chemical agents at particular developmental stages and by genetic mutations. The study of homeotic mutants in *Drosophila* such as *antennapedia* gave the first insight into the pathways of genetic regulation in animals (Hazelrigg & Kaufman, 1983; Schneuwly et al., 1987; Scott et al., 1983) and detailed how Waddington’s ideas of developmental paths and concepts like García-Bellido's selector genes could actually work. Garcia-Bellido studied the developmental genetics of the achete-scute complex in *Drosophila* and found that it acts as a selector gene, required for the decision of a cell to differentiate into sensory organs, like chaete, but not did not otherwise control their development (García-Bellido, 1979). In *Drosophila* the expression of genes from the achete-scute family were shown to be necessary and sufficient to induce neuronal precursors from ectoderm (Jan & Jan, 1994; Jiménez & Modolell, 1993). They are termed proneural genes for their ability to select neuronal

precursors. Homologues of proneural genes were also found to be conserved in vertebrates and required for similar developmental functions (Casarosa et al., 1999; Horton et al., 1999). Selector genes were proposed in order to explain how genes expressed within individual cells could give rise to the supra-cellular organisation within tissues. Homeotic genes were found to act as selector genes, by transducing higher order organisational cues by instructing *realisator genes* which control the differentiation of the cell; thus, establishing the properties of the cell that enact developmental processes e.g. morphology, mitotic rate, receptor expression, etc. It is hypothesised that once a selector gene is activated in a cell, it will remain active in its progeny and maintain the stable determined state of clones. The sum of this work first revealed how the epigenetic landscape is integrated with gene expression in order to direct development.

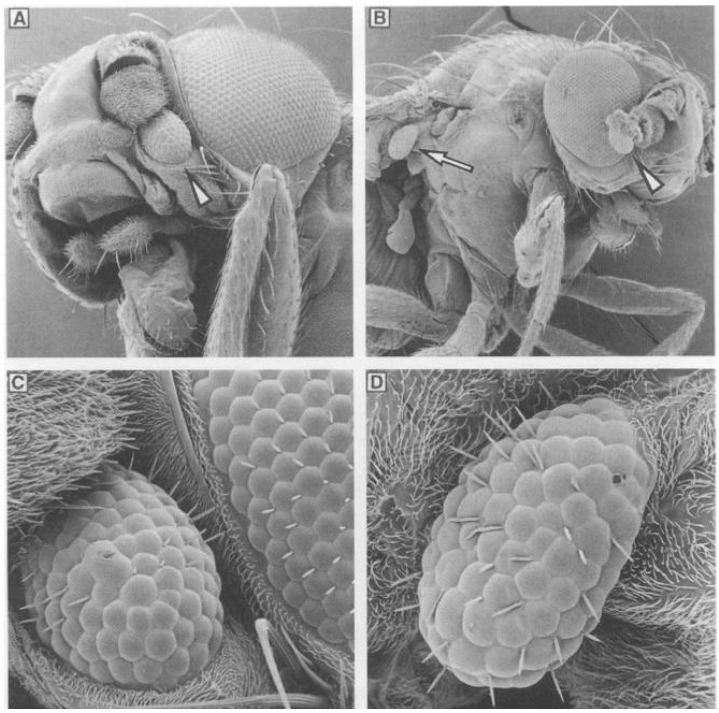

Figure 1.5 Ectopic eyes can be induced by the targeted expression of a homeotic gene

The *Drosophila melanogaster* gene *eyeless*, a transcription factor homologous to human *PAX6* was expressed in targeted imaginal disc primordia. The resultant ectopic eye structures induced on the wings and the antennae are shown here.
(A) Scanning electron micrograph of an ectopic eye (arrowhead) in the head region formed by the antennal disc.
(B) Overview of a fly with an ectopic eye under the wing (arrow) and on the antenna (arrowhead).
(C) Higher magnification of (A). The ectopic eye (to the left) contains hexagonal ommatidia and interommatidial bristles. The organization of the facets in the ectopic eye is very similar to the pattern in the normal eye (to the right). Some facets, however, are fused and some irregularities in the form of the facets are observed.
(D) Higher magnification of the ectopic eye under the wing shown in (B) (arrow). The ectopic eye protrudes out of the thoracic body wall (ventral pleura). The organization of the facets and interommatidial bristles are similar to that of the ectopic eye shown in (C).
From (Halder et al., 1995)

1.2.2 Experimental cell fate modification

Lineage reprogramming

Once cultured embryonic cells became a viable alternative to i*n vitro* experimentation with egg cells, the *in vitro* use of heterokaryons, cells containing nuclei originating from different cells, greatly advanced our understanding of differentiation in mammals. Heterokaryons are created by the fusion of two cells of differing cell type, the resultant cellular phenotype can inform us about how gene expression is affected by the cellular environment and vice versa. For example, when cultured mouse embryonic stem cells were fused with thymus lymphocytes the resulting heterokaryon began to express the stem cell marker *Oct4* over the next 48 hours (Tada et al., 2001). *Oct4* is a key transcription factor expressed in totipotent embryonic stem cells with many roles in differentiation, its levels decline once stem cells begin somatic differentiation during mouse and human embryogenesis (Cowan et al., 2005; Schöler et al., 1989; Zeineddine et al., 2014). In this case the stem-like fate appears to take precedence over the terminally differentiated fate. It is therefore possible to change the potential fate of a determined cell, at the single cell level, its developmental lineage can be said to have been reprogrammed.

It is not always the case that the more primitive phenotype takes precedence however, as heterokaryon experiments involving the fusion of differentiated mouse muscle cells with human foetal amniotic cells show. The resulting cells did not divide (as is usual for fused foetal amniotic cells) and over the next 24 hours produced human muscle protein, suggesting that a cytoplasmic factor is capable of inducing muscle differentiation in primitive possibly multipotent cells (Blau et al., 1983). The determinant cause for this was found to be a single basic helix-loop-helix (bHLH) transcription factor, *MyoD*. *MyoD* was isolated from mouse myoblasts, when it was cloned and expressed in fibroblasts induced myogenesis (Davis et al., 1987). As with selector genes it seems that specific factors in the cytoplasm direct and regulate the phenotype of the cell throughout development. Subsequent work showed that it is possible to reprogram many differentiated cell types to muscle cells under the control of *MyoD*, and it was dubbed a master regulator gene (Weintraub et al., 1989). The

study of immunology and the lymphatic system has shown that lineage reprogramming is also possible *in vivo* where it is surprisingly much more efficient (Nutt et al., 1999). It was found that the development of the B lymphocyte lineage is dependent on the expression of the paired box transcription factor *Pax5* (Nutt et al., 1999) which promotes commitment and suppresses switches to alternate cell fates, such as the T cell lineage (Ikawa et al., 2016). Deletion of *Pax5* in mature B cells resulted in dedifferentiation into an uncommitted progenitor cell fate which could then differentiate into T cells and rescue congenitally T cell deficient mice (Cobaleda et al., 2007). Similarly, through studies of the exocrine system, it was found that by injecting a combination of three virally induced transcription factors into the mouse pancreas, mature exocrine cells expressing the bHLH transcription factor P48 and amylase, could be converted into insulin producing β-cells. BrdU labelling showed very few induced β-cells went through DNA synthesis, indicating that this *in vivo* example of lineage reprogramming can occur without a pluripotent intermediate cell type (Zhou et al., 2008). Similarly acinar cells can be directly converted to β-cells as well as α-like and δ-like cells by various combinations of the transcription factors Ngn3, Mafa, and Pdx1 (Li et al., 2014).

Through the use of reprogramming factors, cultures of cells such as fibroblasts can be reprogrammed to produce various multipotent and mature cell types, in both mice and humans, such as; cardiomyocytes, hematopoietic progenitors, hepatocytes, astrocytes, neural stem cells, various neuronal sub-types, macrophages and pancreatic cells (Reviewed in Xu et al., 2015). In addition, neurons can be produced from various cell types, covered in more detail in section 1.3. With these elegant demonstrations of cell fate plasticity, we can see that it is possible to force a cell from one differentiated state, directly into to another with the expression of a single or few factors. Crucially, the reprogramming of cell fate can happen directly, without a going through a progenitor like state, this is termed direct lineage reprogramming or induced direct transdifferentiation, discussed in more detail in section 1.2.3.

Induced pluripotency

Following the description of various factors that can direct differentiation and change the fate of cells, the search was on for factors which could reprogram differentiated cells into stem cells. Of particular interest were factors that were enriched in mouse embryonic stem cells. It was found that one such transcription factor, NANOG, which contains a homeobox DNA binding domain, common to homeotic genes, is required for the maintenance of the pluripotent state (Chambers et al., 2003; Mitsui et al., 2003). Further work on the known stem cell factor *Oct4*, showed that *Sox2*, a high mobility group transcription factor and neural stem cell fate regulator (Sarkar & Hochedlinger, 2013), forms a complex with *Oct4*. Together they regulate both *Nanog* and *Oct4* expression in embryonic stem cells (Okumura-Nakanishi et al., 2005; Rodda et al., 2005). The landmark papers of Takahashi & Yamanaka, 2006 and Takahashi et al., 2007 tested these and many other factors in mouse and human cells, and narrowed down the minimal set of reprogramming factors to; Oct3/4, Sox2, Klf4, and Myc. Forced expression of these factors, induces differentiated cells to become pluripotent, capable of producing many cell types, including various neuronal cells. In fact, mouse and human fibroblasts were found to be induced into a multipotent neuronal stem cell like state by the expression of SOX2 alone. The SOX2 induced fibroblast can produce, astrocytes and oligodendrocytes as well as various types of neurons (Ring et al., 2012). It is important to note that each of the original four Yamanaka factors can be replaced by other factors depending on the developmental context and still induce pluripotency. Later evidence showed that Myc is dispensable for inducing pluripotency but greatly increases efficiency (Nakagawa et al., 2008) *Myc* is an oncogene and general transcription enhancer (Lin et al., 2012), it's role in promoting cell cycle progression is likely key to the efficiency of induced pluripotent stem cell generation.

Molecular analysis showed that *MyoD* and *MyC* share homology at the DNA binding bHLH sequence and thus defined the class of bHLH transcription factors (Murre et al., 1989). Apart from pluripotency factors, positive cell cycle regulators were found to be critical for induced pluripotent stem cell generation, Cyclin D overexpression was found to increase efficiency (Edel et al., 2010;

Ruiz et al., 2011) and maintaining correct levels of Cyclin A increases pluripotency and reduces tumorigenicity (McLenachan et al., 2012). The opposite holds true for factors that inhibit cell cycle progression and promote differentiation such as the CIP/KIP family of cyclin dependent kinase inhibitors, which act as a barrier to reprogramming (Hong et al., 2009; Kawamura et al., 2009; Li et al., 2009). Once such factors were identified, the mechanisms by which they effect cell fate changes could be investigated.

On top of transcription factors that initiate and direct switches in cell fate and terminal differentiation factors that inhibit such changes, chromatin dynamics play a key role in modulating these actions and determining the balance between pluripotency and differentiation. In fact, the removal of histone H2A variants has been shown to be the rate-limiting step for reprogramming when inducing pluripotency (Pasque et al., 2012), as well as during nuclear transfer (Pasque et al., 2011). Naturally, any drastic changes in cell fate must be accompanied by changes in transcription across the genome. Whereas, large scale changes in gene expression are accompanied by an alteration of chromatin landscape which can promote access to certain genes while making others unavailable (Gifford et al., 2013; Xie et al., 2013; Zhu et al., 2013). This can occur through the restructuring of nucleosomes (Hirschhorn et al., 1992), post translational modifications of their component histones (Luger et al., 1997; Strahl & Allis, 2000), or the addition of chemical marks on DNA (Holliday & Pugh, 1975). These epigenetic modifications do not alter the sequence of DNA but affect interaction with transcription factors. The addition of specific marks on promoters and enhancers can result in increased expression of pluripotency and proliferation genes (Fukuyama et al., 2012; Koche et al., 2011; Liang & Zhang, 2013; Schmidt & Plath, 2012). These factors tend not to be required for the transition of cell fate but are required to maintain changes in fate, for example, knocking out DNA methylation in mouse embryonic fibroblast, does not impair the generation of induced pluripotent stem cells (Pawlak & Jaenisch, 2011). Interaction with epigenetic regulators is a key feature of reprogramming factors.

Despite the very short amount of time since the introduction of induced pluripotent stem cells, there have been great advancements in the technology. We are now witnessing the beginning of clinical applications, for example, cell

replacement therapies for the treatment of some of the major afflictions facing modern medicine, including; neurodegeneration, diabetes, heart disease and spinal cord injury (Trounson & DeWitt, 2016). As induced pluripotent cells can be generated from the patient's own cells, they can then be directed towards specific fates, such as neurons, and grafted back into patient the without the threat of immune response or rejection. However, low chances of initiating reprogramming and reduced chance in completing cell fate transitions after initialisation, results in a low efficiency of reprogramming, significantly hampering progress in the field (Ebrahimi, 2015; Vidal et al., 2014).

Irrespective of the progress made, it is important to note that induced pluripotent stem cells may have significant limitations in clinical applications, as inducing pluripotency inherently introduces the risk of creating teratomas. All induced clones must therefore be carefully screened before being used as a treatment. The constant improvement in methodology will, no doubt, reduce the risks but there may always be the chance of incompletely or unstably differentiated induced cell causing potentially disastrous effects (Tapia & Schöler, 2016). Additionally, precisely targeting induced cells to the affected tissues may be problematic, reducing efficiency, while even correctly induced stem cells could find their way to off-target niches resulting in unwanted side-effects. Inducing transdifferentiation, which changes the differentiated state of a cell but bypasses a pluripotent state, may provide different approaches which could address the issues with induced pluripotent cells. It may be possible to induce transdifferentiation *in situ*, chemically or even through forced expression of exogenous genes, in a highly targeted and transient manner. Exploiting natural mechanisms could increase efficacy and reduce off target effects. Any way in which we can study the natural events which lead to and maintain, stable cell fate transitions, will be enormously helpful in this regard and help reveal hitherto unseen roadblocks.

1.2.3 Natural examples of cell fate plasticity in development and regeneration

While trying to find the mechanisms that change one cell type into another it is useful to study the various ways that it occurs in nature. In this respect, normal development and regeneration in response to injury, provide various interesting cases. Naturally occurring events where one differentiated cell type is stably converted into another are termed transdifferentiation events. This phenomenon was first described in the pupal labial glands of the giant silk moth *Antheraea Polyphemus*. Here, large polyploid differentiated cells responsible for the creating a rigid cuticle that lines the lumen of the silk gland, important for proper silk production, called duct cells are converted to secretory glands (Kafatos, 1968; Kafatos & Williams, 1964, 1968). The cells completely change their differentiated state during pupation; they grow substantially larger, the cuticle is degraded, elaborate invaginations form from the basal then apical membranes, and lastly a mitochondria rich zone forms in between. This specialisation of the secretory gland is required for the uptake and secretion of fluids resulting in the release of the cocoon digesting enzyme cocoonase, which enables the adult to break out of the cocoon. There is no mitosis during this switch in cell fate but H^3-thymidine incorporation autoradiography shows that there is a large amount of DNA synthesis occurring in the first 3 days of the morphological transformation, as the apical and basal zones are becoming identifiable (Selman & Kafatos, 1974). Also, when DNA synthesis is blocked using the ribonucleotide reductase inhibitor hydroxyurea (HU) or the DNA crosslinker mitomycin C a significant proportion of the cells develop into normal adult cells capable of secretion. These results indicate that DNA synthesis itself is not necessarily required for this transdifferentiation. It is clear that in normally cycling cells, the cell cycle must tightly regulate the proliferation/differentiation decision, however, the of role the cell cycle in mitotically inactive but differentiating cells is less apparent. These results hint that there may be an underlying link between the two, for example, cell cycle dependent changes to the epigenetic landscape may be required for or facilitate cellular differentiation. The description of more examples of natural transdifferentiation will be an important tool in answering such questions.

Regeneration of lens tissue has been a classical example of cell fate conversion since Gustav Wolff began publishing papers on newt lens regeneration in 1895. When the lens is damaged or removed, the pigmented epithelial cells of the dorsal iris, that derive from the neuroepithelium, appear to stop producing pigment and proliferate to replace the lost, epidermally derived lens cells, to regenerate new lens tissue. As it was impossible to follow the lineage of the cells during newt lens regeneration, it wasn't until Eguchi & Okada (1973) proved that in clonal cell cultures of retinal pigmented epithelial cells from the chick embryo could produce lens cells in "lentoid" tissue, that this type of regeneration could be properly described as including a transdifferentiation event since the cell lineage could be followed (Figure 1.6). The homeobox gene *Pax6*, a master regulator for eye development (Halder et al., 1995) across many taxa becomes upregulated in proliferating pigmented epithelial cells and is required for the earliest steps of lens regeneration (Ashery-Padan & Gruss, 2001; Madhavan et al., 2006). Injection of *Pax6* coding RNA in *Xenopus* embryos was sufficient to produce ectopic lenses (Altmann et al., 1997), together this suggests that *Pax6* regulates this regenerative transdifferentiation event by controlling differentiation and proliferation status of retinal cells.

Eguchi & Kodama (1993) suggest two criteria in order to avoid confusion with the term transdifferentiation:

"The first prerequisite is that the differentiation state before and after the transdifferentiation can be reliably described and distinguished. Morphological criteria can be used, but preferably should be accompanied by biochemical or molecular biological evidence, to enable an objective decision to be made. The second prerequisite is that a direct ancestor-descendent relationship between cells before and after the switch can be clearly confirmed at the cell level. "

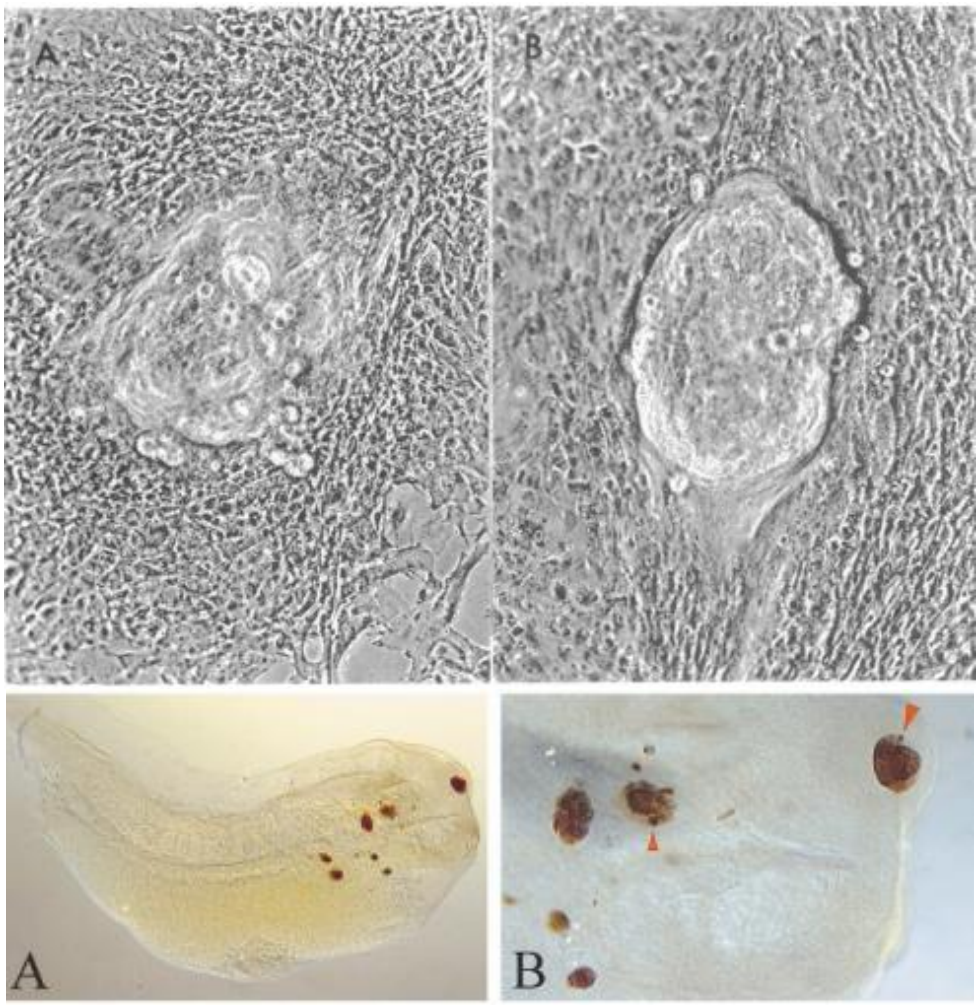

Figure 1.6 Cell fate conversion in lens regeneration

(Top) A "Lentoid" body that appeared in the culture derived from a large number of chick retinal pigment cells (A) and in the culture of a clonal pigment-cell origin (B). From (Eguchi & Okada, 1973)
(Bottom) The homeobox gene *Pax6* induces ectopic lenses in whole *Xenopus* embryos in a cell autonomous fashion. b-Crystallin staining of embryos (stage 38) injected with RNA-encoding Pax6-FLAG revealed the formation of ectopic lenses (brown) in whole mount. From (Altmann et al., 1997)

Tissue regeneration offers many examples of cell fate plasticity, although, perhaps due to the difficulty in determining the above criteria, there are relatively fewer examples of well-defined transdifferentiation, but these are by no means a rare occurrence. The most and longest studied animal for its regenerative capabilities is the axolotl *Ambystoma mexicanum* (Spallanzani, 1768). After an injury such as the loss of a limb, the site forms a blastema; a diverse collection of cells that together are capable of producing all the tissues required to reconstitute a working limb (Muneoka et al., 1986). Cells in the blastema are not pluripotent but are composed of progenitor cells that are restricted in their individual lineage potential depending on the tissue the progenitor cells originate from (Kragl et al., 2009). However, during tail regeneration, individually GFP labelled radial glia cells from the spinal cord

were found to migrate to surrounding tissues divide and transdifferentiate into myosin bearing muscle as well as cartilage cells (Echeverri & Tanaka, 2002). Despite the extensive research on the topic the relative contribution and role of transdifferentiation to salamander limb regeneration is not yet known and makes for fertile ground for future discoveries. The regenerative properties of teleost fish have been well known since Morgan described fin regeneration in 1900 and provide us with more examples of transdifferentiation. With the ability to restore amputated fins, as well as brain, retina, spinal cord and heart lesions, the zebrafish has developed into an excellent model for the study of tissue regeneration (Gemberling et al., 2013). Regeneration in the heart and brain has been shown to involve transdifferentiation (transdifferentiation in the brain will be covered in the section on vertebrate neural development). Zebrafish are capable of heart regeneration throughout life, unlike mammals which only do so in early development (Poss et al., 2002). Cre-recombinase-based lineage-tracing shows a *gata4* expressing population of cardiomyocytes in the ventricular wall of the zebrafish heart lose terminal features (Sarcomeres and high mitochondrial density) and proliferate to regenerate functional muscle (Kikuchi et al., 2010). In the embryo, atrial cardiomyocytes, which differ in gene expression, ultrastructure and function (Ng et al., 2010) and derive from a distinct mesodermal lineage (Bakkers, Verhoeven, & Abdelilah-Seyfried, 2009; Lee, Protze, Laksman, Backx, & Keller, 2017) can transdifferentiate into ventricular cardiomyocytes and contribute to regeneration (Zhang et al., 2013). Intriguingly, this transdifferentiation does not persist in adult heart regeneration, suggesting that alternative means for regeneration exist through development, with reduced transdifferentiation potential in late development.

Another excellent model for the study of regeneration, first described over 250 years ago (Trembley, 1744), is the hydra. It has long been known that regeneration in hydra is possible without the generation of new tissue, called morphallaxis, to distinguish it from regeneration by the development of new tissue, or epimorphosis (Morgan, 1901). Transdifferentiation is known to occur during morphallactic hydra regeneration, for example, neural cells change their neuropeptide expression phenotype depending on their position in the body (Koizumi & Bode, 1986). Similarly, when the head is removed, GFP labelled zymogen gland cells in the trunk of the animal, were observed to directly

change their morphology and gene expression, transdifferentiating to granular mucous gland cells, normally present in the head (Siebert et al., 2008). The most dramatic of hydrozoan regenerative capabilities may be best understood in the context of their mode of reproduction. Mature hydrozoan polyps reproduce asexually by generating miniature adult forms on their trunk which bud off and form their own colony. Many hydroids reproduce sexually through the budding off of a free-living medusa stage, which releases gametes once or several times then disintegrates. Many stages are usually involved and there are various modes through which this can occur, for example, medusae can bud new medusae or polyp morphs or polyps can directly transform into medusae without budding. A few species, such as *Podocoryne carnea*, are capable of ontogeny reversal, that is, development of the entire medusa morph directly into the benthic mature form, this ability is generally lost by the time the medusa reaches full sexual maturity. During this transition it was shown that striated muscle cells could transdifferentiate into nerve cells and this was under the control of the homeobox gene *Otx* (Müller et al., 1999; Schmid, 1992), which has conserved functions in organising the anterior nervous system (Boyl et al., 2001). While many examples of transdifferentiation during regeneration do exist, natural cases of transdifferentiation during development are more uncommon. However, Piraino showed that *Turritopsis dohrnii* is capable of ontogeny reversal at any point of the medusoid lifecycle, the only known case where a sexually mature morph can directly transform into its juvenile form and back (Bavestrello et al., 1992; Piraino et al., 1996). In culture, it appears to be possible for the alternation between morphs to continue indefinitely, earning *T. dohrnii* the moniker, “the immortal jellyfish” (Kubota, 2011). Clearly, ontogeny reversal requires a complete reorganisation of cell types, regeneration and transformation of tissues. The medusa bell consists of various specialised somatic tissues including, striated muscle, endoderm, mesoglea, exumbrellar epidermis, mouth and manubrium, nerve rings and sensory organs (ocelli and statocysts). If the medusoid stage is stressed it can transform into a polyp directly or through a number of stages. Through progressively absorbing the mesoglea, or eversion of the umbrella, then settling as a cyst which then forms a root like branching stolon which acts as an anchor from which the polyp grows. Excision experiments show that the stolon cells, which secrete a tough

cuticle like perisarc, must be produced by the transdifferentiation of exumbrellar epidermis cells, although this has not been directly observed. Intriguingly, a thymidine analogue BrdU assay shows that DNA replication continues in exumbrellar epidermis in *T. dohrnii*, which is not the case in other related species. The potential role of replication in the transformation has yet to be examined.

Piraino defines transdifferentiation as follows;

"Transdifferentiation is defined as a change of commitment and gene expression of somatic, well-differentiated, noncycling cells to other cell types directly or through the return to a condition of undifferentiated cells."

This is the way the term transdifferentiation is employed in most modern usage. A distinction is to be made between direct cellular transdifferentiation which occurs without a division and indirect transdifferentiation, which involves a return to a proliferative state where the daughter cells then adopt a distinct fate. Both direct and indirect transdifferentiation may be accompanied by the loss of terminal features or 'dedifferentiation'. The atypical differentiation of stem cells or the conversion of one stem cell population into another distinct stem cell type, often seen in cancer and tumour formation, is not considered transdifferentiation. While natural transdifferentiation events in development are undoubtedly more rare than other types of differentiation it is important to note that this is by no means an uncommon developmental strategy. The sparsity of transdifferentiation events in our records may be the result of the historical difficulty of unambiguously describing such events, and as such not representative of their true biological prevalence. With adequate tools becoming increasingly available, there is little doubt more examples will come to light in many organisms and will provide an invaluable contribution to our understanding of cellular development. Although often overlooked, it is important to appreciate that transdifferentiation is subtle but pervasive principle in cell biology. The great diversity in what is already known about the landscape, demonstrated by the various examples of cell fate plasticity put forward in this chapter (Figure 1.7), ranging from hydra to mammals, by experimental modification, as well as in normal development or in repair, should encourage us to keep in mind that any particular cell fate transformation may be possible given the right context.

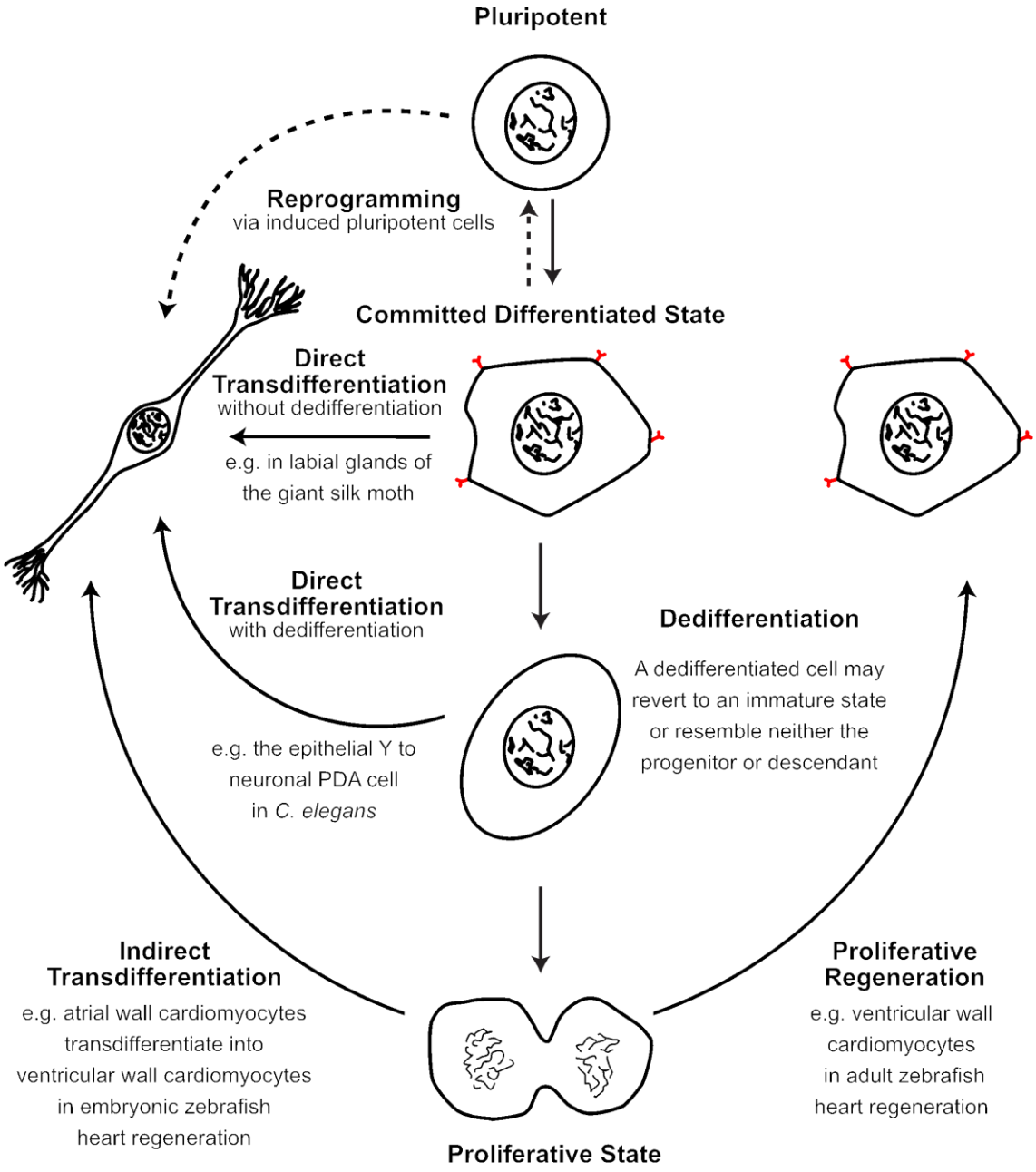

Figure 1.7 Diverse types of cell fate plasticity

A schematic showing different paths cells may take to in order to change their cell fate in normal development, regeneration after injury or by experimental modification.

1.3 Cell fate plasticity in the nervous system

Commitment to a differentiated state and control over the proliferative state is central to cell fate specification. In this respect the study of cell fate plasticity in the nervous system presents special challenges. The ability to rapidly perform complex sets of behaviours, the defining characteristic of animals, requires the requires the production of a comparatively diverse, highly specialised, set of electrically active cells that constitute the nervous system. Unlike most cell types mature neurons are not capable of proliferating, excluding certain exceptional circumstances in disease. Reactivation of the cell cycle in mature neurons rarely occurs, and is usually associated with acute stress, such as DNA damage, excitotoxicity, physical or chemical injury. Moreover, the cell cycle machinery that governs re-entry to the cell cycle and proliferation in other cells, mediate cell death through the apoptotic pathway in neurons (Chen et al., 2013; Park et al., 1998). The unique relationship neurons have with the cell cycle and proliferation in general, demands careful consideration is taken in the study and application of cell fate plasticity in this cell type. Furthermore, the development and maintenance of neuronal cells is dependent on glial cells, the role of this companion cell type must be considered in tandem with neurons themselves. Glial support cells are likewise an extremely diverse class of cells that range from being highly specialised, e.g. participating in electrical processing in vertebrates, to less specialised cells resembling epithelial cells in animals with smaller nervous systems. Invertebrate neural development usually occurs through ectodermal blast cells that give rise to neurons, glia and other cell types in fixed cell lineages (Bate, 1976; Doe, 1992; Sulston, 1983; Truman & Ball, 1998). However, this need not always be the case, as in the sea urchin, development of neurons from the endoderm has been observed (Wei et al., 2011). The rest of this section will focus on the vertebrate nervous system.

1.3.1 Early specification and development of the vertebrate nervous system

In the vertebrate embryo neural tissue is formed from ectoderm, the outermost of the three germ layers. After gastrulation, the process in which the three germ layers are established, a section of the ectoderm, the neuroectoderm, forms the neural plate, in which a neural groove forms then infolds upon itself in order to form a tube structure, the neural tube. The development of the neural plate into the neural tube is termed neurulation. Early embryonic transplant and grafting experiments in amphibians by Spemann & Mangold in 1924 showed that, neurulation is governed by external signals coming from and “organiser region” (Figure 1.8). Functionally analogous organiser regions in various organisms can be temporally and spatially different depending on the organism but molecular analysis shows that these regions generally act by secreting molecules that function antagonistically to global signalling pathways including BMP, Wnt and Nodal; reviewed here (De Robertis et al., 2001; Harland & Gerhart, 1997). While the complex signalling pathways initiated by the organiser ensure correct differentiation into ectoderm or neuroectoderm and appropriate neurulation, screens for early response to neural induction genes provide evidence suggesting that the first steps towards choosing a neural fate are taken earlier (Papanayotou et al., 2008; Streit et al., 2000). Sox2 is the earliest identifiable marker associated with nervous system development it’s expression first seen in the neural plate (Wood & Episkopou, 1999) and is used as a marker for neural fate induction, this pattern of expression is conserved in amphibians, chicks and humans (Collignon et al., 1996; Rogers et al., 2009). Earlier in development, Sox2 has been also shown to be required for maintaining pluripotency in embryonic stem cells (Avilion, 2003). Sox2 regulates differentiation of the embryonic stem cells into ectoderm by suppressing differentiation into mesoendoderm, conversely another pluripotency factor Oct4 suppresses embryonic stem cell differentiation into ectoderm (Thomson et al., 2011). After neuronal specification, Sox2 is required to maintain the proliferative neural progenitor cell pool and prevents neuronal differentiation both in the embryo (Graham et al., 2003) as well as in adult development (Cavallaro et al., 2008; Hagey & Muhr, 2014). The expression pattern of Sox2 is clearly complex and is likely regulated differently throughout

development. Sox2 interacts with other pluripotency factors when maintaining the pluripotent fate of embryonic stem cells as well as supressing certain lineage specifying genes, similarly in neural progenitor cells, it also promotes a stem like state while preventing neuronal differentiation. Sox2 is a key factor throughout nervous system developmental and understanding the mechanisms by which it confers a pluripotent state as well as how its downregulation in post-mitotic neurons and glia relates with neuronal differentiation will be a central question in understanding the early steps of cell fate plasticity in the nervous system.

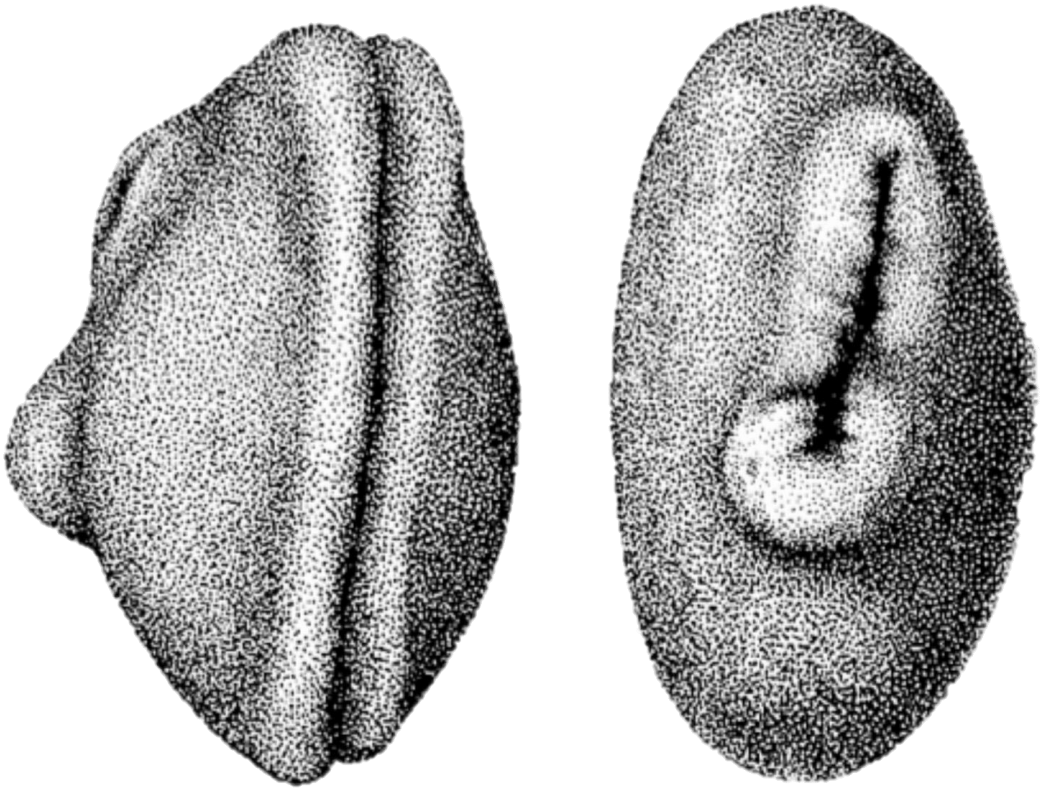

Figure 1.8 Spemann & Mangold organiser transplant

The organizer region taken from a *Triton cristatus* embryo in advanced gastrulation was transplanted into a *Triton* taeniatus embryo of the same stage.

(Left) The primary neural fold can be seen bisecting the *Triton taeniatus* embryo at the neurula stage from top to bottom.

(Right) The *Triton cristatus* implant moved inward in the shape of a shallow cup the secondary neural folds are viewed from the right side and from above. 20X. From (Spemann & Mangold, 1924)

1.3.2 Vertebrate neurons are derived from glia

After neural specification, the traditional view of vertebrate neurogenesis was that a common precursor gave rise to separate lineages of neurons and glia. As lineaging technology progressed various new theories emerged, illustrated in Figure 1.9 (Fujita, 1963; His, 1889; Levitt et al., 1981; Schaper, 1897). A certain set of glia, radial glia, have long been noted for their role in the developing nervous system, however until relatively recently, their exact role as the progenitors of neurons and glia was overlooked. Ramon y Cajal classified radial glia as primitive or modified astrocytes, and noted the importance of radial glial fibres as guides for developing and migrating cortical neurons, the latter was clearly demonstrated by Rakic in 1972. In the rat central nervous system radial glia were found to produce two other major classes of glia, astrocytes and oligodendrocytes (Parnavelas, 1999). However, it wasn't until after the observation of neurogenesis in proliferation "hot spots" rich in radial glial cells in the avian brain, that it was suggested that they may be neural progenitors (Alvarez-Buylla et al., 1990). For some time, there was debate about the exact origin of neurons and even the existence of radial glia. It was eventually established that radial glia were capable of producing neurons and go on to produce two major classes of glia, astrocytes and oligodendrocytes *in vitro* (Malatesta et al., 2000).

Figure 1.9 Various theories about the origin of neurons and glia over time

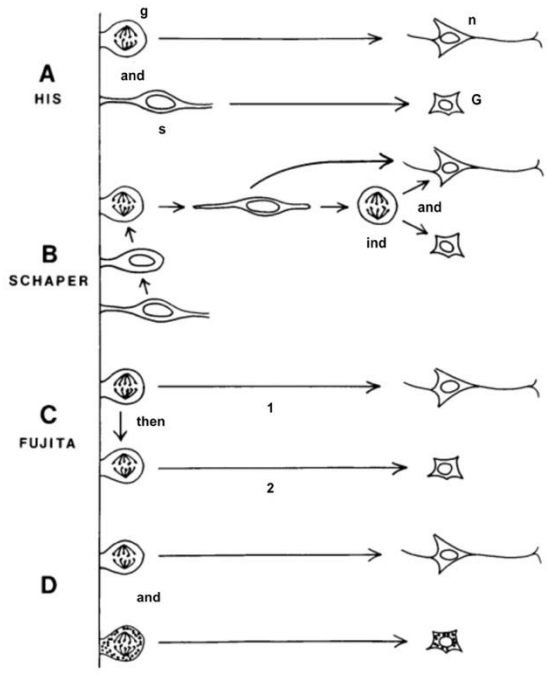

A schematic illustrating competing theories about the origin of neurons and glia, originally printed by Levitt, Cooper & Rakic in 1981 (n= neuron, g=glia)
(A) His describes two classes of cell, germinal cells that give rise to neurons and 'spongiblasts' (s) (which correspond to radial glia), that produce glia.
(B) Schaper contested this model proposing that the two classes of cells observed by His really belonged to the same class of cells which produce an 'indifferent' (ind) intermediate (neither neurons or glia) that are the origin of both neurons and glia.
(C) Thymidine pulse chase autoradiographic experiments led Fujita to propose an indifferent cell type which first produces neurons then switches to produce glia.
(D) Levitt, Cooper & Rakic found both Glial fibrillary acidic protein (GFAP) positive and GFAP negative cells in the mitotic zone at the time of neurogenesis. The interpretation was for two separate progenitior types GFAP- producing neurons and GFAP+ producing glia. Intriguingly they state that "Theoretically, a fraction of the unlabeled cells could be … cells which have ceased producing neurons and subsequently changed over to glial production without having yet expressed GFAP."

Lineaging techniques soon improved enough to allow for high-resolution time-lapse imaging of the proliferative regions of the developing central nervous system. Time-lapse imaging, in combination with fluorescent reporter genes (Figure 1.10), revealed that radial glia divide asymmetrically in the ventricular zone to self-renew and produce post-mitotic neurons; but also divide symmetrically in the subventricular zone producing more radial glia or intermediate progenitor cells which can produce neurons in the embryonic mouse brain (Noctor et al., 2004). Similar observations have been made in the adult mouse hippocampus (Pilz et al., 2018). Since then, there has been some debate about the nature of radial glia, some even questioning if they are actually glia, the term is sometimes used interchangeably with neural stem cells when discussing neurogenesis. It is important to note that having stem-like properties does not preclude a cell from being differentiated, as radial glia have well known important roles in the organisation of the brain and as scaffolds for neuronal migration. As such, when considering the problems regarding neural development and differentiation, the differentiation state of the stem cell and plasticity of this fate should be considered as an integral part of the question.

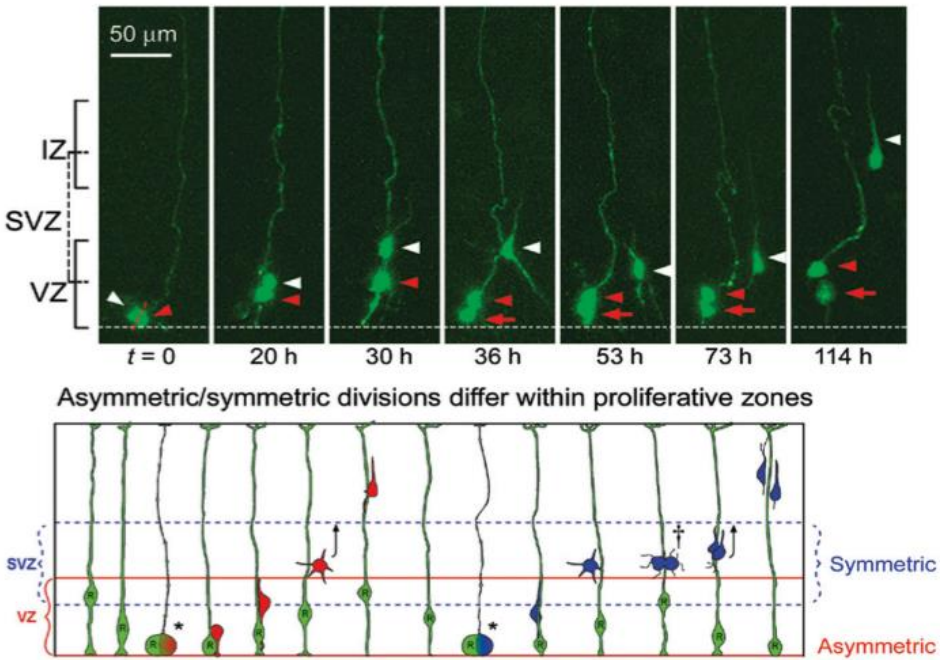

Figure 1.10 Cortical neurons arise via symmetric and asymmetric division of radial glia

Time-lapse imaging shows radial glial cells dividing asymmetrically in the ventricular zone (VZ) (Top) radial glial cell (red arrowhead) divided asymmetrically in the VZ to generate a daughter neuron (white arrowhead) The radial glial cell then divides a second time. One cell inherited the radial process and translocated toward the cortex (red arrowhead), while the other became multipolar (red arrow) and migrated to the sub-ventricular zone (SVZ).
(Bottom) A schematic illustrating to the final division of radial glial cells (green) at the end of neurogenesis. After division, radial glial divide to self-renew and generate neurons (red) or intermediate progenitor cells (blue) that subsequently divide in the SVZ to generate two identical-looking neurons. Adapted from (Noctor et al., 2004)

Experimentally induced cell fate switches in the nervous system

The use of in vitro culture systems opens up new avenues which can be used to interrogate the mechanisms of neural development. Manipulation of factors associated with fate plasticity outside of the complex environment in the developing embryo, can provide answers to fundamental questions about the mechanisms governing fate plasticity. For example, Vierbuchen et al., 2010 generated functional neurons from human fibroblasts by the expression of Ascl1, Brn2 and Myt1l, showing for the first time that it is possible to efficiently switch cell fate across germ layers. A similar experiment soon after produced functional neurons from mouse hepatocytes, using the same three factors (Figure 1.11). This cell fate switch appears to be direct, as the induced neurons did not undergo DNA synthesis (Marro et al., 2011). During the reprogramming, transcripts associated with hepatocyte terminal fate where downregulated as the neuronal fate was acquired, indicating a true switch in lineage occurs and not a mixing of fates. It was later shown that it is possible to induce neuronal differentiation from fibroblasts with the expression of a single proneural factor Ascl1 (Chanda et al., 2014). Chromatin accessibility assays during neuronal induction of mouse embryonic fibroblasts reveal a complete remodelling of the chromatin landscape upon expression of Ascl1. Ascl1 acts first, with Brn2 and Myt1l only able to access fibroblast chromatin subsequently, but only if Ascl1 is present (Wapinski et al., 2013), indicating the Ascl1 acts as a pioneer transcription factor.

Figure 1.11 Neuronal morphology and fate markers induced in hepatocytes

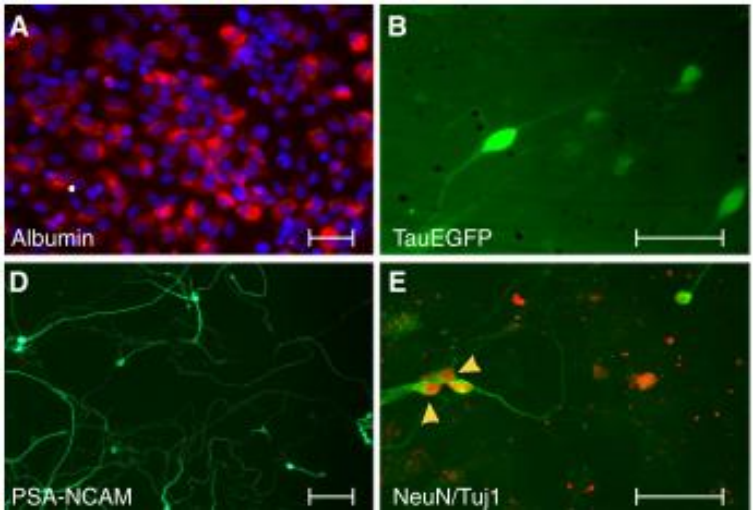

Neurons are induced from mouse hepatocytes by the expression of *Ascl1*, *Brn2* and *Myt1l*.

(A) Primary liver cultures from postnatal mice liver cells express albumin (red)
(B) Neuronal marker TauEGFP-positive cells show a neuronal morphology (green) 13 days after viral induction of *Ascl1*, *Brn2*, *Myt1l*
(D) Induced cells express immature neuron marker PSA-NCAM (green)
(E) Induced cells express neuronal lineage markers NeuN (red) and Tuj1 (green)
Adapted from (Marro et al., 2011)

The pioneer transcription factor model describes how certain factors can bind, transcriptionally inactive, condensed chromatin and quickly recruit other factors usually involved in differentiation (Cirillo et al., 2002; Cirillo & Zaret, 1999; Polach & Widom, 1996; Zaret & Carroll, 2011) (Figure 1.12). Induction of neuronal cells from fibroblasts takes up to 3 weeks but the effects on chromatin can be seen quickly after *Ascl1* induction and the adoption of a stable state, similar to differentiated neurons, by day 5, long before neuronal properties are visible (Wapinski et al., 2017). The rapid switch in chromatin state is likely different than what happens through the gradual lineage fate restriction in embryonic development or induced pluripotency (Wu et al., 2016). It will be important to determine if this difference is a peculiarity of neuronal differentiation or a feature somatic cell fate reprogramming in general. Looking for contrasts with what happens *in vivo* and in genetically amenable model organisms with similar mechanisms of neuronal differentiation, could be particularly helpful in this respect.

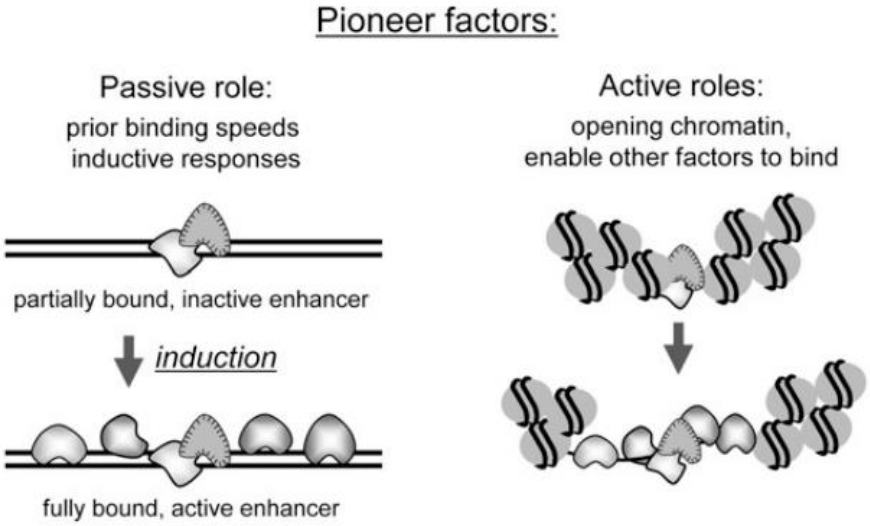

Figure 1.12 Passive and active roles for pioneer factors endow transcriptional competence

A schematic showing the role of pioneer transcription factors in open and compacted chromatin.
In the passive role, stable, prior binding of pioneer factors to a complex regulatory sequence, such as an enhancer element, reduces the number of additional factors that are needed to bind at a later time in order to create an active enhancer. Such priming can increase the rapidity of a transcriptional response.
In the active role, pioneer factors can directly facilitate other factors binding to nucleosomal DNA or open up the local chromatin to allow other factors to bind.
Adapted from (Zaret & Carroll, 2011)

Experimental cell fate modification *in vivo* shows that neurogenic potential in the central nervous system is not necessarily restricted to radial glia, another major type of glia, astrocytes, have the ability to produce neurons (Doetsch et al., 1999; Seri et al., 2001). Similar to the work of Zhou, Brown, Kanarek, Rajagopal, & Melton which reprogrammed mature exocrine cells to β-cells *in vivo* it was shown that astrocytes in the striatum of adult mice could be induced to produce neurons (Niu et al., 2015). Ectopic expression of SOX2 in astrocytes induces them to round up and begin expressing ASCL1, typical of an intermediate progenitor cell, which then go on to divide to produce neuroblasts which proliferate and produce functional neurons (Figure 1.13). During this transition the cells did not express nestin, typical of proliferating radial glia, indicating that they revert to a neural stem cell fate. Intriguingly, unlike the previous *in vitro* examples involving fibroblasts, in this case SOX2 did not promote a stem like fate *in vivo* (Ring et al., 2012) and ASCL1 alone was not sufficient for the transition to neuronal fates (Chanda et al., 2014). In adult mouse astrocytes, SOX2 drives the transition into a neuronal progenitor state where ASCL1 is required but not sufficient to induce neuroblasts capable of producing mature neurons that integrate into local circuits. These differences give insight into the different effects pluripotency factors have on blast cells and mature glial cell types, but more importantly, underlines the importance of studying these type of cell fate transitions in the context of a living brain. The study of animals whose nervous system are composed of fewer cells but have comparable mechanisms of neural fate determination could greatly simplify such a task.

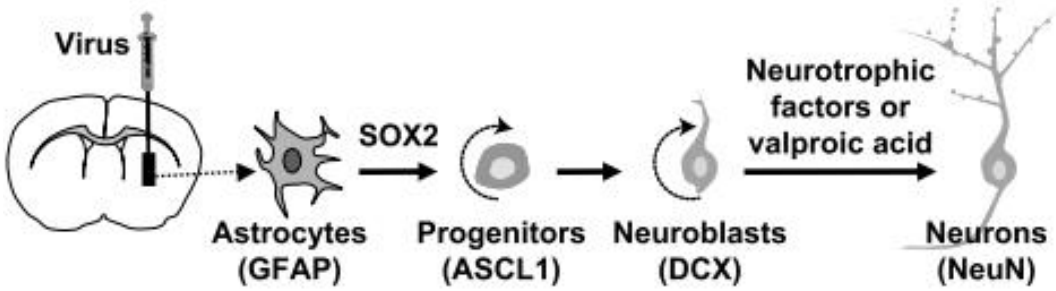

Figure 1.13 Astrocytes in the adult brain induced to produce neurons by SOX2

A schematic representation showing the *in vivo* reprogramming of astrocytes into functional neurons. The reprogrammed cells pass through a distinct series of cell states that mimic adult neurogenesis in the hippocampus.
The virally expressed ectopic SOX2 induces astrocytes to produce ASCL1 expressing progenitor cells which proliferate and generate DCX expressing neuroblasts which are capable of producing mature neurons. Adapted from (Niu et al., 2015)

Glia produce neurons throughout life

Another longstanding idea was that all neurogenesis in mammals occurs in early development. However, this notion was challenged when *de novo* generation of neurons was discovered in the sub granular zone of the dentate gyrus and the sub granular zone (SGZ) of the adult hippocampus (Eriksson et al., 1998; Kempermann et al., 2004; Seri et al., 2001). The adult neural stem cells are glial fibrillary acidic protein (GFAP) and *Sox2* expressing, radial glia like cells with a single arborised projection. Also called Type 1 progenitors, a crucial characteristic central to their role is that they are usually temporarily withdrawn from the cell cycle, termed quiescent, or slowly dividing until they go through heterogenous stages and develop into mature neurons that integrate themselves into pre-existing neuronal circuits (Gebara et al., 2016). The morphological heterogeneity of neural progenitors is accompanied by a difference in cell cycle status, with the quiescent and dividing cell types responding differently to physiological stimuli. For example, physical exercise, which is associated with increased hippocampal neurogenesis, may activate division in the pool of quiescent radial glia (Lugert et al., 2010). In the mammalian brain glia have since been found to produce neurons throughout development reviewed in (Kriegstein & Alvarez-Buylla, 2009) and summarised in Figure 1.14.

Non-mammalian organisms with simpler brains have been used to reveal extraordinary detail about the generation of neurons from glia, particularly late in development. As well as for heart regeneration, the zebrafish is a notable model for neuronal regeneration, as forebrain injury induces proliferation of neuronal precursor cells in the ventricular zone (VZ) which contributes to the recovery of neural tissue in the adult brain (Kishimoto et al., 2012). Radial glial like adult neural stem cells are more prevalent in the zebrafish brain than mammals and are capable of regenerating mature neurons which integrate into existing circuits (Kroehne et al., 2011). It is possible to image the brain zebrafish and trace the activity of individual adult neural stem cells *in vivo* (Barbosa et al., 2015). Over a period one month it was found that most adult neural stem cells in the intact brain remain quiescent (61%). A small proportion of cells divide symmetrically to replenish the stem pool, however unlike in mammals (Obernier

et al., 2018), this is not enough to sustain the stem population into old age. Some stem cells re-enter the cell cycle and divide asymmetrically (12%) to self-renew and produce an intermediate neural progenitor-like cell and rarely multiply symmetrically. Remarkably, a significant proportion (17%) directly began to express neuronal markers and lost the hallmarks of stem cells without undergoing division (Figure 1.15A). Similar imaging after injury showed a striking response where the majority of neural stem cells no longer remain quiescent but divide asymmetrically. A greater proportion now divide symmetrically (Figure 1.15B), however, in contrast to the intact brain this is not a multiplicative division, instead, increasing the output of neurons at the expense of the stem pool. At the same time direct conversions are reduced (Barbosa et al., 2015).

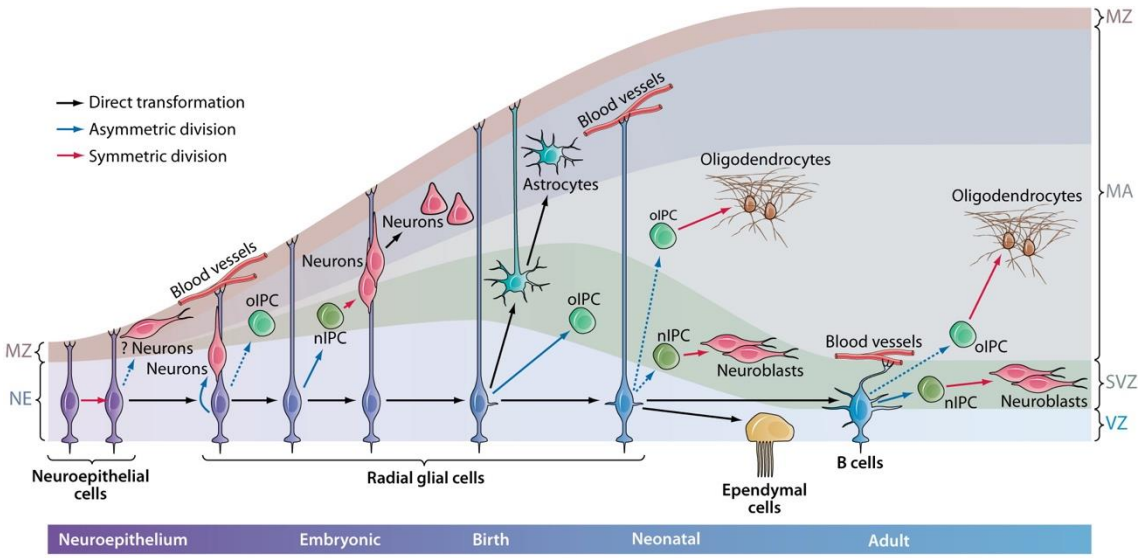

Figure 1.14 Glia produce neurons throughout life

A schematic showing the glial nature of neural progenitor cells in the rodent brain.

In early development neuroepithelial cells proliferate and begin to elongate and convert into radial glial cells. Radial glia divide asymmetrically to generate neurons directly or indirectly through intermediate progenitor cells (nIPCs). At the end of embryonic development, radial glia also begin to convert into astrocytes, some radial glia continue functioning as NSCs in the neonate. These neonatal RG continue to generate neurons and oligodendrocytes through nIPCs and oIPCS; some convert into ependymal cells, whereas others convert into adult SVZ astrocytes (type B cells) that continue to function as NSCs in the adult.
IPC, intermediate progenitor cell; MA, mantle; MZ, marginal zone; NE, neuroepithelium; nIPC, neurogenic progenitor cell; oIPC, oligodendrocytic progenitor cell; SVZ, subventricular zone; VZ, ventricular zone.

In the intact brain, neurons can be continually produced, and homeostasis is achieved by direct conversion of stem cells into neurons, by asymmetric self-renewal or multiplicative division, in this way the stem pool is maintained, declining gradually with age. It is possible however, to switch strategies to rapidly increase the number of neurons in the damaged brain by depleting the pool of adult neural stem cells.

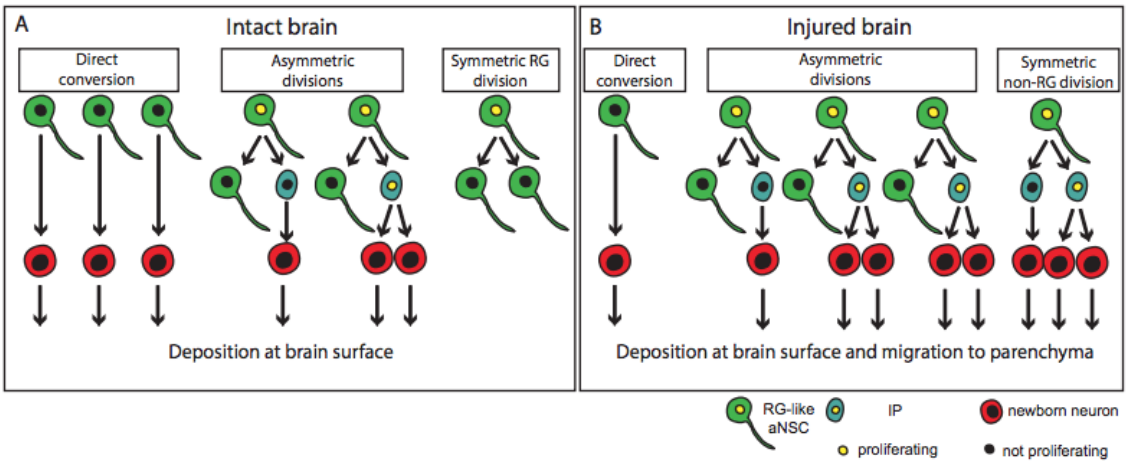

Figure 1.15 Adult neural stem cell dynamics in the intact and injured brain

A schematic image showing two strategies of cell division in the intact and injured zebrafish telencephalon based on live imaging experiments.

(A) In the intact brain adult neural stem cells generate neurons in a way that tend to slowly deplete the stem cell pool with age. Either by direct conversion into neurons or by asymmetric self-renewal and the production of a neuron, the pool is also replenished by multiplicative symmetrical self-renewing divisions. (B) In the injured brain neurogenesis is greatly increased. The neurons are produced by consuming the neural stem cell pool much more rapidly perhaps by drawing on quiescent neural stem cells and limiting replenishment of the stem cell pool.
Adapted from (Barbosa et al., 2015)

The capacity for adult neurogenesis depends entirely on the balance between glial self-renewal and the production of neurons by the depletion of glia. In order to gain a concrete understanding, we must decipher the mechanisms behind the developmental decisions taking place and how each choice affects or instructs the rest. The first and most critical choice is whether to exit the quiescent state and begin, either a multiplicative symmetric division (increasing the number of glia +1) or a neurogenic sequence. If the choice to produce neurons is taken the neurogenic strategy must then be decided; either by asymmetric division (resulting in equal numbers of glia and +1 neurons), direct conversion (-1 glia for +1 neuron), or a consumptive symmetric division (-1 glia, +2 neurons). Since no one strategy occurs at the same frequency, independently of manipulation, it seems that these decisions are taken concurrently, in competition with each other. Describing how balance is maintained between these choices and how these strategies could be altered in injury or disease will undoubtedly be confounded by their competition. Any model in which any each of these decisions can be studied discretely or in combination, will undoubtedly be beneficial informing any such description.

It is the scope of this work to provide tools and techniques and to help decipher the complex sets of developmental decisions that must be taken during a cell fate switch from glia to neurons. The first basic steps in this type of decision; the choice to produce neurons rather than more glia, then choice of neurogenic strategy whether consuming, replacing or directly converting the glial progenitor cells, all hinge about the decision to re-enter the cell cycle from a quiescent state. In the following section I will briefly outline key points in the regulatory control of the cell cycle and cell fate determination.

1.4 Cell cycle control and cell fate plasticity

As cells must exit the cell cycle before terminal differentiation, there is a natural link between the two, but how the extremely complex regulatory networks of the cell cycle are coordinated to influence differentiation is not yet clear. In certain cases, such as, in directly transdifferentiating cells, differentiated cells can undergo full or partial DNA replication when there is no cell division, therefore a well differentiated state need not in itself necessarily preclude the activation of the cell cycle, however the cell cycle is seldom activated in highly differentiated cells and little is known about why this is the case. Getting insight into the mechanisms that coordinate the cell cycle and differentiation could have consequences both in the study of natural development and regeneration as well as in clinical applications for disorders of cellular proliferation and degeneration.

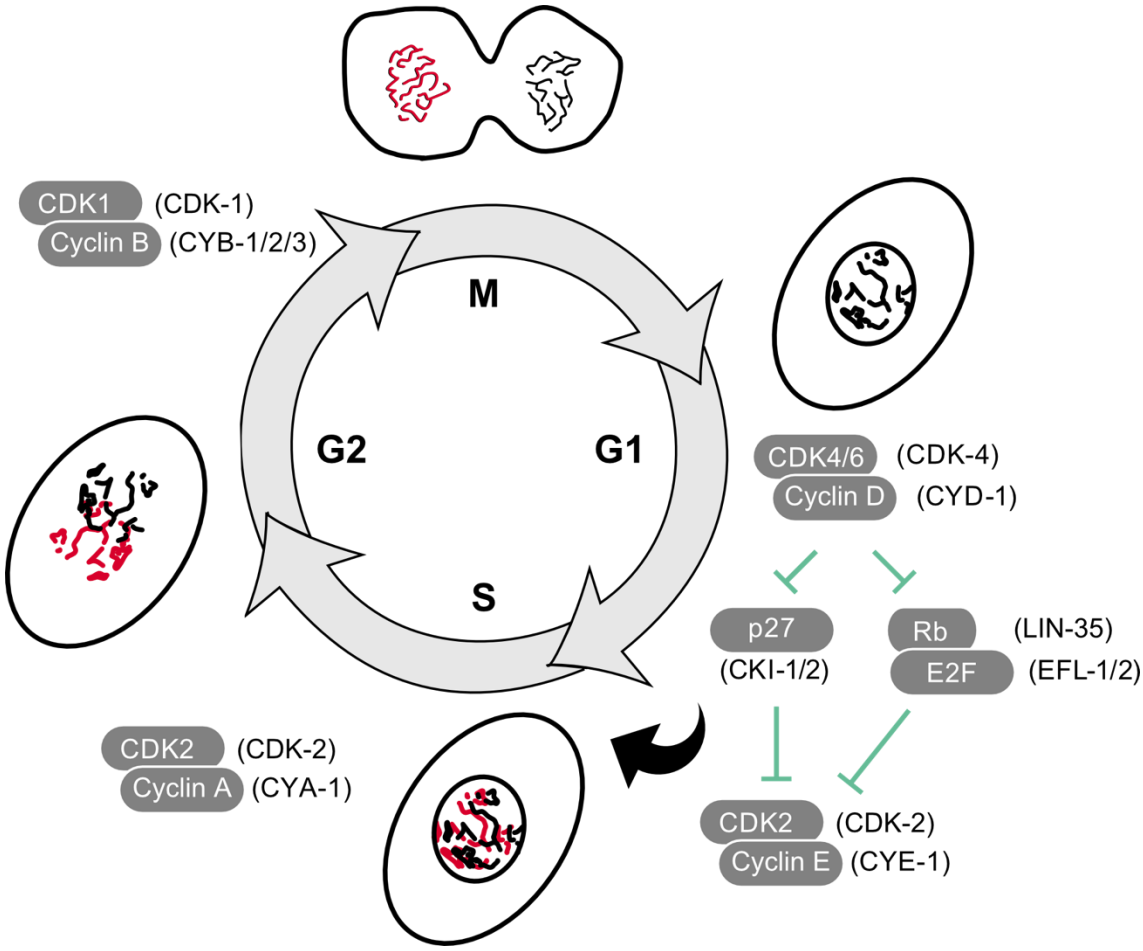

Figure 1.16 The cell cycle

A schematic representing the cell cycle. Showing the four sequential phases G1, S, G2 and M, with the key human gene families associated with each transition and in parentheses the in *C. elegans* homologues involved in the postembryonic cell cycle, with a particular focus on the G1/S transition.

1.4.1 An overview of the cell cycle

This section will give a brief overview of the central genes and regulatory networks involved in cell cycle regulation and their links with cell fate determinants. The canonical cell cycle (Figure 1.16) follows a precise sequence; when a cell is born there is a phase of metabolic growth (G1). The next phase entails the replication of chromosomal DNA in the synthesis phase (S) and is followed by a second gap phase (G2) during which replication is checked for errors and the cell is prepared for the last phase of mitosis (M). During M the replicated chromosomes are segregated into two daughter cells by cytokinesis which again enter G1. A cell may permanently remain in G1 and perform its physiological functions for an extended period of time or immediately proliferate. Cycling cells that are temporarily but reversibly arrested in G1 are referred to as being in G0. G0 or G0/G1 is sometimes used interchangeably with the term quiescence however this term often designates highly specialised, well differentiated cells that have withdrawn from the cell cycle for an extended period of time but retain the ability to re-enter the cell cycle and this is how it will be used in this work. Quiescence need not be limited to G0 however, for example, *Drosophila* stem cells have been found to enter quiescence in the G2 phase as well as G0 and have different properties than G0 quiescent cells, such as re-entering the cell cycle more quickly (Otsuki & Brand, 2018).

By creating heterokaryons of two HeLa cells in different phases of the cell cycle the classic experiments of Rao & Johnson, 1970 showed that the cell cycle is controlled by a highly ordered sequence of regulatory events and checkpoints mediated by diffusible factors. Careful observation of chromosomal structure and BrdU radiolabelling showed that S-Phase nuclei could induce G1 but not G2 cells to enter S while G1 and G2 fusions had little effect on each other (Johnson & Rao, 1970). M cells induced the condensation of chromosomes in G2, S and G1 (Figure 1.17). Since then, thanks to extensive research using various model organisms like yeasts and sea urchin, most of the factors that govern the main checkpoints and transitions from one phase to another have been identified (Evans, Rosenthal, Youngblom, Distel, & Hunt, 1983; Hartwell, Culotti, Pringle, & Reid, 1974; Lee & Nurse, 1987). The main cell cycle related gene families are Cyclins, which fluctuate in concentration

throughout the cell cycle, serine/threonine kinases that associate with cyclins, Cyclin Dependent Kinases (CDKs), and Cyclin Dependent Kinases Inhibitor proteins (CKIs) (Figure 1.18). They collectively regulate the transition between phases and other key aspects of control over the cell cycle, by gene expression, the formation of protein complexes and post-translation modifications, from a multitude of other kinases and phosphatases as well as by subcellular localisation tags.

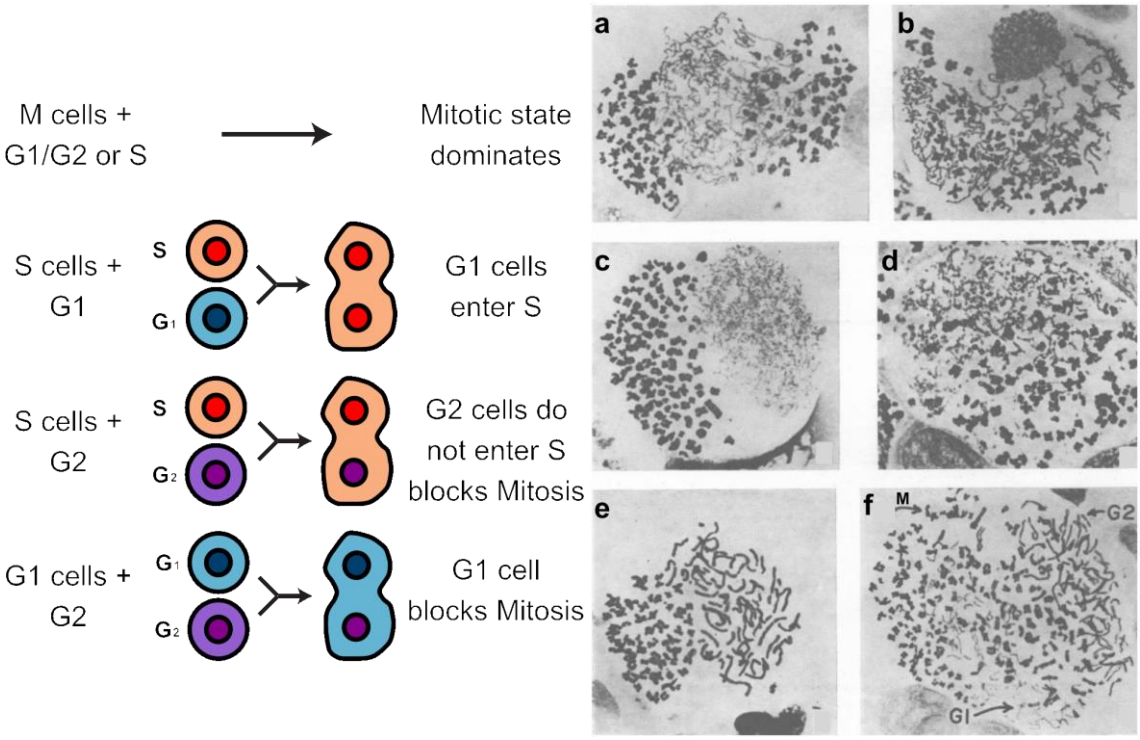

Figure 1.17 The Rao and Johnson cell fusion experiments

(Left) Schematic diagram showing a summary of the results of the heterokaryon experiments of Rao and Johnson fusing cells in assorted stages of the cell cycle together.
(Right) Images of selected experiments showing premature chromosome condensation in heterophasic cells.
(a) Premature chromosome condensation of the G1 nucleus in a heterophasic M/G1 cell at 30 min after fusion. Note the long and slender G1 chromosomes with single chromatids. The more condensed chromosomes are from the mitotic cell blocked by colcemid.
(b) Heterophasic cell formed by the fusion of 2G1 cells with one mitotic cell. Premature chromosome condensation can be observed in the G1 nuclei, one of which still shows its nuclear outline.
(c) Premature condensation of the S chromatin at 45 min after the fusion between mitotic and S-phase cells. The chromatin of the S nucleus presents a fragmented appearance.
(d) Premature chromosome condensation of a nucleus blocked at the G1/S boundary by double thymidine treatment. Note that the pattern of condensation is intermediate between that of G1 and S nuclei.
(e) Premature chromosome condensation of the G2 nucleus in an M/G2 heterophasic cell. The more condensed chromosomes are from the mitotic cell treated with colcemid for 19 h.
(f) A heterophasic cell formed by the fusion between G1, G2 and mitotic cells. Note the differences between G1, G2 and metaphase (M) chromosomes. Adapted from (Johnson & Rao, 1970)

In brief, progression through the somatic cell cycle is controlled by the action of CDKs which are activated in a tightly regulated sequence. Precise regulation is achieved through positive regulation and inhibition, chiefly by cyclins and CKIs. G1/S progression is triggered by Cyclin D in complex with CDK4 or CDK6. The primary target for CDK4 is the Retinoblastoma (Rb) protein, phosphorylation of Rb results in the de-repression of activating transcription factors of the heterodimeric E2F/DP family allowing for the transcription of CDK2, Cyclin A and Cyclin E, and when a certain threshold of CDK activity is reached the cell passes the first restriction point after which it is committed to DNA synthesis. Rb binds to E2F by its transactivation domain (Flemington et al., 1993; Helin et al., 1993) and also helps to recruit chromatin remodelling factors such as histone deacetylases (Magnaghi-Jaulin et al., 1998) which have the effect of locally condensing the chromatin and inhibiting transcription (Kingston & Narlikar, 1999). With increased transcription of Cyclin E/CDK2 and with Cyclin D/CDK4 Rb is hyperphosphorylated ensuring commitment to S-phase. Cyclin E/CDK2 and Cyclin A/CDK2 modulate the transcription of factors critical to the regulation of the early steps of DNA synthesis; Origin of Replication Complex (ORC) subunits and kinases, DNA helicases, like Minichromosome Maintenance (MCM2-7) subunits, histone proteins and chromatin remodelling factors like SWI/SNF, ribonucleotide synthesis and processing, such as DHFR, and Ribonucleotide Reductase (RNR) and DNA polymerases. Rb has also been shown to bind to the MCM helicase complex and inhibit S-phase entry (Mukherjee et al., 2010; Sterner et al., 1998). After replication is completed Cyclin B/CDK1 levels accumulate, once activated by Cyclin A/CDK2, Cdc25 and other complexes, Cyclin B/CDK1 drives entry into Mitosis by the phosphorylation of targets that inhibit replication and promote the assembly of the spindle apparatus and kinetochores. Finally the cell cycle proteins are marked for degradation by the Anaphase Promoting Complex (APC) and once CDK activity is low enough for spindle disassembly, nuclear envelope assembly and cytokinesis the daughter cells enter the new G1 phase; reviewed in (Bertoli, Skotheim, & de Bruin, 2013; Chen et al., 2017; Hydbring, Malumbres, & Sicinski, 2016; Malumbres, 2014; Morgan, 2007; Sun, Bagella, Tutton, Romano, & Giordano, 2007). It is important to note that CDKs can often compensate for one another and rescue relatively minor alterations in

cell cycle dynamics and significantly, cell cycle progression has been shown to be dependent on the pattern of increasing general CDK activity as well as substrate specificity (Oikonomou & Cross, 2011; Swaffer, Jones, Flynn, Snijders, & Nurse, 2016). Nevertheless, aberrant CDK activity due to inappropriate expression of Cyclins or activity of CKIs can have dire consequences including tumour formation or apoptosis. The multiple redundant pathways in vertebrate model systems can make the study of the cell cycle and differentiation problematic.

The activity of CDKs is fine-tuned by modulation via a combination of inhibitory and activating proteins in order ensure orderly progression through the cell cycle. For full catalytic activity CDKs can be phosphorylated by a CDK Activating Kinase (CAK) as well as being bound by a Cyclin. The catalytic site of a CDK is usually occluded by a domain called the activation loop or T-loop (Figure 1.18), upon binding with a Cyclin the catalytic cleft is opened up for interaction with substrates. For full CDK activity phosphorylation of the T-loop on a specific threonine residue by a CAK is often required, keeping the T-loop clear of the catalytic cleft (Jeffrey et al., 1995).

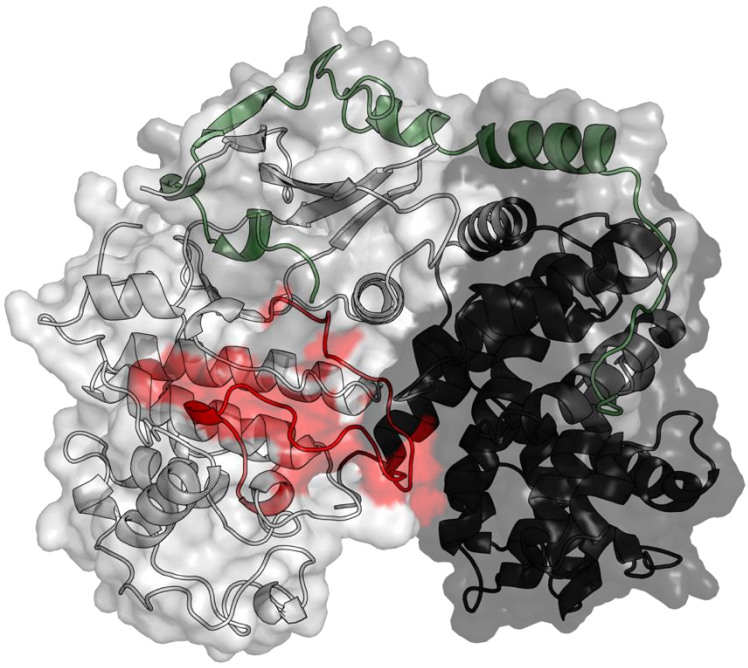

Figure 1.18 CDK2-CYCA-p27 complex crystal structure with functional domains

A 3D rendering of CDK2 (white) in complex with Cyclin A (black) and the CKI p27 (green). The general structure is consistent among the CDK family. The catalytic cleft is formed by the recess between the Cyclin and the CDK. The primary regulatory region of the CDK, the T-loop, is highlighted in red. In its inactive state the t-loop occludes the catalytic cleft and the ATP binding domain.
3D rendering using PBDid 1jsu in The PyMOL Molecular Graphics System, Version 2.0 Schrödinger, LLC. Using the molecular structure from (Russo et al., 1996)

Negative regulation of CDK activity is governed by two main types of CDK inhibitors the INK4 and CIP/KIP families. The INK4 family block G1/S progression by binding to CDK4/6 and disrupting Cyclin binding and kinase activity. In contrast, the CIP/KIP family act throughout the cell cycle and are not strictly CDK inhibitors, as they also modulate Cyclin/CDK complex assembly and nuclear trafficking (Blain, 2008; Bockstaele et al., 2006). CIP/KIP proteins inhibit CDK activity by binding and sequestration of both Cyclins and CDKs, as well as by preventing T-loop phosphorylation (Cheng et al., 1999). In turn, the inhibitory activity of CIP/KIP family CKIs is governed by, cell cycle phase dependent expression, post-translational mechanisms or sequestration by Cyclins and degradation. For example, the inhibitory activity of p27 bound to Cyclin D/CDK4 complexes is dependent on the phosphorylation of certain residues of p27. (James et al., 2008) Reviewed in: (James et al., 2008; Li et al., 2015; Ray et al., 2009; Sherr & Roberts, 1999; Wood & Endicott, 2018). The activity of G1/S CDKs are often modulated through the action of CKIs to control the proliferation/differentiation decision, For example, the mitogenic pluripotency factor Myc indirectly, through FoxO factors, inhibits endogenous transcription of p27/kip (Chandramohan et al., 2008). CKIs, CAK and similar factors that directly affect CDK activity at the G1/S transition are likely to be key components of the differentiation/proliferation decision. A high level of CKI expression is associated with a state of quiescence p27/Kip is used as a marker for quiescent cells and has been found to regulate the proliferation/quiescence decision in various systems (Besson et al., 2006; Georgia & Bhushan, 2006; Oesterle et al., 2011). In the adult mouse hippocampus p27 has been shown to regulate the quiescence of radial glia, the Cyclin-CDK interacting domain is necessary to control this activity, additionally, p27 also directly regulates the cell cycle exit and differentiation of immature neurons (Andreu et al., 2015; Nguyen et al., 2006).

1.4.2 Cell cycle control and cell fate determination

Control of cell division can be a used as means to guide differentiation, for example, establishing asymmetry in the first cell division in *C. elegans* is critical to the correct specification and timing of division of the lineage founder cells in the embryo (Rose & Gönczy, 2014). Similarly, in the facultatively multicellular protist *Dictyostelium discoideum*, which upon starvation, forms social groupings consisting of two cellular specialisations, the stalk and the spore, the phase of the cell cycle is used as cue for differentiation (Jang & Gomer, 2011). If cells happen to be in the S-phase upon starvation they produce prestalk cells and if they are in late G2 they produce prespore cells. It follows that there must be a link between cell cycle components and cell fate determinants. An example of the crosstalk between the cell cycle machinery and cell fate determination factors has been well described during myogenesis. The myogenic master regulator MyoD influences and is influenced by the cell cycle in order to induce differentiation in concert with cell cycle exit. MyoD activity is negatively regulated via hyperphosphorylation by CDK2, this promotes MyoD degradation when CDKs are active in the nucleus (Kitzmann et al., 1999; Song et al., 1998; Tintignac et al., 2000). Additionally, Cyclin D and CDK4/Cyclin D can also complex with MyoD in the nucleus to inhibit its DNA binding activity (Cenciarelli et al., 1999; Zhang et al., 1999). MyoD also negatively regulates cell cycle progression through CKIs. MyoD can cause permanent withdrawal from the cell cycle by inducing the expression of the CKI p21/Cip (Halevy et al., 1995), also p57/kip2 transcription is stimulated by MyoD binding and the reorganisation of chromatin structure to allow access to the p57 promoter (Busanello et al., 2012). In turn p57 stabilises MyoD by forming a complex possibly in competition with the formation of MyoD/CDK4/Cyclin D complexes (Reynaud et al., 2000). Muscle differentiation requires careful coordination with the exit from the cell cycle, this is ensured by a complex series of direct reciprocal interactions between cell fate determinants and cell cycle components. Such interactions are not unique to muscle differentiation and likely play a widespread role in the differentiation of cells of any tissue, including the brain.

Cell cycle control in neuronal fate determination

Apart from regulating cell the transition between different phases of the cell cycle, cell cycle machinery has been shown to have roles in neuronal determination from the earliest stages in the embryo. The classic proneural transcription factor Ngn2 was found to be phosphorylated by CDKs at multiple sites, thus inhibiting its binding to neuronal differentiation targets (Ali et al., 2011; Hindley et al., 2012). Mutation of these CDK phosphorylation sites enhances neuronal differentiation in the developing *Xenopus* embryo and this effect persists even if CDK activity is increased (Ali et al., 2011). In turn, Ngn2 overexpression was found to inhibit cell cycle re-entry of chick spinal neural progenitors, by indirectly downregulating S-phase Cyclins D, E and A, while knockdown of Ngn2 results in S-phase Cyclin upregulation, however, CDK and CKI expression is not affected by Ngn2 levels. Importantly, Ngn2 can induce neuronal differentiation independently of Cyclin levels (Lacomme et al., 2012). In contrast, the CKI, p27 was shown to stabilise Ngn2 in *Xenopus* and mice, thus promoting early neurogenesis independently of its role in Cyclin/CDK complexes (Nguyen et al., 2006; Vernon et al., 2003). Similarly, the deletion of Cdk4 and Cdk2, which bind with Cyclins D and E respectively, results in an increase in neurogenic divisions, in mouse neural stem cells. Proliferative divisions were not blocked in Cdk4 and Cdk2 double knockouts as Cdk1 was found to compensate by binding to both Cyclin D and E, but did result in a shorter S-phase and an increase in spontaneous neuronal differentiation (Lim & Kaldis, 2012). Conversely, the overexpression of CDK4/CyclinD1 delays neurogenesis and promotes the proliferation of progenitor cells (Lange et al., 2009). Interestingly, in the earliest steps of neuronal determination, the loss of Cdk4 and Cdk2 was found to reduce the expression of the Sox2 protein. Cdk1, Cdk2 and minimally Cdk4, were found to phosphorylate Sox2 and it was found that Sox2 must be dephosphorylated in order to bind to neurogenic genes, such as Ngn2 (Lim et al., 2017). This finding suggests that as well as for cell cycle progression (Swaffer et al., 2016) high CDK activity inhibits neural differentiation by phosphorylating Sox2. When CDK activity is lower, Sox2 bound to neuronal differentiation genes can activate transcription, possibly after cleavage with increased serine protease activity (Lim et al., 2017). Similarly, Cdk2 mediated

Sox2 phosphorylation at multiple sites was found to be not to be itself required for mouse embryonic stem cell self-renewal and cell cycle progression (Ouyang et al., 2015). Thus, the beginning steps required for neuronal determination could be induced during cell division; high CDK activity induces phosphorylation of Sox2 and promotes entry into a self-renewing state, after division the no longer actively phosphorylated Sox2 (perhaps through the action of proteases and other modifications) begins to induce its neuronal differentiation program. The interplay between cell cycle machinery and transcription factors associated with neuronal differentiation can act as a sensor for cell cycle activity in order to inform the proliferation/differentiation decision as well as realising differentiation.

Tight regulation of quiescence is essential in adult neural stem cells

The embryonic environment is permissive to embryonic stem cell renewal, but this ability is lost later in development, since neural stem cells can persist in into adulthood in the mammalian brain, they therefore need to maintain control of the differentiation/proliferation decision over long periods of time. One of the key mechanisms by which this is achieved involves the regulation of the quiescent state. The ability of certain cells to remain quiescent is associated with retaining the ability to be multipotent and function during repair and regeneration. While quiescent cells are often said to be inactive or dormant as the name suggests, it is becoming clear that quiescent cells can be functional, and some stem cells have been shown to be capable of high metabolic activity (Lemons et al., 2010). They must also be able to rapidly respond to a changing environment in order to function appropriately, the Notch pathway, which generally promotes proliferative signalling and well as differentiation and apoptosis (Artavanis-Tsakonas et al., 1999), is critical to stem cell quiescence and the maintenance of stem cell pools by proliferation (Bjornson et al., 2012; Philippos et al., 2012). This pathway is also necessary for the proliferation and quiescence of neural stem cells in the developing and adult mammalian brain (Engler et al., 2018; Gaiano et al., 2000; Imayoshi et al., 2010; Iso et al., 2003), where it acts by inducing the expression of transcriptional repressors like *Hes1*, which inhibits proneural gene expression and neuronal differentiation (Del Bene et al., 2008). Live imaging studies show that neural stem cells that have proliferated can return to quiescence but soon

become active again (Pilz et al., 2018), this suggests that there may be different levels of quiescence, deep or shallow. The ability return to quiescence is promoted by Ascl1. Ascl1 is degraded by the E3-ubiquitin ligase Huwe1, in proliferating neural stem cells, high levels of Ascl1 result in the accumulation of Cyclin D which promotes cell cycle re-entry, however knockout of E3-ubiquitin ligase results in the accumulation of Ascl1 and consequently Cyclin D levels, blocking cell cycle re-entry (Urbán et al., 2016). Genome wide association studies reveal that Ascl1 regulates many genes involved with cell cycle progression at the G1/S transition, as well as genes associated with cell cycle exit (Castro et al., 2011). In fact, when *Ascl1* is expressed heterochronically in the mouse retinal ganglion cell lineage it blocks cell cycle exit in retinal ganglion progenitor cells (Hufnagel et al., 2013). The seemingly contradictory roles are reminiscent of the role of the Ascl1 homologue in *Drosophila*, which both promotes neuroblast self-renewal (Southall & Brand, 2009) and prevents further division in neuroblast daughter cells (Wallace et al., 2000). These experiments hint that Ascl1 may have an ancient and conserved role as a direct molecular link that coordinates cell cycle regulation and neural differentiation.

The Notch pathway is required for both proliferation and quiescence and Ascl1 is required not only for neuronal differentiation but also proliferation. In order to ensure that neurons can be produced into adulthood and a sufficient stem pool remains these contradictory programs must be coordinated. A key mechanism by which this coordination is achieved is through the regulation of Ascl1 activity by Hes1. Ascl1 is antagonistically regulated by Hes1, and Hes1 has been shown to negatively autoregulate itself in a feedback loop, resulting in a oscillating levels of Hes1 and Ascl1, in opposing phases (Hirata et al., 2002). Using fusion reporters for Hes1 and Ascl1, their relative levels could be assessed in both proliferating and quiescent neural stem cells (Sueda et al., 2019). It was found that in the quiescent state Hes1 is sustained at a high level and this keeps Ascl1 levels too low to begin to activate cell cycle machinery (Figure 1.19). In active neural stem cells both Ascl1 and Hes1 oscillate at comparable levels and Ascl1 oscillations trigger proliferation. In the newly born neurons, the oscillation of Ascl1 is sustained at a high level, promoting neuronal differentiation. Combinations of a knockout of Hes1 and constitutively active Hes1 showed that high levels and not oscillations are enough to promote a

quiescent state, while optogenetic and lentivirus induced oscillations of Ascl1 in quiescent cells induced neural stem cells to generate neurons. This suggests that high levels of Hes1 determine the quiescent state while oscillation and sustained high levels of Ascl1 govern proliferation and neuronal differentiation, respectively. The molecular mechanisms by which each of these states are activated is not yet well known, and leaves open the search for a potential signal that results in a lowering of Hes1 levels or the possibility of alternative sources of Ascl1 expression that could drive quiescent cells into activity.

It is becoming increasingly clear that apart from their role in the progression of the cell cycle, Cyclins, CDKs and CKIs are also involved in direct and indirect regulation of pluripotency factors and master regulator genes that govern the differentiation of various tissues. Taken together these results indicate the formation of a CDK activity dependent bistable switch, where the inhibitory phosphorylation by CDKs may prevent pioneer factors from binding to inaccessible chromatin and initiating their developmental program during the cell cycle. Concomitantly, the build-up or concentration/activity of cell fate determining factors mutually suppress cell cycle activity preventing continued proliferation. Transition from the G1 phase seems to provide a key window in the cell cycle for cell fate decisions to be made. Any models which can facilitate the study of the interactions between the cell cycle and cell fate is will be valuable not only for our understanding of the basic biology but could quickly find applications in cell replacement strategies.

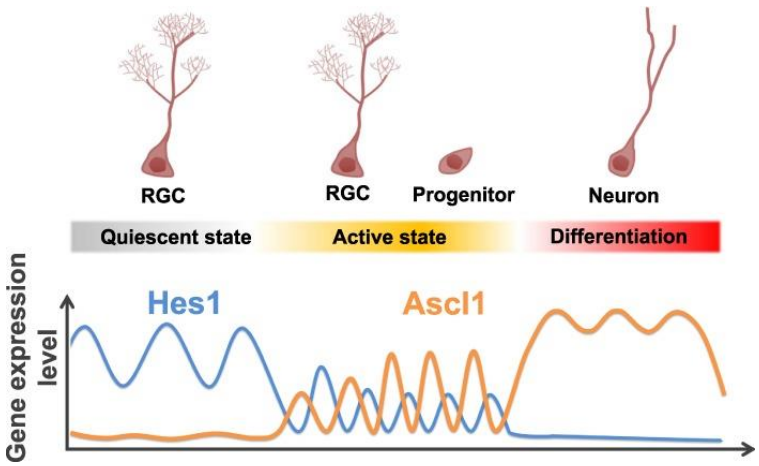

Figure 1.19 Expression of Hes1 and Ascl1 in quiescent and active neural stem cells

A schematic showing the expression dynamics of Hes1 and Ascl1 in quiescent and active radial glia-like neural stem cell (RGC) and differentiating neurons. High levels of Hes1 determine the quiescent state, while oscillation of Ascl1 controls proliferation and sustained high levels of Ascl1 promote neuronal differentiation. From (Sueda et al., 2019)

Along with the increasing pace of advancement of *in vitro* cell culture, complementary *in vivo* studies will be critically important in developing a functional understanding the intracellular events, as well as the effects the microenvironment has on cells undergoing cell fate transitions. It is the goal of this work to further our understanding of cells undergoing cell fate transitions and in particular the production of neurons from glia. Without such an understanding, the study of, and treatments for, brain injury, age related disorders and cell replacement strategies will be at a serious disadvantage. Unfortunately, the enormous complexity of the developing and adult vertebrate brain presents several obstacles to *in vivo* study. Chiefly the identification and lineage determination of individual cells, along with the heterogeneity of cells within the same class, make the determination of both the starting and resultant cell fates during reprogramming a potential source of error. At the same time, the unavoidable ecological and biological constraints of vertebrates, such as long lifecycles and genetic networks with multiple redundant pathways, make unbiased genetic and drug screening approaches expensive and time-consuming prospects. Also, regrettably, such approaches by no means guarantee that even the most promising results will translate to humans. A smaller and more genetically amenable model organism with an even distantly comparable neuronal development could be immensely helpful, speeding up the process of translating our understanding of development to medical application, from discovering new therapeutic targets to testing interventions. In the next section I will present some of the key benefits of using the nematode *Caenorhabditis elegans* as a model organism in which to study neuronal development.

1.5 *Caenorhabditis elegans* as a model for neuronal development and cell fate plasticity

1.5.1 Introduction to C. elegans

C. elegans is a free living nematode commonly found microbe rich environments such as plant stems, rotting plant matter and compost (Schulenburg & Félix, 2017). It is a sexually dimorphic dioecious species, with both a female hermaphrodite and a male. The worm has been used extensively as a model species, originally established by Sydney Brenner to study the genetics of neuronal development and behaviour in 1965 (Brenner, 1973). The hermaphrodite develops from fertilisation, through four larval stages, to sexual maturity over about 3 days (Figure 1.20). The hermaphrodite transiently produces sperm early in development making it capable of self-fertilisation, apart from the sperm stored in the spermatheca, the adult only bears female reproductive organs. The ability of hermaphrodites to quickly produce 200-300 clones is of great benefit to genetic studies. Males naturally occur infrequently, and must mate in order to procreate, this allows for easy cross-fertilisation which is extremely useful in genetic studies, the difference in reproductive drives is the source of their physiological and behavioural differences (Figure 1.21). Simple methods of mutagenesis, the ability to freeze strains for long term storage and ability to produce transgenic strains make the worm extremely genetically amenable (Mello et al., 1991; Mello & Fire, 1995).

The adult hermaphrodite has a simple, optically transparent, body plan consisting of 959 cells, each of which can be identified unambiguously. The lineage of every cell, from the embryo to the adult, has been established and found to be invariant, which is extremely useful, allowing the study of development at a single cell resolution (Sulston et al., 1983; Sulston & Horvitz, 1977; Sulston & White, 1980). Several invaluable and now widespread techniques including fluorescent reporter genes, RNA interference and optogenetics were developed in *C. elegans* (Chalfie et al., 1994; Fire et al., 1998; Nagel et al., 2005). Advances like these lead to discoveries that fundamentally transformed the study of development and cell biology in general, for example, the *lin-12*/Notch pathway (Greenwald et al., 1983; Priess & Nichol Thomson, 1987) and microRNAs (Davis, Haas, & Pocock, 2015; Lee,

Feinbaum, & Ambros, 1993) were first discovered in the worm. These discoveries give us a wealth of tools and techniques which can easily be adapted in order to explore the developmental mechanisms by which glia produce neurons. In order to capitalise on the progress made *in vitro*, a complementary approach in a model system is the obvious next step, despite its relative phylogenetic distance from humans the invertebrate *C. elegans* is an ideal candidate for this purpose.

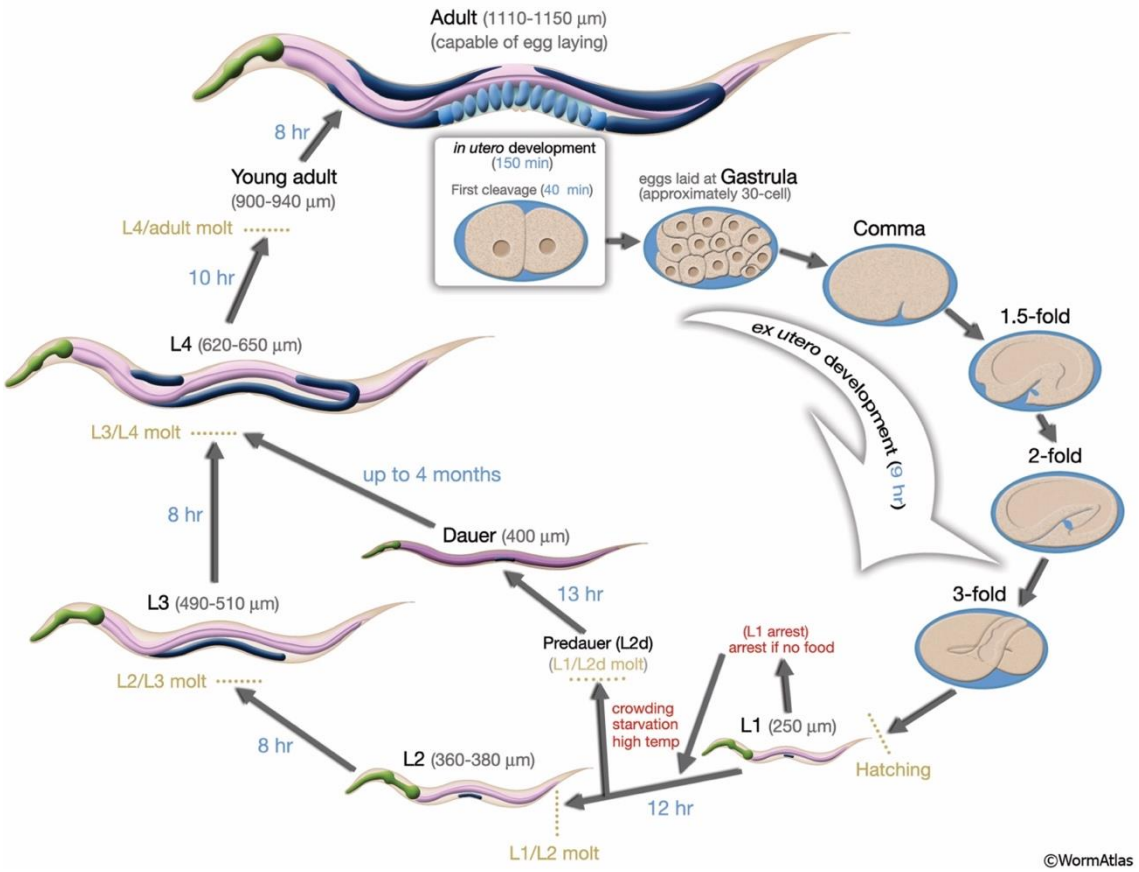

Figure 1.20 Lifecycle of *C. elegans*

The lifecycle of hermaphrodite *C. elegans* at 22 °C, with time spent and approximate length at each stage. Sexual maturation occurs during the fourth larval stage. Taken from Wormatlas.

Genetics and sex determination

C. elegans was the first animal to have a full genome sequence available and has a relatively compact genome of 100Mb with over 20,000 protein coding genes *(C. elegans* Sequencing Consortium, 1998). About 40% of *C. elegans* genes are thought to have human homologues (Shaye & Greenwald, 2011). The worm is diploid and has 5 autosomes, hermaphrodites have two X chromosomes (XX) and males have one (XO). Sex determination is governed by the autosome to sex chromosome ratio (Figure 1.21). XO males are formed as 50% of the progeny of mating or spontaneously by the meiotic nondisjunction of X chromosomes in hermaphrodites, which occurs rarely (<0.001% of births) in laboratory conditions. The X to autosome ratio directs the sex determination pathway to induce male or hermaphrodite fate (Hodgkin, 1987; Zarkower, 2005). By expressing components of this pathway in specific cells or tissues we can effectively feminise genetically XO cells or masculinise XX cells. In combination with the ability to target and genetically manipulate individual cells, we can study neural development from the level of genetic regulation all the way to how this translates to changes in behaviour.

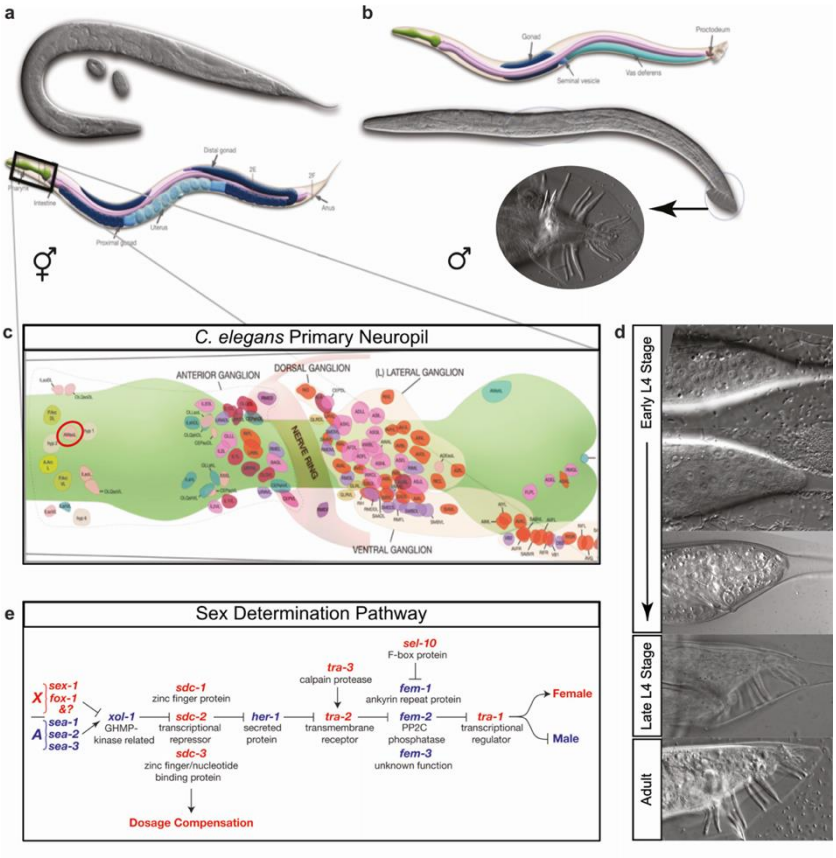

Figure 1.21 Sexual dimorphism and sex determination in *C. elegans*

(a,b) Hermaphrodite and male *C. elegans* DIC and schematic images showing gross anatomical structures. Modified from Wormatlas.
(c) lateral schematic of head showing Nerve ring and head ganglia. Motor, sensory and interneurons in purple, pink and red respectively. Socket cells in brown AMso encircled in red. Modified from Wormatlas.
(d) Development of the male tail from L4 to adulthood.
(e) The *C. elegans* Sex determination pathway. From (Zarkower, 2005)

The cell cycle in C. elegans

The cell cycle has been well studied *C. elegans* showing that many of the major aspects of the eukaryotic cell cycle are conserved from yeast to worms to humans. *C. elegans* has helped in the discovery of novel regulators, for example, *lin-5*, part of the conserved NuMa complex, which is involved in anchoring the mitotic spindle for correct positioning of cleavage in asymmetric cell divisions, and chromosome segregation, was first found in the worm (Lorson et al., 2000; Srinivasan et al., 2003). Screens for cell cycle regulator homologues, show that the multiple often redundant Cyclin/CDK gene families of mammals are present as individual genes in the worm (Boxem et al., 1999), greatly simplifying analysis. In many organisms with a requirement for rapid embryogenesis over cell growth, such as amphibians or insects, the early cell cycle is modified, such that one or both of the gap phases of the cell cycle can be skipped and the S-phase shortened (Farrell & O'Farrell, 2014; Lee & Orr-Weaver, 2003; O'Farrell, 2015), this is the case in the worm. For most of *C. elegans* embryonic development, the cell cycle oscillates between S and M, with very stereotypical timing which is dependent on the cell lineage and tissue type down to the individual cell (Bao et al., 2008). There is therefore little need for G1/S control until the final embryonic divisions and post-embryonic divisions. Due to the importance of the G1/S transition in differentiation I will chiefly focus on this aspect of the worm cell cycle.

The worm homologues of Cyclin D and Cdk4/6, *cyd-1* and *cdk-4* are required for G1/S progression in all post-embryonic cell divisions (Lu & Horvitz, 1998; Park & Krause, 1999) and late embryonic development (Yanowitz & Fire, 2005). Additionally, ectopic expression of CDK-4/CYD-1 can induce cell cycle entry in arrested cells (Korzelius et al., 2011; Park & Krause, 1999). The canonical function of Rb in G1/S progression is also conserved in the worm homologue *lin-35* where *cyd-1* acts upstream of both *lin-35* and *efl-1*, the worm homologue of E2F, to negatively regulate cell cycle entry (Boxem & van den Heuvel, 2002) but functions redundantly with parallel pathways (Boxem & van den Heuvel, 2001; Fay et al., 2002; Ferguson & Horvitz, 1989; Lu & Horvitz, 1998). The knock down of *lin-35* and an activator of the APC/C ubiquitin ligase, *frz-1,* completely eliminates the need of *cyd-1* and *cdk-4* during development

(The et al., 2015), indicating that these two together are the main targets of CDK-4/CYD-1. The CDK-4/CYD-1 complex was also shown to phosphorylate Rb and FZR-1, on residues associated with their activation, *in vitro*. Interestingly, loss or reduction of *fzr-1* activity results in the activation of the S-phase helicase *mcm-4,* specifically in post mitotic neurons but this does not result in DNA replication, while *lin-35* loss has similar results in muscle tissue (The et al., 2015). This suggest that as the direct targets of CDK-4/CYD-1, Rb and FZR-1 not only inhibit cell cycle progression in quiescent cells but also work together to actively inhibit the expression of DNA replication machinery in differentiated post mitotic cells.

The worm has two CIP/KIP family CKI homologues *cki-1* and *cki-2* (Hong, Roy, & Ambros, 1998), the sequence of *cki-1* is highly conserved with the *Drosophila* CKI Dacapo, p21 and p27, specifically the sites necessary for CDK inhibition and Cyclin binding (de Nooij et al., 1996; Lane et al., 1996) however, no INK4 related genes appear to be conserved in *C. elegans*. In the embryo CKI-1 expression is essential to cell cycle arrest, knock down of *cki-1* results in large amounts of extra cell divisions while this is not the case for *cki-2*, indicating that *cki-1* acts as the main inhibitor of the cell cycle entry in the worm (Fukuyama et al., 2003) Importantly, the extra divisions caused by the knock down of *cki-1* in are likely due to a single extra round of cell division at the end of each in each lineage, suggesting that CKI-1 functions at a crucial stage of the cell lineage to regulate the correct number of divisions required. The expression of *cki-1* occurs in the G1 phase in post-embryonic blast cells of various lineages, such as the; vulva precursor cells (VPC) and other cells in the somatic gonad, neuroblasts in the P lineage, in intestinal cells that undergo endoreduplication and the seam cell lineage (Hong et al., 1998). In the seam cells, which have bouts of cell division at each larval stage with resting periods in between moults, *cki-1* is highly expressed in the periods of quiescence and downregulated during division, but are kept high during differentiation after the terminal mitosis in L4 (Hong et al., 1998). The pathway of heterochronic genes, which govern the precise timing of larval development (Ambros & Horvitz, 1987; Lee et al., 1993; Moss, Lee, & Ambros, 1997), controls the timing and developmental specification VPCs by regulating the G1/S decision partly through *cki-1* (Euling & Ambros, 1996; Hong et al., 1998). Knockdown of *cki-1*

results in a single extra early blast cell division in the VPC, and extra divisions in the lateral hypodermal and intestinal lineages (Hong et al., 1998). Similarly, knockdown of *cki-1* and *cki-2* restores the ability both of *cdk-4* and *cyd-1* mutants to enter S-phase in postembryonic intestinal lineage. While loss of *lin-35* alone, partially restores the amount of cell division in *cdk-4* and *cyd-1* mutants and knocking down *lin-35*, *cki-1* and *cki-2* together, results in a large amount of supernumerary divisions, together this indicates that *lin-35* and *cki-1* act together in parallel pathways to control the G1/S transition through CDK-4/CYD-1 (Boxem & van den Heuvel, 2001). *cki-2* shows similar defects in regulating cell cycle quiescence and may act in the same pathway as *cki-1*, as double mutants and RNAi knockdown enhances proliferation defects in VPC lineage mutants, but there is likely also a distinct mechanism as *lin-35* mutants do not enhance *cki-2* defects as is the case with *cki-1* (Buck et al., 2009). The phosphatase CDC-14 is also required for cell cycle quiescence, similar to *cki-1*, *cdc-14* loss of function mutants show extra divisions in the intestinal, hypodermal and VPC lineages. Interestingly, CDC-14 is localised in the cytoplasm in quiescent cells but localised in the nucleus in post-mitotic cells like neurons, and likely functions to promote accumulation of CKI-1 in the nucleus and stabilisation against degradation (Saito et al., 2004). Postembryonically, the G1/S transition in the worm is chiefly governed by the action of *cdk-4*/*cyd-1*, which acts at least partially through *lin-35*/Rb and *fzr-1*, while quiescence is modulated by the Cip/Kip CKIs *cki-1* and *cki-2* (Figure 1.16)

Cell cycle components at G1/S entry are tightly linked with the asymmetric distribution of key developmental factors during development and could direct sexual dimorphism in cell fate as well as general cell division timing during larval development. For example, the somatic gonad precursor (SGP) cell division, which is central to axis formation and sex determination during gonadogenesis is mediated by *cyd-1*, likely through its canonical function in regulating *efl-1*. Asymmetry in the downstream effectors of Wnt signalling, POP-1/TCF and SYS-1/β-catenin, determines the proximal/distal axis of the developing gonad of both males and hermaphrodites (Siegfried et al., 2004). During several asymmetric cell division both in the embryo and the developing larva, the posterior daughter in the division detects a Wnt signal and export POP-1 from the nucleus resulting in the expression of Wnt responsive genes.

Upon SGP division the daughter with less nuclear POP-1 goes on to determine the distal end of the gonad while the daughter with more nuclear POP-1 establishes the proximal end. This asymmetry is modulated by *cyd-1*, in the *cyd-1(q626)* mutant, POP-1 asymmetry was sometimes abolished specifically in SGP daughter cells and appeared normal in other postembryonic lineages (Tilmann & Kimble, 2005). *cyd-1(q626)* mutants are sometimes missing one or both gonad arms due to the misspecification of distal cells early in gonadogenesis, intriguingly, *cyd-1(q626)* mutants also often resulted in a feminised gonad in males. Masculinisation of the gonad is determined in the SGP by the forkhead transcription factor *fkh-6*, which is initially expressed in SGPs in both sexes but is turned off in hermaphrodites. *fkh-6* null mutant males have similar feminised gonads and FKH-6 expression is abolished in *cyd-1(q626)* animals. The *fkh-6* promoter has putative E2F binding sites suggesting that G1/S machinery relieve *efl-1* repression to induce the male fate. Indeed, the defects in axis formation and sex-determination were suppressed by RNAi of, *lin-35*, *efl-1*, *dpl-1*, and *cki-1* and *cki-2* indicating that the canonical G1/S pathways act to determine cell fate in tandem with sex-determination (Tilmann & Kimble, 2005). Mechanisms such as these could provide a link between the sex determination pathway and sex-specific cell cycle entry.

The nervous system of C. elegans

The nervous system is by far the most complex system in the animal, the 300 hermaphrodite neuronal cells are organised in 118 morphologically distinct subclasses. Most neuronal cell bodies are clustered around the nerve ring; the central neuropil of the animal (Figure 1.21), consisting of approximately 100 axons that encircle the pharyngeal isthmus, and serve as the brain of the worm (Ward et al., 1975; JG White, 1986). The neuronal cells are supported by 56 glial cells. There are two main classes of glial cell, socket cells and sheath cells that together with ciliated sensory neurons form sensilla, the sensory organs of *C. elegans*. The amphid sensilla are the primary chemosensory organs of the animal and are located bilaterally in the head. The cell bodies of the 12 amphid sensory neurons are located posterior to the nerve ring, the dendrites run laterally to the nose (Figure 1.22). The Amphid Socket (AMso) are polarised cells with cell bodies anterior the 1st pharyngeal bulb, they extend a process

anteriorly to the nose where they form a pore in the tough cuticle of the animal, allowing certain amphid neuron endings to contact the outside environment. The Amphid Sheath (AMsh) are similarly polarised cells, with cell bodies located posterior to the nerve ring, projecting to the nose where they ensheath the dendrites of amphid neurons and are anchored by the socket to epithelium by adherens junctions (Doroquez et al., 2014). The glial cells are not required for neuronal survival and are not myelinating but are essential for development and maintaining the structure and function of neuronal receptive endings (Bacaj et al., 2008; G. Oikonomou & Shaham, 2011; Shaham, 2005). The socket and sheath glia cells derive from an epithelial lineage, however, the last class of glia consists of the 6 GLR cells that ensheath the inner circumference of the nerve ring are mesodermally derived.

This small but complex nervous system is ideal for the study of behaviour and development. It is simple enough to study in detail but also governs a diverse range of behaviours, such as, feeding, food searching and mating, allowing for the dissection of the neural circuits involved. Additionally, the connectivity of the entire nervous system has been mapped down to the level of the synapse, showing very stereotypical development (Hall & Russell, 1991; Jarrell et al., 2012; Sulston & Horvitz, 1977; Sulston & White, 1980; J White et al., 1976). The first complete wiring diagram of an animal's nervous system, including both sexes, has recently been published by the Emmons Lab (Cook et al., 2019).

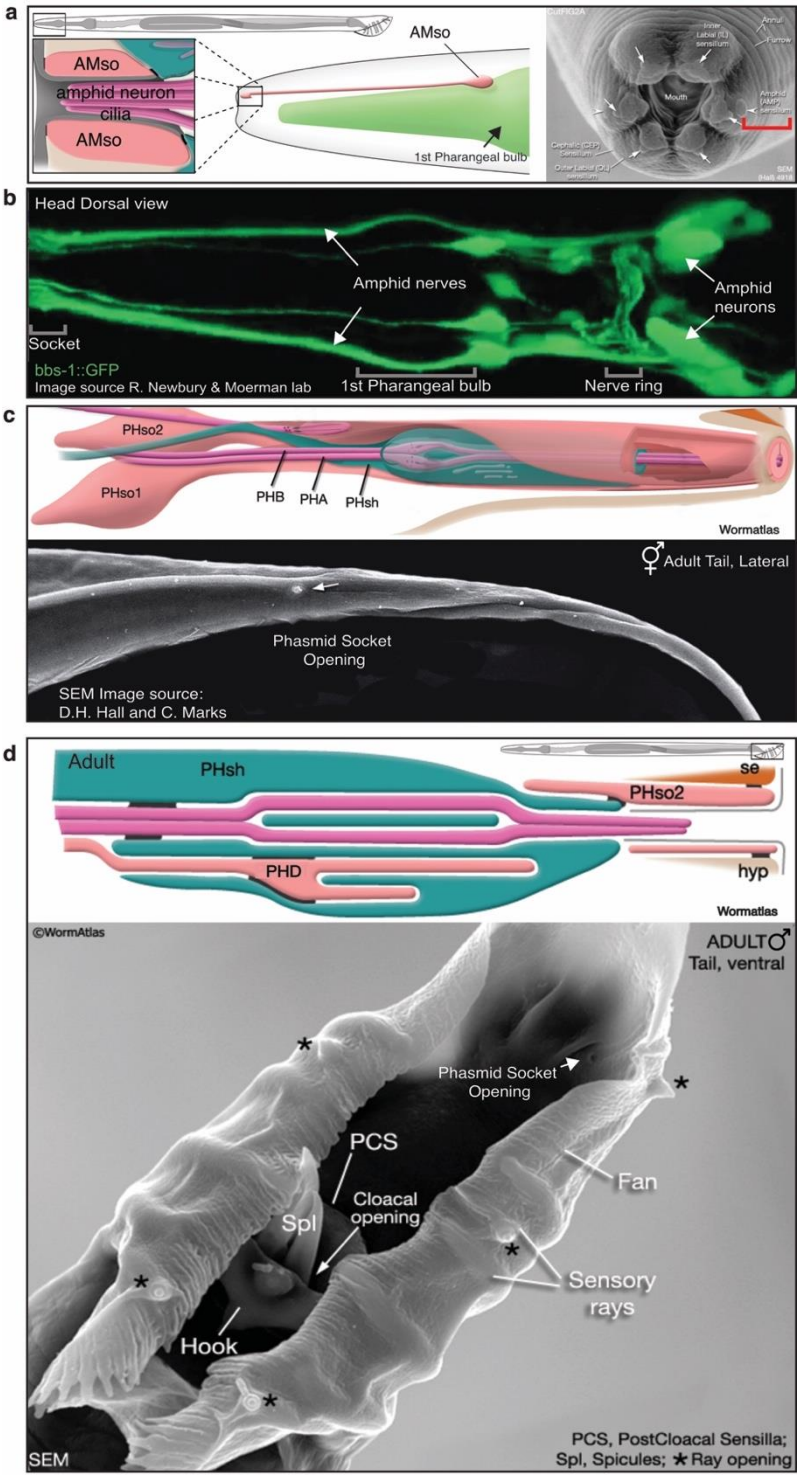

Figure 1.22 The structure of the amphid and phasmid sockets

a) Lateral schematic of head showing the amphid socket cell body with the pore opening boxed (left). Anterior view SEM of hermaphrodite head showing location of amphid sensilla. Modified from Wormatlas.org

(b) Confocal image in dorsal view of hermaphrodite head showing the ciliated neurons of the amphid with bbs-1::gfp

(c) Lateral schematic of the adult hermaphrodite phasmid sensillum showing; phasmid sockets 1 and 2, phasmid sheath and phasmid neurons A and B (top) and lateral SEM of the hermaphrodite tail showing the phasmid socket opening (bottom)

(d) Lateral schematic of the adult male phasmid sensory ending showing; the phasmid socket 2 opening, endings of phasmid neurons A, B and D in the phasmid sheath (top). Ventral SEM of the adult male tail showing fan shaped copulatory structures and sensory openings (bottom) Modified from Wormatlas

Sexual dimorphism in the nervous system

The *C. elegans* male is highly dimorphic from the hermaphrodite, in both morphology and behaviour, by far the major dimorphism between the sexes is that of the nervous system. The male has a total of 1031 somatic cell nuclei, most of the additional cells form part of the nervous system in the tail, until recently there were thought to be there are 90 glia and 383 neurons, 89 of which are male specific in total (Hodgkin, 1988; Sulston & White, 1980), however, work from the Barrios and Poole Lab, which I will present in Chapter 3 has shown that it is comprised of 387 neurons (93 of which are male-specific) and 88 glia. Outside of the gonad, almost all the sexual dimorphisms in the worm develop post-embryonically, for the first three larval stages male and hermaphrodites look and behave very similarly. During sexual maturation in the late L3-L4 stage the male tail goes through a dramatic remodelling when the fan and copulatory structures are formed (Figure 1.21). The cuticular fan extends over of 9 pairs of rays, male specific sensilla, each composed of two neurons and a structural cell that the performs the role of the socket. The rays originate from the posterior epithelial seam cells. The hindgut becomes highly differentiated, rectal epithelial cells act as blast cells, producing the hook, spicules, hook sensillum, and post cloacal sensillum, and allow the joining of the reproductive tract with the gut. Together with accompanying muscles these are all required for the intricate steps of mating (Chapter 3). The rays are chiefly responsible for the response to contact with hermaphrodites and turning, the spicules and hook sensilla for location of the hermaphrodite vulva, insertion and ejaculation (Garcia et al., 2001; Liu & Sternberg, 1995).

The nervous system is sexually dimorphic at various levels, for example, sex-shared neurons can function in neuronal circuits that are sexually dimorphic; depending on the sex neurotransmitter expression can differ in shared neurons (Serrano-Saiz, Pereira, et al., 2017), sex-specific sensory inputs can affect the function of sex-shared circuits and there can be differences in the strength of connections between the sexes (Cook et al., 2019; Sulston et al., 1980; Sulston & Horvitz, 1977; Weinberg et al., 2018). Sexual dimorphisms such as the development of sex-specific neurons can arise by various mechanisms (Figure 1.23), for example, the sex-specific cell death of

the HSN neurons in males and the death of the CEM neurons in hermaphrodites (Sulston et al., 1983), or there can be sex-specific neurogenesis, as is the case with the male sensory rays. These type of dimorphisms are governed by the *tra* pathway, For example, proapoptotic genes are directly repressed by TRA-1 in the HSNs of hermaphrodites while in males *tra-1* function is not enough to prevent cell death (Conradt & Horvitz, 1999). Sex-specific neurogenesis can be triggered by the sex-specific expression of transcription factors, in the ray precursor cells the bHLH transcription *lin-32* factor specific (Zhao & Emmons, 1995). Apart from generating and removing neurons the connectivity of the nervous system is also altered in a sex-specific way. The PHB phasmid neuron in L1 animals of either sex synapses with both the backward locomotion command interneuron AVA and the sex-shared interneuron AVG, however in adult hermaphrodites only the AVA synapses are preserved and in males, only the AVG. This sex-specific synaptic pruning is governed by the *tra-1* via the Doublesex/MAB-3 domain transcription factors, *dmd-5* and *dmd-11* (Oren-Suissa et al., 2016). Similarly, the postembryonically born PHC sensory neuron does not synapse with many cells in the hermaphrodite but in males is highly connected to many of the male specific cells born during sexual maturation (Jarrell et al., 2012). The Doublesex/MAB-3 domain transcription factor *dmd-3* is necessary and sufficient for the male specific connectivity as well as many other aspects of its differentiation, while the action of DMD-3 is cell autonomously repressed by TRA-1 in hermaphrodites (Serrano-Saiz, Oren-Suissa, et al., 2017).

The sexual dimorphisms in the shared nervous system can affect the behaviour of the animal. For example, the genetic sex of shared sensory cells can increase or decrease the quantity of chemoreceptors expressed, depending on the sex and thus sex-specifically alter the behaviour of shared circuits, For example, the reduction of a key chemoreceptor ODR-10 in males reduces attraction to food (Ryan et al., 2014). Most of the sexual dimorphisms in the male nervous system are part of neural circuits directly involved in mating and are not shared, however, some cells (sex-shared or male specific) allow males to exhibit more subtle decision-making behaviours not seen in the hermaphrodite. For example, if a hermaphrodite or larva of either sex, is allowed to roam on a patch of *E. coli* on an agar pad they will normally remain

upon the food patch indefinitely. If a single adult male is placed on a patch of food, however, they will explore the food but eventually leave and begin to explore the agar. This exploratory behaviour has been shown to be driven by mature male specific expression of DAF-7 a TGF-β ligand in the sex-shared sensory neuron ASJ (Hilbert & Kim, 2017). Interestingly, if there is a hermaphrodite present on the food the male will no longer leave. This is interpreted as competition between the reproductive nutritional drives. Specifically, it is periodic contact with hermaphrodites, detected through ray neurons and the male specific EF interneurons, that supresses the drive to leave (Barrios et al., 2008; Lipton et al., 2004).

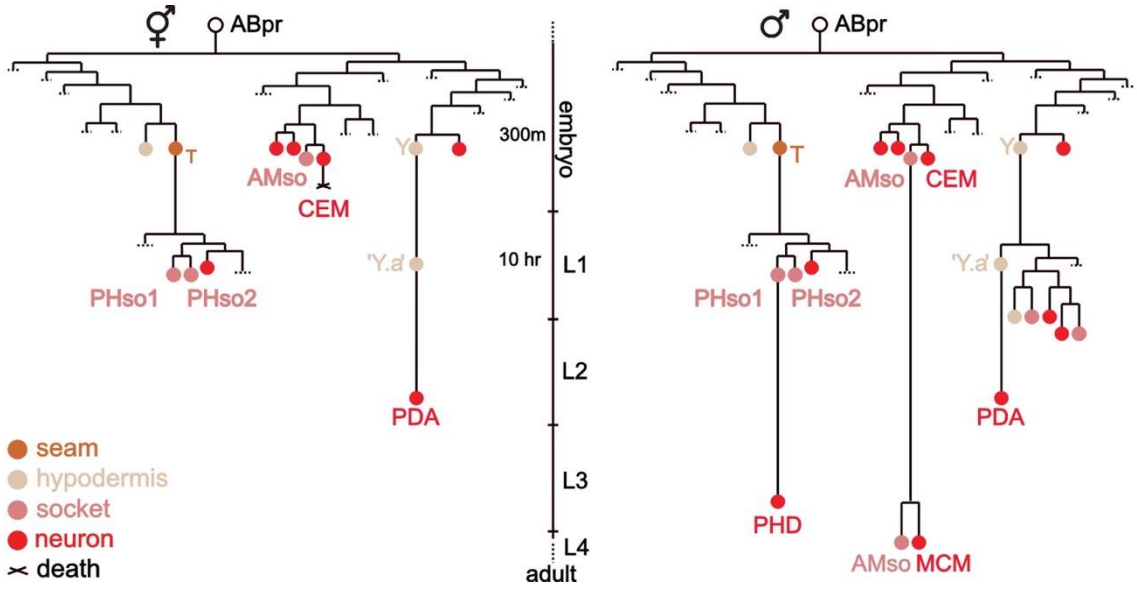

Figure 1.23 Selected sex dimorphic lineages in *C. elegans*

Lineage diagram showing part of a sexually dimorphic lineage in hermaphrodites and males, illustrating the various strategies by which neuronal sex-specificity is generated. The vertical length of each branch represents relative duration between cell cycles.

1.5.2 C. elegans as a model for cell fate specification and plasticity

Establishing cell fate with terminal selectors

The small but diverse nervous system of the *C.* elegans is ideal for the study cell fate specification and plasticity. The hermaphrodite has only 118 neuronal subtypes, making it possible to use unbiased methods of interrogation and interpret results in the light of the entire system. Most of the analysis and experimentation in development follows the conceptual framework suggested by the Waddington landscape model of development. As such, this approach seeks an understanding from the beginning of development, at the top of the landscape, down through the decisions of which valleys to take in order to end up at a particular state of differentiation at the bottom. *C. elegans* is particularly well suited to do the reverse, using a bottom-up approach in order to determine how the terminal features of specific neuron types and subtypes are genetically encoded. The fully defined cell lineage, well characterised function and features of individual neuronal cells and wealth of genetic tools are crucial for this sort of approach. For two straightforward examples we can look at the specification of the thermosensory type neurons AFD and the gustatory chemosensory neurons ASE. Genetic screens for defects in behaviours like thermotaxis are easily undertaken and quickly provided many genes that are required for normal thermotaxis , such as *ttx-1* (Hedgecock & Russell, 1975). Ultrastructural analysis of this mutant showed defects in the sensory ending of the amphid neuron AFD (Perkins et al., 1986). Laser ablation of AFD causes major defects in thermotaxis (Mori & Ohshima, 1995), *ttx-1* was found to be a homeobox transcription factor of the *Otx* family and *ttx-1* mutants have the same phenotype as AFD ablated animals (Satterlee et al., 2001). Interestingly, *ttx-1* is not required for the generation of the neuron but for the specification of its subtype identity, by regulating many of the terminal features of the AFD type neuron. Similarly, early screens for salt chemotaxis defective mutants yielded alleles for many genes, such as *che-1* (Lewis & Hodgkin, 1977). Later, laser ablation experiments showed that the pair of ASE neurons are chiefly responsible for salt chemotaxis (Bargmann & Horvitz, 1991) and that, the GLASS related Zn finger transcription factor *che-1*, is essential for the

specification of ASE neurons (Uchida et al., 2003). Analysis of the transcriptome of ASE neurons showed that genes expressed in these cells have a small regulatory motif which acts as a binding site for CHE-1. Furthermore, using GFP reporter constructs it was shown that this binding motif is both required and sufficient to drive expression in ASE (Etchberger et al., 2007). Importantly, without *che-1* the ASE neurons still express pan neuronal genes but lose the expression of their sub-type specific genes, appearing as nonspecific sensory neurons and do not adopt an alternative fate. These examples show that by examining the gene batteries that define the terminal identity of a neuron and interrogating the regulatory networks required for this specific expression, a bottom up approach can turn up unique insights. Following these and several other examples led to the proposal of the terminal selector concept of neural identity (Hobert, 2008, 2011). Hobert extrapolates on Garcia-Bellido's selector gene concept, where selector genes work transiently, in a specific phase of development, acting upon genes that realise and effect the developmental processes in the cell and surrounding tissue. Terminal selectors act on the final step of development by determining the differentiated state of a cell (Figure 1.24).

Hobert (2016) describes terminal selectors in this way;

"Terminal selectors control the terminally differentiated state of a neuron, i.e., they initiate and maintain the stable identity of nondividing differentiated cells"

A defining feature of terminal selectors is their ability not only to initiate the terminal identity of a cell but to continuously maintain it, usually via autoregulation. Not only do they maintain identity but there is good evidence that they also simultaneously repress alternative fates, suggesting coordination between the control of terminal differentiation and the restriction of cell fate plasticity (Patel & Hobert, 2017).

There is evidence for the requirement of early developmental factors that also specify cell identity in mammalian neurons, for example, Otx2 is required post-mitotically for neuron subtype identity in adult mouse ventral tegmental area (Di Salvio et al., 2010). Continuous expression of Otx2 is required for the function and survival of the retinal pigment epithelium (Béby et al., 2010; Housset et al., 2013). Similarly, the LIM homeodomain protein Lmx1b is

required for ventral midbrain dopamine neuron development, as well as for correct functioning throughout life (Laguna et al., 2015). The two examples discussed above showed that single selectors controlled the expression of the majority of the terminal fate makers of a cell, however some terminal selectors are required for only part of the terminal features (Pereira et al., 2015). With its small nervous system, the effort is well underway to completely describe the neuronal differentiation programs of every neuron in the worm. How widely this strategy of cell fate specification is adopted in the animal kingdom has yet to be investigated but knowledge gained in this model system will undoubtedly open up new avenues and approaches that can be applied to the study of cell fate specification, pluripotency and reprogramming.

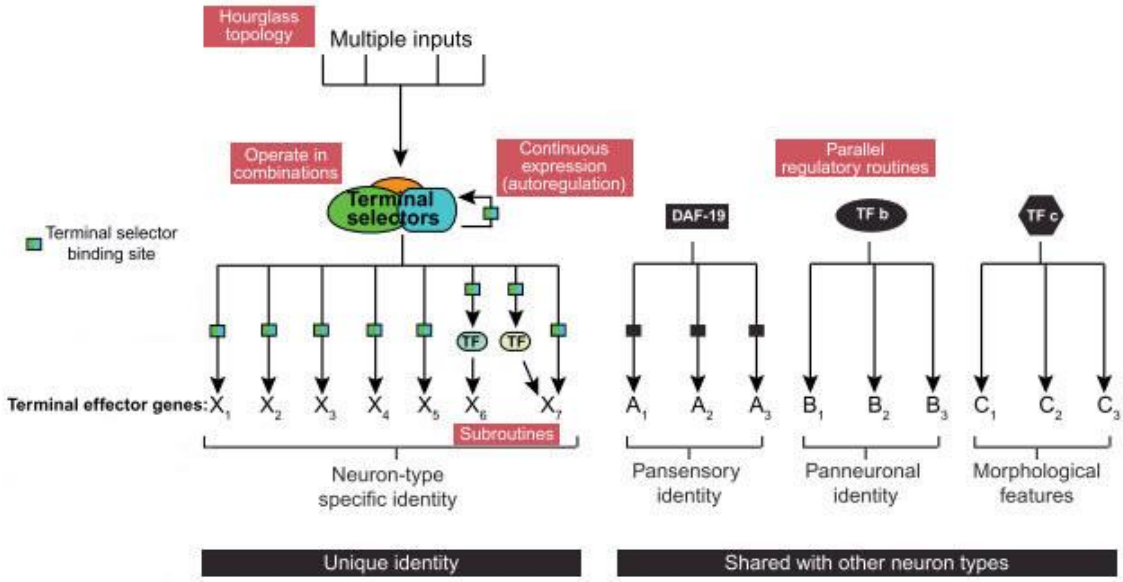

Figure 1.24 Terminal selector regulons

Red squares highlight key concepts. Sustained expression of terminal selectors is often, but not always ensured by autoregulation. Small rectangles illustrate binding sites for transcription factors and indicate direct regulation of effector genes by terminal selectors. Terminal selectors shown on the left control neuron-type specific identity features that assign a unique identity to a neuron. Parallel regulatory routines such as those that regulate pan-sensory features (via DAF-19) are controlled by factors that could also considered to be terminal selectors; but they do not assign unique identities. Morphology regulators control generic aspect of a neuron's morphology, such as placement of axons/dendrites into specific fascicles or polarity. TF, transcription factor. Adapted from (Hobert, 2016)

Maintaining cellular identity

As cell fate is progressively established in development, the capacity to adopt alternative fates are also lost (Gurdon, 1960a, 1960b). Epigenetic regulation via chromatin remodelling or histone modifying complexes are important factors in the establishment and maintenance of cell fate and again *C. elegans* can be uniquely useful for the study of epigenetic regulation and reprogramming. As cell fate is stabilised the general nuclear architecture appears to change with chromatin becoming more compact and reducing plasticity. In *C. elegans* intestinal development, EM studies show that there is very little electron dense heterochromatin at the early stages of embryonic development but the amount of transcriptionally silent electron dense regions increases as cell progressively differentiate (Leung et al., 1999). Since then similar findings of transcriptionally active euchromatin have been observed in human embryonic stem cells and mouse induce pluripotent stem cells (Park et al., 2004) (Efroni et al., 2008). The Polycomb repressive complex chiefly binds to and methylates histone H3 on lysine 27 to repress transcription and maintain cell fate (Schuettengruber et al., 2007), disabling Polycomb in worms using *mes-2* mutants prolongs the period of plasticity in development and keeps chromatin in an open position (Yuzyuk et al., 2009). Using tissue specific integrated transgenes, it was found that in differentiated cells, active genes shift toward the nuclear lumen while inactive genes become heterochromatic and bound to the nuclear envelope while in the early embryo they are localised randomly (Meister et al., 2010). The spatial dynamics of chromatin are key to proper maintenance of the differentiated state as well as for promoting pluripotency. The maintenance of a stable differentiated state is the defining characteristic of terminal selectors and indeed it has been found that terminal selectors can limit plasticity by inducing the formation of transcriptionally inactive chromatin in *C. elegans* neurons. Inducing the expression of the terminal selector for ASE neuron fate, *che-1*, in early embryonic development results in ASE neuron markers being expressed but this plasticity in cell fate is not possible in adults. However, removal of the terminal selectors of other neuron fates, such as *unc-3*, which induces a cholinergic fate, enables the fate of adult cells to be changed upon expression of *che-1*. Furthermore the removal

of the competing terminal selector *unc-3* along with *mes-2* greatly increased the amount of cells changing fate with *che-1* expression (Patel & Hobert, 2017). Therefore, this work suggests that along with the ability to activate genes specific to the unique identity of a cell, terminal selectors concomitantly restrict alternate cell fates.

Experimental cell fate reprogramming in C. elegans

C. elegans has also been used in order to find new natural barriers to cell fate plasticity, which maintain the identity of cells *in vivo*. By undertaking forced reprogramming, it is possibly to look for factors that aid and protect against cell fate alteration *in vivo*. As mentioned above, expressing terminal selectors constitutively in all tissues, for example, *che-1* the terminal selector of the ASE neurons, does not normally result in ectopic expression of terminal markers such as *gcy-5*, which marks ASER. However, by expressing terminal selectors constitutively and knocking down genes using RNAi it is possible to screen for barriers to reprogramming by looking for ectopic expression of the terminal selectors to identify the factors and mechanisms that safeguard cell fate. Using this method it is possible to directly convert mitotic germ cells into ASE type neurons by knocking down the histone chaperone *lin-53* (Tursun et al., 2011). *lin-53/RBBP* is a component of both histone acetyl and deacetyl transferase complexes, and as such can either act to activate or repress transcription of genes by adding or removing, respectively, acetyl groups to DNA bound histones, its role is mainly involved with the maintenance of cell fate. Many other chromatin factor genes were found in to work in a similar way to *lin-53* in a subsequent automated screen, such as *mrg-1* (Hajduskova et al., 2019). The human homologue of *mrg-1*, MRG15, is also a component of both histone acetyl and deacetyl transferase complexes, involved in neural precursor cell proliferation and neural fate choice (Chen, Takano-Maruyama, Pereira-Smith, Gaufo, & Tominaga, 2009). The germline cells converted by *che-1* in the *mrg-1* knockdown background lose germ cell specific characteristics such as *pie-1* expression and P-Granules as they gain ASE neuron fate. Interestingly, ChIP-seq of MRG-1 exclusive to the germline, where it acts to preserve cell fate, shows that it binds cell cycle and DNA processing genes (Hajduskova et al., 2019). In a separate screen, subunits of the chromatin regulator FACT

(facilitates chromatin transcription) were also identified (Kolundzic et al., 2018), FACT is conserved to humans and was found act in histone assembly and disassembly to facilitate transcription of chromatin bound DNA (Orphanides et al., 1998). The role of FACT in cell fate maintenance is also conserved in humans, as depletion of FACT subunits in human fibroblasts increases neuronal reprogramming efficiency by *Ascl1*, *Brn2* and *Myt1l* expression. Similarly, FACT depletion enhances reprogramming of fibroblasts into induced pluripotent stem cells but do not do so by enhancing the expression of the pluripotency factors themselves (Kolundzic et al., 2018). Such work highlights the importance of chromatin factors both in maintaining differentiation state by controlling access to actively transcribed genes but also in repressing alternative fates by acting as barriers. Furthermore, by exploiting this model organism's amenability to powerful, *in vivo*, unbiased and automated experimental approaches, it demonstrates that it is possible to swiftly transfer new findings to experimentation in human models offering the best of both worlds.

Natural epithelial to neuronal transdifferentiation in C. elegans

An example of the phenomenon of natural direct transdifferentiation has been extremely well characterised in the *C. elegans* hermaphrodite, the Y-PDA transition. In this case, the embryonically born rectal epithelial cell Y migrates anteriorly during the first larval stage, then without division or fusion with other cells, loses all epithelial characteristics, migrates and directly transdifferentiates into the cholinergic motor neuron PDA (Jarriault et al., 2008). The role of the rectal epithelium is taken over by the posterior-most ventral epithelial cell, P12.pa. ablation experiments showed that the rectal epithelial cells do not play a role in the transdifferentiation of Y (Jarriault et al., 2008). In the male, Y acts as a blast cell (Figure 1.23) that divides in the first larval stage to produce Y.a which goes on to become PDA, and Y.p which divides a number of times to give rise to the cells of the post-cloacal sensillum (Sulston et al., 1980). Before the transdifferentiation event in hermaphrodites, the Y cell expresses various epithelial markers and rectal cell markers but no neuronal markers, after the event the opposite is true, with no overlap between the two (Jarriault et al.,

2008; Richard et al., 2011). The transdifferentiation is observed to occur in a stepwise process between the L1 to the L3 stages; as Y begins to dissociate from the rectum, its epithelial identity is lost; then Y begins to migrate anteriorly, once in its final position the cell acquires a neuronal fate (Figure 1.25). Utilising genetic labels of the epithelial fate as well as its final neuronal fate, forward and reverse genetic screens were designed in order to discover the factors governing the process (Kagias et al., 2012; Zuryn et al., 2010).

The classes of mutants isolated from these screens suggested that there were various discrete successive steps involved in transdifferentiation process. There is some debate if alterations in cell fate, especially drastic alterations such as during direct reprogramming occur as a gradual process with a mixing of identities, until the new identity takes over, or if this occurs in a stepwise process with definite boundaries between steps. For example, the induced reprogramming of pancreatic exocrine cells into β-cells, that occurs without cell division, is thought not to go through a dedifferentiated state but directly switch from one state to another (Zhou et al., 2008). In other induced reprogramming events, markers of terminal fate are expressed but parts of the original program remain (Marro et al., 2011; Weintraub et al., 1989). Determining if experimental cell fate modifications recapitulate what happens a natural context will have important ramifications in the study of development and reprogramming. To determine if the Y-PDA transdifferentiation occurs gradually or in discrete steps, mutants that appeared to affect different parts of the process were interrogated. Several mutants that appeared to initiate the transdifferentiation but not acquire the correct PDA neuronal fate, were found to affect the DNA binding domain of the COE family transcription factor UNC-3, which is the terminal selector for cholinergic fate (Kratsios et al., 2012). In such *unc-3* mutants, Y cells were born at the appropriate time, lost epithelial features and migrated away from the rectal epithelium normally and did not appear to gain alternate fates (Richard et al., 2011). Interestingly, the general cell cycle inhibitor *cki-1* is highly expressed in Y through L1 but is permanently switched off as Y begins its migration and loses its epithelial marker expression, additionally, as might be expected for a terminal selector, in some *unc-3* mutants a pan neuronal marker was expressed during the migration, although there is never any overlap between neuronal and epithelial fluorescence reporters. The lack of overlap suggests that the

transdifferentiation occurs in a series of discrete steps. There is a long period of *cki-1* expression after the birth of Y in the embryo, which lasts until L2 when the epithelial markers also decline. The dynamic expression of this key cell cycle control gene suggests that the non-dividing hermaphrodite Y cells may exhibit an extended quiescent like state, exit from which could be associated with the transdifferentiation process. Expressing transcription factors that determine, endoderm, muscle, or a different neuronal subtype, during the time that wild type Y cells, or *unc-3* mutants did not express either neuronal or epithelial markers did not result in the adoption of these new fates, indicating that this intermediate does not adopt a pluripotent state (Richard et al., 2011). This resistance to reprogramming and restriction fate may suggest that its specific differentiation program (or part of one) may have already been determined. Also, it is important to bear in mind the sexually dimorphic context of this lineage, where in the male, Y acts as a blast cell that divides at the same time as the Y migration begins in hermaphrodites (Figure 1.23).

Using a reverse genetic approach focussed on chromatin remodelling and pluripotency related factors, the very first steps in initiating the transdifferentiation event itself were found to be dependent on the three members of the transcriptional repressor NODE (Nanog and Oct4-associated deacetylase) complex, the pluripotency related transcription factors *ceh-6/Oct*, *sem-4/Sall*, and *sox-2/Sox* and the chromatin remodelling factor *egl-27/Mta*. The combination of these transcription factors and chromatin remodelling factors act to alter higher order chromatin structure in order to specifically regulate pluripotency. Coimmunoprecipitation assays indicate that *ceh-6/Oct*, *sem-4/Sall*, *egl-27/Mta* associate together, suggesting that these four factors work together, or in combinations as a plasticity module that control the expression of the rectal epithelial cell marker *egl-5* (Kagias et al., 2012). A key difference between induced and natural reprogramming events, is that natural events are much more reproducible occurring up to 100% of the time (Zuryn et al., 2014), studies using this model show that chromatin modifications are also key to this robustness. In order find factors that ensure robustness, a screen for low penetrant Y-PDA mutants was designed, as this would help select for genes that normally ensure a 100% robust and efficient cell fate conversion every time (Zuryn et al., 2014). Several mutants from this screen were found to affect the

conserved H3K27me3/me2 demethylase, JMJD-3.1, that promotes the expression of pluripotency related transcription factors. These alleles lost their ability to demethylate H3K27me3. A reverse genetic RNAi screen identified the conserved H3K4 methylating subunit *set-2*, knockdown of which acted similarly to *jmjd-3.1* mutants, indicating that multiple histone H3 modifications are required for robust Y-PDA transdifferentiation. *set-1* mutants failed to downregulate epithelial markers in Y-PDA transdifferentiation mutants, or when successfully downregulating these markers they failed to turn on the correct PDA program, indicating failures in both 'dedifferentiation' and redifferentiation, while *jmjd-3.1* mutants show that it is only involved in the redifferentiation process. Together this suggest that these factors act in sequence throughout the transdifferentiation process. Fluorescent reporter analysis showed that both *set-2* and *jmjd-3.1* are present in the nucleus throughout the transdifferentiation, except *jmjd-3.1* levels become undetectable during the loss of epithelial fate. Suggesting, that the role of JMJD-3.1 in the redifferentiation process is governed by nuclear levels of the protein. Analysis of *set-2* and *jmjd-3.1* double mutants showed that they likely act in parallel pathways and act upon a common target to promote redifferentiation. Taken together this suggests that chromatin remodelling factors like *set-2* and *jmjd-3.1* act in parallel to ensure robust transdifferentiation while transcription factors like *unc-3* and the drive the process.

The ability to break down the transdifferentiation process in such a fine-grained manner is unprecedented and provides exceptional insights into the process. It is intriguing that conserved pluripotency factors instruct this cell fate switch, but the process nevertheless appears inflexible to experimental manipulations of cell fate. Future efforts in this direction hold great promise towards increasing the efficiency and safety of potential regenerative or cell replacement strategies. An understanding of the steps that occur during the transition from one cell type to another will be crucial to the translation and implementation of safe techniques, learning from natural examples will be invaluable in helping us to ask the right questions. Supressing the initial fate of a cell before or during a cell fate conversion occur may be a significant factor in maintaining a stable fate. The worm as a model has proven itself in the testing

of these and other important questions regarding cell fate determination and maintenance.

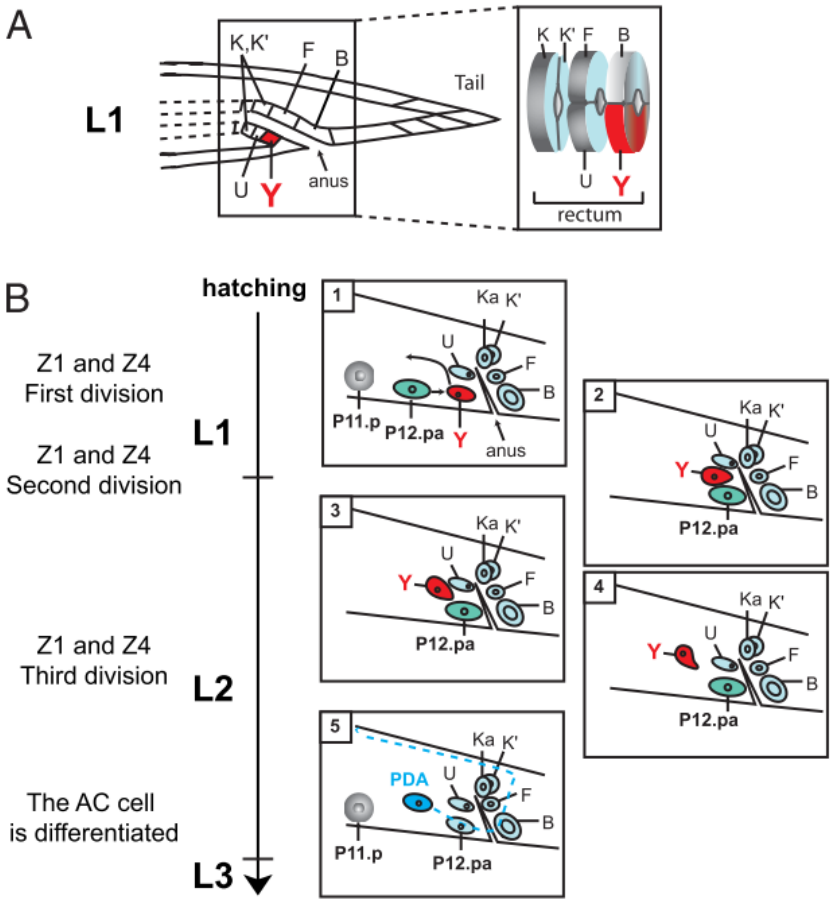

Figure 1.25 Natural transdifferentiation of Y-PDA in *C. elegans*

A) The rectum at the L1 stage is composed of three pairs of cells forming a tube.

B) Timing is matched to gonadal development.
(1) at the end of L1 Y retracts and is replaced by P12.pa.
(2) Y begins to lose epithelial properties.
(3) The cell continues to migrate anteriorly.
(4 and 5) The transdifferentiating cell reaches its final position and acquires neuronal characteristics.
Adapted from (Jarriault et al., 2008).

1.6 Summary

Development in general and in particular that of nervous system, requires impeccable coordination between progenitor cell proliferation, renewal or permanent withdrawal from the cell cycle and cellular differentiation. We are developing a deep practical understanding of the genetic, molecular and cellular events that drive neuronal development and how these are involved with fate plasticity. Unavoidably however, the drastic developmental changes that occur during embryogenesis and the complex microenvironments of stem cell niches required to keep the intricate balance between maintaining progenitor populations and the production of diverse differentiated cell types, can impede research. In this study I will present the discovery of two late in development cases of neurons being born from glia-like cells in the *C. elegans* male. Each case occurs through a related but distinct mechanism, one by asymmetric division and one by direct transdifferentiation. Surprisingly, both bear striking similarities to neuronal development in vertebrates, providing a unique opportunity to study a single snapshot of the events that trigger neuronal development. With minimal interference from the myriad variables in the developmental environment of more complex brains, this model may offer singular insight into the basic biological processes governing plasticity in cell fate coupled with neuronal differentiation. Additionally, the versatility of *C. elegans* as a model organism promises benefits outside developmental biology. Any findings could rapidly be applied in regenerative medicine and cell fate reprogramming strategies for the treatment of neurogenerative and neurodevelopmental disorders or drug screening for anticancer therapeutics.

1.7 Aims

The overall aim of this project is to gain a greater understanding of the cellular and molecular mechanisms of how neurons are produced from glia. In order to do so I seek to assist in continuing to establish the *C. elegans* a model for late-in-development neuronal cell fate plasticity. Specifically, I use of the male as a model and provide tools, strains and new methodology for the investigation of the regulatory strategies that confer neurogenic potential to differentiated glia.

In this work I will:

In Chapter 3 present two distinct cases of glia-derived neurons in the male *C. elegans*. This exciting finding is the first time glia-derived neurogenesis is observed outside of vertebrate systems and presents a unique opportunity for study. The first case occurs through the asymmetric division and self-renewal of the AMso to produce the MCM interneurons and the second through the direct transdifferentiation of the PHso1 into the sensory neuron PHD. As part of this work I helped to characterise the development of these two novel cases of glia-to-neuron cell fate switches. Full accounts of their connectivity, behavioural function and cellular development have been published by the Poole and Barrios labs in collaboration with the Emmons and Hall lab. A third manuscript based on the findings presented in the remaining chapters is currently in preparation.

In Chapter 4 I describe a forward genetic screen performed in order to isolate and mutants that affect sequential steps of AMso to MCM development.

Chapter 5 shows the mapping and cloning of two mutants that affect the earliest steps of MCM development and show that both mutants are novel alleles of the key G1/S cell cycle regulator CDK-4.

Finally, Chapter 6 provides new insights into potential mechanisms that occur in both the proliferative and cell fate switches, by carrying out a developmental analysis of key cell fate determinants and cell cycle components, with interesting implications for the study of glia derived neurogenesis.

Chapter 2

Materials and Methods

2.1 General worm methods

2.1.1 Maintenance

Worms were maintained under standard conditions (Brenner, 1974) on 6cm NGM plates seeded with *E. coli*. Experiments were conducted at 20°C unless otherwise stated. Except for mapping purposes strains are in the N2 background, males are induced using *him-8(e1489)* IV or *him-5(e1490)* V.

2.1.2 Synchronisation and cleaning

Strains are kept clean from bacterial contamination by periodically treating a small number of gravid hermaphrodites with a drop of sodium hypochlorite solution in a fresh plate. The progeny are allowed to develop and this step repeated until there is no longer any contamination. For synchronisation and cleaning of large numbers of animals, strains can be egg prepped. Several plates are washed off with M9 buffer solution buffer, collected in 15ml Falcon tubes and spun down at low speed on a centrifuge. Animals may be cleaned again with a second M9 wash at this stage. Eggs are isolated by treating with a high pH sodium hypochlorite solution, and agitation for about 10 minutes or until adults and larvae are fully dissociated. The eggs are then washed in M9 three times and plated.

For experiments that benefit from highly synchronised animals, such as for time-lapse imaging of single animals, a timed egg lay was performed. Animals are cleaned as above, and 20-30 gravid adults transferred to a fresh plate and allowed to lay eggs over 1 or 2 hours. The adults are then removed thus ensuring that all animals on the plate are as close to each other in development as possible. A timed egg was preferred to L1 synchronisation as a

means of synchronisation so as to reduce the potential of stress caused by starvation interfering with normal development.

2.1.3 Storage

Strains were frozen for long term storage at -80°C using equal amounts of M9 and Freezing solution (M9 Buffer with 30% glycerine).

2.1.4 Recipes

KPO_4 Buffer (100ml)	
1M KH_2PO_4	76ml
1M K_2HPO_4	24ml

M9 Buffer (1L)	
KH_2PO_4	3g
Na_2HPO_4	6g
NaCl	5g
1 M $MgSO_4$	1ml
H_2O	to 1L

Egg Prep Solution (10ml)	
Bleach (Mexcel)	2ml
10M NaOH (Sigma-Aldrich)	0.5ml
mQ H_2O	7.5ml

Nematode Growth Media (1 L)	
NaCl (Sigma-Aldrich)	3g
Agar (Sigma-Aldrich)	17g
Bactopeptone (BD Biosciences)	2.5g
mQ H_2O	975ml
Autoclave	
1M KPO_4 (Fluka-Honeywell)	25ml
1M $CaCl_2$ (Sigma-Aldrich)	1ml
Cholesterol (5mg/ml in EtOH) (Sigma-Aldrich)	1ml
Nystatin (10mg/ml in H_2O) (Sigma-Aldrich)	2.5ml

2.2 Microscopy and imaging

2.2.1 Microscopy

Nikon SMZ2745 dissecting microscopes were used for general *C. elegans* work and maintenance. For scoring and imaging at high magnification Zeiss Axio Imager M2 compound microscopes with a Cool LED pE-2, LED epi-fluorescent illumination system were used. Images were acquired using a mounted pco.sensicam sCMOS camera. All images are shown at 100X magnification unless otherwise stated. Animals are generally mounted on a microscope slide for imaging in a 5µL droplet of 50mM sodium azide on a pad of 5% agarose. Confocal volumes were taken using a Leica SP8vis high resolution single photon microscope, with 22m field of view scanner, Leica HyD™ (Hybrid photodetector), and 60X objective lens. The LAS AF 3 (Leica Application Suite Advanced Fluorescence) was used to acquire volumes.

2.2.2 Image processing

Images were analysed using ImageJ (Schneider et al., 2012) using the FIJI plugin package. Fluorescent images are analysed using the Image5D plugin, this allows the entire depth of the worm to be imaged creating Z-stacks of approx. 1µm slices. Fluorescence channels can then be superimposed, most images presented here are flattened projections of several slices in order to clearly show the morphology of whole or pairs of cells.

3D models were created from confocal volumes using the Fluorender interactive rendering tool (Yong Wan et al., 2009).

Molecular graphic diagrams were prepared using PyMOL v2.2.2 (The PyMOL Molecular Graphics System, Version 2.0 Schrödinger, LLC.).

Figures were assembled in the Affinity graphics editor, Serif (Europe) Ltd.

2.3 EMS Mutagenesis and screening

The screen was performed with BAR82 *[ida-1::gfp];him-8(e1489)* P0 animals. First, in order to clean and synchronise the animals, they were egg prepped by treating gravid adults with sodium hypochlorite to dissociate adults and larvae and ensure only the eggs survive, the eggs are then washed in M9 three times and plated. The P0s as eggs are left to develop until the late L4/early adult stage and mutagenized by exposure to 50mM ethyl methane sulfate (EMS) for 4-5 hours. The P0s were washed, left to recover and become gravid overnight then egg prepped. This step is to reduce bacterial contamination and synchronise the F1s which are plated as eggs and left at 25°C, the extra care taken in cleaning the animals helps minimise the accelerated bacterial growth at this temperature. Next, approximately 200 hermaphrodite F2s were either singled to a plate (the first four rounds were clonal) or picked two per plate (the subsequent rounds were semi-clonal) and left at to generate progeny at 25°C. The male F3 progeny were screened animals for the absence of *inIs179[ida-1::gfp]* expressing MCMs on a fluorescence dissecting microscope (Figure 4.3). The screen was performed at 25°C in order to be able to identify temperature sensitive mutants which conditionally present a *nom* phenotype at 25°C but do not at lower temperatures. From plates with the desired phenotype, approximately 50 animals were singled and scored in order to ensure that the mutation bred true, and this step repeated. Once it was ensured that the mutation was homozygous, males were scored under a compound microscope, frozen and stored at -80°C. The penetrance of the *nom* phenotype in each mutant line was scored, by the lack of expression of *inIs179[ida-1::gfp]* in one or both cells in the region of interest, at both 20°C and 25°C.

2.4 Temperature shift experiments

Plates of animals were incubated for at least two generations at either the permissive temperature 20°C or non-permissive temperature 26°C. Animals incubated at 20°C were synchronised and upshifted to the non-permissive temperature at various points throughout their lifecycle, as eggs, shortly after hatching at L1, at 22hrs, 24hrs and 26hrs post hatching during L3, and in early and late L4. 50-100 animals were scored for the *nom* phenotype at each stage. Conversely, animals incubated at the non-permissive temperature were downshifted to the permissive temperature at the same developmental timepoints and scored. The critical period for the development of the MCMs was determined to be within the time when the *nom* phenotype is first observed in downshifted animals and no longer observed in upshifted animals.

2.5 Integration of fluorescent markers

Integration of extrachromosomal arrays into the genome was carried out by gamma irradiation. Animals were staged to mid L4 and subjected to 4000 rads of γ radiation. 200 array-carrying hermaphrodites were picked, 5 to a plate. After the food was consumed a chunk was taken and placed onto a fresh plate and this step repeated at least 3 times. In this way array carrying animals are outcompeted by animals with the marker integrated into the genome. Next 20 fluorescent animals were singled from each plate and their progeny scored for 100% fluorescent animals over two generations. The new strain was then backcrossed a few times into a *him* strain and scored for Mendelian segregation. Two transgenes *drpIs1* and *drpIs2* expressing GFP under the promoter for *grl-2*, which is expressed only in the AMso, PHso and excretory cell, were created in this way.

2.6 Mapping

Method for mapping male specific phenotypes. N2 males from the starting strain, in which the male specific phenotype can be seen, were crossed into hermaphrodites of the mapping strain, CB4856 HA. Several crosses were set up in order to ensure enough progeny were produced, crosses were set overnight and the P0 males removed the next day.

Male and hermaphrodite F1 cross-progeny were then in-crossed. Approximately 10 in-crosses should be set with a ratio of 5 males per hermaphrodite, crosses set overnight and the F1 males removed the next day. At the appropriate developmental stage 300-500 F2 recombinant, males in which the male specific phenotype was identifiable were picked. F2 recombinant males were allowed to crawl on an unseeded NGM plate in order to reduce the amount of bacteria they carry, then using a mouth pipette, aspirated and placed in 1mL of M9 buffer in an 1.5mL Eppendorf tube. The animals agitated gently, spun down at low speed and washed with more M9. The washed F2 recombinant males were then left gently agitating in M9 for 6-8hrs in order to minimise bacterial contamination. When thoroughly washed the animals were spun down and half the M9 removed, the animals were then transferred to a fresh 1.5mL Eppendorf tube, washed and spun down a final time. As much of the M9 buffer as possible was removed by aspiration and the animals stored at -80°C. When enough F2 recombinants were collected, they were pooled and their genomic DNA purified with the Gentra puregene kit, using the protocol for the purification of genomic DNA from 5-10mg fresh or frozen tissue. The purity and concentration of the purified DNA was checked by spectrophotometry.

The genomic library preparation and sequencing was performed by the UCL Genomics team at the UCL Great Ormond Street Institute of Child Health. The bioinformatic processing was performed using CloudMap (Minevich et al., 2012).

2.7 Genotyping by PCR and sequencing

To confirm the genotype of *nom-5/8* mutants DNA was isolated by washing off a plate of worms with 750ml of ddH20 into PCR Eppendorf tubes. Then spun at high speed for 1 min and the supernatant removed. 200ul lysis buffer (50mM HCL, 10mM Tris-HCL pH 8.2, 2.5mM MgCl2, 0.45% Triton, 0.45% Tween20, and 0.6ul of 20mg/ml fresh Protease K) were added to the sample. Samples were then freeze cracked at -80°C for 15-20min. After freezing, samples were placed into PCR machines set to 2-5hrs at 65°C then 30min at 95°C to denature the Protease K.

Approx. 589μl lysate (10ng of DNA) was then added to PCR mix consisting of: 189μl of 10μM primers appropriate for generating the selected fragment, 589μl HiFi Bio buffer, 0.3 589μl PCRBIO HiFi Polymerase, topped up with ddH_2O to desired reaction volume. PCR is carried out using an optimised PCR program, for the *cdk-4*(*drp5/8)* MS9-MS10 primers as follows:

Step	Temperature (°C)	Duration (min)	Cycles
Heated lid	112		
Initial Denaturation	95	1	1
Denaturation	95	1	30
Annealing	52.3	0.5	
Extension	72	0.5	
Final Extension	72	10	1
Hold	10	∞	1

For genotyping by digest the amplified DNA product is purified with the Gentra puregene kit, using the protocol for the purification of genomic DNA from 5-10mg fresh or frozen tissue.

2.8 Primers list

Gene/allele	Name	Sequence
him-8(e1489)	MS1 Forward primer	AATATTCAATGTCATTTCCCGG
	MS2 Reverse primer	GTGATAACGCATTTGACGG
cdk-4(drp5/drp8)	MS9 Forward primer	TGTCTGTCAACTGCTCAGCC
	MS10 Reverse primer	CAAGCAAAACATGTCACTGCAC
him-5(e1490)	MS13 Forward primer	AGGTGCACGTTTCAAGAGTC
	MS14 Reverse primer	TGCGTCTATCAGCTTCGTCA

Primers designed using ApE- A plasmid editor.

2.9 Strain list

	Strains used in this study
BAR4	*otIs356[rab-3p::2xNLS::TagRFP] V;him-5(e1490) V*
BAR37	*nsIs198[mir-228pro::GFP + lin-15(+)];otIs356(rab-3::RFP) V; him-5(e1490) V*
BAR77	*oleEx24[grl-2(1kb)::fem-3::SL2::mCherry (8 ng)+ elt-2p::GFP (40 ng)];inIs179[ida-1p::GFP] II;him-8(e1489) IV*
BAR82	*inIs179[ida-1:gfp] II;him-8(e1489):las-3(ole1) IV*
BS1175	*cdk-4(gv3);ozEx76[cdk-4p::CDK-4:GFP + sur-5:dsred]*
BL5717	*inIs179[ida-1:gfp] II;him-8(e1489) IV*
CB4088	*him-5(e1490) V*
CB1489	*him-8(e1489) IV*
JH1288	*cdk-7(ax224) I*
KM48	*+/szT1 [lon-2(e678)] I; cdk-4(gv3)/szT1 X*
NG4080	*gmIs20 [hlh-14::hlh-14::GFP] II*
OH10690	*otIs356[rab-3:2xNLS:tagRFP] V;him-8(e1489)*

PT2248	*pdf-1(tm1996);him-5(e1490)*
SV1067	*heSi45[mcm-4::mCherry + unc-119(+)] IV*
SV1669	*heSi193[mcm-4p::CDK sensor::eGFP::tbb-2 3'UTR + Cbr-unc119(+)] II*
VT825	*dpy-20(e1282) IV; maIs113[cki-1::GFP + dpy-20(+)]*
	Strains from this study
CHL36	*inIs179[ida-1:gfp] II;drpIs3[lin-48::tdTomato];him-8(e1489) IV*
CHL64	*inIs179[ida-1:gfp] II;drpIs3[lin-48::tdTomato];him-5(e1490) V*
CHL100	*nom-1(drp1);inIs179[ida-1:gfp] II;him-8(e1489) IV*
CHL101	*nom-1(drp1);inIs179[ida-1:gfp] II;otIs356[rab-3p::2xNLS::TagRFP] V; him-8(e1489) IV*
CHL102	*nom-1(drp1);inIs179[ida-1:gfp] II;drpIs3[lin-48::tdTomato]; him-8(e1489) IV*
CHL103	*nom-2(drp2);inIs179[ida-1:gfp] II;him-8(e1489) IV*
CHL104	*nom-2(drp2);inIs179[ida-1:gfp] II;otIs356[rab-3p::2xNLS::TagRFP] V; him-8(e1489) IV*
CHL105	*nom-2(drp2);inIs179[ida-1:gfp] II;drpIs3[lin-48::tdTomato]; him-8(e1489) IV*
CHL106	*nom-3(drp3);inIs179[ida-1:gfp] II;him-8(e1489) IV*
CHL107	*nom-3(drp3);inIs179[ida-1:gfp] II;otIs356[rab-3p::2xNLS::TagRFP] V; him-8(e1489) IV*
CHL108	*nom-4(drp4);inIs179[ida-1:gfp] II;him-8(e1489) IV*
CHL109	*nom-4(drp4);inIs179[ida-1:gfp] II;otIs356[rab-3p::2xNLS::TagRFP] V; him-8(e1489) IV*
CHL110	*cdk-4(drp5) X;inIs179[ida-1:gfp] II;him-8(e1489) IV*
CHL111	*cdk-4(drp5) X;inIs179[ida-1:gfp] II;otIs356[rab-3p::2xNLS::TagRFP] V; him-8(e1489) IV*
CHL112	*cdk-4(drp5) X;inIs179[ida-1:gfp] II;drpIs3[lin-48::tdTomato];*

	him-8(e1489) IV
CHL113	*cdk-4(drp5) X;inIs179[ida-1:gfp] II;him-8(e1489) IV; oleEx24[grl-2prom::fem-3::SL2mCherry (8ng/µl)+elt-2::GFP (40ng/µl)]*
CHL114	*cdk-4(drp5) X;inIs179[ida-1:gfp] II;him-8(e1489) IV;OzEx76(cdk-4 (+))*
CHL115	*nom-6(drp6);inIs179[ida-1:gfp] II;him-8(e1489) IV*
CHL116	*nom-6(drp6);inIs179[ida-1:gfp] II;otIs356[rab-3:2xNLS:tagRF])V; him-8(e1489) IV*
CHL117	*nom-6(drp6);inIs179[ida-1:gfp] II;drpIs3[lin-48::tdTomato]; him-8(e1489) IV*
CHL118	*nom-7(drp7);inIs179[ida-1:gfp] II;him-8(e1489) IV*
CHL119	*nom-7(drp7);inIs179[ida-1:gfp] II;otIs356[rab-3p::2xNLS::TagRFP] V; him-8(e1489) IV*
CHL120	*nom-7(drp7);inIs179[ida-1:gfp] II;drpIs3[lin-48::tdTomato]; him-8(e1489) IV*
CHL121	*cdk-4(drp8) X;inIs179[ida-1:gfp] II;him-8(e1489)IV*
CHL122	*cdk-4(drp8) X;inIs179[ida-1:gfp] II;otIs356[rab-3p::2xNLS::TagRFP] V; him-8(e1489) IV*
CHL123	*cdk-4(drp8) X;inIs179[ida-1:gfp] II;drpIs3[lin-48::tdTomato]; him-8(e1489) IV*
CHL124	*cdk-4(drp8) X;inIs179[ida-1:gfp] II;him-8(e1489) IV;OzEx76(cdk-4 +)*
CHL125	*nom-9(drp9);inIs179[ida-1:gfp] II;him-8(e1489) IV*
CHL126	*nom-9(drp9);inIs179[ida-1:gfp] II;otIs356[rab-3p::2xNLS::TagRFP] V; him-8(e1489) IV*
CHL127	*nom-9(drp9);inIs179[ida-1:gfp] II;drpIs3[lin-48::tdTomato]; him-8(e1489) IV*
CHL128	*drpIs1[grl-2::gfp];pie-1:histone::rfp;him-8(e1489) IV*
CHL129	*CDKsensor:hesi193;drpIs3[lin-48::tdTomato];him-8(e1489) IV*
CHL130	*gmIs20[hlh-14prom::hlh-14::gfp rol-6(+)] II;drpIs3[lin-48::tdTomato]*

CHL131	*unc-119;drpIs3[lin-48::tdTomato]*
CHL132	*unc-119;inIs179[ida-1:gfp] II*
CHL133	*unc-119;inIs179[ida-1:gfp] II;drpIs3[lin-48::tdTomato];him-8(e1489) IV*
CHL134	*unc-119;inIs179[ida-1:gfp] II;drpIs3[lin-48::tdTomato]*
CHL135	*gmIs20[hlh-14prom::hlh-14::gfp rol-6(+)] II;drpIs3[lin-48::tdTomato]*
CHL130	*drpIs1[grl-2::gfp, dpy-5(+)] X;dpy-5(e907)*
CHL32	*drpIs1[grl-2::gfp, dpy-5(+)];otIs356[rab-3p::2xNLS::TagRFP] V; dpy-5(e907)*
CHL137	*drpIs2[grl-2::gfp, dpy-5(+)]:dpy-5(e907)*
CHL140	*drpIs3[lin-48::tdTomato]*
CHL141	*drpIs4[lin-48::tdTomato]*
CHL142	*maIs113[cki-1:gfp+dpy20(+)];drpIs3[lin-48::tdTomato]*
CHL143	*pie-1:histone:rfp;drpIs1[grl-2::gfp] X;him-8(e1489) IV*
CHL144	*drpIs3[lin-48::tdTomato];heSi193[mcm-4p:CDKsensor:GFP;tbb-2] II; him-8(e1489) IV*
CHL145	*drpIs3[lin-48::tdTomato]; heSi193 [mcm-4p:CDKsensor:GFP;tbb-2] II*
CHL146	*cdk-1(n3046)/qC1[dpy-19:glp-1] III;inIs179[ida-1:gfp] II; drpIs3[lin-48::tdTomato];him-8(e1489) IV*
CHL147	*cdk-7(ax224) I:inIs179[ida-1:gfp] II;drpIs3[lin-48::tdTomato]; him-8(e1489) IV*
CHL148	*maIs103[rnr-1prom::gfp+unc-36 (+)] X;inIs179[ida-1:gfp] II; drpIs3[lin-48::tdTomato];him-8(e1489) IV*
CHL149	*cdk-7(ax224) I;nsIs198[mir-228::gfp + lin-15(+)];him-8(e1489) IV; otIs356[rab-3p::2xNLS::TagRFP] V*

Chapter 3

Two cases of sex-specific glia-derived neurons in *C. elegans*

3.1 Overview

Research in *C. elegans* has mainly focussed on the hermaphrodite sex, mainly due to the many inherent advantages the worm offers as model organism in the first place. More recently however, the male sex has garnered the interest of increasing numbers of researchers. The male possesses more complex postembryonic development and behaviour, with the vast knowledgebase and tools developed from the study of the hermaphrodite as a solid foundation, makes it an appealing target for research in these areas. We have discovered two cases where glial cell types that are stably differentiated and at the end of their lineage in the hermaphrodite give rise to neurons in the male. My MSc and now PhD work focussed primarily on the developmental characterisation of both of these glia-to-neuron cell fate switches and has contributed to the preparation of two manuscripts which describe the development, connectivity and function and of these novel neurons. The first regarding the MCMs has been published in October 2015 the second regarding the PHDs has recently been published in eLife.

3.2 Results

Here I summarise briefly the main findings relevant to this thesis from the two pieces of published work (Sammut et al 2015: Annexe I and Molina et al 2020: Annexe II). In the first paper, I help identify a novel pair of male specific neurons never previously observed, despite the extensive characterisation of *C. elegans* neuroanatomy (Figure 1: Sammut et al., 2015). The reason for this is likely due to their birth late in development and the description of males being focussed on the areas differing most from the hermaphrodite, the male tail, the nerve ring and sensillar endings at the nose. I go on to show this novel pair of cells derive from a male-specific division of a fully differentiated pair of glial cells that form part of the amphid sensory organ in both sexes (Figures 5 and 6: Sammut et al., 2015). I found that in males, during sexual maturation (at the L4 stage), the AMso glial cells (Figure 1.22) divide asymmetrically to self-renew and give rise to the mystery cells of the male (MCM) neurons (summarised here in Fig 3.1). In hermaphrodites, the AMso remains stably differentiated and does not divide. We find that during the division the AMso retains its polarised morphology and connection to the cuticle (Extended Data Figure 3: Sammut et al., 2015). Following the division, the anterior daughter retains this morphology and continues to express glial markers, while the posterior daughter downregulates glial markers, upregulates neuronal markers and sends a posterior projection to the nerve ring (Extended Data Figure 5: Sammut et al., 2015). I found that this glia-to-neuron cell fate switch is cell autonomously regulated by the sex determination pathway (Extended Data Figure 4: Sammut et al., 2015). Together with the Barrios lab at UCL and our collaborators in New York we went on to show the MCM neurons incorporate into male neural circuits that regulate reproductive behaviours and are required for a male-specific associative learning event (Sammut et al., 2015: Annexe I).

More recently the Barrios and Poole labs discovered a second glia-to-neuron cell fate switch, which I have also helped to characterise (Molina et al 2020: Annexe II; my contribution to this work was in the general planning and carrying out of developmental analyses as well as providing strains. Specifically, I helped carry out the initial cellular developmental and genetic expression analyses of the PHD neurons and detailed the timing and nature of the PHso1-to-PHD transition. I performed the single animal live imaging

experiments, following PHD development from PHso1 both directly and by division. Additionally, I designed the nucleoside incorporation experiments with Carla Lloret-Fernández who carried them out). The PHso1 cells in males had been observed to possess the basal bodies of cilia, these structures are specific to ciliated neurons in *C. elegans*, but as no other neuronal properties were then noted the PHso1 were classified as glia (Sulston & White, 1980). We have found that the PHso1 cells undergo a direct (no cell division) glia-to-neuron transdifferentiation specifically in males to generate a cholinergic, ciliated sensory neuron pair termed PHD (Figures 2 and 3: Molina et al., 2020). As with the posterior daughter of the AMso division, PHso1 downregulates a battery of glial markers and upregulates a battery of neuronal markers during the transdifferentiation, concomitantly losing their glial morphology and acquiring a neuronal morphology (Figures 2 and 3: Molina et al., 2020; summarised here in Figure 3.1). Surprisingly, we find that on some occasions PHso1 divides before transdifferentiating (in a background-dependent manner) raising intriguing questions about how the cell cycle is regulated in PHso1 and whether aspects of the cell cycle are somehow involved in the transdifferentiation process (Figure 3 and Figure 3 supplements 2 and 3: Molina et al., 2020). We then examined a number of factors that have been shown to be involved in direct transdifferentiation of Y-to-PDA (see Chapter 1.5.2) and find they are largely dispensable for both PHso1-to-PHD and AMso-to-MCM transdifferentiation, suggesting distinct molecular events regulate different transdifferentiation events in the worm (Figure 5 and Figure 5 supplements 1 and 2). Again, in collaboration with the Barrios lab and our collaborators in New York we went on to show the PHD neurons are incorporated into male-specific neuronal circuits that regulate sensory-motor coordination during the intricate steps of male mating (Molina et al., 2020).

3.3 Summary

Overall the work summarised above has revealed that glia can act as neuronal progenitors across the animal kingdom. In many ways these two glia-to-neuron transdifferentiation events resemble certain aspects of vertebrate neurogenesis, in particular adult neurogenesis, during which quiescent radial glia become re-activated and act as neural progenitors (Figure 3.1). This provides us with two paradigms in which we can now interrogate the molecular and cellular mechanisms that regulate these distinct transdifferentiation events in a genetically tractable organism and with single-cell resolution. In the following chapters I will present my work in this regard, where I begin by performing a forward genetic screen in order to identify genetic regulators of the AMso-to-MCM cell fate switch.

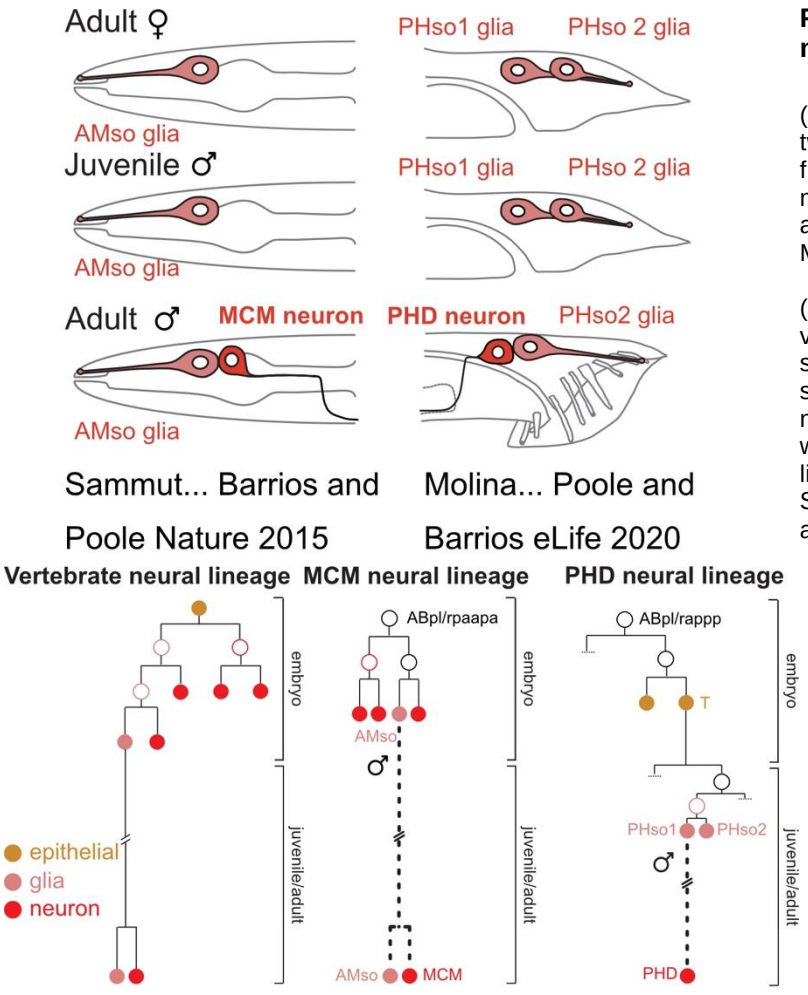

Figure 3.1 Glia derived neurons in *C. elegans*

(Top) A schematic showing the two sets of neurons generated from glia in the *C. elegans* male, described in Sammut et al., 2015 and Molina et al., 2020.

(Bottom) A representative vertebrate neural lineage showing differentiated glia, such as, radial glia can retain neurogenic potential, compared with the MCM and PHD lineages in *C. elegans.* Showing male specific lineages as dashed lines.

Chapter 4

The Molecular regulation of MCM development

4.1 Overview

The development of the MCM interneurons from the AMso glial cells present an unprecedented opportunity for the study of glia-derived transdifferentiation. These cells allow us to exploit the advantages of an invertebrate model organism in order to discover the genetic and cellular mechanisms that govern glia derived neuronal development. Experiments can be done relatively quickly and more exhaustively than using vertebrate models and may lead to novel discoveries or alternative interpretations of known neuronal differentiation events. With the discovery that glia act as neuronal progenitors in such distant taxonomic groups, there is also an opportunity to discover if the genetic events driving these processes are also conserved. If they are broadly conserved then this would indicate shared regulatory pathways may have existed before the protostome and deuterostome branches diverged, making them evolutionarily ancient indeed. Furthermore, if the genetic and cellular events are closely shared between worms and vertebrates, the worm and other invertebrates may provide a quick and cheap means of dissecting genetic pathways involved in vertebrate-like neuronal differentiation and testing potential therapies. On the other hand, if the vertebrate and invertebrate glia to neuron events are independent much can be learned from an alternative method of solving similar developmental problems perhaps providing novel theoretical perspectives.

Playing to the strengths of *C. elegans* as a genetic model organism, I performed a fluorescent reporter based forward genetic screen to isolate mutants in which MCMs fail to be specified, denoting them as having a *nom* (No MCM) phenotype. By mapping and cloning such mutants the hope is to identify molecular factors, in an unbiased way, that direct every step of MCM neuronal development, from the potential of the AMso to divide and produce neurons, to MCM terminal specification. With the help of MSc/BSc. students Kishan

Khambhaita and Munim Husain, I isolated nine mutants affecting MCM development. Next, using fluorescent reporter gene analysis, the mutants were classified according to the general stage of MCM development affected in each mutant; AMso specification, AMso division, MCM neuronal specification and MCM neuronal subtype specification. The most common, heritable and stable mutant phenotypes were those of AMso division, MCM neuronal specification and MCM neuronal subtype specification. There are several candidates genes that could be involved in MCM development, such as those in the sex determination pathways that we know are involved or the plasticity cassette genes identified in the Y-PDA transdifferentiation (Kagias et al., 2012). These genes would likely affect the first steps that initiate the AMso-MCM cell fate switch, possibly resulting in a loss of AMso glial characteristics or failure of the proper acquisition of neuronal fate. In order discover genes involved in every step of MCM neuronal development a forward genetic screen was carried out as follows.

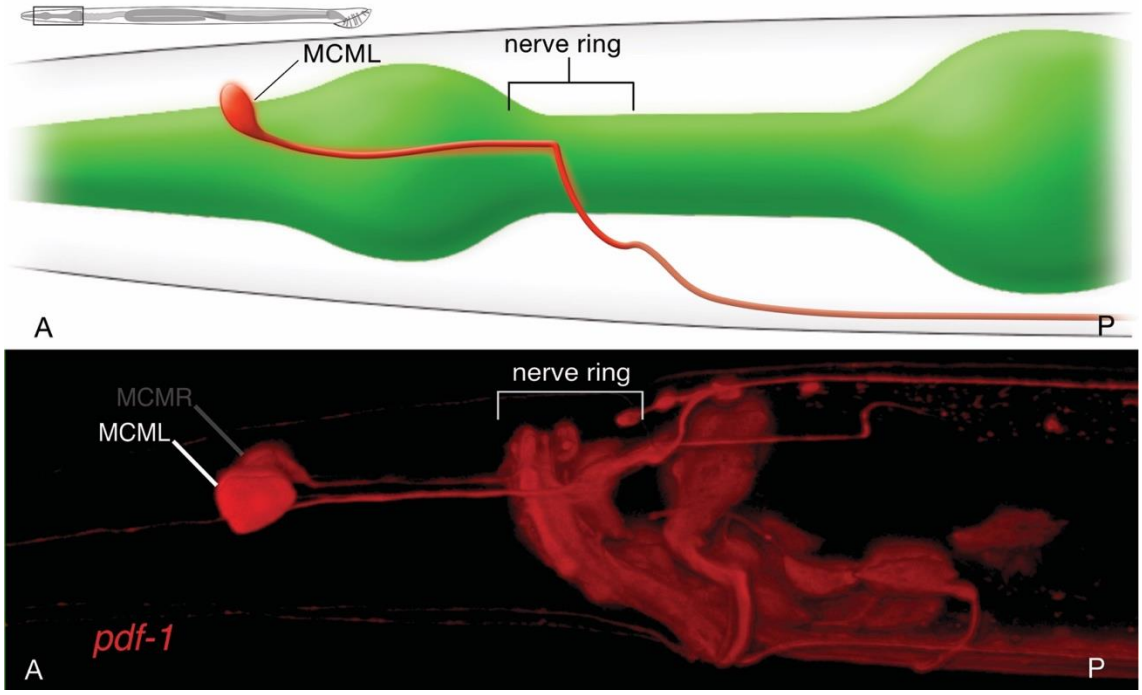

Figure 4.1 The location of the MCMs in the head of the male

(Top) Lateral schematic of the male head showing the position of the MCM cell body lying just anterior of the first pharyngeal bulb (pharynx in green) and projection into the nerve ring. (Bottom) Lateral oblique from a confocal volume of male head showing the MCMs and other *pdf-1::rfp* expressing cells.

4.2 Forward genetic screen yields nine No MCM mutants

A forward genetic screen was designed specifically in order to identify novel genetic regulators of the AMso to MCM cell fate switch. The aim of the screen was to identify male animals capable of surviving to adulthood but failing to express a transgene for the MCM neuronal subtype marker *ida-1* in the head. The BAR82, *inIs179*[*ida-1::gfp*];*him-8(1489)* strain was used as there are no other *ida-1::gfp* expressing cell bodies in the region of interest. The head region with the MCM and nerve ring labelled with *pdf-1::rfp* is shown in Figure 4.1. The *inIs179* promoter GFP fusion was generated by insertion of a 7652-bp fragment upstream of the *ida-1* start codon into the GFP vector pCR2D (Zahn et al., 2001). In order to screen for the male specific phenotype a high incidence of male mutant background was needed. In this way we selected for factors affecting the mature AMsos and developing MCMs and reduce the likelihood that essential genes and factors that affect early development or well-known genes affecting general cellular development are selected.

The screen was carried out in the following manner (Figure 4.2) adapted from (Brenner, 1974; Jorgensen & Mango, 2002) as described in Chapter 2.

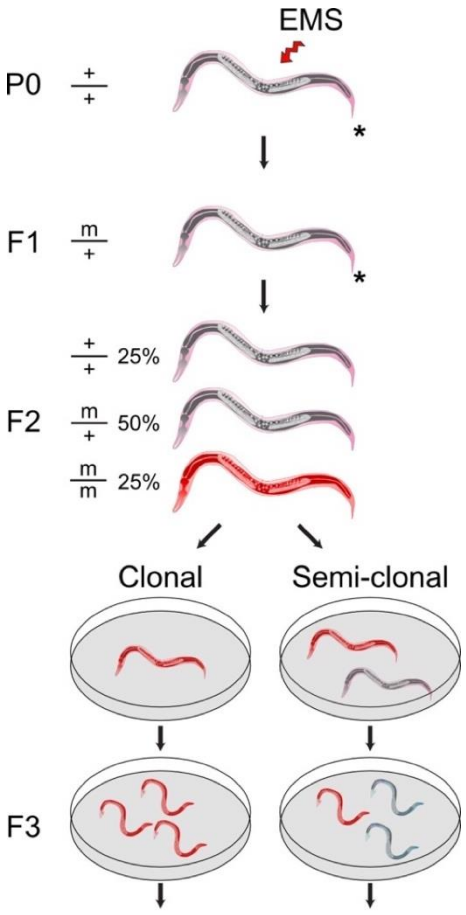

Figure 4.2 Forward genetic screen strategy

A schematic showing the strategy undertaken for a simple forward genetic screen for *nom* mutants.

Gravid P0 hermaphrodites are staged and mutagenised with EMS (* denote egg prep steps). Either the sperm or the egg is mutagenised in the P0, making the F1s heterozygous for any causal mutation.

Next 200 F2 hermaphrodites are either put 1 to each plate for a clonal screen or 2 to a plate in a semi clonal screen.

As the MCMs are male specific, the male F3 progeny are screened for plates bearing a high percentage of males which lack MCMs. Any mutant lines are singled two more times to ensure the mutation breeds true and stored.

From the screening of 3918 F1 haploid genomes, nine mutant lines with no MCMs visible by *inIs179[ida-1::gfp]* expression were isolated (Figure 4.3). EMS mutagenesis is strongly biased towards generating single nucleotide polymorphisms (SNPs), specifically G:C to A:T alterations which account for up to 87.5% of EMS mutations while deletions, transpositions or other rearrangements are relatively rare (Noma and Jin, Filbotte, Coulondre and Miller,1977). As shown in Chapter 3, AMso division and MCM development is intrinsically regulated under the control of the sex determination pathway, however no signs of sex reversals typical of a transformer (*tra*) phenotype (e.g. the appearance, in males, of hermaphrodite characteristics, such as vulva or the *ida-1::gfp* expressing HSN neurons or conversely, in hermaphrodites, the loss of vulva or appearance of MCMs or male specific structures) were stably observed in the *nom* mutant lines after outcrossing.

The penetrance of the *nom* phenotype by *ida-1::gfp* expression was also established for each of the nine mutants. 1 day old adult males were scored at 20°C and 25°C in order to determine if the mutants are temperature sensitive. A minimum of 50 animals were scored at each temperature. Several mutants were found to have a higher penetrance of the *nom* phenotype at 25°C, with *nom-1(drp1)*, *nom-6(drp6)*, and *nom-8(drp8)* being very strongly temperature sensitive (Figure 4.4).

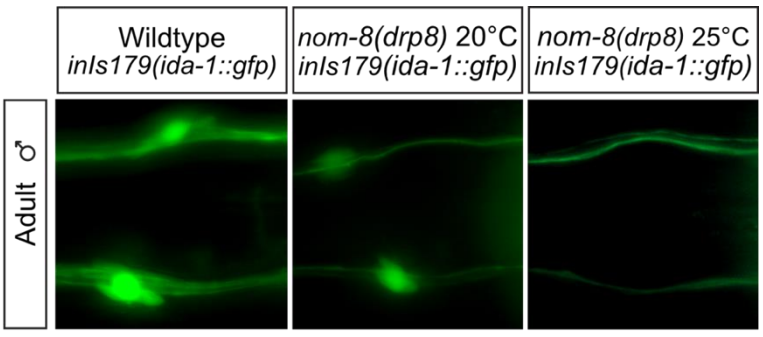

Figure 4.3 The MCMs and the *nom* phenotype

Dorsal view of the region anterior to the first pharyngeal bulb in 1 day adult males expressing the MCM neuronal subtype marker *inIs179[ida-1::gfp]*. Wild type incubated at 25°C and the temperature sensitive mutant *nom-8(drp8)* incubated at 20°C or 25°C.

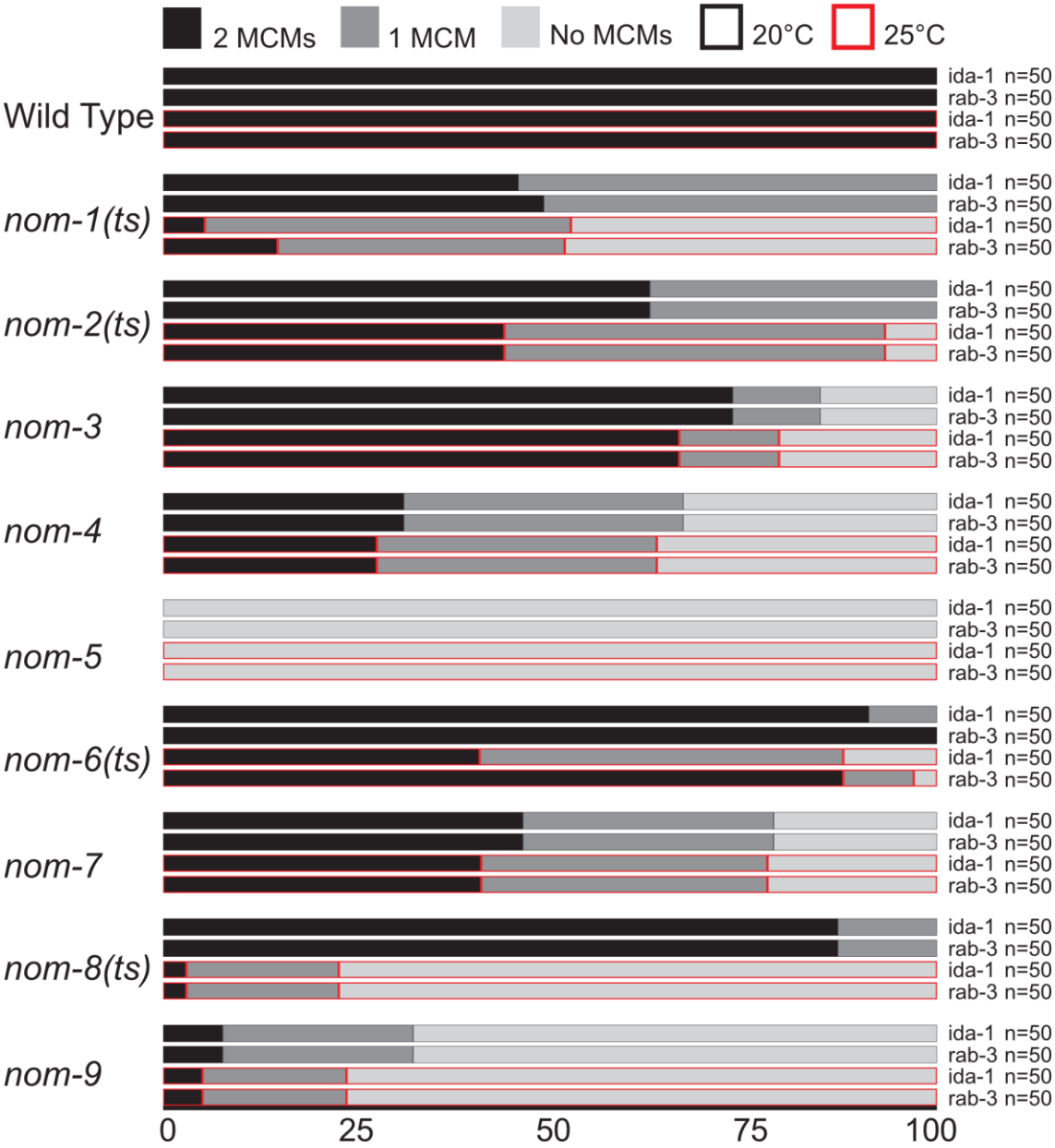

Figure 4.4 The penetrance of nine mutants isolated from the forward genetic screen

EMS mutagenesis of 3918 haploid genomes yields 9 mutants with no visible *ida-1::gfp* in the MCMs at 25°C. Defects in expression of pan-neuronal marker *otIs356[rab-3::rfp::NLS]* and neuronal subtype marker *inIs179[ida-1::gfp]* are quantified at 20°C and 25°C.

4.3 Isolated mutants affect sequential steps of MCM development

In order to be able to dissect the cellular events of MCM development it is essential to know as much as possible about the nature of each mutant phenotype, specifically how and when MCM specification is affected. Along with Kishan Khambhaita, I began examining the expression of neuronal and glial markers in each mutant, in order to determine the point at which the MCM developmental program is affected (Figure 4.5). As a glial reporter I generated the spontaneously integrated reporter *drpIs3* from a *lin-48::tdTomato* construct that contains a 6.8kb promoter fragment upstream of the coding sequence of *tdTomato* and the *unc-54* 3' UTR that was a kind gift from Mike Boxem, LIN-48 is an OVO related transcription factor and is known to act as a target of the Pax homologue EGL-38 in hindgut cells (Stefanakis et al., 2015). As a pan-neuronal marker I used the synaptic vesicle associated RasGTPase nuclear localised *rab-3* construct, *otIs356[rab-3(prom1)*::*2xNLS*::*TagRFP.* As a neuronal subtype marker, I used the same cytoplasmic *inIs179[ida-1::gfp]* construct used as the screening strain, which codes for the *C. elegans* homologue of the secretory vesicle associated receptor Insulinoma-Associated Protein, IA-2.

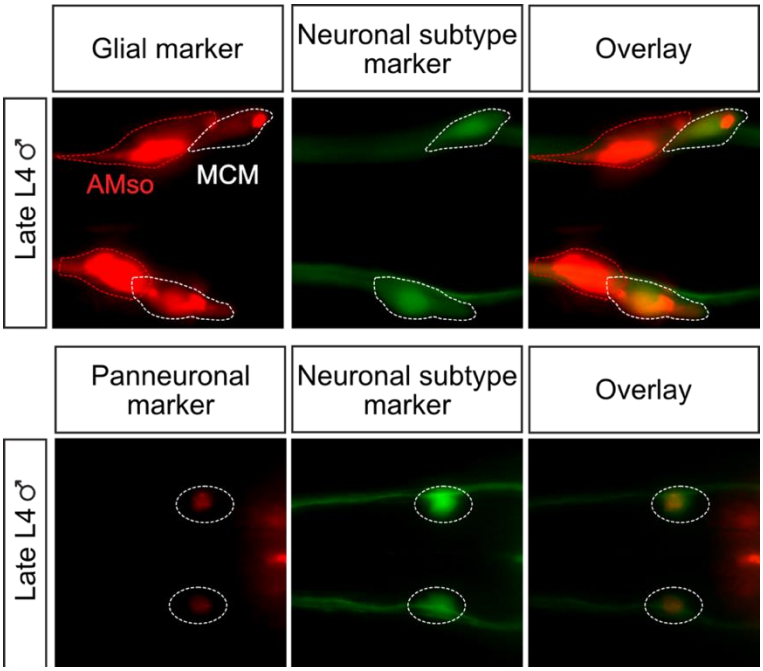

Figure 4.5 Wild type expression of neuronal and glial markers in the AMso and MCM

Wild type male expression of glial marker, *drpIs3[lin-48::tdTomato]*, pan-neuronal marker *otIs356[rab-3::rfp::NLS]* and neuronal subtype marker *inIs179[ida-1::gfp]* in the AMso and MCMs. The glial marker *drpIs3[lin-48::tdTomato]* is strongly expressed in the AMso, some perdurance from dividing AMso can still be seen in newly born MCMs until the late L4 stage and fades quickly in adult MCMs. By examining the AMso at the late L4 stage it is possible to determine if the AMso has divided. Both the pan-neuronal *otIs356[rab-3::rfp::NLS]* and neuronal subtype marker *inIs179[ida-1::gfp]* are visible in the MCMs from the mid to late L4 stage.

There are four broad stages in MCM development that could result *inIs179[ida-1::gfp]* expression being lost in the mutants, which can be classified into sequential stages of MCM development affected as follows (Figure 4.6):

Class I- Absence of the AMso cells: Due to the design of the screen it would be less likely to isolate this class of mutants since severe defects in the amphid sensilla would cause defects in neuronal development and function (Shaham, 2006) and hence reduce the chance of survival or development of the animal to adulthood. Mutants of this class which present with an incompletely penetrant phenotype, could also result in the MCM development defects even if the AMso is present, however none were detected in the screen so far.

Class II- Absence of AMso cell division: If the AMso is born normally but its normal developmental program is abrogated, this class should include genes controlling the most upstream events that confer neurogenic potential to the AMso. For example, as revealed in Chapter 3 we know that the AMso do not divide when genetically feminised, therefore, sex determination pathway mutants would be expected to fall into this category.

Class III- Failure of MCM neuronal specification: this class of mutants will show no neuronal differentiation of the MCMs following AMso division. Plasticity factors or master regulators of neuronal fate or might fall into this category.

Class IV- Failure of MCM subtype specification: this could be due an alteration of the entire terminal gene battery of the MCMs or may be due to a specific silencing of *ida-1* expression. The MCM terminal selector/s would likely fall into this category.

It is possible for a mutant to fit into more than one class for example, partial division defects that may or may not affect neuronal or subtype specification, in this case mutants would be classified according to the earliest stage of development affected.

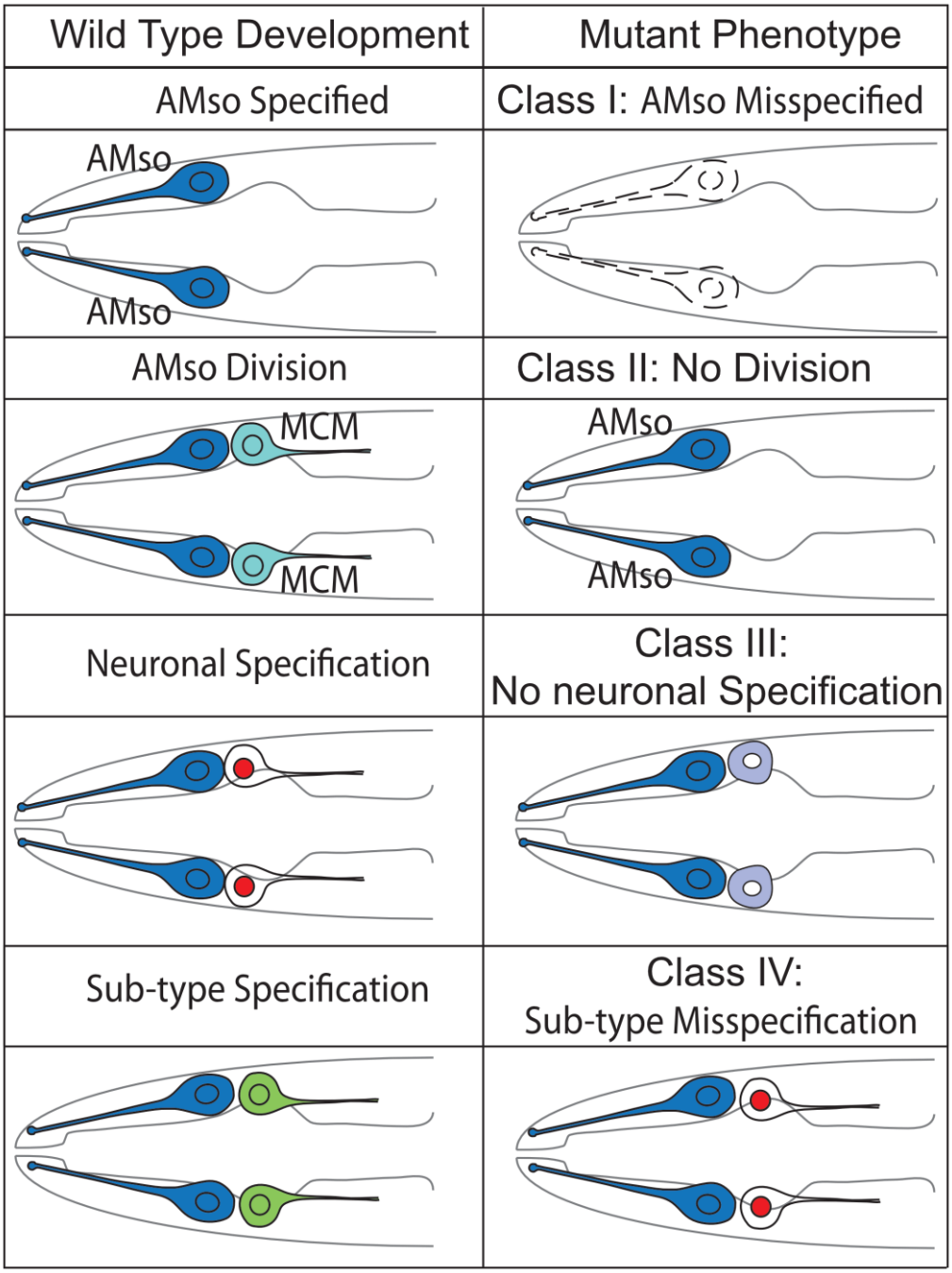

Figure 4.6 Mutant classes affect sequential steps of MCM development

A schematic showing dorsal views of the male head comparing wild type expression of neuronal and glial markers with 4 developmental classes of MCM mutants:

Class I- Absence of the AMso cells

Class II- Absence of AMso cell division

Class III- Failure of MCM neuronal specification

Class IV- Failure of MCM sub-type specification

4.3.1 Characterisation of Class I and Class II mutants

To identify Class I and Class II mutants, I used the integrated reporter *drpIs3[lin-48::tdTomato]* as a marker of AMso glial fate. In both male and hermaphrodite 1 day old adults, the *drpIs3[lin-48::tdTomato]* construct strongly labels the AMso, PHso1 but not PHso2, as well as, the excretory duct and pore cells and rectal epithelial cells and weakly labels other unidentified, likely socket cells, in the head. The AMso and PHso1/PHD are easily identifiable by their position, as the most anterior and posterior strongly labelled cells respectively. Next, *drpIs3* was crossed into the *nom* mutants containing *inIs179[ida-1::gfp]. drpIs3* has not as yet been crossed into mutants *nom-3(drp3)* and *nom-4(drp4)* they may be linked with *drpIs3* and cannot yet be assessed to be in Class I or Class II. Each other mutant was scored for the presence of the AMso, 50 1 day old adult males were scored at 25°C.

It was possible to identify both AMso in all mutants, upwards of 96% of the time, indicating that none of the mutants assessed belong to Class I (Table 4.1). Next in order to identify Class II mutants the division of the AMso can be visualised by perdurance of *lin-48::tdTomato* in the daughter cell which persists into early adulthood (Table 4.1). For each mutant line 25-60 mid L4 males were scored for the division of AMso at 25-26°C, in all mutants except *nom-5(drp5)* and *nom-8(drp8)* it was possible to identify the AMso daughter cells upwards of 97.5% of the time (Table 4.1). In both *nom-5(drp5)* and *nom-8(drp8)* the AMso division defect was fully penetrant. *nom-8(drp8)* is temperature sensitive showing 100% AMso division defect above 26°C, indicating that ***nom-5(drp5)*** **and** ***nom-8(drp8)*** **are Class II mutants**.

Table 4.1 AMso *drpIs3* expression and AMso division 26°C

	drpIs3 phenotype			
	number of AMso expressing *lin-48::tdTomato*	%	number of AMso divide	%
Wild type	100/100	100	100/100	100
nom-1(drp1)	96/100	96	78/80	97.5
nom-2(drp2)	117/120	97	119/120	99
nom-3(drp3)	n.d	-		-
nom-4(drp4)	n.d	-		-
nom-5(drp5)	100/100	100	0/80	0
nom-6(drp6)	100/100	100	59/60	98
nom-7(drp7)	100/100	100	50/50	100
nom-8(drp8)	100/100	100	0/60	0
nom-9(drp9)	100/100	100	70/70	100

4.3.2 Characterisation of Class III and Class IV mutants

Class III and Class IV mutants were identified by crossing the pan-neuronal reporter, *otIs356[rab-3::rfp::NLS]*, into the *nom* mutants containing neuronal subtype marker *inIs179[ida-1::gfp]*. A minimum of 50, one day old adult males were scored at 20°C and 25°C (Figure 4.4). By scoring for co-expression of the markers it was determined if the AMso daughter cells possessed general neuronal properties, including pan-neuronal components necessary for synaptic transmission, like *rab-3* and MCM neuronal subtype specific properties such as *ida-1* expression which is associated with neurosecretory communication.

Class III mutants have AMso that express *drpIs3(lin-48:tdtom)* normally and that also divide normally, however the posterior daughter cells, fail to express both pan-neuronal and neuronal subtype markers. The majority of the mutants isolated; ***nom-1(drp1), nom-2(drp2), nom-3(drp3), nom-4(drp4)***, ***nom-7(drp7)*** **and** ***nom*****-9(drp9)**, **fit into Class III** (Figure 4.7). AMso phenotype for *nom-3(drp3)* and *nom-4(drp4)* have not been determined yet, therefore will be in this class provisionally. It will be important to determine if the daughter cells that do not acquire a neuronal fate remain in an undefined or "dedifferentiated" state similar to what is described during the Y-PDA transition or if they express glial markers like the AMso mother cells or if there is mixed neuronal/glial fate.

Class IV mutants also have AMso that express *drpIs3(lin-48:tdtom)* normally and that divide normally. Pan-neuronal gene expression, visualised by *otIs356[rab-3::rfp::NLS]*, is also normal however the neuronal subtype assessed by *inIs179[ida-1::gfp]* expression is affected. At 25°C the temperature sensitive mutant *nom-6(drp6)* was found to have small rab-3 defect, being expressed in both daughter cells in 88% of animals but only 41% also expressed *ida-1::gfp* in both daughter cells (Figure 4.7). The discrepancy between the pan-neuronal and neuronal subtype marker expression shows that the cells tend to retain a general neuronal fate, but the neuronal subtype is misspecified, indicating that ***nom-6(drp6)*** **is a Class IV mutant**.

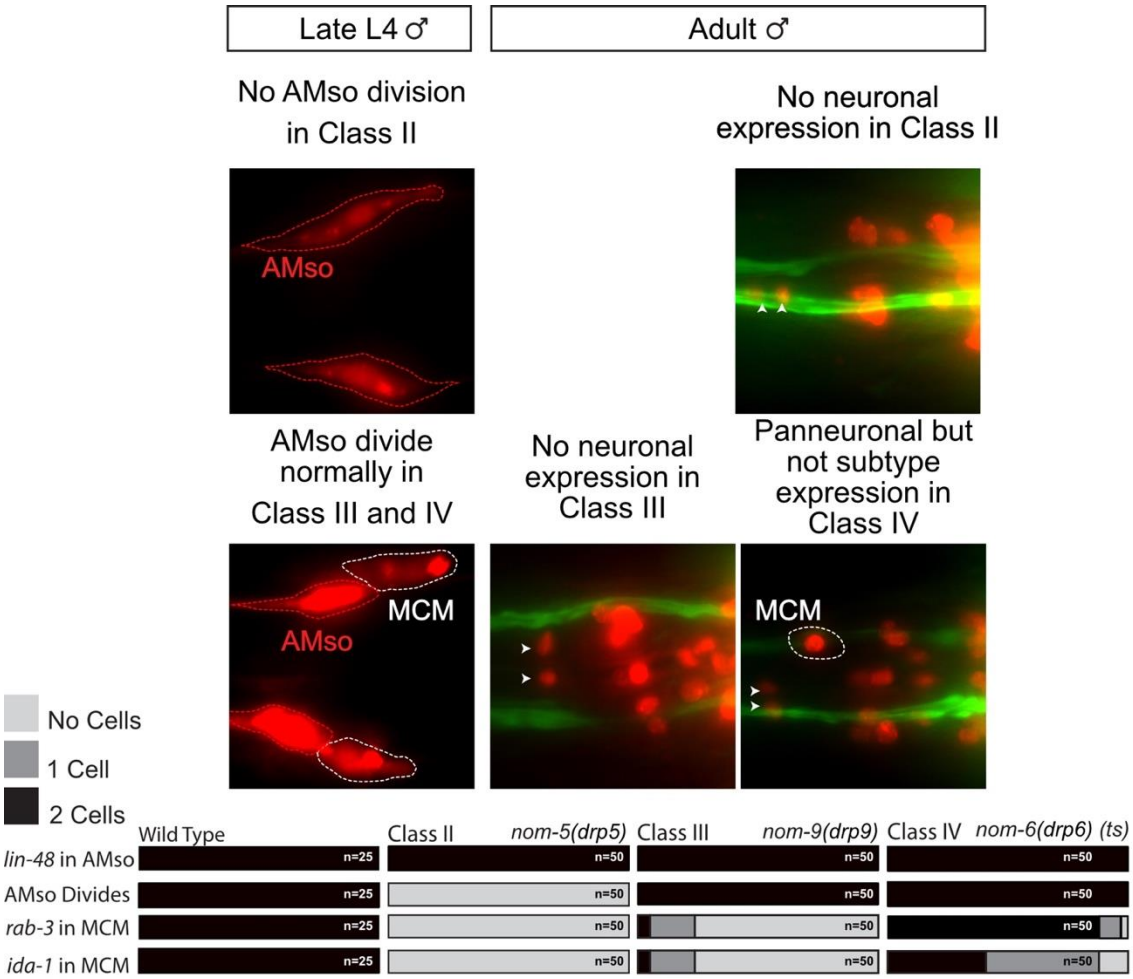

Figure 4.7 Characterisation of mutant classes

To classify mutants into classes affecting sequential stages of development, the combinatorial expression of glial marker, *drpIs3[lin-48::tdTomato],* pan-neuronal marker *otIs356[rab-3::rfp::NLS]* and neuronal subtype marker *inIs179[ida-1::gfp]* in the AMso and MCMs is assessed.

(Top) Illustrative images showing the appearance of possible common phenotypes of glial and neuronal marker expression in the region anterior or the 1st pharyngeal bulb of late L4 and adult males. Used in order to aid the classification mutants into Classes I to IV.

Class I mutants would not show any glial marker in the region of interest in the head and are not shown.

Class II mutants have normal glial marker expression in the AMso, however, the AMso fail to divide. This is assessed by looking for perdurance of the glial marker in the daughter cell at late L4. As the MCMs are not born there is no pan-neuronal or neuronal sub-type marker expression in the region of interest in the head. White arrowheads indicate nuclear marking of I1L and ILR pharyngeal neurons which are anterior to the first pharyngeal bulb but lie completely within the pharynx and are easily distinguished.

Class III mutants have normal glial marker expression in the AMso, and they can be seen to produce daughter cells by looking for glial marker perdurance at L4. However, there is no pan-neuronal or neuronal sub-type marker expression in the region of interest in the head when viewed as adults.

Class IV mutants have normal glial marker expression in the AMso, and they can be seen to produce daughter cells at L4. Cells bearing the nuclear pan-neuronal marker can be seen in the region of interest, however these cells may lack neuronal sub-type marker expression.

(Bottom) Scoring of each of the phenotypes described above in a representative mutant from each class. (Scoring is at non-permissive temperature, n is the number of animals scored).

4.4 PHD development is minimally affected in *nom* mutants

In order to assess if PHD development was similarly affected in the mutants the morphology of PHD was scored in *drpIs3(lin-48:tdtom)* expressing animals (see Chapter 3). Preliminary analysis of each strain indicates that none of the mutants showed any consistent defects Table 4.2. PHD specification has not been assessed in *nom-3(drp3)* and *nom-4(drp4)*.

Table 4.2 Assessment of PHD morphology by *drpIs3* expression

	number of PHD with WT morphology by *lin-48::tdTomato*	%
Wild type	100/100	100
nom-1(drp1)	74/77	96
nom-2(drp2)	126/133	95
nom-3(drp3)	n.d.	n.d.
nom-4(drp4)	n.d.	n.d.
nom-5(drp5)	47/48	98
nom-6(drp6)	48/50	96
nom-7(drp7)	44/48	92
nom-8(drp8)	52/54	96
nom-9(drp9)	52/54	96

4.5 Summary

I have undertaken a forward genetic screen in the search for factors involved in MCM specification. Additionally, I helped develop a method to identify defects in the sequential stages of MCM development, and identified two Class II mutants, six Class III mutants and one Class IV mutant from the screen. I also examined the potential effect these mutants had on PHD specification, a preliminary examination showed no gross irregularities in the number or gross morphological features of PHD in the mutants tested. After completing the developmental characterisation of the MCM mutants I chose to focus on the most upstream events of MCM development and thus began a more in depth analysis of the Class II mutants. The next chapter will present the data showing the mapping and cloning the two Class II mutants, including techniques developed for the genetic analysis of male specific mutant phenotypes.

Chapter 5

Class II mutants *nom-5* and *nom*-8 are novel alleles of *cdk-4*

5.1 Overview

I have isolated mutants that affect the various stages of development of the first example of glia derived neurons in an invertebrate. An understanding of the earliest events in the process is essential to framing the entire context of this cell fate plasticity. The mechanisms governing cell division in particular are one of the least understood aspects of transdifferentiation. I have therefore chosen to investigate the Class II mutants first.

In this chapter I will: (i) present a novel genetic crossing scheme for mapping male specific phenotypes by sequencing, that was used to map both the Class II mutants *nom-5* and *nom-8* to a 1Mb region on the X chromosome; (ii) show by mapping, rescue, and complementation that *nom-5(drp5)* and *nom-8(drp8)* are alleles of *cdk-4*, thence renamed *cdk-4(drp5)* and *cdk-4(drp8)* respectively. The unavoidable biological limitations of XO male specific phenotypes caused by mutations on the single X chromosome complicates standard genetic analysis. However, by using cell type specific masculinisation of the mother cell, as described in Sammut et al 2015: Annexe I, I was able to investigate the basic genetic nature of *cdk-4(drp5)* allele.

5.2 *nom-5(drp5)* and *nom-8*(*drp8*) map to the *cdk-4* locus

5.2.1 Mapping-by-sequencing of nom-5(drp5) and nom-8(drp8)

In order to map a male specific phenotype by sequencing it was necessary to adapt the genetic crossing scheme developed for mapping-by-sequencing of hermaphrodite phenotypes (Doitsidou et al., 2016). This method of sequencing relies on a polymorphic strain of *C. elegans*, in this case the Hawaiian strain CB4865 (HA), which has regular single nucleotide polymorphisms (SNPs) on average every 1000 base pairs compared with the genome of ancestral wild type Bristol (N2) strain used in most *C. elegans* work (Batzoglou et al., 2002; Koch et al., 2000; Wicks et al., 2001). With a highly accurate list of defined HA SNPs available (Minevich et al., 2012), the allele frequencies of HA to Bristol SNPs can be compared in the progeny of a cross between the two strains. Without any selection, meiotic recombination in the F1 would result in a 1:1 of HA to Bristol SNPs at any particular point along the F2 genome. However, if mutants in a Bristol background are crossed with a HA and the homozygous recombinant mutant F2 progeny are selected they cannot have recombined with HA at the location of the causal variant on the chromosome. Therefore, if homozygous mutant F2 progeny are selected and enough recombination events are pooled and sequenced, a region of pure Bristol SNPs in a background of 1:1 HA to Bristol SNPs would indicate the location of the mutation to a high resolution, the exact resolution depends chiefly on how many recombination events are pooled, as increasing the number of events increases the likelihood that some events occur closer to the site of the selected mutation, 50 are enough to give mapping to 0.5Mb (Figure 5.1). Using CloudMap (Minevich et al., 2012) the bioinformatic processing can be done automatically using pre-designed workflows. By sequencing the original strain used for mutagenesis, CloudMap can subtract the identified non-causal background variants to provide a short list of candidate causal mutations in the mapping region.

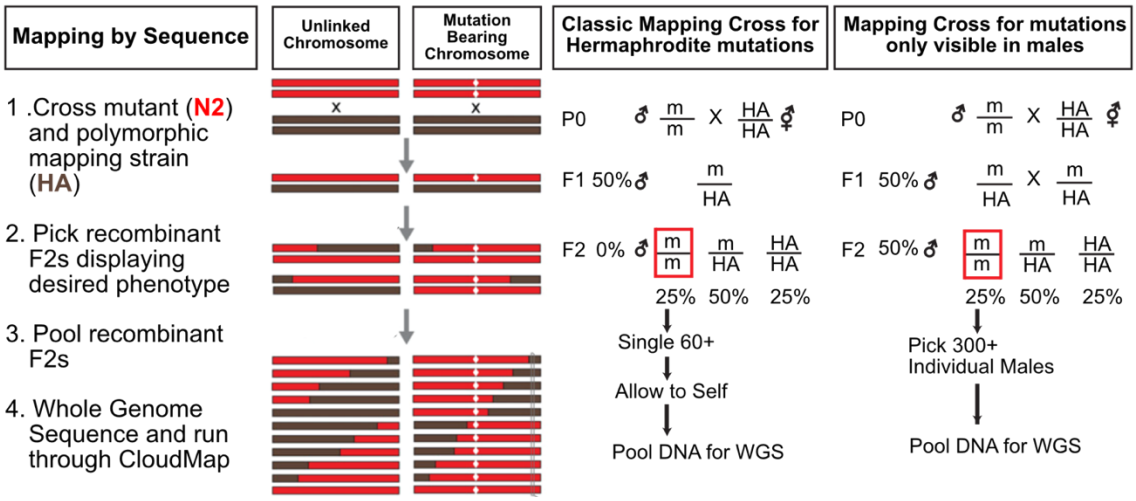

Figure 5.1 A novel scheme for mapping male specific phenotypes

Hawaiian variant mapping by whole genome sequencing strategy, adapted from (Minevich et al., 2012). With crossing schemes for the generation of homozygous F2 recombinant mutants with phenotypes visible in hermaphrodites and a modified scheme for male specific phenotypes, with the expected proportion of males at each stage of the cross.

When selecting F2 recombinants with a visible phenotype in hermaphrodites, the standard protocol is to single enough F2s to get 30-50 recombinants, therefore, if 50 recombinants are desired, 200 of F2s must be singled and their F3 progeny screened in order to find the 25% that, by mendelian segregation, will be homozygous. As explained above, the greater the number of homozygous recombinants the higher resolution the mapping will be, 50 plates of recombinants is enough to give tight mapping to 0.5Mb region (Minevich et al., 2012). The F3 worms in these plates are then pooled, their DNA purified, sequenced and analysed. In many cases the target mutation is only visible in a specific genetic background, in this case, the fluorescent transgene *ida-1::gfp* and *him-8* are required. Every additional unlinked gene required in the background increases the total number of F2s required by a factor of 4, and this can quickly become an unfeasible number. For example, for 50 F2 recombinants, if three separate alleles or transgenes are required to be homozygous, this would amount to 4^3 X 50 = 3200 being singled and screened. It is important to note that if less than approx. 95% of sequenced recombination events are homozygous F2s the mapping attempt can fail. I developed a simple method for male specific phenotypes that addresses these issues.

As a proof of principle, I began by mapping the *nom-8(drp8)* mutation which presents a nearly completely penetrant phenotype at 25-26°C (Figure 4.4). To begin with *nom-8(drp8)*;*inIs179[ida-1::gfp]*;*him-8(e1489),* (N2 background) males were crossed into CB4856 HA hermaphrodites. 50% of the cross progeny will be male, allowing F1 in-crosses to be set in order to ensure half the F2 progeny are male and 75% contain the either heterozygous or homozygous *inIs179[ida-1::gfp]* transgene, greatly assisting in the identification of the recombinant F2 *nom* progeny. This avoids the necessity of having a homozygous *him* mutation in the background in order to be able to see the male specific phenotype. In this way, through several F1 in-crosses 300 individual F2 males carrying the *nom-8(drp8)* causal mutation were picked. These were washed for 2 hours in M9 in order to decrease the amount of bacterial DNA contamination, the genomic DNA was purified and sent for whole genome sequencing. Using this novel genetic crossing scheme and processing in CloudMap, I was able to get a good but fairly weak mapping for *nom-8(drp8)* to between 13 and 14Mb on the X chromosome (Figure 5.2). The scatter plot shows the proportion of the mapping HA strain SNPs along the chromosome nearly reaching 0 in the region of 13Mb. While, the red bars in the plots represent 0.5 Mb bins and grey bars are 1 Mb bins of the proportion of parental Bristol SNPs normalised against the distribution of HA SNPs along the chromosome reaching a peak at 13-14Mb.

This method provides the potential of very tight mapping by sequencing, due to the high number of F2 recombinants selected at the cost of being more laborious, in picking the individual recombinants and greater care in the purification of the small quantity of DNA. A high enough DNA concentration for sequencing, of 18.1ng/L, is possible, however a large proportion did not map to the *C. elegans* genome, probably due to a high degree of bacterial contamination. Unfortunately this resulted, in large regions of the *C.* elegans genome remaining uncovered by sequencing, as the excess of bacterial DNA resulted in a lower coverage of the *C.* elegans genome than theoretical estimates predicted before sequencing (resulting in many HA SNP position not being able to be assessed and hence the weaker mapping signal), in order to address this problem high coverage sequencing is recommended.

Next, I mapped the *nom-5(drp5)* mutation by the same method, with minor modifications; this time picking 500 F2 recombinants, implementing a more thorough cleaning regime (6-8hrs) in order to minimise bacterial contamination. Using this method *nom-5(drp5)* was mapped to a 0.5Mb region around 13.5 Mb on the X chromosome (Figure 5.2). The scatter plot shows the proportion of the mapping HA strain SNPs along the chromosome reaching 0 between 13Mb and 14Mb. While, the red bars in the plots represent 0.25 Mb bins and grey bars are 0.5 Mb bins of the proportion of parental Bristol SNPs normalised against the distribution of HA SNPs along the chromosome peaking at 13.5Mb.

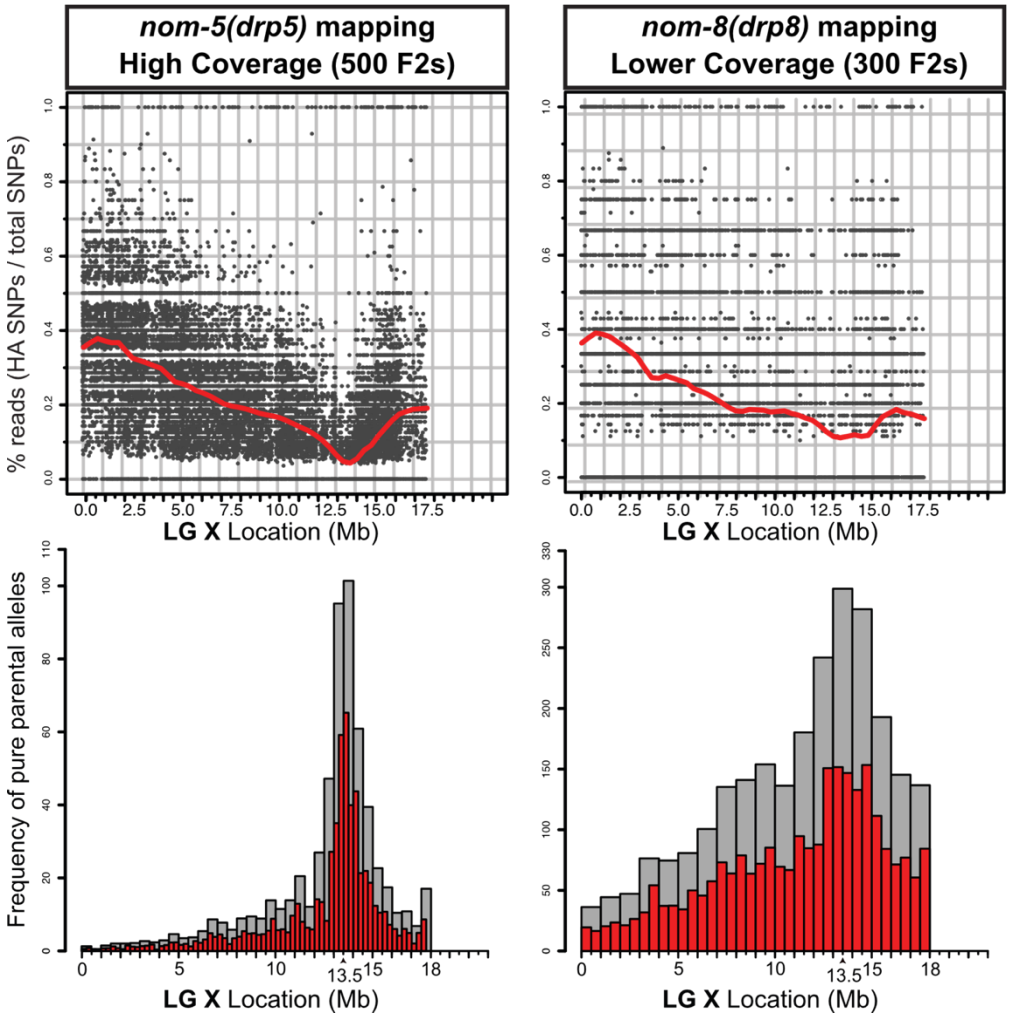

Figure 5.2 Both *nom-5(drp5)* and *nom-8(drp8)* map to 13.5Mb on the X chromosome

(Top) Scatter plot of the ratio of mapping strain (HA) alleles/total reads at each of the mapping strain SNPs on the chromosome with a regression line (red) through all the points. For both *nom-5(drp5)* and *nom-8(drp8)*.

(Bottom) Corresponding frequency plots that display the regions of the chromosome where pure parental allele SNP positions are concentrated normalised against HA SNPs distribution along the chromosome. X-axis shows position along the X chromosome, major gradations are 1Mb. Red bars represent bins of 0.25Mb for *nom-5(drp5)* and 0.5 Mb for *nom-8(drp8)* and grey bars represent 0.5Mb for *nom-5(drp5)* and 1Mb bins for *nom-8(drp8)*.

Consistent with this *nom-5(drp5)* was shown to be X-linked by genetic testing. As 100% of F1 males produced from *nom-5(drp5)* males crossed into wild type CB4856 hermaphrodites do not have a *nom* mutant phenotype; in this scenario, the single X of the F1 males would come from the mother and therefore not contain the *nom-5(drp5)* mutation. When the reciprocal cross is made with *him-8(e1489)* males (not containing the *nom-5(drp5)* mutation) crossed into *nom-5(drp5)* hermaphrodites 50% of their progeny show the *nom* phenotype (Table 5.1). Under normal circumstances 100% of the progeny should bear the maternal X and therefore the *nom* phenotype, however *him-8(e1489)* being a X non-disjunction mutant produces 38.7% nullo X ova and thus resulting in a proportion of XO male cross progeny bearing the paternal X (Hodgkin et al., 1979). Crossing *nom-5(drp5)* males into *him-8(e1489)* hermaphrodites also resulted in 51% of their progeny presenting the *nom* phenotype (Table 5.1) confirming that the progeny of *him-8(e1489)* hermaphrodites do bear the paternal X phenotype, although this is 10-15% more than would be explained by the 38.7% nullo X ova alone. Nevertheless, taken together the mapping and genetic testing are consistent with X linkage.

With both mutants showing that the bins nearest to 13.5Mb on X had the highest proportion of starting strain Bristol SNPs, this raised the possibility that the *nom-5(drp5)* and *nom-8(drp8)* mutations are two alleles of the same gene. Analysis of possible causal variants within a 2Mb region around 13.5Mb on X initially, before subtraction of non-causal variants, provided several candidate genes for nom-*5(drp5)* and *nom-8(drp8)*. The original screening strain used for mutagenesis, BAR82 and the mapping stain, were also sequenced, (as was the BL5717 strain, from which the BAR82 strain originated and is also known not to have a *nom* phenotype), and any variants in common were subtracted from the list as non-causal variants. Conspicuously, after subtraction, out of the possible causal variants the *cdk-4* locus (Figure 5.3) was the only one that had protein coding variants in both mutants.

Figure 5.3 The *cdk-4* locus

The *cdk-4* locus with known molecular lesions. Adapted from (Boxem & van den Heuvel, 2001).

Table 5.1 X-linkage of *nom-5(drp5)* mutation

♂ P0 Genotype	♀ P0 Genotype		
	CB4856 WT		
	F1 *nom* Phenotype		
	Wild type %	*nom* %	n=
inIs179[ida-1::gfp];him-8(e1489)	100	0	75
	F1 *nom* Phenotype		
nom-5(drp5);inIs179[ida-1::gfp];him-8(e1489)	98.5	1.5	65
	F1 *nom* Phenotype		
nom-5(drp5);inIs179[ida-1::gfp];otIs356[rab-3::rfp];him-8(e1489)	100	0	81
	nom-5(drp5);inIs179[ida-1::gfp];him-8(e1489)		n=
	F1 *nom* Phenotype		
	Wild type %	*nom* %	
otIs356[rab-3::rfp];him-8(e1489)	54	46	26
	otIs356[rab-3::rfp];him-8(e1489)		n=
	F1 *nom* Phenotype		
	Wild type %	*nom* %	
nom-5(drp5); inIs179[ida-1::gfp];him-8(e1489)	51	49	35

5.2.2 drp5 and drp8 alter conserved residues predicted to affect the activation loop

Sequence analysis of *nom-5*(*drp5*) and *nom-8*(*drp8*) offers intriguing insight into the potentially specific function *cdk-4* may have in MCM development, in the next section we show by complementation and rescue that *drp5* and *drp8* are alleles of *cdk-4*. Both protein coding variations are very close to each other and are likely to affect the same region of the protein and suggests that this region is important for MCM development. The affected region, known as the catalytic loop, canonically extends from the HRD to the S/APE motifs and is a common feature of protein kinases. As the name suggests it functions directly in the catalytic process and the switch between the active and inactive conformations of the kinase domain. Part of the catalytic domain, the activation loop or T-loop, is a key regulatory region, which when phosphorylated on a particular Threonine residue (T172) is required for full CDK activity in human cells. The region of the catalytic loop is highly conserved in metazoans from worm to humans (Figure 5.4) including both of the residues affected by the *cdk-4*(*drp5*) and *cdk-4*(*drp8*) molecular lesions. The location of the *cdk-4*(*drp5*) allele corresponds to an amino acid residue just two residues away from T172 in humans, here a conserved Alanine is converted into a Threonine residue. The activation loop extends from the DFG to the S/APE motif, the *cdk-4*(*drp8*) lesion substitutes a Leucine residue for Phenylalanine in a highly conserved region at the end of the activation loop (Figure 5.4). A 3D rendering based on the crystal structure of human CDK4 in complex with CyclinD1 (Day et al., 2009) shows that the residues predicted to be affected in *cdk*-4(*drp5*) and *cdk*-4(*drp8*) are in close proximity to the catalytic cleft (Figure 5.4) suggesting that regulation of CDK-4 activity at this site directs MCM development.

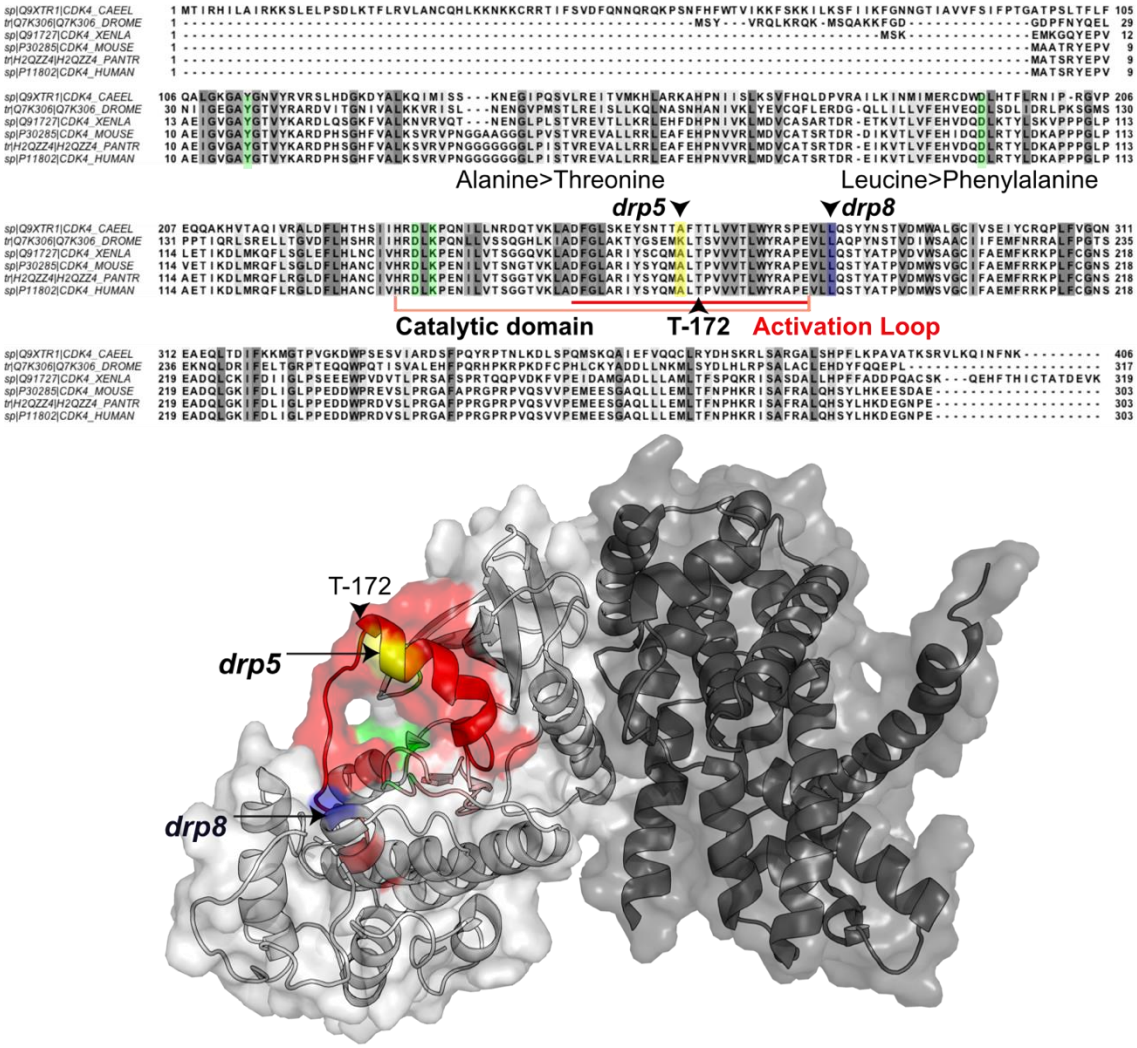

Figure 5.4 *drp5* and *drp8* are predicted to alter key residues of CDK-4

(Top) Multiple sequence alignment of the CDK4 protein sequence in *C. elegans*, *D. melanogaster*, *X. laevis*, mouse, chimpanzee and human. Conserved residues are highlighted. The activation or T-loop (red) within the catalytic domain contains a Threonine residue at 172 on the human sequence. Phosphorylation of T-172 is a key step in the regulation of CDK4 activity in human cells. Also highlighted are residues involved in ATP binding (green). The predicted *cdk-4* allele *drp5* (yellow) results in a protein coding variant converting a conserved Alanine to Threonine two residues short of the Threonine residue corresponding to T-172 in humans. The *cdk-4*(*drp8*) (blue) variation results in a Leucine to Phenylaniline conversion of a conserved residue in close proximity to the T-loop. Sequence alignment using Clustal Omega (Sievers & Higgins, 2018) viewed in Jalview.

(Bottom) Crystal structure of human CDK4 in complex with CYD1 (Day et al., 2009). Cyclin is in black and CDK4 is in white. The activation loop is highlighted in red and the location of T-172 marked with an arrowhead. The activation loop is stabilised in an inactive conformation occluding the catalytic site with ATP binding regions (green). The predicted locations corresponding to the genetic lesions *drp5* (yellow) and *drp8* (blue) are marked by arrows. 3D rendering using PBDid 2w9z in the PyMOL Molecular Graphics System, Version 2.0 Schrödinger, LLC.

5.3 Genetic analysis indicates that *nom-5(drp5)* and *nom-8*(*drp8*) are alleles of *cdk-4*

5.3.1 The critical period for MCM development in nom-8 animals is in L3

Taking advantage of the temperature sensitive mutant isolated from the screen, I investigated the period in development that *nom-8(drp8)* is required. Temperature shift experiments show that when males are shifted up to the non-permissive temperature at any point prior to the late L3 stage then they will not produce MCMs, but if incubated at the permissive temperature and then shifted to the non-permissive temperature in the L4 stage they are able to produce MCMs (Figure 5.5). Conversely if animals are incubated at the non-permissive until mid L3 then downshifted they will appear wild type, if downshifted after L3 they will then exhibit the *nom* phenotype, presence of MCMs was scored by the expression *inIs179[ida-1::gfp]*. There is therefore a short critical period in the L3 stage during which the altered *nom-8(drp8)* gene product can block MCM development, this timing is coincident with the time of AMso division and is consistent with a functional disruption of the cell cycle. In order to discover if mutations of *cdk-4* were indeed the cause the *nom* phenotype I planned to carry out complementation tests. However, in order to do so, I first had to develop a way to test an X-linked male specific phenotype, which is impossible to do classically, as XO males only have a single copy of X and naturally, two alleles are required to assess complementation. To circumvent this problem I attempted complementation testing, using XX hermaphrodites with genetically masculinised AMso. In the next three sections I will use a masculinising array expressed in XX hermaphrodite AMso to, first of all show that show that *cdk-4*(*drp5)* acts downstream of the masculinising determinant and then use the masculinised XX AMso to perform, dominance and complementation tests impossible in XO animals.

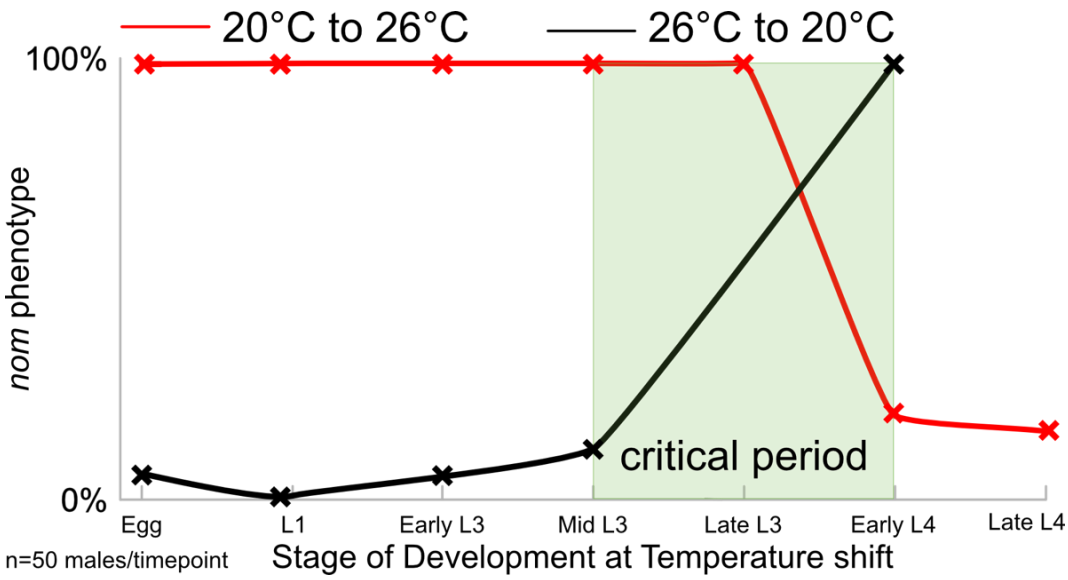

Figure 5.5 The *cdk-4(drp8)* allele blocks MCM development at mid to late L3

Temperature shift experiments show that the critical period for MCM development in *cdk-4(drp8)* is between mid-L3 and early L4 which is around the time AMso division occurs. The presence of the MCMs was scored by *inIs179[ida-1::gfp]* expression. The red line denotes animals incubated at a permissive temperature of 20°C upshifted to the non-permissive temperature of 26°C at each time point (x). The black line denotes animals incubated at a non-permissive temperature of 26°C and shifted down to a permissive temperature of 20°C at each time point (x). Shifting animals up to the non-permissive temperature at any time before late L3 results in a completely penetrant *nom* phenotype while up-shifting after L3 allows for the production of MCMs. While, shifting animals down to a permissive temperature at any time before mid L3 permits the production of MCMs but doing so after results in a *nom* phenotype. The green window shows the period where *cdk-4(drp8)* is inferred to be required to produce MCMs.

5.3.2 cdk-4(drp5) likely acts cell autonomously downstream of fem-3 in the AMso

As described in Chapter 3, MCM specification is cell intrinsically under the control of the sex-determination pathway. The o*leEx24 [grl-2prom::fem-3::SL2mCherry + elt-2::GFP]* extrachromosomal array, drives the masculinising determinant *fem-3* (Figure 1.21) under the control of the *grl-2* promoter, and therefore is expressed only in the AMso, excretory pore, excretory duct and the PHso1 and PHso2 cells. Via mosaic analysis using *oleEx24* I could investigate the nature of the *cdk-4*(*drp5*) allele in genetically XX but phenotypically masculinised AMso. The inheritance of o*leEx24* in the AMso was determined for each cell by the looking for the expression of mCherry under a compound microscope. In *cdk-4*(+/+);*inIs179[ida-1::gfp]* hermaphrodites 76% of AMso that carry *oleEx24* produce MCMs (n=37 cells) while no non-array carrying AMso develop MCMs (n=58 cells), see Figure 5.6 (a). In contrast, *cdk-4*(*drp5/drp5*);*inIs179[ida-1::gfp]* hermaphrodites whose AMso also carried

o*leEx24* never produced MCMs (n=25 cells) likewise *cdk-4*(*drp5/drp5*);*inIs179[ida-1::gfp]* non-array carrying AMso do not produce MCMs (n=25 cells), see Figure 5.6 (c). As the *nom* phenotype of *drp5* is also apparent in AMso masculinised hermaphrodites, this indicates that the *drp5* allele acts downstream of the sex determination pathway, most likely cell specifically. This result allows for further genetic testing using this system.

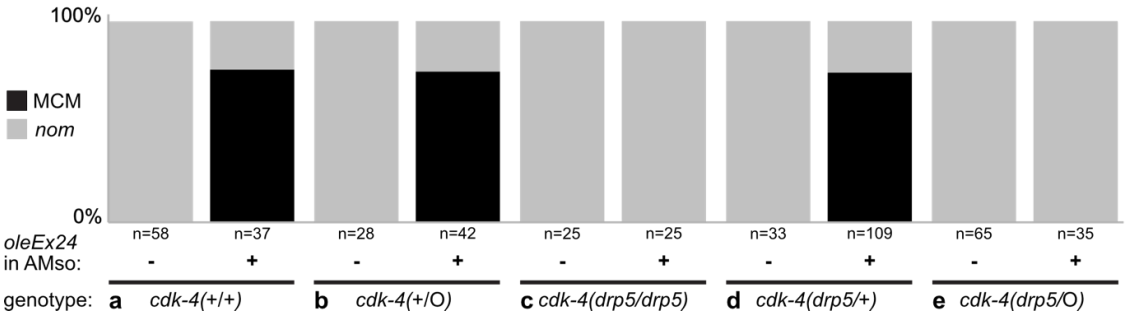

Figure 5.6 Masculinisation of XX AMso allows for genetic analysis of *nom* phenotype in *cdk-4* alleles

The masculinising factor *fem-3* is driven in the AMso by the extrachromosomal array, o*leEx24[grl-2prom::fem-3::SL2mCherry +elt-2::GFP]*. Mosaic analysis of o*leEx24* in hermaphrodite AMso allows for the investigation of the nature of X linked *cdk-4* alleles in the context of the male specific *nom* phenotype. The null allele (O) is *cdk-4*(*gv3*) from BS1175. The *nom* phenotype is assessed by the expression of *inIs179[ida-1::gfp]*.

(a) Confirms that, as shown in Chapter 3, the AMso of homozygous wild type *cdk-4(+/+)* animals, which carry the masculinizing array (**+**) can produce MCMs while non array carrying AMso (**-**) never do.

(b) The AMso of animals bearing only a single functioning copy of *cdk-4(+/O)* and carry the masculinizing array (**+**) can produce MCMs just as well as homozygous wild type *cdk-4(+/+)* animals. Indicating that one copy of wild type *cdk-4* is enough to allow AMso to produce MCMs normally and that *cdk-4(gv3)* does not produce a dominant negative *nom* phenotype.

(c) Homozygous *cdk-4(drp5/drp5)* AMso never produce MCMs ,whether they carry the masculinizing array (**+**) or not (**-**). Suggesting that *cdk-4* acts downstream of the sex determination pathway in the AMso.

(d) In heterozygous *cdk-4(drp5)* animals *cdk-4(drp5/+)* the AMso produce MCMs when they carry the masculinizing array (**+**) showing that one copy of wild type *cdk-4* is enough to completely rescue the *nom* phenotype seen in homozygous *cdk-4(drp5/drp5)* animals, indicating that *cdk-4(drp5)* does not produce a dominant *nom* phenotype.

(e) The AMso bearing the two recessive mutations *cdk-4(drp5) and cdk-4(gv3)* have a completely penetrant *nom* phenotype as transheterozygotes *cdk-4(drp5/O)* when they carry the masculinizing array (**+**). Indicating that they do not complement each other and are therefore alleles of the same gene.

5.3.3 cdk-4(drp5) does not show dominance effects

Using the method outlined in the previous section I used the masculinising o*leEx24* array to investigate the nature of the *cdk-4*(*drp5*) in genetically XX but phenotypically masculinised AMso. By examining the *nom* phenotype by *inIs179[ida-1::gfp]* expression of the F1 progeny of *cdk*-4(+) and *cdk-4*(*drp5)* animals carrying o*leEx24* it is possible to assess any possible dominance effects of *cdk-4*(*drp5)*. There is a complete lack of a *nom* phenotype in the masculinised AMso of heterozygous *cdk-4*(+/*drp5*) animals (n=109 cells), comparable to what is observed in homozygous *cdk*-4(+/+), see Figure 5.6 (d). Therefore *cdk-4*(*drp5)* does not appear to have a dominant negative effect or semi-dominant effect and likely acts as a classical recessive allele.

In order to assess the possibility of a haploinsufficiency of *cdk-4* or a dominant negative effect of *cdk-4(gv3)* causing a *nom* phenotype, I examined the F1 progeny of *cdk*-4(+) and *cdk-4*(*gv3)* null animals from BS1175 carrying o*leEx24*. The masculinised AMso of *cdk-4*(+/*O*) show no defect in the production of MCMs compared with *cdk*-4(+/+) animals (n=42 cells), indicating that a lowered dosage of wild type *cdk-4* and the presence of *cdk-4(gv3)* does not result in a *nom* phenotype, see Figure 5.6 (b).

5.3.4 cdk-4(gv3) does not complement the cdk-4(drp5) nom phenotype

The ability to assess the male specific *nom* phenotype in XX animals and finding that *cdk-4*(*drp5*) and *cdk-4*(*gv3*) are recessive for the *nom* phenotype allows for the testing of complementation of *cdk-4*(*drp5*). In order to test for complementation, I examined the *nom* phenotype of the F1 progeny of *cdk*-4(*drp5*) and *cdk-4*(*gv3)* null animals *cdk-4*(O). Since *cdk-4* is required for G1/S progression in all post-embryonic cell divisions, the null allele *cdk-4(gv3)* has an extremely strong larval arrest phenotype (Park & Krause, 1999), therefore a means of permitting them to produce progeny is required. A strain containing an extrachromosomal array bearing a wild type copy of *cdk-4*, BS1175 *cdk-4(gv3)*;*ozEx76 [(pKMii1177) cdk-4p::CDK-4::GFP + (pAD46) sur-5::DsRed)]* has been shown to rescue the larval arrest phenotype (Fox et al., 2011) and therefore allow for the testing of their progeny. The last step

before testing was to create a single strain bearing the *cdk*-4 null allele *gv3*, the *cdk-4*(+) rescuing array and the AMso masculinising array o*leEx24*, *cdk-4(gv3)*;*ozEx76;*o*leEx24*.

Finally, to perform the complementation test I crossed *cdk-4(drp5);inIs179[ida-1::gfp];him-8(e1489)* males into *cdk-4(gv3)*;*ozEx76;*o*leEx24* animals. Next, I selected the non *cdk-4* rescue array *ozEx76,* carrying hermaphrodite F1 cross progeny, that did however, bear the AMso masculinising o*leEx24* array, and examined their *nom* phenotype by *inIs179[ida-1::gfp]* expression.

The masculinised AMso of *cdk*-4(*drp5*/O) hermaphrodites did not produce any MCMs (n=35 cells), matching what was found in *cdk-4*(*drp5/drp5*) animals, see Figure 5.6 (e). The null allele of *cdk-4*(*gv3*) failed to complement the *nom* phenotype of *cdk-4*(*drp5*) providing evidence that they are both alleles of the same gene.

5.3.5 Wild type cdk-4 rescues the nom phenotype of cdk-4(drp5) and cdk-4(drp8)

In order to confirm if *nom-5(drp5)* and *nom-8(drp8)* are indeed alleles of *cdk-4* it is essential to verify if a wild type copy of *cdk-4* rescues the *nom* phenotype. I was able to obtain two constructs containing wild type *cdk-4, vmIs9[unc-119;cdk-4p::cdk-4::FLAG::cdk-4 3'UTR]* (The et al., 2015) a gift from Sander van den Heuvel and *ozEx76 [(pKMii1177) cdk-4p::CDK-4::GFP + (pAD46) sur-5::DsRed)]* (Fox et al., 2011) which both rescue the *cdk*-4 null allele *gv3* (Fox et al., 2011; The et al., 2015). I began by crossing *nom-5(drp5);inIs179[ida-1::gfp]*;*him*-8*(e1489)* into SV929 which contains the null allele *cdk-4(gv3)* and the integrated wild type *cdk-4* construct *vmIs9*. I selected *inIs179[ida-1::gfp]*;*him-8(e1489)* F2s that threw only non-larval arrested animals with mixture of *nom* and wild type MCM phenotype males, inferred to be homozygous for *drp5* and hemizygous for *vmIs9*, the presence of MCMs is assumed to be due to the rescue of the *nom* phenotype by *vmIs9*. Hermaphrodites from plates with this phenotype were singled for one more generation to ensure the *cdk-4* null allele *gv3* was not in the background, by confirming there were no larvally arrested animals and the progeny checked for mendelian segregation. These segregated as expected (n=52) with 54% having

a mixture of males with *nom* and wild type MCMs, 23% only *nom* males and 23% only wild type males. One plate of F4s of each of these phenotypes was genotyped using the MS9 & MS10 primers which amplify a 563bp region around the *cdk-4(drp5)* lesion. When this fragment is digested with the BceAI restriction enzyme, wild type *cdk-4* will produce two bands of 399bp and 164bp however the *cdk-4(drp5)* lesion masks the BceAI cut site, therefore an undigested 563bp band indicates the presence of *cdk-4(drp5)* while two bands of 399bp and 164bp indicate wild type *cdk-4* see the control in Figure 5.7. As all plates show an undigested band (Figure 5.7 arrowhead) this indicates that *drp5* was homozygous in the F3s. The F4 plate which only produced males with wild type MCMs also has digested bands indicating the presence of both wild type *cdk-4* from the vmIs9 transgene and *cdk-4(drp5)*, thus demonstrating that *vmIs9* fully rescues the *nom-5* phenotype see Figure 5.7/Table 5.2.

Table 5.2 *vmIs9* rescues *nom-5(drp5)*

	Genotype	♂*nom* phenotype	n=
Control	WT *inIs179[ida-1::gfp]*;*him-8(e1489)*	**0%**	50
	nom-5(drp5);inIs179[ida-1::gfp];*him-8(e1489)*	**100%**	50
nom-5(drp5);inIs179[ida-1::gfp];*him-8(e1489)* X SV292			
F3 sibs	*cdk-4*(*drp5*);*vmIs9 cdk-4*(+)	**0%**	50
	cdk-4(*drp5*);no *vmIs9*	**100%**	50

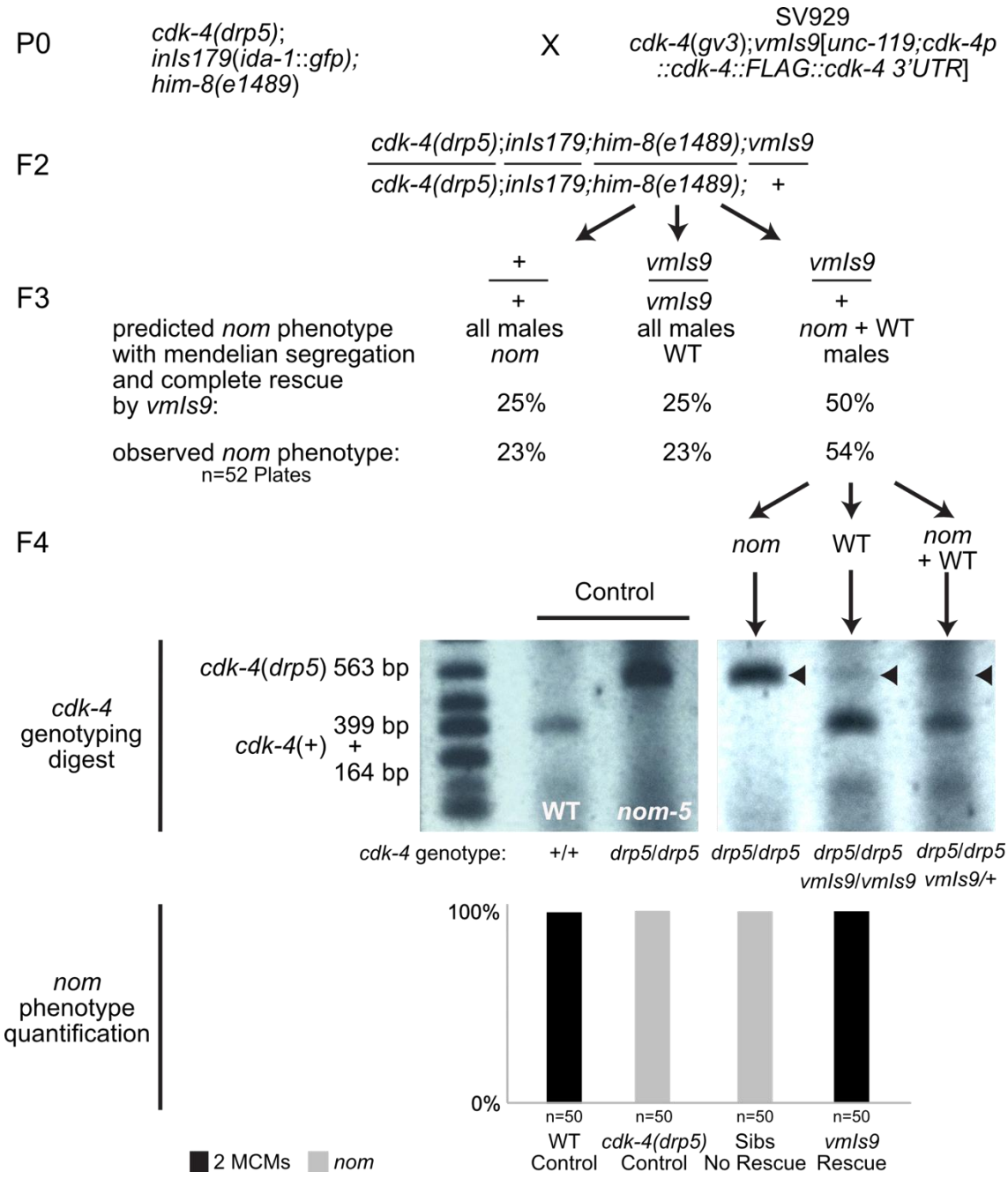

Figure 5.7 *VpIs9* rescues *nom-5(drp5)*

Crossing scheme and genotyping showing the rescue of the *nom* phenotype of *nom-5(drp5)* by the *vmIs9* construct which contains wild type *cdk-4*. The only source of wild type *cdk-4* is the from the *vmIs9* construct, therefore the presence of MCMs in the F3 generation can only be explained by the inheritance of *vmIs9*, as *cdk-4(drp5)* or *cdk-4(gv3)* animals cannot produce MCMs. The *nom* phenotype, assessed by *inIs179[ida-1::gfp]*, is observed to segregate in a mendelian fashion with approximately 25% of F2 animals' male progeny completely lacking MCMs, another 25% in which the *nom* phenotype is completely rescued and 50% with a mixture of *nom* and wild type males. This is most simply explained by the mendelian segregation of *vmIs9* which completely rescues the *cdk-4(drp5) nom* phenotype. Genotyping by means of a digest with the restriction enzyme BceAI, which cuts a 563bp fragment of wild type *cdk-4* but not *cdk-4(drp5)* confirms that *cdk-4(drp5)* animals that do not carry *vmIs9* are 100% *nom* while *cdk-4(drp5)* animals that carry *vmIs9* are 100% rescued and appear wild type for the *nom* phenotype.

Next, I introduced the extrachromosomal array *ozEx76[(pKMii1177) cdk-4p::CDK-4::GFP + (pAD46) sur-5::DsRed)]* (Fox et al., 2011) into both *cdk-4(drp5)* and *cdk-4(drp8), inIs179[ida-1::gfp]* strains in order to confirm that wild type *cdk-4* rescues the *nom* phenotype in both alleles. The *nom* phenotype was completely rescued in array carrying *cdk-4(drp8)* animals (n=50/50) incubated at a non-permissive temperature (26 °C), while non-array carrying sibs were not rescued (n=50/50). The *nom* phenotype was rescued in 96% of array carrying *cdk-4(drp5)* animals in either one or both MCMs (n=48/50) (Figure 5.8), while non-array carrying sibs were not rescued (n=50/50).

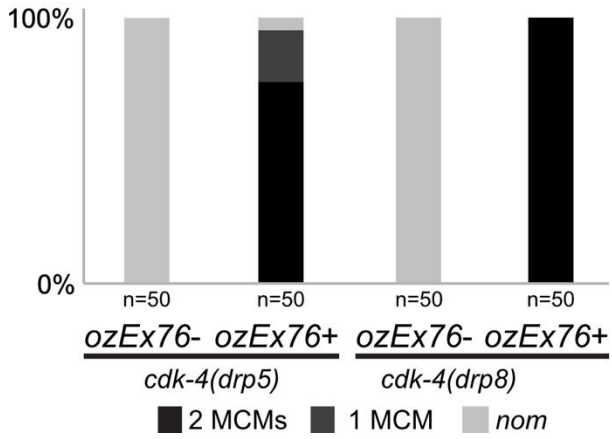

Figure 5.8 *nom* phenotype of *cdk-4(drp5)* and *cdk-4(drp8)* is rescued by *ozEx76*

The *nom* phenotype of *cdk-4(drp5)* and *cdk-4(drp8)* (26°C) strains, assessed by *inIs179[ida-1::gfp]*, was observed in siblings that carry (+) the *ozEx76*, which contains wild type *cdk-4* and siblings that do not (-). The *nom* phenotype is rescued in both *cdk-4(drp5)* and *cdk-4(drp8)* when they carry *ozEx76* but not in non-array carrying animals. n=number of animals.

5.4 *cdk-4(drp5)* and *cdk-4(drp8)* appear to specifically affect AMso division

5.4.1 cdk-4(drp5) complements the larval arrest phenotype of cdk-4 null animals

As *cdk-4* is required for G1/S progression in all post-embryonic cell divisions the null allele *cdk-4(gv3)* has an extremely strong larval arrest phenotype (Park & Krause, 1999). The progeny of BS1175 *cdk-4(gv3)*;*ozEx76 [(pKMii1177) cdk-4p::CDK-4::GFP + (pAD46) sur-5::DsRed)]* animals, that do not carry the rescuing array, all arrest as larvae before reaching adulthood (n=200) (Figure 5.9). Only a minute proportion(2.8%) of *cdk-4* wild type BAR82 *inIs179[ida-1::gfp]*;*him-8(e1489)* animals fail to develop to adulthood (n=214). *cdk*-4(*drp5*) animals develop similarly to wild type animals with only 4% of animals not making it to adulthood (n=170). This is an indication that post-embryonic blast cell division is not apparently affected in *cdk*-4(*drp5*) animals. By counting the (non-array carrying) F1 cross progeny of wild type male BAR82 and BS1175 hermaphrodite animals we can see that a single copy of *cdk-4* is enough for normal development. The vast majority of hemizygous *cdk-4*(+/O) hermaphrodites survive to adulthood, as 45% of animals arrest (n=140), these correspond to the male progeny which only inherit a single copy of *cdk-4*(*gv3*) and thus fail to develop. The same proportion of larval arrest (45%) is seen in the F1 cross progeny of male *cdk*-4(*drp5*) and BS1175 animals (n=172) indicating that, like the wild type, a single copy of *cdk*-4(*drp5*) is enough to rescue the larval arrest phenotype (Figure 5.9). Surprisingly, despite *cdk*-4(*drp5*), acting as a null for AMso division in XO males and in XX masculinised hermaphrodites, a single copy of *cdk*-4(*drp5*), is sufficient to for apparently normal hermaphrodite development into adulthood. In combination with the finding that a single copy of wild type *cdk-4* or *cdk*-4(*drp5*) are equally capable of AMso division in XX masculinised hermaphrodites (Figure 5.6 d,e) this implies that a general reduction of *cdk-4* activity is unlikely to be the driving factor in the AMso division defect of *cdk*-4(*drp5*).

5.4.2 cdk-4(drp5) is not defective in most post-embryonic blast cell division

At first glance it may appear unsurprising that a key cell cycle regulator may be implicated in Class II mutations, which are defined by AMso division defects. However, due to the design of the screen any mutants resulting in major deleterious effects on key cell cycle regulators would be unlikely to survive to adulthood and therefore not be pulled out of the screen. Indeed, various molecular lesions of *cdk-4* resulting in modification of conserved residues (Figure 5.3), truncated versions of the protein, or deletions have the effect of inhibiting post-embryonic divisions and have a strong larval arrest phenotype (Boxem & van den Heuvel, 2001). Both *cdk-4(drp5)* and *cdk-4(drp8)* appear phenotypically wild type in gross morphology and general behaviour, they have uninterrupted alae which are produced by the seam cells, have functioning rectal epithelia, while males are capable of mating indicating that there is no major defect of the somatic gonads, vulva or male tail development, all of which develop post-embryonically. As *cdk-4* is required for all post-embryonic blast cell divisions it seems highly unusual for one specific post-embryonic division such as the AMso to be singularly affected in the *cdk-4* alleles isolated from this screen.

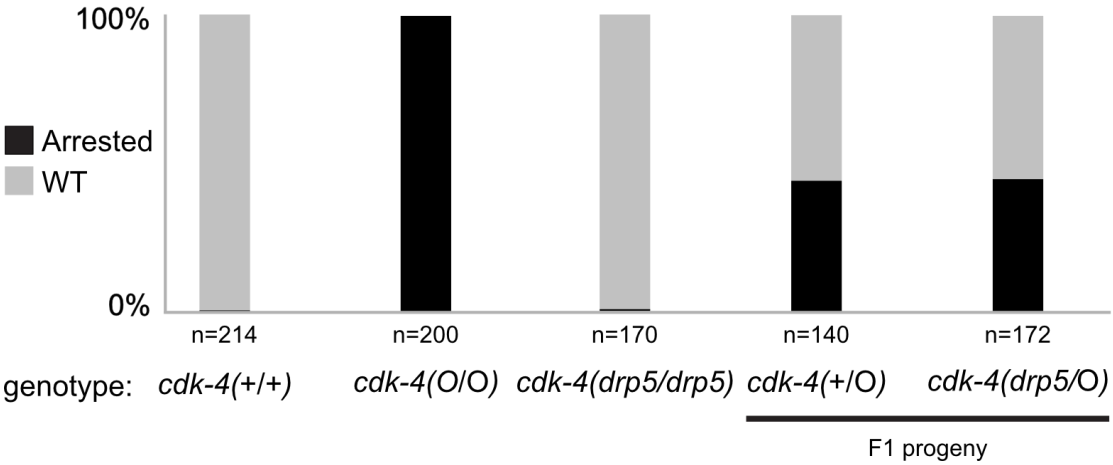

Figure 5.9 *cdk-4(drp5)* complements the larval arrest phenotype of *cdk-4* null animals

The *cdk-4*(*O/O*) null allele *gv3* blocks all post-embryonic blast divisions and results in a completely penetrant larval arrest phenotype. Strikingly however the *cdk-4*(*drp5/drp5*) allele does not result in defects of larval development and performs largely like wild type *cdk-4*(*+/+)*. Examining the F1 progeny of *cdk-4*(*+)* and *cdk-4*(*drp5)* males with *cdk-4*(*O/O*) hermaphrodites shows that a single copy of wild type *cdk-4*(*+/O)* is enough to completely rescue the larval arrest phenotype, the 45% of arrested progeny correspond to males which inherit a single null copy of *cdk-4* on the X chromosome from their *cdk-4*(*O/O*) mothers. Similarly, a single copy of *cdk4(drp5)*, *cdk-4*(*drp5/O*) is enough to completely rescue the larval arrest phenotype.

It is possible that altering the T-loop of CDK-4 might diminish CDK at G1/S, resulting in failure of AMso division and perhaps other postembryonic divisions. The AMso may also require a higher G1/S CDK activity threshold or have differences in G1/S signalling compared with other postembryonic blast cells. In order to determine if other post-embryonic divisions were affected, the AMso division null allele *cdk-4(drp5)* was used, I counted the number of male rays and the hermaphrodite specific ventral cord neurons VC neurons which are visible with *inIs179[ida-1::gfp]*. The number of rays in *cdk-4(drp5)* males is normal as is the number of *cdk-4(drp5)* hermaphrodite VC neurons which descend from the P lineage (Table 5.3). While not exhaustive most post-embryonic lineages in both males and hermaphrodites appear at least superficially wild type.

Table 5.3 Sex-specific post-embryonic blast cell lineage divisions in *drp5*

Genotype	♂ Animals with 18/18 rays present	n=
WT *inIs179[ida-1::gfp];him-8(e1489)*	**100%**	50
drp5;inIs179[ida-1::gfp];him-8(e1489)	**100%**	50
	♀ Animals with 6/6 VC neurons present	n=
WT *inIs179[ida-1::gfp];him-8(e1489)*	**100%**	20
drp5;inIs179[ida-1::gfp];him-8(e1489)	**100%**	20

5.4.3 A complex behavioural response is unaltered in cdk-4(drp8) mutants

An excellent way to test for general pleiotropies that may be caused by cell division defects, particularly in the nervous and locomotor systems, is to test a complex behavioural response that required the proper functioning of all major systems in the animal. The sexual conditioning response described in Chapter 3 is an ideal such test. The conditional mutant *cdk-4*(*drp8*) was selected for testing of sexual conditioning to olfactory cues (performed by Lucy Lin in the Barrios Lab). Similar to what was shown in Chapter 3 males respond to the olfactory cues, benzaldehyde and diacetyl in sexual conditioning switch assay, the same way as they do to salt as a gustatory cue. *cdk-4*(*drp8*) animals at the permissive temperature behave similar to wild type animals, while at the non-permissive temperature when they lack MCMs, they do not display the sexual conditioning switch response (Figure 5.10), they behave similarly to MCM laser ablated animals show in Chapter 3. While this is not an exhaustive analysis of post-embryonic development or behaviour, taken together these results suggest that any pleiotropies are minimal and the cell division defect in the *cdk-4*(*drp5*) and *cdk-4*(*drp8*) mutants may be specific to the AMso.

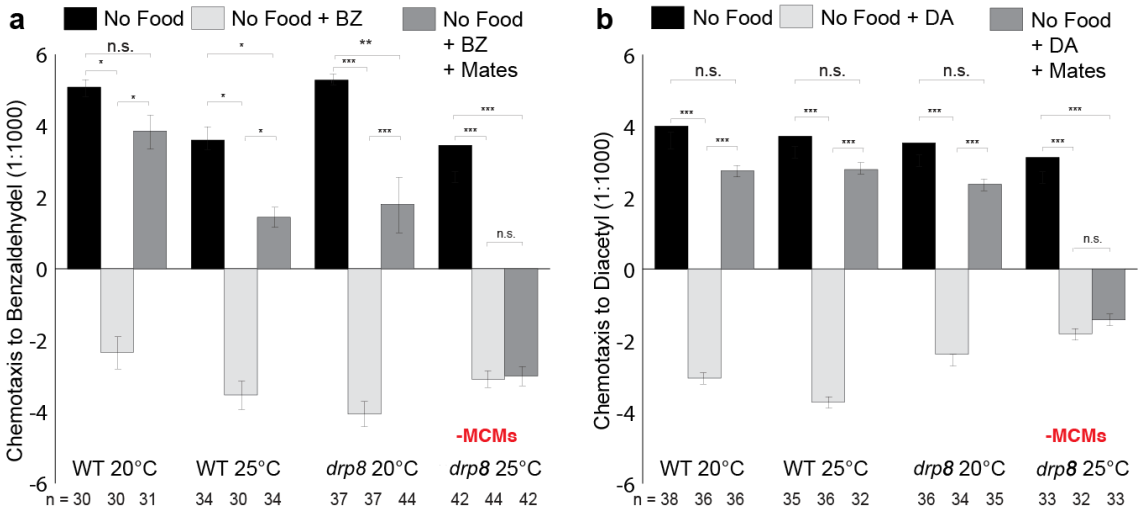

Figure 5.10 The sexual conditioning response is normal in *cdk-4(drp8)*

(a) Benzaldehyde and (b) diacetyl chemotaxis scores of *cdk-4(drp8);inIs179[ida-1::gfp]; otIs356[rab-3::rfp];him-8(e1489)* mutant males maintained at 20℃ and 25℃ and wild-type inIs179*[ida-1::gfp];otIs356[rab-3::rfp];him-8(e1489)* males maintained at 20℃ and 25℃ tested for the sexual conditioning switch.
cdk4-(drp8) males at the permissive temperature do not behave significantly different from wild type showing that there are no pleiotropies that generally affect behaviour. At the non-permissive temperature *cdk-4(drp8)* males behave as MCM laser ablated animals. (Experiments performed by Lucy Lin) Error bars indicate S.E.M. Mann- Whitney U-test with Bonferroni correction was used for statistical analysis. ***P < 0.001; **P < 0.01; *P < 0.05; NS = no statistically significant difference (P ≥ 0.05).

5.5 Summary

Using a novel mapping by sequencing technique for male specific phenotypes I mapped both the Class II mutants *nom-5* and *nom-8* to 13.5Mb on the X chromosome. Through rescue and complementation, I showed that *nom-5* and *nom-8* are alleles of *cdk-4*, and rename them *cdk-4(drp5)* and *cdk4(drp8)* respectively. The construct *vpIs9*, which contains wild type *cdk-4* rescues the *nom* phenotype in *nom-5*, while a second independently generated construct, *ozEx76*, also containing wild type *cdk-4*, similarly rescues both *nom-5* and *nom-8*. By using cell type specific masculinisation of the mother cell, I was able to investigate the basic nature of *cdk-4(drp5)* allele. The known a *cdk-4* null allele *gv3*, which is required for all post-embryonic divisions, does not complement the *nom* phenotype in the masculinised XX AMso of *nom-5* mutants, however, the larval arrest phenotype of *cdk-4(gv3)* is 100% complemented by *nom-5*. Additionally, the lack of a *nom* phenotype in *cdk-4(+)*/*cdk-4(drp5)* heterozygotes indicates that the *cdk-4(drp5)* allele does not have a dominant effect.

Sequence analysis predicts that both *cdk-4(drp5)* and *cdk-4(drp8)* affect the T-loop, implicating the important regulatory region of CDK-4, in MCM development. Together the evidence presented in this chapter implicates the key cell cycle G1/S regulator, *cdk-4*, in this glia-to-neuron transition in the worm. Thus, laying the groundwork necessary for the continued investigation of the cell cycle in the early regulation of MCM development and suggesting new avenues for investigation, such as potential CDK interactors and canonical or non-canonical G1/S regulators. The apparent specificity of this defect in a gene required for all post embryonic divisions opens up intriguing questions about the mechanism behind this glia-to-neuron transition. In the next chapter I will investigate the mechanisms guiding the early steps of both MCM and PHD specification in order to develop a basic understanding of the factors involved in these distinct glia-to-neuron cell fate transformations.

Chapter 6

Cell cycle inhibition and key cell fate determinants are coordinated in both proliferative and direct glia-to-neuron cell fate switches

6.1 Overview

With the evidence acquired about the basic nature of the Class II *cdk-4* alleles, I began investigating the possible mechanisms involved in AMso division and MCM development and how they compare to PHD development. Based on the sequence features of *cdk-4(drp5)* and *cdk-4(drp8*) an attractive idea is that specific activation of CDK-4, through T-loop phosphorylation, is required in the male AMso for MCM development. CDK7 has been shown to act as the general CAK in mammalian cells and can phosphorylate most CDKs (Fisher & Morgan, 1994; Kato et al., 1994), it is likely to phosphorylate the T-loop of CDK4 and promote G1/S progression (Bisteau et al., 2013; Schachter et al., 2013). CDK7 also has a dual role in the transcription promoting complex, where it phosphorylates RNA polymerase II to initiate transcription. There is a single homologue of CDK7 in *C. elegans*, and using the conditional allele *cdk-7(ax224*), Wallenfang & Seydoux (2002) provide evidence that *cdk*-7 is required for cell cycle progression in the embryo and likely acts as a CAK at various points in the cell cycle. I therefore investigated if *cdk-7* is required for MCM development, however, this does not appear to be the case. Next, I examined the involvement of CKIs in the earliest steps of MCMs and PHD development. Surprisingly, I found that *cki-1* is expressed in hermaphrodite AMso, PHso1 and PHso2 throughout development despite the fact that no divisions or cell fate transformations occur. *cki-1* expression is similar in the male until the time of the cell fate transformations, where immediately after AMso division both daughter cells continue to express *cki-1*, however, *cki-1* levels decline in the MCM daughter in adulthood but are still sustained in the self-renewed AMso. Concomitantly, during the PHso1-to-PHD transformation,

cki-1 expression is sharply downregulated. The finding of a key G1/S inhibitor being dynamically regulated in a cell fate transition, which does not require cell division, is in itself perplexing but following up on this I examined typical S-phase markers and found that they too are expressed during PHD specification.

Finally, I also examined the possible involvement of known cell fate determinants in MCM and PHD development. Specifically, I examined the downstream effectors of the Wnt asymmetry pathway, as these factors are known to affect the asymmetric fate of daughter cells and are involved in sexual specification, and the proneural factor *hlh-14*, the worm homologue of ASCL1. I found that POP-1 is localised in the AMso and MCMs in a fashion consistent to what is seen in SGP cell development and that *hlh-14* is transiently expressed early in MCM and PHD development.

6.2 AMso division does not depend on *cdk-7* activity

In order to assess the possibility of *cdk-7* acting as a CAK that directly regulates G1/S in AMso to MCM transition, introduced the conditional *cdk-7* allele *ax224* into two strains each containing an MCM neuronal and an AMso marker. The loss of *cdk*-7 activity does not seem to affect AMso division, as *cdk-7*(ax224*)*;*nsIs198[mir-228::gfp]*; *otIs356[rab-3::rfp::NLS]* L1 males shifted to the non-permissive temperature of 25°C have AMsos that divide 99% of the time (n=99/100 AMso divide), comparable to what is seen in *cdk-7*(ax224) animals kept at the permissive temperature (n=50/50 AMso divide) as well as *cdk-7*(+) animals at 25°C (n=40/40 AMso divide) (Table 6.1). Similarly, the AMso of *cdk-7*(ax224*)*;*inIs179[ida-1:gfp];drpIs3[lin-48::tdTomato]* L1 males shifted to 25°C divide 100% of the time (n=108/108 AMso divide), comparable to what is seen in *cdk-7*(ax224) animals kept at the permissive temperature (n=80/80 AMso divide) as well as *cdk-7*(+) animals at 25°C (n=40/40 AMso divide) (Table 6.1). Additionally, a small proportion of *cdk-7(ax224);inIs179[ida-1:gfp];drpIs3[lin-48::tdTomato]* posterior daughters showed a neuronal marker expression defect at 25°C (7.4%), the same proportion of AMso, ectopically expressed the neuronal subtype marker *ida-1*::*gfp* (7.4%) after division. A smaller *rab-3*::*rfp* expression defect (5%) was seen in *cdk-7*(ax224*)*;*nsIs198[mir-228::gfp]*; *otIs356[rab-3::rfp::NLS]* animals at 25°C but no ectopic *rab-3*::*rfp* expression was seen in the AMso. These results indicate that *cdk-7* is not likely to direct AMso division but may affect MCM neuronal gene expression via its role in transcription.

Table 6.1 *cdk-7* does not affect AMso division

Genotype	AMso division Phenotype		
	Wild type %	*nom* %	n=
cdk-7(ax224);mir-228::gfp;rab-3::rfp	99	1	100
cdk-7(ax224);mir-228::gfp;rab-3::rfp	100	0	50
mir-228::gfp;rab-3::rfp 25°C	100	0	40
	Wild type %	*nom* %	
cdk-7(ax224);lin-48::tdtom;ida-1::gfp	100	0	108
cdk-7(ax224);lin-48::tdtom;ida-1::gfp	100	0	50
lin-48::tdtom;ida-1::gfp 25°C	100	0	40

6.3 The regulation of cell cycle quiescence is associated with both proliferative and direct glia-to-neuron cell fate switches

6.3.1 Hermaphrodite amphid and phasmid sockets are kept in a state of quiescence throughout life

As vertebrate neural progenitors are kept in a state of quiescence and as one of the chief negative regulators of the G1/S transition and interactors of CDK4, I investigated the potential involvement CKIs in MCM development. I performed a developmental analysis of *cki-1* expression, the primary CKI in the worm, using *maIs113*[*cki-1::GFP* + *dpy-20*(+)] (Y. Hong et al., 1998), in combination with *drpIs3[lin-48::tdTomato]* in order to identify the AMso and PHso1/PHD. The expression of *cki-1* is an indicator of cells that have exited the cell cycle and has been used as a marker of cell cycle quiescence. Surprisingly, despite the typical developmental role of *cki-1*, in maintaining progenitor cells quiescent in G1 until subsequent proliferation, the hermaphrodite AMso as well as PHso1 and PHso2 which do not divide or undergo cell fate transformations express *cki-1::GFP* throughout life (Figure 6.1). The AMso are born in the embryo (Figure 1.23) and seem to maintain *cki-1::GFP* expression well into adulthood, when viewed at L1, *cki-1::GFP* in the AMso can be seen at the same levels as many other cells which have recently exited the cell cycle. The PHso1 and PHso2 are not born until mid L1 (Figure 1.23), by L3 *cki-1::GFP* is strongly expressed in the phasmid sockets. In L3 *cki-1::GFP* is still evident in the AMso while in most other non-cycling cells it is no longer visible, cells known to divide during larval development such as the seam cells are also seen to strongly express *cki-1::GFP*. The PHso2 can be identified by morphology, location immediately posterior to PHso1 and close association with the socket structure. From L4 through to 2 day old adults *cki-1::GFP* is maintained in the AMso and PHso1 and PHso2 (Figure 6.1) when most other *cki-1::GFP* in the animal is diminished, expression in PHso1 and PHso2 remains particularly strong. I next examined the effect of the *cki-1*(*gk132*) (Buck et al., 2009) mutation (which gives rise to a putative deletion of the start codon) on AMso and PHso1 development in hermaphrodites. Homozygous *cki-1*(*gk132*) animals are larval lethal, I therefore examined *mln1* balanced animals bearing *drpIs3*, and found

that balanced animals may exhibit extremely weak haploinsufficiency, AMso were not observed to divide, however PHso1 very rarely show some PHD like morphology (n=5/300 animals).

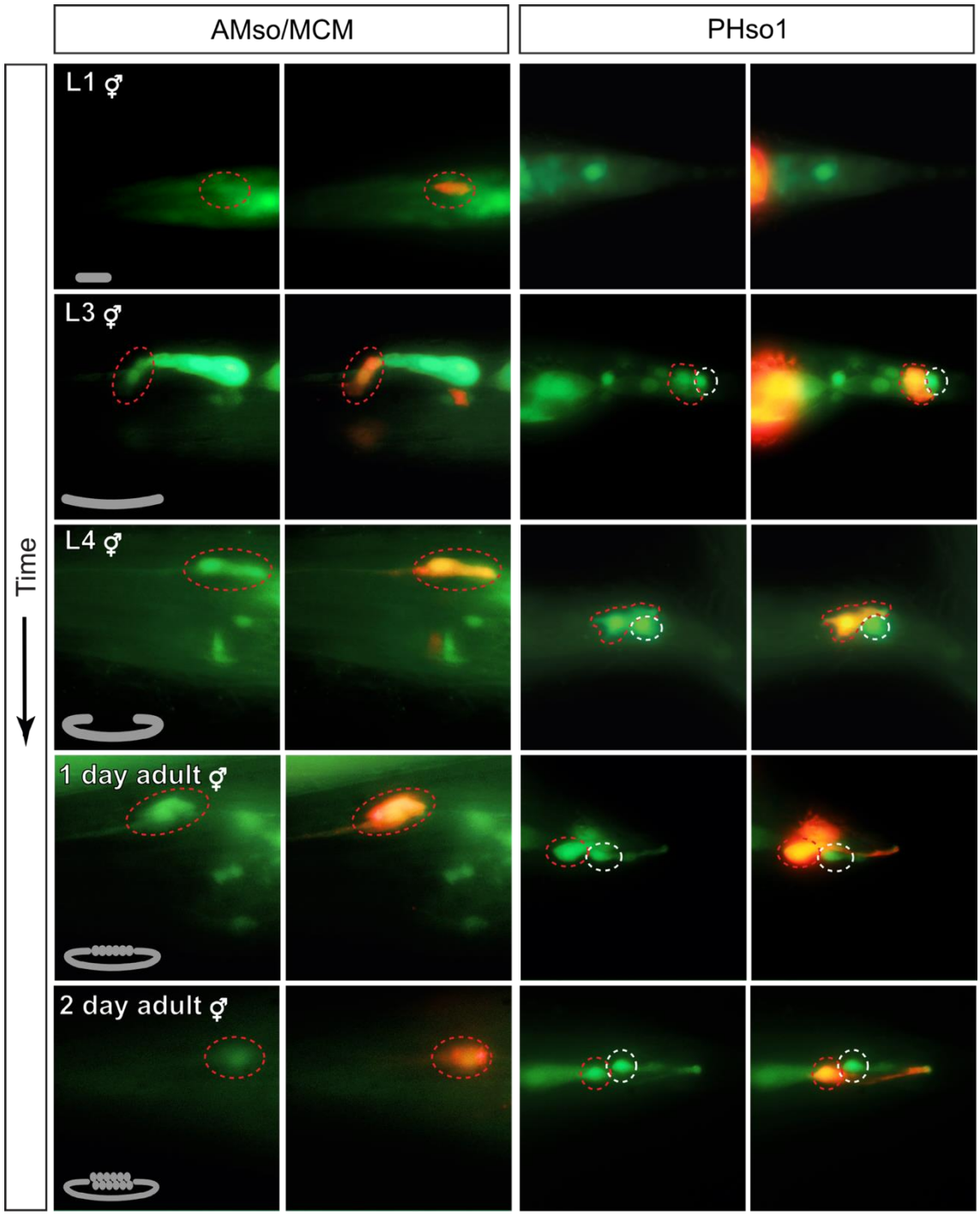

Figure 6.1 The hermaphrodite amphid and phasmid sockets express *cki-1* throughout life

A time course showing representative fluorescence images of the expression of the quiescence marker *cki-1*, in the AMso and PHso1 through development in hermaphrodite animals of different ages. AMso and PHso1 are labelled in red with *drpIs3[lin-48::tdTomato], cki-1* expression is visualised with *maIs113*[*cki-1::GFP* + *dpy-20*(+)] in green.

Figure 6.1 The hermaphrodite amphid and phasmid sockets express *cki-1* throughout life

Each row shows fluorescence images with the green channel side by side with composite images of the red and green channels together; of the head (left) and tail (right) region of the same animal. The relative ages of animals are assessed by the extent of gonad progression.

In L1 *cki-1* expression can be seen in many cells in the head including cells that have recently terminally divided in the embryo, this includes the AMso (circled in red) which can be seen to express *cki-1* at approximately the same level. The PHso1 cannot yet be visualised by the expression of *lin-48* as it is born in mid L1.

By L3 most of the cells in the head outside of the pharynx can no longer be seen to express *cki-1* with the exception of the large seam cells which reiteratively divide during larval development and strongly express *cki-1*. Notably however, after many other embryonically born cells cease to express *cki-1*, the AMso still appear to maintain the expression of *cki-1* long after their terminal division. In the tail, the newly born PHso1(circled in red) and PHso2(circled in white) can be seen to strongly express *cki-1* which is typical of recently divided cells. PHso2 is identified by its location immediately posterior to PHso1 and the typical morphology or the socket structure. Again, the seam cells and some recently divided cells in the rectal epithelium can also be seen to express *cki-1*.

In L4 *cki-1* the head looks similar to L3 where the AMso can still be seen to strongly express *cki-1*. In the tail PHso1 and PHso2 can still be seen to strongly express *cki-1* while other cells that were born at a similar time no longer do so. This pattern of expression persists even 2 days into adulthood and is particularly pronounced in the PHso1 and PHso2, when almost all other cells have ceased to express *cki-1*. It is remarkable that the embryonically born AMso appear to express the quiescence marker throughout the life of the animal well into old age, a capability which is unique in the animal.

6.3.2 In males cki-1 is downregulated in the MCMs after proliferation as well as in the PHso1/PHD after the direct cell fate switch

A developmental analysis of *cki-1* expression in males was performed in the same way as was done for the hermaphrodite. At early L3 the male amphid and phasmid sockets appear much the same as they do in the hermaphrodite, all strongly expressing *cki-1::GFP*. In the AMso *cki-1::GFP* is continuously expressed, leading up to division in early L3 and is maintained after division in the self-renewed AMso daughter cells after the birth of the MCMs (Figure 6.2). In the newly born MCMs *cki-1::GFP* is strongly expressed and is clearly visible in the late L4 stage, as might be expected for cells exiting the cell cycle, however, by adulthood *cki-1::GFP* is downregulated in the MCMs. Surprisingly however, *cki-1::GFP* expression is maintained in the AMso daughter cells well after it is no longer detectable in their sister cells, the MCMs, despite now having terminally exited the cell cycle. In this way the male AMso are similar to the hermaphrodite. In contrast to the AMso which continue to express *cki-1* despite having terminally divided in both males and hermaphrodites, the male PHso1 appear downregulate *cki-1* after their cell fate transformation into neurons, despite not undergoing division. The PHso1 express *cki-1::GFP* throughout their cell fate transformation into the PHD neurons during L3, after which *cki-1::GFP* is downregulated and is no longer detectable in young adults (Figure 6.2). The *cki-1::GFP* dynamics in the PHso1/PHDs appear to be closely coordinated in time with those of the MCMs. An additional remarkable finding is that the male Phso2 cells maintain *cki-1::GFP* throughout their life much in the same way as they do in the hermaphrodite, in spite of the fact that the PHso2 do not appear to undergo any division or cell fate transformations in either sex. Taken together these results suggest that the male AMso, PHso1 and PHso2, may regulate cellular quiescence, as assessed by *cki-1* expression, in a distinct way in each of the three sets of cells. Furthermore, the coincidence of a decline in the cellular quiescence factor with the PHso1 to the PHD transformation implies a relationship between the cell cycle and this direct cell fate switch.

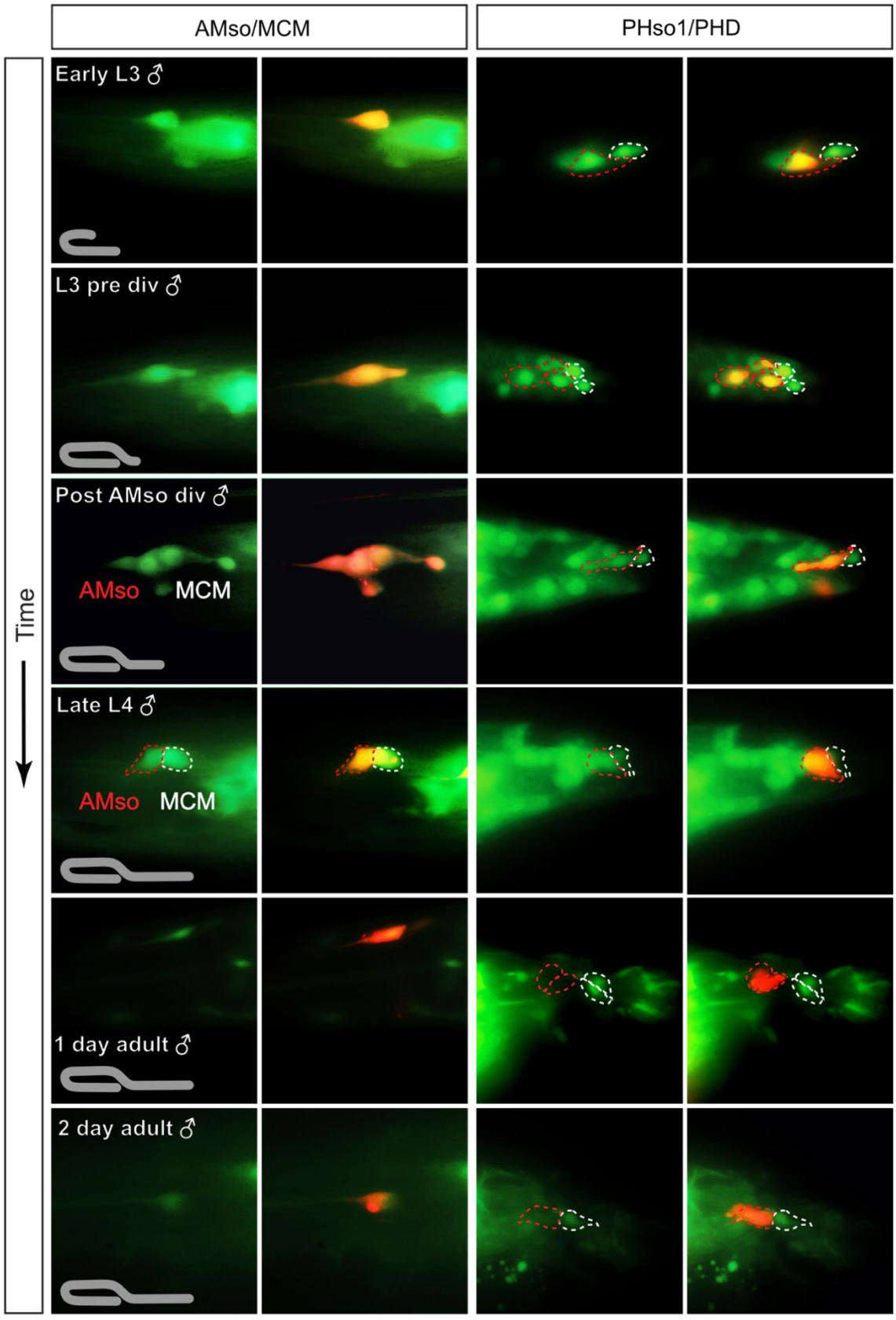

Figure 6.2 *cki-1* dynamics in males correlate with neuronal differentiation

Figure 6.2 *cki-1* dynamics in males correlate with neuronal differentiation

A time course showing representative fluorescence images of the expression of the quiescence marker *cki-1*, in the AMso and PHso1 through development, in male animals of different ages. AMso and PHso1 are labelled in red with *drpIs3[lin-48::tdTomato*], *cki-1* expression is visualised with *maIs113*[*cki-1::GFP* + *dpy-20*(+)] in green. Each row shows fluorescence images with the green channel side by side with composite images of the red and green channels together; of the head (left) and tail (right) region of the same animal. The relative ages of animals are assessed by the extent of gonad progression and by tail development in L4.

Up to the L3 stage the *cki-1* expression pattern is the same in the male as it is in the hermaphrodite. In the L3 stage *cki-1* is strongly expressed in the AMso before and after the division, while immediately after the division *cki-1* is strongly expressed in the newly born MCMs. In the male tail *cki-1* expression can be seen in many cells at this time as the copulatory structures develop. In PHso1/PHD (circled in red) and PHso2 (circled in white) *cki-1* appears to be strongly expressed.

During the L4 stage when most of sexual maturation occurs *cki-1* is still strongly expressed in both the AMso and MCMs. Similarly, in the tail *cki-1* expression remains in PHso1/PHD and PHso2

In adulthood *cki-1* expression declines in the MCMs but surprisingly, persists in the AMso well into old age, despite having undergone its terminal division. In the adult PHD, *cki-1* expression is completely lost despite not having undergone cell division. Interestingly *cki-1* expression remains in PHso2, as it does in the hermaphrodite.

6.4 S-phase markers are expressed at the time of the PHso1-to-PHD transition

Following the unexpected finding of a key G1/S regulator being associated with the direct PHso1-to-PHD transition, I questioned whether the PHso1 enters the S-phase during this transition. I examined fluorescent reporter gene expression in PHso1, driven by the promoters of two S-phase genes; *mcm-4*, a DNA helicase subunit and necessary component of the pre-replication complex, and the ribonucleotide reductase, *rnr-1*, required for the final step of deoxyribonucleotide synthesis, both required for DNA synthesis. The AMso/MCM and PHso1/PHD were labelled using *drpIs3[lin-48::tdTomato]*, and examined around the time of the birth of the neurons, for co-expression with *maIs103*[*rnr-1p*::*GFP+unc-36*(+)] and *heSi193*[*Pmcm-4*::*CDK sensor*::*eGFP*::*tbb-2 UTR + Cbr-unc119*(+)] which drives eGFP as a part of a CDK sensor (Van Rijnberk et al., 2017). The developmental expression pattern was found to be highly similar for both S-phase markers. In early L3 the S-phase markers are scarcely detectable, however between the time the gonad begins to extend posteriorly and the point at which it crosses back over its point of origin both *mcm-4* and *rnr-1* are upregulated in both the AMso and PHso1 (Figure 6.3). At this stage the AMso is as yet undivided and the characteristic socket morphology can still be clearly observed in PHso1. The S-phase markers perdure into the L4 stage, after the birth of the MCM and the neuronal morphological features of PHDs begin to become apparent. The expression of two S-phase markers introduces the possibility that replication may occur in the direct glia-to-neuron cell fate switch as well as the proliferative division. Furthermore, the developmental analysis again reveals a tight coordination of the cell cycle markers during the generation of both neuron types.

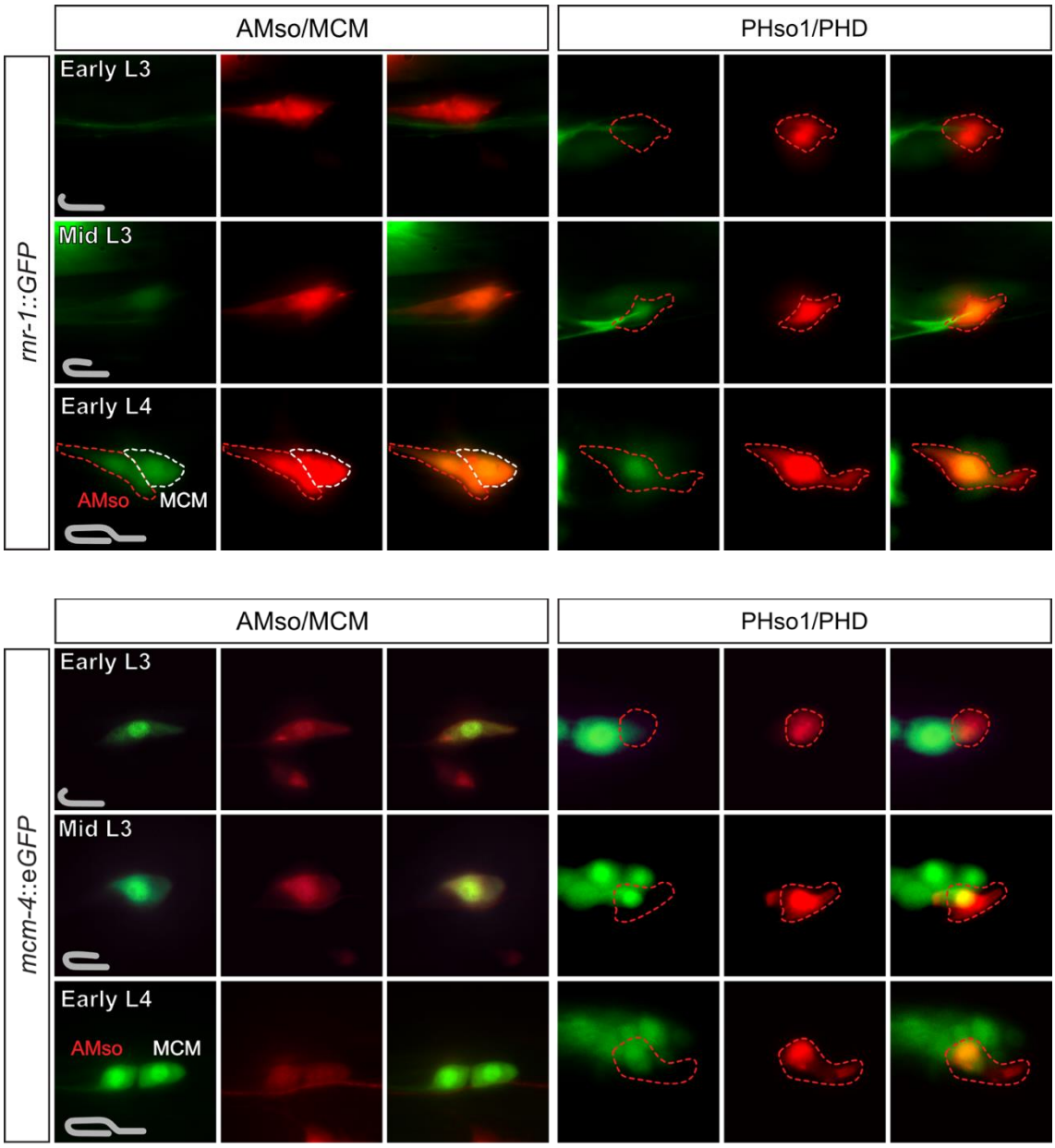

Figure 6.3 S-phase markers are expressed in the PHso1-to-PHD transition

Time course showing representative fluorescence images of the expression of S-Phase markers *rnr-1*(top) and *mcm-4* (bottom), in the AMso and PHso1 through development in male animals of different ages. AMso and PHso1 are labelled in red with *drpIs3[lin-48::tdTomato], rnr-1* expression is visualised with *maIs103*[*rnr-1p*::*GFP+unc-36*(+)] and *mcm-4* with *heSi193*[*Pmcm-4*::*CDK sensor*::*eGFP*::*tbb-2 UTR* + *Cbr-unc119*(+)] in green. Each row shows fluorescence images with the green and red channels, with composite images of the red and green channels together; of the head (left) and tail (right) region of the same animal. The relative ages of animals are assessed by the extent of gonad progression and by tail development in L4.

By mid L3, as the gonad begins to extend posteriorly, both S-Phase markers begin to be strongly expressed in the AMso before the division and perdure in both daughter cells for a short time after. Intriguingly however, both of the S-phase genes are also expressed in PHso1/PHD at the time of the transition, despite the fact that cell division is not required for this transition. This hints that there may be an unforeseen link between cell cycle regulation and neuronal differentiation in these cells.

6.5 Wnt asymmetry pathway markers are expressed early in MCM development

The downstream effectors of Wnt asymmetry pathway have been shown to affect the asymmetric development of daughter cells and regulate sex-specific features, such as in the somatic gonad. As a likely Wnt signal leads to the export of *pop-1* from nucleus which is known to affect the asymmetric daughter cell fate, I examined the JK3437 *him-5*(*e1490*);*qIs74*[*sys-1p*::*GFP*::*POP-1*] (Siegfried et al., 2004) strain in order to assess POP-1/TCF localisation in the AMso and MCMs at the time of AMso division.

In early L3, as the male gonad turns to grow posteriorly, a lone bilateral pair of cells in the head begin to express *sys-1*/β-catenin, POP-1 driven under the *sys-1* promoter localised to the nucleus (Figure 6.4). By location and morphology this pair of cells are likely to correspond to the AMso. By early L4, POP-1 is seen in the nuclei of a second pair of cells immediately posterior to the original pair (Figure 6.4). As the AMso are the only cells to divide at this time, in this region it is likely that the posterior cells correspond to the MCMs. After division nuclear localisation of POP-1 is asymmetrical, visibly stronger in the anterior daughter cells, akin to what is seen in the SGP precursor cells in early gonad development. Expression of *qIs74* is also seen in sets of cells in extreme posterior of the animal these may include PHso1 and PHso2 however they have not been conclusively identified.

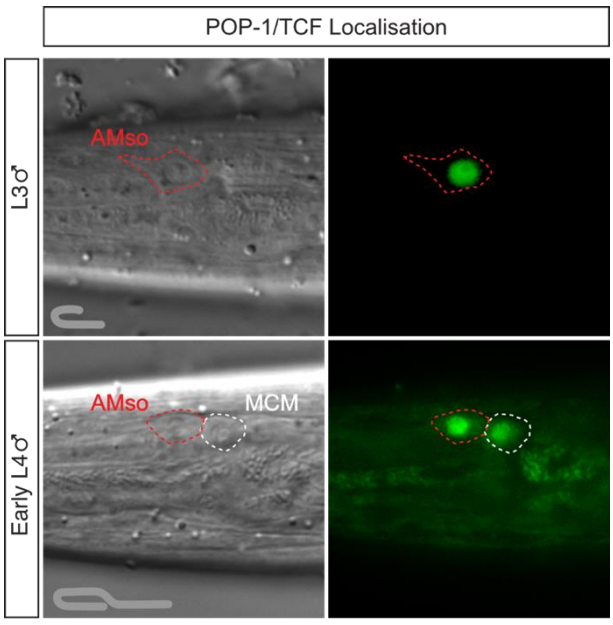

Figure 6.4 Wnt asymmentry pathway effector POP-1/TCF expression in the AMso and MCMs

Representative images of *qIs74* [*sys-1p::GFP::POP-1*] expression in the area anterior to the first pharyngeal bulb in males, before (top) and after (bottom) the time of AMso division. As there are no other divisions in the region at this time these cells likely correspond to the AMso and MCMs. The relative ages of animals are assessed by the extent of gonad progression indicated by the cartoon in the bottom left. Images by R. Poole

6.6 *hlh-14* is transiently expressed in the MCMs and PHD

As Ascl1 is both expressed in and a requirement for the production of neurons from glia in vertebrates, I investigated the possibility that *hlh-14*/ASCL1 is involved in MCM and PHD development. To do so I combined the *gmIs20*(*hlh-14p::HLH-14*::*GFP*) (Frank et al., 2003) transgene with the AMso and PHso1/PHD marker *drpIs3*[*lin-48::tdTomato].* Animals were carefully staged in order to examine the period immediately before and after the birth of the MCMs and the PHso1-to-PHD transformation. The PHso1 is born in mid L1 and by late L1, *lin-48* is expressed (Johnson et al., 2001), during L3 when the socket structure of PHso1 is still clearly visible, no *gmIs20* expression is evident in the AMso or PHso1 (Figure 6.5). However, over a short period, spanning no more than two hours after the birth of the MCMs, before tail tip retraction is completed, nuclear localisation of *hlh-14::HLH-14*::*GFP* is clearly visible in both the AMso and the PHso1, the latter marking the earliest indication that the transformation into the PHD neuron has begun (Figure 6.5). By later in L4, after tail tip retraction is complete and *lin-48::tdTomato* levels decline in the MCMs, *hlh-14p::HLH-14*::*GFP* is no longer detectable. These results indicate that there is a short burst of *hlh-14* expression very soon after the birth of the MCMs after which *hlh-14* is rapidly downregulated and/or the HLH-14::GFP is metabolised. At each stage, images are of the head and tail regions of the same animals indicating that the timing of proneural gene activity in the newly born MCMs seems to be closely coordinated in time with initiation of the direct transformation of the PHso1 into the PHD neuron. No similar expression is seen in the PHso1 of hermaphrodite animals, however due to the rapid temporal dynamics this cannot be ruled out based on fluorescent reporter gene expression alone.

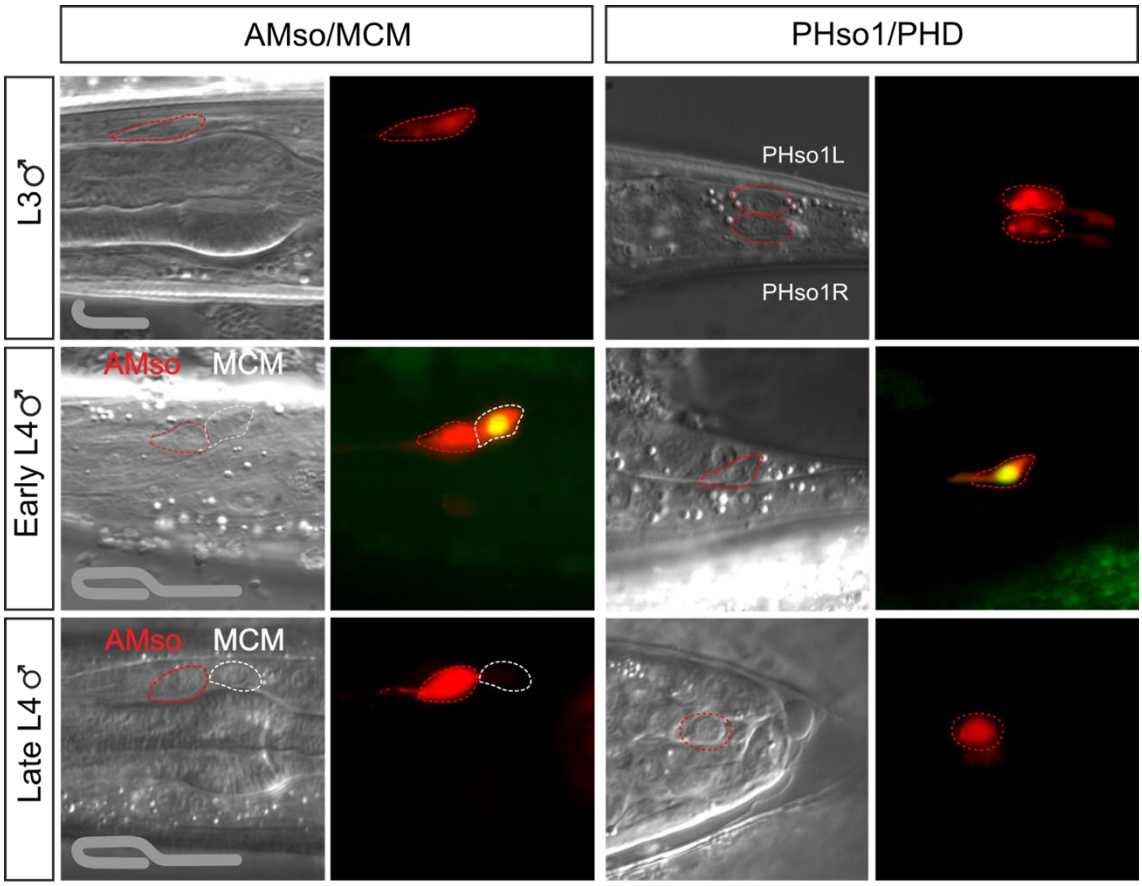

Figure 6.5 Transient expression of hlh-14/ASCL1 in the early MCM and PHD

Representative images of *gmIs20*[*hlh-14p::HLH-14*::*GFP*] expression in males before (top), shortly after (middle) and several hours after AMso division (bottom). AMso and PHso1/PHD are labelled with *drpIs3[lin-48::tdTomato].* Each row shows DIC and composite fluorescence images of the red and green channels of the head (left) and tail (right) region of the same animal. The relative ages of animals are assessed by the extent of gonad progression and by tail development in L4.

6.7 Summary

Following the implication of potential *cdk-4* regulation specifically in AMso division, the prospect of G1/S regulators and possible interactors of *cdk-4* became attractive targets in the investigation of glia derived neuron development. I used a conditional allele of *cdk-7* to test the possibility that it acts a CAK in the AMso where it may activate CDK-4. Perturbation of *cdk-7* after embryonic development does not interfere with AMso division, indicating that if a CAK is involved in *cdk-4* activation it is unlikely to be *cdk-7*. Careful developmental analysis of selected cell cycle components and cell fate determinants has provided insight into the earliest stages of both MCM and PHD development. Remarkably, the fact that that the AMso glial cells are able to produce neurons is not the only unusual property of these cells, as these cells are atypical in their development as well as their lineage. The G1/S regulator *cki-1*, which has been used as a marker of quiescence, is continuously expressed in the AMso, from its birth in the embryo until late adulthood. Despite the fact that the AMso only divides once in the male, features of a quiescent cell cycle are observed in the self-renewed AMso daughter and lost in the MCM daughter, hinting at a possible stem cell like property. This molecular evidence suggests that the resemblance of the AMso to radial glial cells in vertebrates may be more than superficial and may be associated with comparable cellular developmental mechanisms. The hermaphrodite AMso as well as both PHso1 and PHso2, also appear to express the quiescence marker throughout their life, even though these cells do not divide or undergo any cell fate transformation. This subset of glial cells appear to be qualitatively different in development to most other cells in the worm and these distinctive features are associated with sex-specific neuronal production. In fact, at the time of the direct PHso1-to-PHD transdifferentiation in the male, the quiescence marker is downregulated suggesting that there is a progression into the cell cycle. Analysis of S-phase markers indicates that the PHso1 does indeed begin to express the machinery necessary for DNA replication. If synthesis occurs or is required for the transdifferentiation is as yet unknown but will be an important avenue to pursue in order to get a better understanding of the processes of direct cell fate transitions. Additionally, I found that the downstream effectors of Wnt signalling

are implicated in the earliest stages of AMso division and MCM development, and that localisation in the AMso and MCMs is consistent to what is seen in SGP cell development. The homologue of the proneural factor ASCL1 is transiently expressed early in MCM and PHD development before any neuronal properties are apparent. Additionally, proneural gene expression appears to be temporally coordinated during MCM and PHD early specification. Taken together these results suggests that regulation of the cell cycle machinery may be integral to glia-to-neuron transdifferentiation in the worm, even in the absence of DNA replication and cytokinesis. These three related sets of cells appear to share features of a common mechanism but each result in radically different developmental outcomes. A detailed description of what is held in common and unique to each of these cells, in tandem with a comparison between the sexes promises to reveal new mechanisms that promote cell fate transformations as well as those that maintain a stable fate.

Chapter 7

Discussion

7.1 General Discussion

In its most stripped down form, eukaryote development can be described in terms of a program that directs changes in cell fate, i.e. how the cells that constitute an organism establish and maintain the transcriptional pattern of one cell fate, and switch to the maintenance of successive cell fates, until a stable mature form results. The transition between cell fates is often accompanied by a cell division but is not required. For example, in a more conceptually simple case of a developmental program, such as that of single celled protists or yeasts, fate decisions must be made about when to switch between a feeding, resting or growing state, they only re-enter the cell cycle to reproduce. Importantly, the program does not proceed in a blind sequence, rather the expression of each step of the program is informed by the other parts, such that, reproduction cannot begin until there has been enough growth and a lack of food might induce a specialised resting state, while the reproductive step may require the prior development of specialised morphological features involved in the exchange of genetic material. Therefore, switching between substantially different cell states is not, in itself, fundamentally tied to cell division, however in multicellular organisms, switching between different cell fates is tied to cell division. Cellular specialisation in multicellular organisms, offers various evolutionary benefits but also necessitates successive layers of complexity in development. The evolutionary strategy adopted by obligate multicellular organisms requires an elaboration of the unicellular developmental program, effectively separating the program into iterative steps with subprograms distributed in discrete packages of cells and cell types. Perhaps due to the iterative nature of the program, regulation of the cell division cycle and cellular differentiation have tended to become amalgamated. Proper development depends as much on proliferation, cell cycle dynamics, timing and synchronisation between cells as on the robust and timely differentiation of

specialised cell types. Consequently, both must occur in concert and a balance between the renewal of progenitor cells and differentiated specialised cells must be struck. Furthermore, control of cell division can be a used as means to guide differentiation, for example, in the establishment of asymmetry in the first cell division in *C. elegans* or the stalk and the spore cell fate choice in *Dictyostelium*, directly depend on the state of the cell cycle. Of course, during development, the fate of many cells is to produce other specialised cells, therefore, cell division can be both the cause of cellular specification as well as the consequence of cell fate specification. This state of affairs results in a difficulty for developmental biologists, such that any manipulations of cell fate can result in confounding effects on the cell cycle, which limits avenues for experimentation. For example, in the study of pluripotent stem cells, regeneration, reprogramming and transdifferentiation, manipulations of cell cycle associated factors, pluripotency factors, or cell fate determinants can result in inappropriate cell cycle arrest, proliferation, cellular differentiation or cell death (Soufi & Dalton, 2016; Zaveri & Dhawan, 2018). These concerns take on particular importance when it comes to translational studies where, while there have been great advances, the efficiency and fidelity of cell fate transformations is still a technical hurdle. A deeper understanding of how cell fate is determined in the context of the cell cycle and if it is possible to separate the two will be key to overcoming such hurdles. It is my hope that this work will contribute to the establishment of a model in which neuronal differentiation from glia-like cells can be readily studied in both proliferative and direct cell fate switches at once. Comparison between the shared and independent components of the mechanisms that govern these cell fate switches offers a so far unique opportunity which may elucidate some of the fundamental biology that connects the cell cycle and cell fate.

7.2 The Molecular regulation of MCM development

One of the ultimate goals of the project introduced here is to piece together a complete picture of the sequence of genetic and cellular events that lead to the terminal specification of the MCM neurons. To this end, an unbiased forward genetic screen for genes that regulate MCM development was undertaken. Nine mutants were isolated from the screen that affect sequential stages of MCM development. In order to facilitate further study each mutant line was characterised in order to be able to classify the general stage of MCM development affected. Two Class II mutants, defective in AMso division, six Class III mutants and one Class IV mutant which affect pan-neuronal and MCM neuronal subtype specification respectively, were isolated. While several mutants were obtained from this small screen it is will be important to continue the screen to saturation, however, the tools and techniques developed here will expedite the process. Apart from the *drp5* and *drp8* alleles which have been studied in detail the rest of the mutants will need to be more deeply characterised, their specific phenotypes examined in greater detail, then mapped and cloned. The classification of mutants allows us to narrow our focus of study to particular stages of MCM development. For example, Class I and particularly Class II mutants would allow us to discover and manipulate the most upstream factors that confer neurogenic potential on the AMso glial cell and determine if inherited factors are important for MCM specification. Class III and Class IV mutants will tell us about the sequence of steps of neuronal specification from after cell division, up until it is terminally differentiated.

No mutants that act primarily before AMso division were isolated from this screen, this is likely in part due to the design of the screen, it is possible that genes that affect AMso cell fate, have pleiotropic roles which affect survival. For example, mutants of the aristaless homologue alr-*1* which is known to be involved in AMso fate maintenance (Tucker et al., 2005), have a tendency to crawl out of plates as adults and desiccate, a common phenotype in mutants affecting chemosensation (Starich et al., 1995). Screening for an adult specific phenotype would reduce the chances of mutations with similar effects from being isolated, nevertheless mutants that effect AMso specification would still be expected. Phenotypes other than those described here are possible; such as the AMso exhibiting neuronal properties or the production of multiple MCMs,

indeed, *inIs179[ida-1::gfp]* expressing AMso were seen rarely in some mutants but not consistently enough to score for penetrance. This type of phenotype could either indicate defects in AMso specification, or a defect of division where neural fate promoting determinants are expressed in the AMso either due to a failed mitosis or mis-segregated to the AMso in a defective asymmetric division. These types of mutants could inform us about the mechanisms that maintain AMso fate and establish MCM fate. To assess the potential importance of asymmetric segregation of neuronal determinants, a temperature-sensitive allele of *lin-5*/NUMA, a key component of the mitotic spindle, can be used to alter the plane of cell division. Animals in which the division of the AMso occurs in the dorsal-ventral rather than anterior-posterior orientation can be assessed for any alterations in cell fate. Preliminary data suggest that in some circumstances *rab-3* expressing AMso cells can be observed in *lin-5* mutants, which would suggest that segregation of cell fate determinants is an important part of the mechanism of MCM development.

To understand how MCM fate is established it will also be essential to determine the fate of the daughter cells in Class III and Class IV mutants as well as what happens in the wild type. It must be determined if the daughter cells (that do not acquire a neuronal fate) remain in an undefined intermediate or “dedifferentiated” state similar to what is seen during the Y-PDA transition, if they express glial markers like the AMso mother cells or if there is mixed neuronal/glial fate. If an undefined state exists, the next step would be to determine if this type of cell has to potential to differentiate into other neuron or cell types. This would be done by forcing expression of transcription factors that determine endoderm, mesoderm or other neuron types, it may be possible to establish if the early MCMs are more stem cell like or if there exist specific barriers against reprogramming an alternate fate. If however, the daughter cells are born as glial cells this might more closely resemble a direct transdifferentiation after the production of an AMso like cell, where there is competition between glial and neuronal fates. Discovering factors that govern either outcome, and in particular how this is coordinated with the cell cycle, may have an important impact on our understanding of cell replacement strategies and fate reprogramming. Preliminary analysis of Class III AMso daughter cells shows that they do not conspicuously express *drpIs3(lin-48:tdtom)*, indicating

that loss of neuronal fate does not result in a default AMso like fate taking over. Unfortunately, due to the limits of the temporal resolution of transgene expression analysis, it is not possible to accurately determine if *lin-48* expression ceases in the newly born MCMs or non-neuronal AMso daughter cells. In order to make this determination active transcription must be monitored using a technique that can measure active transcription, such as smFISH.

In addition to continuing the analysis of the AMso and MCMs in the *nom* mutants it will be essential to perform an in depth characterisation of the PHso1/PHDs in these mutants. Although preliminary analysis indicates that PHDs develop normal morphology in the mutants tested so far, further analysis is required to determine if the PHD develop normally. Markers with which the PHDs can be clearly identified and morphology assessed would be required, such as an integrated version of the *oig-8::gfp* reporter shown in Chapter 3 will be used. Despite the many similarities of the two cell fate transformations, the fact that several mutants affecting MCM development do not seem obviously to affect PHD morphological development points to at least partially distinct mechanisms that govern the two events. A similar screen for factors affecting PHD development is also to be undertaken. The comparison of the AMso to MCM and PHso1 to PHD cell fate transformations will hopefully uncover the common and distinct mechanisms of proliferative and non-proliferative neuronal fate determination.

7.3 On the role *drp5* and *drp8* as novel alleles of *cdk-4*

Following the classification of MCM mutants into classes that affect sequential stages of their development, the Class II mutants were prioritised for study as they affect the most upstream events affecting MCM development in the AMso. The study of the *C. elegans* male offers the opportunity for novel insights but genetic analysis of male specific phenotypes can come with unique challenges. Nevertheless, we have shown that well established techniques for hermaphrodite genetic analysis can be adapted for use in the male. By mapping rescue and complementation, the Class II mutants *drp5* and *drp8* were determined to be alleles of *cdk-4*. As CDK-4 is key to regulating the G1/S transition and initiation of the cell cycle it is perhaps not surprising that mutations affecting such a critical gene could result in a defect of AMso division. What is unusual however is the apparent specificity of these alleles, where null alleles of *cdk-4* disrupt all post-embryonic cell divisions, *cdk-4(drp5)* and *cdk-4(drp8)* mutants develop normally and do not exhibit obvious pleiotropic effects in morphology or behaviour. Consequently, the question now becomes; if *cdk-4(drp5)* and *cdk-4(drp8)* are generally capable of normally initiating the cell cycle in post-embryonic divisions then how does it come to be that so few other cells other the division of the AMso is blocked?

There are two main possibilities that could account for such a situation; first that the AMso is particularly sensitive to G1/S CDK activity levels or second, there is the expression of specific factors which could specifically activate or be targets of CDK-4 that promote G1/S. These possibilities are not mutually exclusive, and it is possible this phenomenon is a result of a combination of these factors.

The simpler explanation would be that the AMso requires a particularly high threshold of CDK activity for division and *cdk-4(drp5)* and *cdk-4(drp8)* are simply hypomorphic alleles, resulting a slightly lowered CDK-4 activity. This level of activity would need to be high enough to allow other post-embryonic division but not high enough to allow AMso division. The persistent expression of *cki-1* in the AMso of either sex suggests that the AMso might be primed to enter the cell cycle throughout life and a higher G1/S CDK activity threshold

might help protect against accidental AMso division. However, three pieces of indirect evidence suggest that this hypothesis is unconvincing:

First, that there is an extremely strong phenotype, in both *cdk-4(drp5)* and *cdk-4(drp8)* at the non-permissive temperature, 100% of AMso divisions are blocked and there is no indication of a progressive phenotype. It is not impossible that hypomorphic alleles could result in an acute 100% penetrant phenotype but if this were to be the case, it suggests that there would be a large difference in the G1/S CDK activation threshold of the AMso when compared against other cells. This is because there is no overlap between the *nom* phenotype and other post-embryonic cell division phenotypes. For this to be true would mean that two independent alleles were isolated that lowered CDK-4 activity enough to completely abolish MCM development but never enough to affect any other divisions, this is possible, as they do affect the same domain but a cumbersome explanation.

Second, in the masculinised AMso of XX hermaphrodites halving the dose of *cdk-4* does not result in haploinsufficiency as it does not cause a *nom* phenotype. Dosage compensation ensures that XX hermaphrodites and XO males maintain comparable rates of sex chromosome transcription. There is evidence that, while both sexes retain similar ratios of sex chromosome to autosome transcription, the X chromosome is more active than autosomes in both sexes, thus allowing for similar X:A transcription rates in XO males (Kruesi et al., 2013; Lau & Csankovszki, 2015). There is no excess X transcription in hermaphrodites however, as it compensated for by hypotranscription of X linked genes on both X chromosomes, which is governed by the dosage compensation complex (Meyer, 2005). Masculinisation of the AMso in XX hermaphrodites was achieved by the expression of *fem-3* which acts downstream of the dosage compensation complex genes (Zarkower, 2005) see Figure 1.21e. Therefore, dosage compensation should be unaffected in XX cells masculinised by *fem-3* overexpression and XX animals should have similar levels of X-linked gene expression as XO males. Therefore, the masculinised AMso of XX animals that bear only a single copy of wild type *cdk-4* should have a lowered dose of *cdk-4*. However, when a wild type copy of *cdk-4* is introduced over null copy of *cdk-4* (Figure 5.6b) it does not cause a *nom* phenotype. In most organisms a general increased expression of *cdk4* promotes G1/S

progression, overexpression of *cdk4* is associated with many cancers (Goel et al., 2018; Hamilton & Infante, 2016) and increased levels of CDK4 limit or abolish the efficacy of CDK4/6 inhibiting drugs (Cen et al., 2012; Olanich et al., 2015; Wu et al., 2011). While increased *cdk4* expression levels result in increased CDK4 activity and proliferation, and can overcome DNA damage associated G1 arrest in hematopoietic cell lines (Reed et al., 1998). Therefore, assuming that increased *cdk-4* expression levels results in increased CDK-4 activity, finding that a reduction in the dose of *cdk-4* in XX masculinised AMso does not impair their ability to divide suggests that a they are unlikely to be highly sensitive to a lowering of G1/S CDK activity.

Lastly, the sequence analysis of the residues affected by *drp5* and *drp8* indicate that the T-loop is affected, a key regulatory region of CDK4. The *drp8* mutation may alter the conformation of the T-loop as it substitutes a small aliphatic Leucine for Phenylaniline which has a bulky aromatic ring, at a higher temperature it may be incorporated into the hydrophobic spine and alter the conformation of the T-loop or interfere with the hydrophobic interactions of the HRD and DFG motifs that occur when kinases are in their active state (Kornev et al., 2006; Meharena et al., 2013). In the *drp5* allele, a conserved Alanine is converted into a Threonine residue just two residues away from critical T172 phosphorylation site in mammals, it is possible that the introduction of a second Threonine so close to a phosphorylation site could result in erroneous phosphorylation and cause conformational changes that have deleterious effects on the proteins function. While it is conceivable that mutations in this region simply lower the general efficiency of the enzyme complex below a required threshold, it opens up the possibility that CDK4 must be specifically activated in the AMso for division to occur. It is possible that the T-loop domain control is only required in the AMso but seems unlikely considering the importance of this domain in other organisms (Bockstaele et al., 2006). An assay of CDK-4(*drp5)* activity will be helpful in order to determine whether its activity is substantially different than wide type CDK-4.

The other main possibility that accounts for the selective nature of the *drp5/8* mutations is that there is a unique interactor of CDK-4 in the AMso. There are not many known interactors of CDK4, which makes this possibility of particular interest as there is a chance that we might uncover novel

mechanisms of CDK4 regulation. Apart from the Rb family, CDK4 is not known to phosphorylate many substrates (Anders et al., 2011). Negative regulators like CKIs do interact with CDK4 and INK4 family proteins are known to interact with the catalytic domain of CDK4/CDK6 to strongly repress kinase activity (Jeffrey et al., 2000; Russo et al., 1998), however INK family proteins are not found in *C. elegans.* It is possible that an alternate protein plays this role in the worm, and is expressed specifically in the AMso, the *drp5/8* mutations may mimic the action of such an inhibitor. A simpler solution would be that an AMso specific candidate could activate the CDK-4 T-loop preferentially in the AMso. CDK7 is thought to be the main CAK that acts on CDK4 (Kaldis et al., 1996; Schachter et al., 2013) however, as the conditional allele *cdk-7(ax224)* never produces a *nom* phenotype, *cdk*-7 does not appear to play a major role in this postembryonic cell division, despite being required in the embryo (Wallenfang & Seydoux, 2002). Nevertheless, as it is likely not a null allele (Wallenfang & Seydoux, 2002) in order to confirm that *cdk-7* does not play a role in AMso division, *cdk-7(ax224)* mutants in combination with *cdk-7* RNAi should be tested. Recently however, certain Mitogen Activated Protein Kinases (MAPKs), the c-Jun N-terminal kinases (JNKs) have also been found to phosphorylate CDK4 on T-172 (Colleoni et al., 2017) suggesting that it is possible that other CAKs may be involved.

The most important alternative possibility for a specific target of CDK-4 target in the AMso would be that it may not act mainly through the canonical Rb pathway but target another pathway. In the worm, *lin-35(n745)* Rb null mutations are able to suppress the effects of the *cdk-4(gv3)* and *cyd-1* null mutations. Such animals can reach normal size and their intestinal nuclei undergo replication similar to wild types, however a significant number of post-embryonic divisions fail. The incomplete suppression suggests that *lin-35* Rb is not the only target of CDK-4/CYD-1 (Boxem & van den Heuvel, 2001). Similarly, double mutant *cdk-4(drp5)* and *lin-35* animals can be used to check the extent to which *lin-35* Rb suppresses *cdk-4(drp5)* and restores the MCMs. If *lin-35* Rb fails to suppress *cdk-4(drp5)* then it suggests that CKD-4 could be acting through a novel target. Preliminary experiments (data not shown) suggest the *lin-35(n745)* completely fails to suppress *cdk-4(drp5)*. Therefore, a suppressor screen of *cdk-4(drp5)* will be undertaken in order to look for possible interactors

of CDK-4. The identification of new targets or novel mechanisms of action of CDK-4 could open up new avenues for therapeutic strategies. The selective inhibition of CDK-4/6 is a fast developing approach to cancer treatment (Schettini et al., 2018). The CDK-4/6 inhibitors abemaciclib, palbociclib, and ribociclib have recently been approved for use in patients however, intrinsic or acquired resistance to these drugs is restricting their effectiveness (Knudsen & Witkiewicz, 2017; Pandey et al., 2019). Any models in which the known or novel mechanisms of CDK4/6 inhibitor resistance can be quickly studied may prove extremely useful. It will be relatively simple to test these drugs in the AMso/MCM as a model, firstly to confirm the involvement of CDK-4 and to potentially quickly translate findings to improve the therapeutic approach.

7.4 Cell cycle inhibition and key cell fate determinants are coordinated in both proliferative and direct glia-to-neuron cell fate switches

We sought to understand and compare the earliest steps in these two types of glia-to-neuron cell fate switches, in order to discover if the mechanisms involved are in any ways similar or completely distinct. Cellular developmental analysis via genetic fluorescent reporters of cell cycle components and cell fate determinants, showed various shared features in both the proliferative and direct glia-to-neuron cell fate switches. The proneural factor ASCL1 is transiently expressed in the newly born in MCMs and at the earliest stage of the PHso1-to-PHD transdifferentiation before any neuronal properties are apparent. Finding that the timing of expression appears coordinated in both cells suggest that a common mechanism may be at play in both cell fate switches. Additionally, the implication of ASCL1 in non-vertebrate glia derived neurons suggests that there may be a surprisingly close relationship between the mechanisms of neuronal development from glia in humans and invertebrates. Similarly, Wnt asymmetry pathway appears to be involved in the proliferation and differentiation of the AMso and MCMs, a feature also shared with vertebrate neurogenesis. How the complex centralised nervous systems of bilaterians evolved from the pre-bilaterian distributed nerve nets is a longstanding unsolved question in biology. A fundamental but debated question is, if the centralisation of the nervous systems found in all bilaterians evolved by convergence, independently in separate phyla or if this type of nervous system was present in an ancestor common to all bilaterians and so descends to all metazoa homologously (Strausfeld & Hirth, 2016). Cells that closely resemble radial glia in morphology, gene expression and have roles as central nervous system support cells, have been found in taxa representing all major branches of protostomes and deuterostomes, suggesting that a common ancestor for radial glia is likely to exist (Helm et al., 2017). However, the potential of glial cells to produce neurons and glia have not been described outside of chordates, this developmental analysis of the MCMs and PHDs from the AMso and PHso1 glial cells, shows that various features of neural development are shared with vertebrates. Specifically, the expression of conserved neuronal

differentiation factors, the direct cellular conversion of glia into neurons, asymmetric division of glia to produce a neuron and a glial cell, and the maintenance of neural progenitors in a quiescent state. Together this suggests a homology may likewise exist in the development of neurons and glia.

Irrespective of whether these cell types evolved by homology or convergence an interesting question remains, specifically, how is cellular quiescence related to the neurogenic potential glia? One of the more surprising findings of this study is that the AMso and PHso1 remain in a state of quiescence, as marked by *cki-1* expression, for a comparatively long time compared to other cells in the worm. An extended period of quiescence is a characteristic but not necessary property of stem cells. This trait is shared with the AMso and PHso1 which can be viewed as sex-shared cell types that achieve multipotency by remaining quiescent in both sexes but going on to proliferate or differentiate in only one of the sexes. This could point to the existence of an evolutionarily ancient predecessor of stem-like cells where the ability to maintain an extended state of quiescence and the ability to differentiate in various cell types are combined. Apart from posing fundamental theoretical questions, these cells may also have more practical value, for example, discovering how the AMso and PHso1 are maintained in a state of quiescence, particularly in the hermaphrodite can be useful for cancer therapy. There are known sex differences in the incidence and outcomes of many cancers, such as glioblastoma (Yang et al., 2019), the underlying causes of which are poorly understood. A better understanding of the mechanisms that differentially regulate the proliferation decision in each sex could help explain the differences in susceptibility and sensitivity to therapies between the sexes. Similarly, understanding what regulates the quiescent state could be useful to learning what triggers division in quiescent cancerous cells, which are generally resistant to classical cancer therapies (Yeh & Ramaswamy, 2015). As such, the AMso/MCM and PHso1/PHD model is well suited to interrogate the mechanisms that govern quiescence, proliferation and differentiation. It will be important to determine whether MCM and PHD development is directly under the control of *cki-1*, similar to what is found in VPCs during vulva development. Knocking down cell cycle inhibitors heterochronically and in hermaphrodites then looking for the production of ectopic neurons would help determine if the

differentiation program is largely intrinsic and not greatly influenced by the microenvironment. If there are sex differences or uncontrolled proliferation without neuronal differentiation then this could point to additional differentiation cues or protective factors involved in the mechanism. Alternately, *cki-1* may not be chiefly in control of MCM or PHD development which might suggest novel roles for the gene.

Soon after their birth the MCMs stop expressing the quiescence marker, as do the PHDs after they differentiate into neurons, how the transition from quiescence to permanent cell cycle exit is achieved in the daughter cells is another important question. Proneural factors have been shown to induce cell cycle exit (Bertrand et al., 2002; Dennis et al., 2018; Ross et al., 2003) and it is likely that the transient expression of *hlh-14*/ASCL1 may be involved in this process. Less is known about how such factors are so closely controlled in order to control differentiation and cell cycle exit. The expression of ASCL1 must at some point fundamentally change the epigenetic landscape and do so through binding with compacted chromatin but relatively little is known about how ASCL1 opens up the chromatin and what other factors may be involved. In this model the effect on *hlh-14* expression of various candidate upstream factors, that may be involved in the cell cycle and differentiation processes, can be closely followed at the single cell resolution. For example, preliminary RNAi experiments of *lin-48*/OVO show a *nom* phenotype, but no division defects, making it a prime candidate that may be involved in the expression of early specification factors such as *hlh-14*. Additionally, with a comparison of how these processes occur with a cell division and in direct transdifferentiation will allow us a better understanding of how the epigenetic landscape is changed during division and what may or may not be effective in therapeutic strategies.

7.5 Considering the role of S-phase machinery during direct transdifferentiation in the absence of DNA replication

Another unexpected finding is that S-phase markers are expressed during the direct transdifferentiation of the PHso1 to the PHD. The expression of S-phase markers strongly suggests that synthesis may be occurring, possibly leading to a endoreduplication event or the amplification of certain genes, similar to the amplification of chorion genes in the *Drosophila* ovarian follicle cells (Calvi et al., 1998). However, preliminary Edu incorporation experiments shows that direct transdifferentiation can occur without synthesis. This leads to an unusual question; if DNA synthesis does not occur then what is the role of S-phase machinery, are they necessary for the transdifferentiation process or are they an epiphenomenon? An important step to answer this question would be blocking synthesis with hydroxyurea, a potent ribonucleotide reductase inhibitor. While it is difficult to imagine a role for a ribonucleotide reductase outside of the synthesis of deoxyribonucleotides for DNA replication it is possible that it is expressed as part of the cassette of genes expressed under the control of E2F, where another gene may have a role in differentiation; i.e. it may possible that S-phase machinery is required for differentiation but the cell replication and division itself is bypassed. During replication chromatin must be opened up, nucleosomes disassembled and reassembled, new histones manufactured and the epigenetic information carried by them modified (Aze & Maiorano, 2018; Budhavarapu et al., 2013; Chen & Dent, 2014; Serra-Cardona & Zhang, 2018). This process could be exploited in order to induce differentiation but replication itself avoided. Certain S-phase related genes have potential function outside of DNA replication, the MCM 2-7 complex proteins, for example, are thought to have roles outside of strict DNA unwinding activity during replication. This protein family has several puzzling features, there is a great excess of MCM 2-7 proteins that are located outside of origins of replication, distributed evenly on the chromatin of replicated DNA, this is referred to as the MCM paradox (Das et al., 2014). During replication the MCM 2-7 complex is known to dislodge nucleosomes by recruiting histone chaperones like the FACT complex (Avvakumov et al., 2011) and it is also known to be inhibited by CKIs like p27 to inhibit replication (Nallamshetty et al.,

2005). Outside of replication MCM 2-7 subunits are also known to bind with RNA pol II (Yankulov et al., 1999) and promote transcription (Zhang et al., 1998). The MCM 2-7 complex has also been found to be localised to the histones of actively transcribing genes, along with RNA Pol II and the intact complex is essential for transcription (Snyder et al., 2009). It is possible that certain S-phase related genes are also playing a role in transcription and modification of the epigenetic landscape, making them prime candidates as differentiation factors. By manipulating Cyclin E expression, we could help determine if general S-phase gene expression is required for the transdifferentiation of PHso1 into PHD. Alternatively, if S-phase genes are found to be expressed during transdifferentiation events but not play any significant role, it would nevertheless be interesting to discover how such a state occurs and how it is regulated. Discovering how such S-phase gene activity is restrained from inducing synthesis, whether this is chiefly translational or post translationally, could have implications for the interpretations of many experiments where these genes are used as definitive markers for replication.

If indeed there exist mechanisms by which the epigenetic landscape altering properties of S-phase can be exploited but actual synthesis or mitosis avoided, then the model system presented here and *C.* elegans in general would be ideally suited for their study. It would be interesting to examine the Y-PDA transdifferentiation with an eye on the bypassing of cell division, it would be important to see if S-phase genes are expressed there too even though replication is not thought to occur (Richard et al., 2011). Discovering new mechanisms by which cell division could be bypassed during differentiation could be extremely useful to cell replacement strategies, particularly in addressing fear of potential tumorigenicity of induced reprogrammed stem cells and in the treatment of cancers.

7.6 Concluding remarks

In summation, the work presented here has begun to give us an understanding of basic developmental features of both the AMso to MCM and PHso1 to PHD cell fate transformations. Providing a loose framework and the basic tools and techniques necessary to continue to use the AMso to MCM and PHso1 to PHD cell fate transformations as a model. A model that is ideally suited to study neuronal development from glia and the general biological principles that bring together the cell division cycle and cellular differentiation.

In so doing, this work also opened up unexpected new avenues, in the specific nature of mutations of the key cell cycle regulator *cdk-4* that appears to only affect a single pair of (or at most very few) cell divisions in the worm, the discovery of cells with neuronal potential that remain quiescent throughout their life, and in the implication of DNA replication components in a direct cell fate switch.

Annexe II

eLife

RESEARCH ARTICLE

Direct glia-to-neuron transdifferentiation gives rise to a pair of male-specific neurons that ensure nimble male mating

Laura Molina-García[1†], Carla Lloret-Fernández[1†], Steven J Cook[2‡], Byunghyuk Kim[3§], Rachel C Bonnington[1], Michele Sammut[1], Jack M O'Shea[1#], Sophie PR Gilbert[1], David J Elliott[1], David H Hall[3], Scott W Emmons[2,3], Arantza Barrios[1]*, Richard J Poole[1]*

[1]Department of Cell and Developmental Biology, University College London, London, United Kingdom; [2]Dominick P. Purpura Department of Neuroscience, Albert Einstein College of Medicine, New York, United States; [3]Department of Genetics, Albert Einstein College of Medicine, New York, United States

Abstract Sexually dimorphic behaviours require underlying differences in the nervous system between males and females. The extent to which nervous systems are sexually dimorphic and the cellular and molecular mechanisms that regulate these differences are only beginning to be understood. We reveal here a novel mechanism by which male-specific neurons are generated in *Caenorhabditis elegans* through the direct transdifferentiation of sex-shared glial cells. This glia-to-neuron cell fate switch occurs during male sexual maturation under the cell-autonomous control of the sex-determination pathway. We show that the neurons generated are cholinergic, peptidergic, and ciliated putative proprioceptors which integrate into male-specific circuits for copulation. These neurons ensure coordinated backward movement along the mate's body during mating. One step of the mating sequence regulated by these neurons is an alternative readjustment movement performed when intromission becomes difficult to achieve. Our findings reveal programmed transdifferentiation as a developmental mechanism underlying flexibility in innate behaviour.

***For correspondence:** a.barrios@ucl.ac.uk (AB); r.poole@ucl.ac.uk (RJP)

[†]These authors contributed equally to this work

Present address: [‡]Department of Biological Sciences, Columbia University, New York, United States; [§]Department of Life Science, Dongguk University-Seoul, Goyang, Republic of Korea; [#]Centre for Discovery Brain Sciences, Edinburgh University, Edinburgh, United Kingdom

Competing interests: The authors declare that no competing interests exist.

Funding: See page 27

Received: 10 May 2019
Accepted: 02 October 2020

Reviewing editor: Piali Sengupta, Brandeis University, United States

© Copyright Molina-García et al. This article is distributed under the terms of the Creative Commons Attribution License, which permits unrestricted use and redistribution provided that the original author and source are credited.

Introduction

The coordinated execution of innate, stereotyped sexual behaviours, such as courtship and mating, requires sexually dimorphic sensory-motor circuits that are genetically specified during development (reviewed in ***Auer and Benton, 2016***; ***Barr et al., 2018***; ***Yang and Shah, 2014***). Studies in the nematode *Caenorhabditis elegans*, in which the development and function of neural circuits can be interrogated with single cell resolution, have revealed two general developmental mechanisms underlying sexual dimorphism in the nervous system. The first involves the acquisition of sexually dimorphic features in sex-shared neurons during sexual maturation, which include changes in terminal gene expression, such as odorant receptors, neurotransmitters and synaptic regulators (***Hilbert and Kim, 2017***; ***Jarrell et al., 2012***; ***Oren-Suissa et al., 2016***; ***Ryan et al., 2014***; ***Serrano-Saiz et al., 2017a***; ***Serrano-Saiz et al., 2017b***; ***Pereira et al., 2019***; ***Weinberg et al., 2018***). The second mechanism involves the generation of sex-specific neurons (***Sammut et al., 2015***; ***Sulston and Horvitz, 1977***; ***Sulston et al., 1980***). Sex-specific neurons are primarily involved in controlling distinct aspects of reproductive behaviours, such as egg-laying in the hermaphrodite and mating in the male (reviewed in ***Emmons, 2018***). Generation of sex-specific neurons requires sex-specific cell death (***Sulston et al., 1983***) or neurogenesis events resulting from sex differences in the cell division patterns and neurodevelopmental programmes of post-embryonic cell lineages

(reviewed in **Barr et al., 2018**). Here we identify a novel way in which sex-specific neurons are generated in the nervous system: through a direct glia-to-neuron transdifferentiation of sex-shared cells.

In one of his seminal papers, John Sulston described a sexual dimorphism in the phasmid sensilla of adult animals (**Sulston et al., 1980**). The phasmid sensillum is one of the seven classes of sense organs that are common to both sexes in *C. elegans*. These sense organs are organised in sensilla which are concentrated in the head and the tail (**Bird and Bird, 1991**; **Ward et al., 1975**; **White et al., 1986**; **Doroquez et al., 2014**). Each sensillum is composed of the dendrites of one or more sensory neurons enveloped by a channel, usually composed of a single sheath glial cell and a single socket-glial cell. These sensilla can be viewed as part of an epithelium, continuous with the skin, and are shaped by mechanisms shared with other epithelia (**Low et al., 2019**). Socket-glial cells are highly polarised and adhere to the hypodermis at the distal end of their process where they form a small, ring-like hollow pore in the cuticle through which the sensory dendrites can access the outside world. The bilateral phasmid sensilla (**Figure 1**), situated in the tail, are unusual in that they are each composed of two socket-glial cells (PHso1 and PHso2). John Sulston observed that in juvenile animals (L2 stage) of both sexes, PHso1 forms the primary pore (**Sulston et al., 1980**; **Figure 1A**). At adulthood, the hermaphrodite retains a similar structure (**Figure 1B**). In males, however, it is PHso2 that forms the main pore and PHso1 was described as having retracted from the hypodermis and to protrude into the phasmid sheath (**Figure 1C**). It was also described to contain basal bodies, a structural component of cilia, in the region enveloped by the phasmid sheath. As sensory neurons are the only ciliated cells in *C. elegans* (**Perkins et al., 1986**), this is suggestive of neuronal fate, yet Sulston observed no other neuronal characteristics (**Sulston et al., 1980**). We previously showed that in the amphid sensillum (a similar organ located in the head) the amphid socket-glial cell (AMso) acts as a male-specific neural progenitor during sexual maturation, dividing to self-renew and generate the MCM neurons (**Sammut et al., 2015**). We therefore sought to investigate the PHso1 cells in more detail.

We find that during sexual maturation (L4 stage), the pair of sex-shared PHso1 glial cells acquire sexually dimorphic function by undergoing a direct (without cell division) glia-to-neuron transdifferentiation that results in the generation of male-specific neurons, which we term the phasmid D neurons (PHDs). This cell-fate plasticity is regulated by the sex-determination pathway, likely cell-intrinsically. However, we find the cell-fate plasticity does not depend on certain molecular

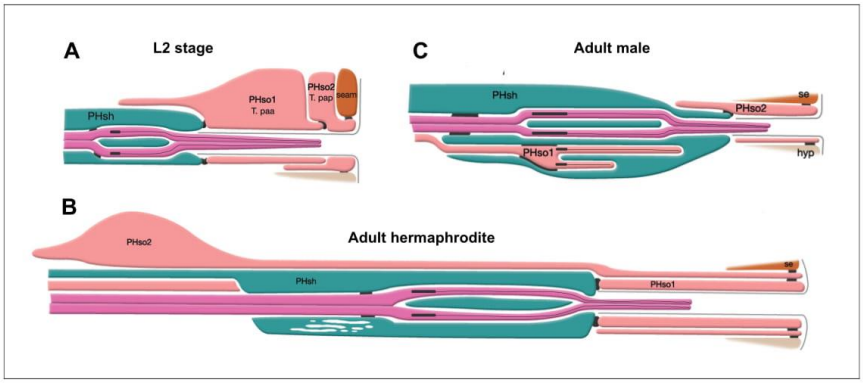

Figure 1. The phasmid sensillum. Diagram of the phasmid sensillum in either sex at the L2 larval stage (**A**), in adult hermaphrodites (**B**) and in adult males (**C**). The socket-glial cells (PHso1 and PHso2) are coloured in light pink; the sheath glial cells (PHsh) in green; and the ciliated dendrites of the phasmid sensory neurons, in dark pink. The adherens junctions are depicted as black lines between cells. Axonemes and cilia are marked as black bars and black lines inside the dendrite tips. Each phasmid opens to the exterior on the extreme right (posterior), where grey lines mark the cuticle borders of the phasmid pore and fan. Hypodermis (hyp), seam (se). Diagram has been modified from and is used with permission from http://www.wormatlas.org.

©2010 Wormatlas. Figure 1 is modified with permission from http://www.wormatlas.org/. It is not covered by the CC-BY 4.0 licence and further reproduction of this figure would need permission from the copyright holder.

mechanisms known to regulate the only other well-described direct transdifferentiation in *C. elegans* (**Kagias et al., 2012**). This bilateral pair of previously unnoticed neurons are putative proprioceptors that regulate male locomotion during specific steps of mating. One of these steps is a novel readjustment movement performed when intromission becomes difficult to achieve. Our results reveal sex-specific direct transdifferentiation as a novel mechanism for generating sex-specific neurons and also show the importance of proprioceptive feedback during the complex steps of mating for successful reproduction.

Results

The sex-shared PHso1 cells undergo glia-to-neuron transdifferentiation in males

Using a *lin-48/OVO1* reporter transgene to identify and visualise the PHso1 cell bodies both before and during sexual maturation (**Johnson et al., 2001**; **Wildwater et al., 2011**), we observed no distinguishable differences between the hermaphrodite and male PHso1 cells at the L3 stage (**Figure 2A**). The PHso1 cells display a polarised morphology and a visible socket structure in both sexes. In hermaphrodites, this morphology is maintained during the transition to adulthood and PHso1 cells elongate as the animal grows. In males, by contrast, the PHso1 cells display morphological changes that can be observed during the L4 stage, the last larval stage before adulthood (**Figure 2A**). We find that during this stage PHso1 retracts its socket process and extends a short dendrite-like posterior projection into the PHsh cell and a long axon-like anterior process projecting towards the pre-anal ganglion region. For this reason and those described below, we use the name PHD to refer to the PHso1 cells after these morphological changes take place. A time-lapse of an individual male reveals that socket retraction is initiated at early L4, when the male gonad has almost reached the tail, and that the nascent axon is first observed at mid-L4, when the vas deferens has joined with the cloaca (**Figure 2B**). The axon-like outgrowth is complete by the end of tail-tip retraction, when ray precursor cells start to fuse into the tail seam syncytium (**Figure 2—figure supplement 1**). These observations corroborate those of John Sulston and identify the stage of sexual maturation as the time during which the PHso1 cells undergo radical remodelling in males. This remodelling involves quite a remarkable change in morphology from a socket-glial morphology to a neuron-like morphology.

To determine whether the PHso1 cells also acquire neuronal characteristics at the level of gene expression, we analysed and compared the expression of glial and neuronal markers in the PHso1 and PHso2 cells of males and hermaphrodites. In adult hermaphrodites, we find that both cells express the panglial microRNA *mir-228* (**Wallace et al., 2016**) and the AMso and PHso glial subtype marker *grl-2* (a Hedgehog-like and Ground-like gene protein: **Hao et al., 2006**) at similar levels (**Figure 3A**). In males, by contrast, *mir-228* and *grl-2* expression is noticeably dimmer in PHso1 than in PHso2 by the mid-to-late L4 stage and completely absent by day 2 of adulthood (**Figure 3A, B and C**). Importantly, expression of these reporters appears equal in brightness in both cells at the late L3 stage and only becomes noticeably dimmer in PHso1 following the morphological changes, such as the retraction of the socket, that occur during the L4 stage (**Figure 3B and C**, **Figure 3—figure supplement 1**). In contrast, in hermaphrodites, no morphological changes of PHso1 are observed and the reporters appear equal in brightness through to adulthood (**Figure 3A**, **Figure 3—figure supplement 1**). After the posterior hypodermal cells begin to retract leaving the characteristic fluid-filled extracellular space at the tail, PHso1 begins to express the pan-neuronal marker *rab-3* (a synaptic vesicle associated Ras GTPase: **Stefanakis et al., 2015**) in males but not in hermaphrodites, and this expression persists throughout adulthood (**Figure 3A, B and C**). In addition to *rab-3* expression we also observe sequential expression of other neuronal markers such as: the vesicle acetylcholine transporter *unc-17* (**Alfonso et al., 1993**; **Pereira et al., 2015**; **Figure 3D**); the phogrin orthologue for dense-core vesicle secretion *ida-1* (**Zahn et al., 2001**; **Figure 3E**); the intraflagellar transport component required for proper sensory cilium structure *osm-6* (**Collet et al., 1998**; **Figure 3F**); and the IG domain containing protein *oig-8* (**Howell and Hobert, 2017**; Figure 6A). None of these neuronal markers are observed in PHso2 or in the hermaphrodite PHso1. The switch in gene expression in PHso1 is therefore initiated concomitantly with morphological changes during sexual maturation and in a male-specific manner. Together, these data demonstrate that the male

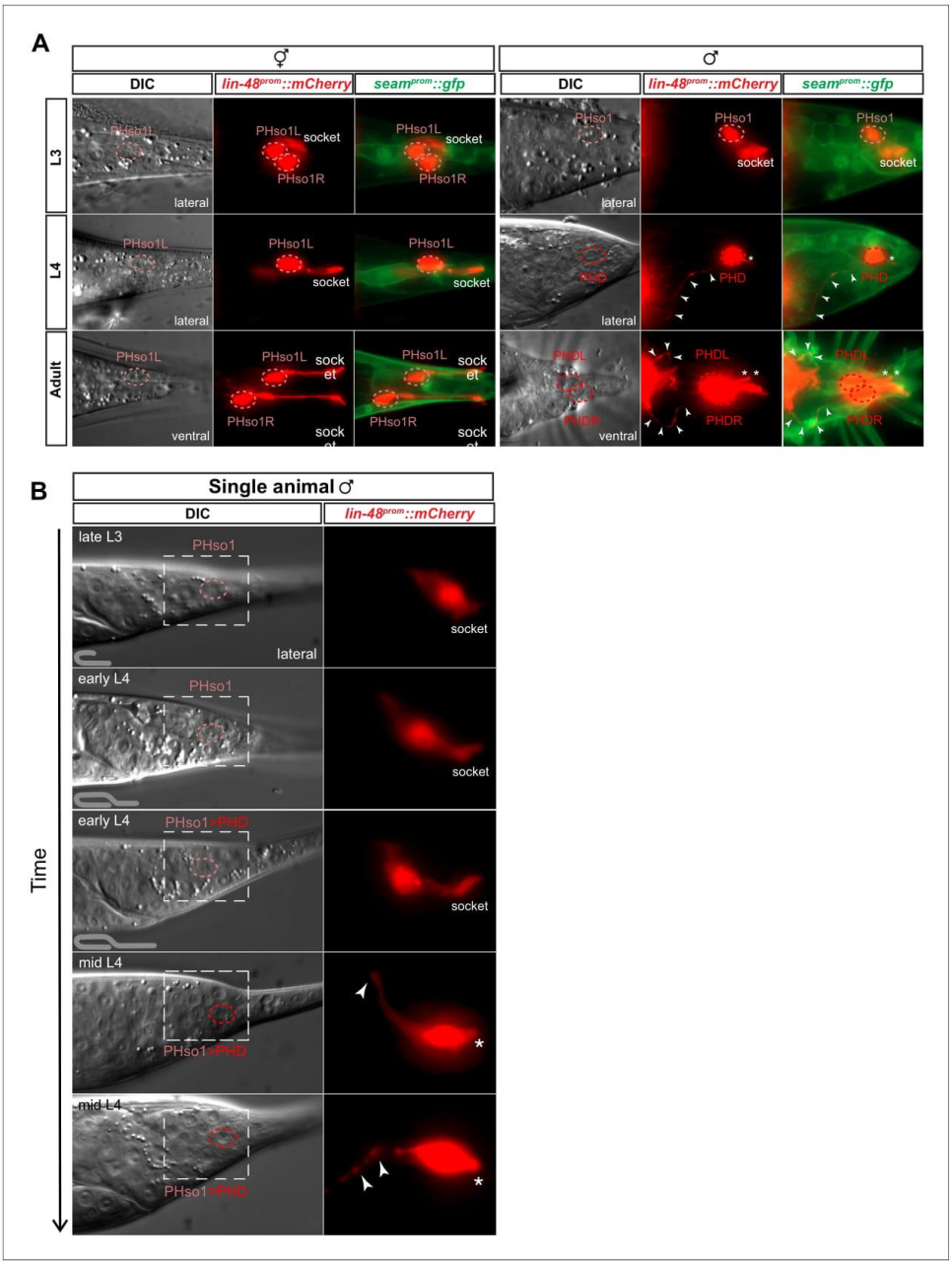

Figure 2. The sex-shared PHso1 cells undergo glia-to-neuron morphological changes in males. (**A**) Expression of *lin-48*^{prom}*::mCherry* and the *seam*^{prom}*::gfp* (*wrt-2*^{prom}*::gfp)* reporter transgenes in PHso1 of hermaphrodites (left panel) and males (right panel) at the third (L3) and fourth (L4) larval stages and in adults. The images show the morphological transformation of male PHso1 into the PHD neuron during sexual maturation. Arrowheads label the axonal process extending from the PHD into the pre-anal ganglion. Asterisks indicate the dendritic process of PHD. (**B**) DIC and fluorescent images of a

Figure 2 continued on next page

Figure 2 continued

time-lapse of PHso1-to-PHD remodelling in an individual male (see Materials and methods). The top two time-points show the late L3 stage after the gonad has looped back and early L4 after the gonad has crossed over itself (see cartoon at the bottom left side of the left panel). The subsequent time-points range from early-to-mid-L4, when the vas deferens has joined with the cloaca, to late mid-L4, when tail-tip retraction is almost complete. The dashed boxes on the DIC images indicate the position of the fluorescent images. Arrowheads indicate the nascent axon.
The online version of this article includes the following figure supplement(s) for figure 2:

Figure supplement 1. PHD axon outgrowth.

PHso1 bilateral pair of glial cells transdifferentiate into a novel class of cholinergic and likely peptidergic ciliated neurons, which we have termed phasmid D neurons (PHDs).

PHso1-to-PHD transdifferentiation is usually but not always direct

We sought to further validate that PHso1 transdifferentiation is direct. Division followed by programmed cell death of one of the daughters is common throughout *C. elegans* embryonic and post-embryonic development (***Sulston and Horvitz, 1977***; ***Sulston et al., 1983***). We therefore explored the possibility that PHso1 could divide asymmetrically, to give rise to the PHD neuron and a sister cell that undergoes rapid apoptosis. For this purpose, we analysed mutants of the canonical cell death protein CED-4, homologue to the apoptotic protease activating factor 1 (Apaf-1), required to activate the CED-3 effector caspase (***Ellis and Horvitz, 1986***; ***Yuan and Horvitz, 1992***; reviewed in ***Conradt et al., 2016***). Strong loss-of-function mutations in *ced-4* result in the survival of somatic cells that normally undergo programmed cell death during development. We observe no statistically significant increase in the frequency of 'survivor cells' in *ced-4(n1162)* mutants compared to controls, when scoring the number of cells per side of each animal. This suggests there is no cell death in the PHso1 lineage (***Figure 3—figure supplement 2A***). Moreover, we never observed an apoptotic cell body in the vicinity of the PHD neuron.

To our surprise, we observed the presence of an extra cell that co-expressed *lin-48^{prom}::tdTomato* and *rab-3^{prom}::yfp* in 13–24% of sides of both *ced-4* mutant and control animals (***Figure 3—figure supplement 2A***). This extra cell had a similar morphology to PHD, was located immediately anterior to PHD and was detected from the early L4 stage onwards. It also expressed all the markers known to be expressed by the PHD neurons (***Figure 3—figure supplement 2B–G***). We realised, however, the percentage occurrence of this extra cell was variable between strains suggesting its presence/absence is background-dependent (***Figure 3—figure supplement 2H***). In the cases where we did observe an extra cell, we wanted to distinguish between the following possibilities: additional expression of the transgenes in a highly similar neuronal subtype, perduring expression of the transgenes from earlier in the lineages of the phasmid sockets or an infrequent division of PHso1. To this end, we performed 5-ethynyl-2′-deoxyuridine (EdU) staining in a *lin-48^{prom}::tdTomato* background. EdU is a thymidine analogue that is incorporated into the replicating DNA of dividing cells. EdU was fed to a synchronised population of animals at late L2-to-early L3 (22 hr after L1 arrest), after the PHso1 cells are born and before they remodel into the PHD neurons, and adult animals were scored. As a positive control, the divison of the bilateral AMso cells that give rise to the MCM neurons were also scored, as it occurs at a similar time as the PHso1-to-PHD transition (***Sammut et al., 2015***). In the majority of cases (79% of sides scored), no EdU signal was detected, indicating that PHso1 mainly transdifferentiates directly into the PHD neuron. In 21% of sides however, EdU signal was detected in two *lin-48^{prom}::tdTomato*-expressing cells per side in the tail of male animals (***Figure 3G***) but never in hermaphrodites (data not shown). Importantly, EdU is never present in the PHD neuron unless observed in two cells on the same side, eliminating the possibility of cell death via non-apoptotic machinery, as is the case of the male linker cell (***Abraham et al., 2007***). In addition, we were able to observe the division of PHso1 in a single animal in a time-lapse of an individual male (***Figure 3—figure supplement 3***).

All together, these observations indicate that PHso1 can sometimes divide symmetrically to give rise to two neurons, which we term PHD1 and PHD2. However, in the vast majority of cases, the PHso1 cells undergo direct remodelling, without wholesale DNA replication or cell division, during which they directly acquire neuronal fate.

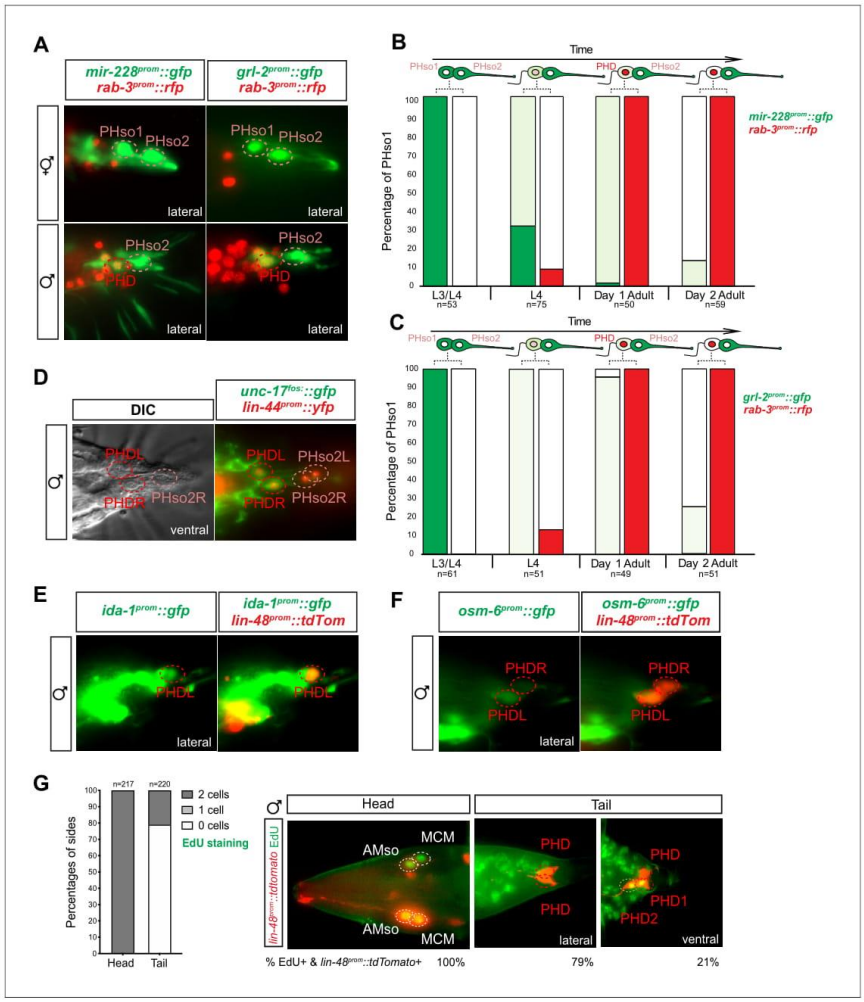

Figure 3. The sex-shared PHso1 cells undergo glia-to-neuron molecular changes in males occasionally accompanied by a division. (**A**) Expression of the glial marker reporter transgenes *mir-228^{prom}::gfp* and *grl-2^{prom}::gfp* and pan-neuronal marker *rab-3^{prom}::rfp* in the phasmid socket cells (PHso1 and PHso2) and the PHD neuron in adult male animals. (**B**) Bar chart showing the percentage of PHso1/PHD cells expressing the pan-glial marker reporter transgene *mir-228^{prom}::gfp* and the pan-neuronal marker reporter transgene *rab-3^{prom}::rfp* scored concomitantly in males at different stages of development and at adulthood. Intensity of the *mir-228^{prom}::gfp* reporter transgene in the PHso1/PHD cells was assessed by eye in comparison with PHso2: dark green indicates PHso1/PHD = PHso2, light green indicates PHso1/PHD < PHso2 and white is non-detectable in PHso1. (**C**) As B but for the subtype-specific glial marker *grl-2^{prom}::gfp* scored concomitantly with *rab-3^{prom}::rfp*. (**D**) Expression of the acetylcholine vesicle uploader reporter transgene *unc-17^{prom}::gfp* in the PHD neurons of adult males. The *lin-44^{prom}::yfp* reporter transgene has been coloured red. (**E**) Expression of an *osm-6^{prom}::gfp* reporter transgene in the PHD neurons of adult males, which are co-labelled with a *lin-48^{prom}::tdTomato* transgene. (**F**) Expression of an *ida-1^{prom}::gfp* reporter transgene in the PHD neurons of adult males, which are co-labelled with a *lin-48^{prom}::tdTomato* transgene. (**G**) EdU staining to assess PHso1 division. Left panel: quantification of EdU labelling in cells per side in adult males. The AMso division that gives rise to AMso and MCM cells was scored as a positive control. Right panel: representative images of EdU DNA labelling (green) present in the nuclei of the AMso socket cell and MCM neuron (head), and absent in the PHD neuron (tail), unless two cells per side are observed (PHD1 and PHD2). All cells scored were labelled with a *lin-48^{prom}::tdTomato* transgene.

The online version of this article includes the following source data and figure supplement(s) for figure 3:

Source data 1. Scoring data of glial and neuronal fluorescent reporters and EdU labelling in the PHD neurons of *wildtype* animals.

Figure 3 continued on next page

Figure 3 continued

Figure supplement 1. Expression of glial markers is downregulated in the PHso1 of males.
Figure supplement 2. PHso1 divides at low frequency in a background-dependent manner.
Figure supplement 2—source data 1. Scoring data of PHD background-dependent division.
Figure supplement 3. Live division of PHso1 in a single-animal time-lapse.

Biological sex regulates PHso1-to-PHD transdifferentiation cell-autonomously

We next addressed whether the PHso1-to-PHD cell fate switch is regulated by the genetic sex of the cell rather than the sex of the rest of the animal, in a manner similar to that of several other sexual dimorphisms in *C. elegans* (**Fagan et al., 2018**; **Hilbert and Kim, 2017**; **Lee and Portman, 2007**; **Oren-Suissa et al., 2016**; **Ryan et al., 2014**; **Sammut et al., 2015**; **Weinberg et al., 2018**; **White and Jorgensen, 2012**; **White et al., 2007**). To uncouple the sex of PHso1 from the rest of the animal, we drove expression of *fem-3* in PHso1 (and PHso2) under the *grl-2* promoter. *fem-3* inhibits the expression of *tra-1*, a downstream target of the sex-determination pathway that activates hermaphrodite development and inhibits male development (**Hodgkin, 1987** and reviewed in **Zarkower, 2006**). Therefore, cell-specific expression of a *fem-3* transgene will masculinise a cell in an otherwise hermaphroditic background. We find that *fem-3* expression specifically in the PHso1, and not PHso2, transforms PHso1 into a PHD-like neuron, resulting in the upregulation of *ida-1* and *rab-3* expression and the acquisition of neuronal morphology (**Figure 4A–C**). This indicates that the competence of PHso1 to transdifferentiate into PHD is likely cell-intrinsic and based on genetic sex.

Factors required for Y-to-PDA transdifferentiation are largely dispensable for PHso1-to-PHD and AMso-to-AMso+MCM transdifferentiation

The first well-described transdifferentiation event in *C. elegans* is the direct conversion of the rectal epithelial cell Y into the motor neuron PDA (**Jarriault et al., 2008**). As with PHso1-to-PHD, Y-to-PDA occurs directly, without a division and in a sex-specific manner. However, Y-to-PDA happens exclusively in hermaphrodites (in males the Y blast cell divides and PDA is generated from the anterior daughter of this division) and during the late L1 stage, much earlier than sexual maturation. In Y-to-PDA, the erasure of the original epithelial fate requires the action of a complex of conserved nuclear factors (SOX-2, CEH-6/Oct, SEM-4/Sall, and EGL-27/Mta) and the acquisition of the final motor neuron fate involves the cholinergic terminal selector EBF transcription factor UNC-3, in addition to specific combinations of histone modifier complexes (**Kagias et al., 2012**; **Richard et al., 2011**; **Zuryn et al., 2014**). We investigated how broadly the molecules involved in the initiation of Y-to-PDA transdifferentiation could be acting in *C. elegans*, as we hypothesised that the factors involved in the re-specification would depend on the specific terminal neuronal cell fate. Hence, we analysed loss-of-function mutants for *sem-4, egl-27,* and *sox-2* in PHso1-to-PHD transdifferentiation, and in the previously described AMso-to-AMso+MCM cell fate switch (**Sammut et al., 2015**).

We observed no statistically significant defect in the number and cell identity of MCM and PHD neurons in *sem-4(n1971)* null mutants (**Figure 5A**). In *egl-27(ok1671)* strong loss-of-function mutants, although a significant defect is observed in the number of *lin-48^{prom}::tdTomato*-positive MCM neurons, normal *rab-3^{prom}::yfp* expression suggests a defect in *lin-48::tdtTomato* reporter transgene expression levels but not in the division of the AMso or in the acquisition of neuronal fate by the MCM. No *lin-48^{prom}::tdTomato* expression is ever observed in the region of PHso1/PHD in *egl-27* mutants at any stage or in either sex (**Figure 5A** and data not shown). This is consistent with previous results that show that *egl-27* affects the division pattern of the T lineage and consequently the production of PHso1 (**Herman et al., 1999**). This early role of *egl-27* in the PHso1 lineage precludes its study in the generation of the PHD neuron using loss-of-function mutants.

As *sox-2* null mutations cause L1 lethal larval arrest, we used two parallel strategies to investigate the role of *sox-2* in PHso1-to-PHD and AMso-to-AMso+MCM: RNAi knock-down and analysis of a rescued *sox-2* null allele. For the former, we made use of the RNAi-sensitised strain *nre-1(hd20) lin-15B(hd126)* (**Schmitz et al., 2007**). No statistically significant defect is observed in the PHD neuron in *sox-2* RNAi-treated animals (**Figure 5B**). An increase in the number of *rab-3^{prom}::yfp*-expressing

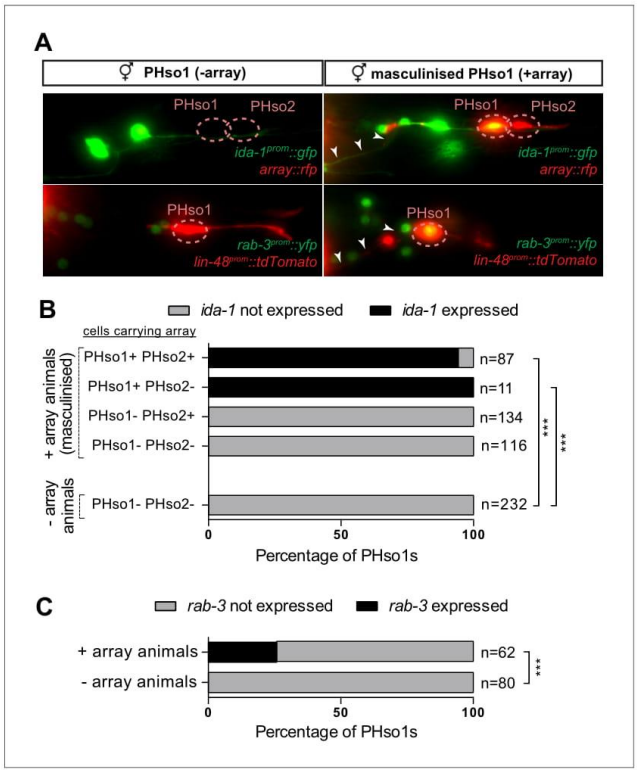

Figure 4. PHso1-to-PHD plasticity is intrinsically regulated. (**A**) Expression of the *ida-1*^{prom}*::gfp* and *rab-3*^{prom}*::yfp* reporter transgenes in adult hermaphrodites carrying the masculinising array *grl-2*^{prom}*::fem-3::mCherry* in PHso1 (right panel) and in non-array-carrying hermaphrodites (left panel). (**B**) Bar chart showing the percentage of PHso1 and PHso2 cells expressing the *ida-1*^{prom}*::gfp* reporter transgenes in adult hermaphrodites carrying or not carrying the masculinising *grl-2*^{prom}*::fem-3::mCherry* array. Of note, the *grl-2* promoter fragment is also expressed in the AMso, excretory pore and excretory duct cells in the head (***Hao et al., 2006***). Fisher's exact test was used to compare all categories between genotypes and only statistically significant differences from the non-array carrying animals are indicated (*p≤0.05, **p≤0.01, ***p≤0.001). (**C**) Bar chart showing the percentage of PHso1 cells expressing the *rab-3*^{prom}*::yfp* reporter transgene in adult hermaphrodites carrying or not carrying the masculinising *grl-2*^{prom}*::fem-3::mCherry* array. Fisher's exact test was used to compare all categories between genotypes and only statistically significant differences from non-array carrying animals are indicated (*p≤0.05, **p≤0.01, ***p≤0.001).

The online version of this article includes the following source data for figure 4:

Source data 1. Scoring data of PHso1 masculinised cells in hermaphrodite worms.

MCM cells was detected (***Figure 5B***) but analysis of *lin-48*^{prom}*::tdTomato* expression revealed that the extra *rab-3* positive cells derive from ectopic AMso cells that divide efficiently to produce MCM neurons (***Figure 5—figure supplement 1A***). Interestingly, the ectopic MCM cells recapitulate normal development as they not only express the pan-neuronal marker *rab-3*^{prom}*::yfp*, but also the neuron subtype marker *ida-1*^{prom}*::gfp* (***Figure 5—figure supplement 1B***). Moreover, although ectopic AMso cells are observed in both sexes, they exclusively divide in males and not in hermaphrodites (***Figure 5—figure supplement 1A***). This, together with the fact that ectopic *lin-48*-positive cells are induced in RNAi-treated animals only in the F1 generation (and not the P0 generation – see

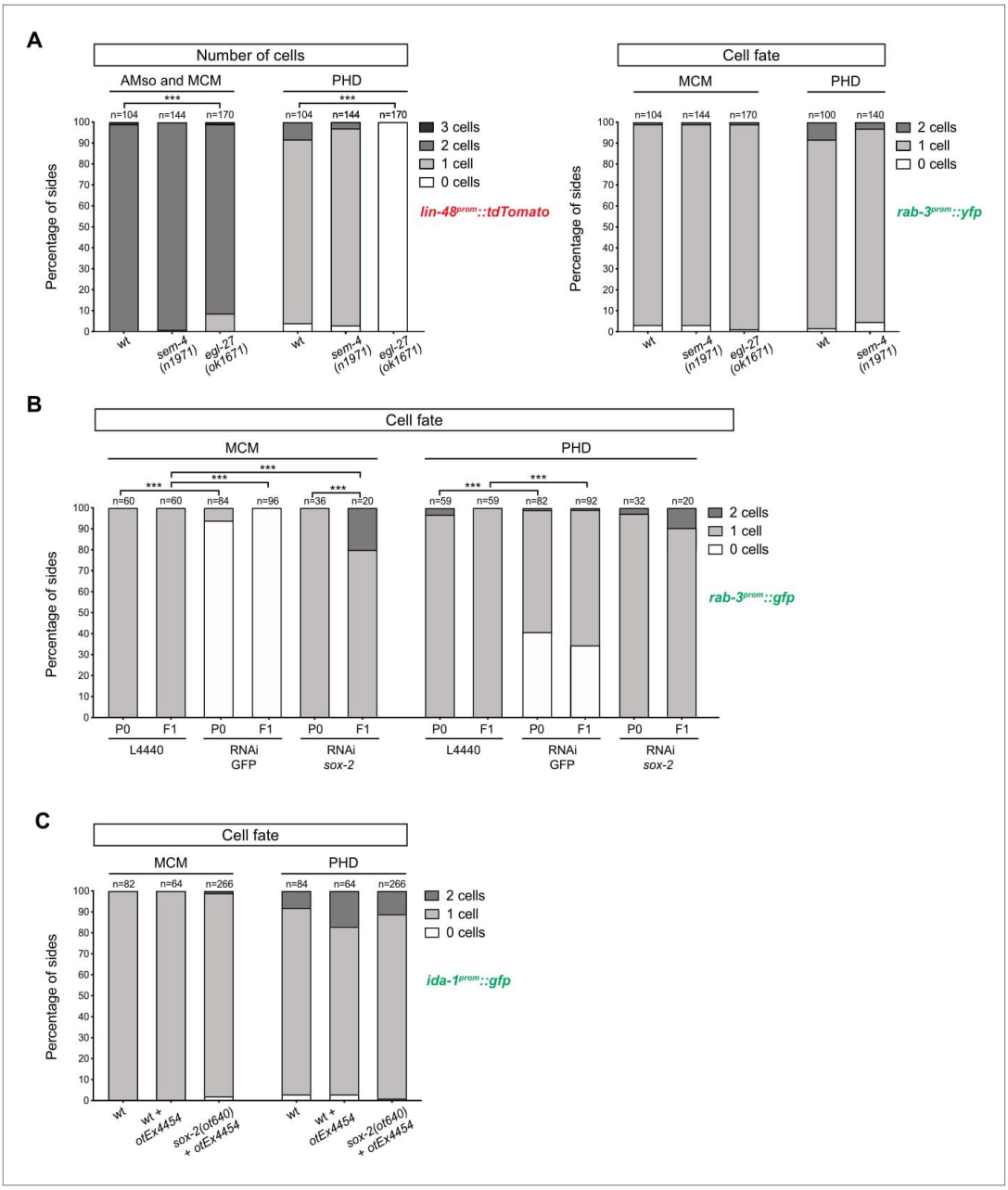

Figure 5. Factors required for Y-to-PDA transdifferentiation are largely dispensable for PHso1-to-PHD and AMso-to-AMso+MCM transdifferentiation. (**A**) Bar chart showing the percentage of AMso, MCM, and PHD cells expressing the *lin-48*^{prom}*::tdTomato* transgene (*drpIs3;* left panel) and the pan-neuronal marker *rab-3*^{prom}*::yfp* reporter transgene (*otIs291*; right panel), in *sem-4(n1971)* putative null and *egl-27(ok1670)* strong loss-of-function mutant animals. The presence and morphology of cells was assessed by *lin-48*^{prom}*::tdTomato* that is expressed, in the head, in the MCM mother (the AMso)

Figure 5 continued on next page

Figure 5 continued

and retained in the AMso and MCM daughters after the division (two cells per side). In the tail, *lin-48^{prom}::tdTomato* is expressed in PHso1 before the cell remodelling and after, in the PHD neuron (one cell per side unless PHD1 and PHD2 are observed). Cells per side were scored in male animals from late L4 to adult stages. Neuronal identity was assessed by *rab-3^{prom}::yfp*. For the PHD neuron *rab-3^{prom}::yfp* was scored concomitantly with *lin-48^{prom}::tdTomato* due to the high number of *rab-3^{prom}::yfp*-expressing neurons in the tail. Fisher's exact test was used to compare all categories between genotypes and only statistically significant differences from the *wildtype* phenotype are indicated (*p≤0.05, **p≤0.01, ***p≤0.001). Of note, 4/7 cells lacking *rab-3^{prom}::yfp* expression in the tail of *sem-4* mutants retained a socket morphology, which is never observed in the cells lacking the reporter in the control strain. This could suggest a block to the initiation of transdifferentiation in PHso1 or that the severe morphological defects of male tails in these mutant animals impair the remodelling process. (**B**) Bar chart showing the percentage of MCM and PHD neurons expressing *rab-3^{prom}::yfp* after RNAi-knockdown of *sox-2*. L4440 empty vector was used as a negative control and GFP RNAi-knockdown as a positive control. Fisher's exact test was used to compare all categories between genotypes and statistically significant differences from the *wildtype* phenotype are indicated (*p≤0.05, **p≤0.01, ***p≤0.001). (**C**) Bar chart showing the percentage of MCM and PHD neurons expressing the *ida-1^{prom}::gfp* neuron subtype marker in *sox-2 (ot460)* null mutant animals rescued for lethality with a *sox-2* fosmid-based extrachromosomal array: (*otEx4454[sox-2(fosmid)::mCherry + elt-2^{prom}::DsRed*]). A mixed population of of *sox-2* mutant (mosaic or non-rescued) and *wildtype* (mutant-rescued) cells were scored. No statistical difference is observed between any of the groups using Fisher's exact test.

The online version of this article includes the following source data and figure supplement(s) for figure 5:

Source data 1. Scoring data of glial and neuronal fluorescent reporters in the PHD neurons of *sem-4*, *egl-27*, and *sox-2* mutant animals.
Figure supplement 1. Factors required for Y-to-PDA transdifferentiation are largely dispensable for PHso1-to-PHD and AMso-to-AMso+ MCM transdifferentiation – additional data.
Figure supplement 1—source data 1. Additional scoring data of glial and neuronal fluorescent reporters in the PHD neurons of *sem-4*, *egl-27*, and *sox-2* mutant animals.

Materials and methods), suggests an early role of *sox-2* in an unknown lineage to supress the production of supernumerary AMso cells.

We additionally analysed a strain containing a *sox-2(ot640)* null allele that was not available at the time of Y-to-PDA characterisation (***Vidal et al., 2015***). To bypass lethality, this strain contains an extrachromosomal *sox-2* fosmid-based rescue array. The presence of this array in individual worms can be tracked by a fluorescent co-injection transgene, *elt-2^{prom}::DsRed*. Within an individual animal the array is inherited in a mosaic fashion and this is validated by the presence of dead embryos positive for the array. As with RNAi-knockdown, no statistically significant defect is observed in the PHD neuron (***Figure 5C***). In the head, one ectopic *ida-1^{prom}::gfp*-expressing MCM neuron is overserved in 3/266 sides per animal, coinciding with an extra AMso (***Figure 5C*** and ***Figure 5—figure supplement 1C***) and phenocopying the F1 RNAi results. However, four out of 269 total *lin-48^{prom}::tdTomato* expressing MCM cells lack *ida-1^{prom}::gfp* expression (***Figure 5C*** and ***Figure 5—figure supplement 1C***), suggesting a possible minor role of *sox-2* in AMso-to-AMso+MCM, not detected in the RNAi-knockdown experiments.

Mutants in the same genes implicated in Y-to-PDA transdifferentiation were employed in this work and with the exception of *sox-2*, identical alleles were used. However, while the Y cell completely fails to transdifferentiate into PDA in these mutants (70–100% of the cases - ***Kagias et al., 2012***), the PHso1-to-PHD and AMso-to-AMso+MCM cell fate switches show no or only very mild defects. Altogether these results suggest that different molecular mechanisms from the ones regulating Y-to-PDA must govern the PHso1-to-PHD and AMso-to-AMso+MCM cell fate switches.

PHDs are sensory neurons of male-specific copulation circuits

To further establish the neuronal characteristics of PHDs, we examined their synapses and ultrastructure, and mapped their full wiring diagram. We identified a ~1 kb promoter region that specifically drives the expression of *oig-8* in the PHD neurons. Expression of a *rab-3* translational fusion under the control of this *oig-8* promoter reveals that PHDs form synapses in the pre-anal ganglion, where the synaptic vesicle associated mCherry-tagged RAB-3 protein can be observed (***Figure 6A***). At the ultrastructural level, we observed both synaptic and dense-core vesicles in PHD, proximal to the cell body (***Figure 6B***). Ultrastructural analysis of the PHD dendrite in seven different animals independently confirms John Sulston's original observation on the presence of cilia, including the basal body and axonemes (***Sulston et al., 1980***). The basal body of PHD lies just dorsal and anterior to the phasmid sheath channel containing the PHA and PHB cilia. It has 2, 1, or 0 short cilia extending

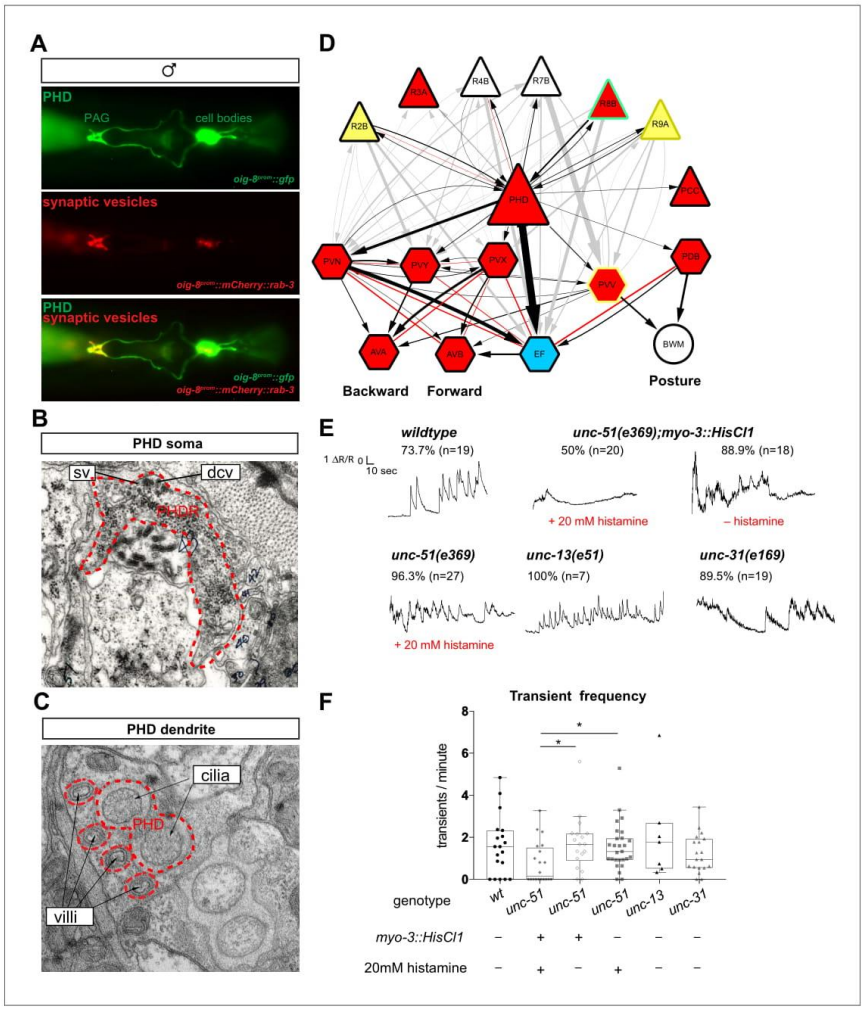

Figure 6. The PHDs are putative proprioceptive neurons of male-specific copulation circuits. (**A**) Expression of the *oig-8*^{prom}*::mCherry::rab-3* and *oig-8*^{prom}*::gfp* reporter in the PHD neurons of adult males. The synapses made by the PHDs in the pre-anal ganglion (PAG) can be observed (ventral view). (**B**) Electron micrographs of the soma of a PHD neuron of an adult male. sv, synaptic vesicle; dcv, dense-core vesicles; PHDR, right PHD neuron. (**C**) As B for a PHD dendrite. (**D**) Diagram depicting the connectivity of the PHD neurons with their main pre-synaptic inputs (ray neurons) and post-synaptic targets. The connections between the ray neurons (RnA/B) and their post-synaptic targets independently of PHD are indicated in grey. Arrows and red lines indicate chemical and electrical synaptic connections, respectively. The thickness of the arrows is proportional to the anatomical strength of their connections (# serial sections). Neurons are colour-coded according to their neurotransmitter: red, cholinergic; yellow, glutamatergic; dark yellow, dopaminergic; blue, GABAergic; green, serotonergic; white, orphan. Note that some neurons (R8B, R9A, PVV) express more than one neurotransmitter. (**E**) Example traces showing PHD activity as normalised GCaMP/RFP fluorescence ratio in restrained animals. Traces are shown for a *wildtype* male, an *unc-51(e359)* mutant with and without a histamine-inducible silencing transgene in muscle (*myo-3*^{prom}*::HisCl1*), a mutant in synaptic transmission (*unc-13*), and a mutant in dense-core vesicle exocytosis (*unc-31*, CADPS/CAPS). The proportion of traces where calcium peaks were identified is indicated for each genotype and treatment. n = number of neurons imaged. (**F**) Plots of frequency values of calcium transients per neuron. Dots represent

Figure 6 continued on next page

Figure 6 continued

individual neurons imaged. Tukey box-and-whisker plots indicate the interquartile ranges and median. *p<0.05; One-way ANOVA with multiple comparisons. Two groups were compared: *unc-51* genotypes and treatments and another group including *wt*, *unc-13*, and *unc-31*. Only statistically significant comparisons are indicated.
The online version of this article includes the following source data and figure supplement(s) for figure 6:

Source data 1. Value of calcium transients elicited by PHD in different genetic backgrounds.
Figure supplement 1. Ultrastructure of the male phasmid sensilla.

within the phasmid sheath very close to PHA and PHB cilia, but within a separate sheath channel. Interestingly, the PHD cilia can lie in variable positions relative to the PHA and PHB cilia: medial, lateral, dorsal, or ventral. In addition, we observe that the dendrite is more elaborate than previously described and has a number of unciliated finger-like villi within the phasmid sheath cell, proximal to the basal body (***Figure 6C*** and ***Figure 6—figure supplement 1***). Through reconstruction of serial electron micrographs all the synaptic partners of PHD were identified (***Supplementary file 1***; ***Jarrell et al., 2012***). PHD neurons project from the dorsolateral lumbar ganglia anteriorly and then ventrally along the posterior lumbar commissure and into the pre-anal ganglion. In the pre-anal ganglion, these establish chemical synapses and gap junctions with sensory neurons and interneurons, most of which are male-specific (***Figure 6D***). Previously, the axonal process of PHD was attributed to the R8B ray neuron (***Jarrell et al., 2012***). A re-examination of the lumbar commissure allowed us to disambiguate PHD's axon. PHDs receive synaptic input from male-specific ray sensory neurons involved in the initiation of the mating sequence in response to mate contact (***Barr and Sternberg, 1999***; ***Liu and Sternberg, 1995***; ***Koo et al., 2011***). The main PHD output is to the male-specific EF interneurons (35.4% of chemical synapses), both directly and through their second major post-synaptic target, the sex-shared PVN interneuron. The EF interneurons are GABAergic (***Serrano-Saiz et al., 2017b***) and synapse onto the AVB pre-motor interneurons which drive forward locomotion. Other PHD outputs include the PVV (male-specific) and PDB (sex-shared but highly dimorphic in connectivity; ***Jarrell et al., 2012***; ***Cook et al., 2019***) interneurons, which synapse onto body-wall muscle, and the cholinergic male-specific interneurons PVY and PVX whose output is to the AVA pre-motor interneurons, which drive backward locomotion. PVN, PVY, and PVX form disynaptic feed-forward triplet motifs that connect PHD strongly to the locomotion circuit interneurons AVB and AVA. The pattern of connectivity of PHD suggests a possible role in male mating behaviour.

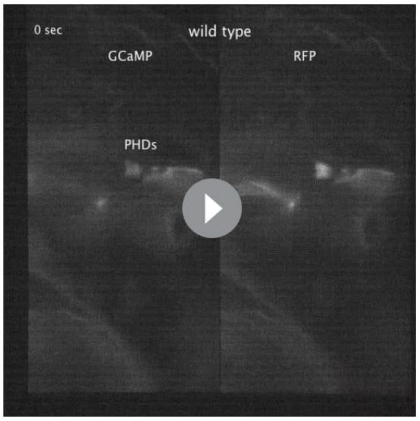

Video 1. Imaging of neuronal activity in PHD neurons with GCaMP6f (left channel) and RFP (right channel) in restrained animals: *wildtype* male. Animals are expressing an *oig-8^{prom}::GCaMP6f::sl2::rfp* transgene. Videos play at 100 fps (recorded at 20 fps).
https://elifesciences.org/articles/48361#video1

PHDs are putative proprioceptive neurons

We next sought to establish the function of the PHD neurons. We began by asking what sensory stimuli might activate them. To monitor neuronal activity, we co-expressed GCaMP6f and RFP in the PHDs and performed ratiometric measurements of fluorescence. We imaged calcium transients in restrained animals glued to a slide without anaesthetic. To our surprise, without applying any exogenous stimulation, we observed intermittent calcium transients in the PHDs of *wildtype* animals, every 30 s on average (***Figure 6E–F*** and ***Video 1***). We observed calcium transients in 73% of the neurons imaged and no peaks could be identified in the remaining traces (n = 19). Since in restrained animals there are small tail and spicule movements due to the defecation cycle and sporadic muscle contractions, one explanation could be that PHDs

may be proprioceptive. We reasoned that if PHD activity resulted from internal tissue deformation caused by muscle contractions, inhibition of muscle activity should eliminate or reduce calcium transients. To inhibit muscle contractions, we generated transgenic worms in which muscles can be silenced in an inducible manner through the expression of the *Drosophila* histamine-gated chloride channel HisCl1 (**Pokala et al., 2014**), under the *myo-3* promoter. To increase the efficiency of muscle silencing, we introduced this transgene into an *unc-51(e369)* mutant background that renders animals lethargic. *unc-51* encodes a serine/threonine kinase required for axon guidance and is expressed in motor neurons and body-wall muscle (**Ogura et al., 1997**). Histamine-treated *myo-3^{prom}::HisCl1;unc-51(e369)* animals were highly immobile and the frequency of calcium transients in the PHDs was strongly reduced (**Figure 6E–F** and **Videos 2** and **3**). Transients were completely eliminated in half of the neurons (**Figure 6F**). The reduction in transient frequency was specific to the silencing of the muscles because in histamine-treated *unc-51(e369)* and histamine non-treated *myo-3^{prom}::HisCl1;unc-51(e369)* control animals, frequency was similar to that of *wildtype* animals (**Figure 6E,F** and **Video 4**).

Although PHDs are sensory neurons, they do receive some small synaptic input from other neurons (**Figure 6D**) and therefore the activity observed in restrained animals in response to muscle contractions could arise either directly through PHD sensory input or indirectly through pre-synaptic neurons. To test this, we imaged PHD activity in *unc-13(e51)* mutant males with impaired synaptic neurotransmission (**Miller et al., 1996**) and in *unc-31(e169)* mutant males with impaired dense-core vesicle secretion (**Speese et al., 2007**). In both these mutants, PHD calcium transients persisted at similar frequencies to those in *wildtype* animals (**Figure 6E and F**). This suggests that PHD activity does not require chemical input from the network. However, we cannot completely rule out that residual neurotransmission in the hypomorphic *unc-13(e51)* mutants may be sufficient to trigger *wildtype* levels of PHD activity in response to muscle contractions. Together, these results suggest that PHDs may respond directly to internal cues arising from muscle contractions, and that they may be proprioceptive neurons. PHDs may sense internal tissue deformations through their elaborate ciliated dendrites, which are deeply encased in the phasmid sheath and not exposed to the outside environment.

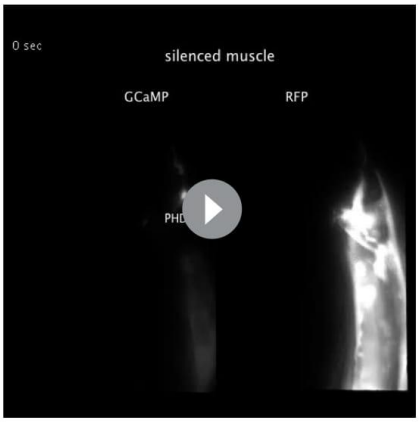

Video 2. Imaging of neuronal activity in PHD neurons with GCaMP6f (left channel) and RFP (right channel) in restrained animals: *unc-51(e359)* male expressing a histamine-inducible silencing transgene in muscle (*myo-3^{prom}::HisCl1::mCherry*) and treated with 20mM histamine. Animals are expressing an *oig-8^{prom}::GCaMP6f::sl2::rfp* transgene. Videos play at 100 fps (recorded at 20 fps).
https://elifesciences.org/articles/48361#video2

Video 3. Imaging of neuronal activity in PHD neurons with GCaMP6f (left channel) and RFP (right channel) in restrained animals: *unc-51(e359)* male expressing a histamine-inducible silencing transgene in muscle (*myo-3^{prom}::HisCl1::mCherry*) and treated with 20mM histamine. Animals are expressing an *oig-8^{prom}::GCaMP6f::sl2::rfp* transgene. Videos play at 100 fps (recorded at 20 fps).
https://elifesciences.org/articles/48361#video3

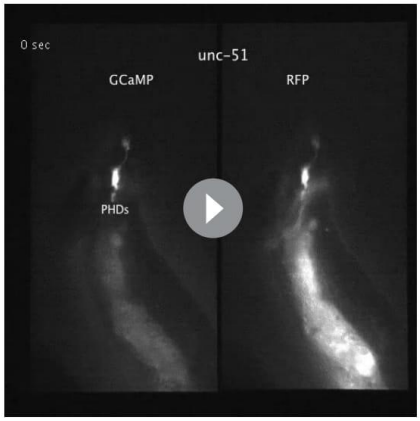

Video 4. Imaging of neuronal activity in PHD neurons with GCaMP6f (left channel) and RFP (right channel) in restrained animals: *unc-51(e359)* male treated with 20mM histamine. Animals are expressing an *oig-8^{prom}::GCaMP6f::sl2::rfp* transgene. Videos play at 100 fps (recorded at 20 fps).
https://elifesciences.org/articles/48361#video4

A novel readjustment step during male mating

The connectivity of PHD to male-specific neurons in the tail suggests that they may play a role in male reproductive behaviours controlled by tail circuits. In *C. elegans*, these include food-leaving behaviour, an exploratory strategy to search for mates (***Lipton et al., 2004***; ***Barrios et al., 2012***; ***Barrios et al., 2008***), and mating behaviour. Mating consists of a temporal sequence of discrete behavioural steps: response (to mate contact); scanning (backward locomotion while scanning the mate's body during vulva search); turning (at the end of the mate's body to continue vulva search); location of vulva (stop at vulva); spicule insertion (intromission); and sperm transfer (reviewed in ***Barr et al., 2018***; ***Figure 7***). The coordinated execution of these mating steps relies on sensory cues from the mate (***Barr and Sternberg, 1999***) and also, presumably, proprioceptive inputs within the male's copulation circuit as well (***Sulston et al., 1980*** and reviewed in ***García, 2014***). This sensory information guides the male to either initiate the next step of the sequence or to reattempt the current, unsuccessful step through readjustment of movement and/or posture (reviewed in ***Barr et al., 2018***).

During our behavioural analysis of *wildtype* males, we identified a novel readjustment movement that has not been previously described which we have termed the 'Molina manoeuvre'. This movement occurs when the male has been trying to insert its spicules in the mate's vulva for a period of time without success and subsequently loses vulva apposition. Unsuccessful spicule insertion attempts occurred in 65% of males, resulting in either a long displacement from the vulva, which led to the re-initiation of the scanning sequence, or in a small displacement (less than two tail-tip length) from the vulva (98% of vulva losses), as previously described (***Correa et al., 2012***). We find that these small displacements from the vulva lead either to local shifts to relocate the vulva (68% of total vulva losses) or to a Molina manoeuvre (32% of vulva losses) (***Figure 7***). The Molina manoeuvre consists of the initiation of forward locomotion along the mate's body away from the vulva to the end of the mate's body (or at least two male tail-tips distance away from the vulva), at which point the male tail acquires a deeply arched posture, followed by a return to the vulva with backward locomotion along the same route (***Video 5***). Males perform this movement towards either end (head or tail) of the mate as a smooth, continuous sequence. Although we used paralysed *unc-51* mutant hermaphrodites to aid our mating analysis, males also perform this readjustment movement with moving *wildtype* mates (***Video 6***).

The PHD neurons are required for coordinated backward locomotion and effective intromission during mating

To test the hypothesis that PHDs regulate reproductive behaviours, we performed behavioural tests of intact and PHD-ablated males and functional imaging of PHD activity in freely behaving males during mating. Target specificity of the laser ablations was confirmed 1-day after ablation by absence of fluorescence returning from the transgene used to label the PHD neurons (***Figure 7—figure supplement 1A–C***). We found no defects in food-leaving behaviour, response to mate contact, turning, location of vulva, or spicule insertion (***Figure 7A,B,D,E and H***). However, these experiments revealed a role for PHDs in initiation and/or maintenance of backward locomotion during scanning and during the Molina manoeuvre. PHD-ablated males often switched their direction of locomotion during scanning, performing fewer continuous backward scans during vulva search compared to

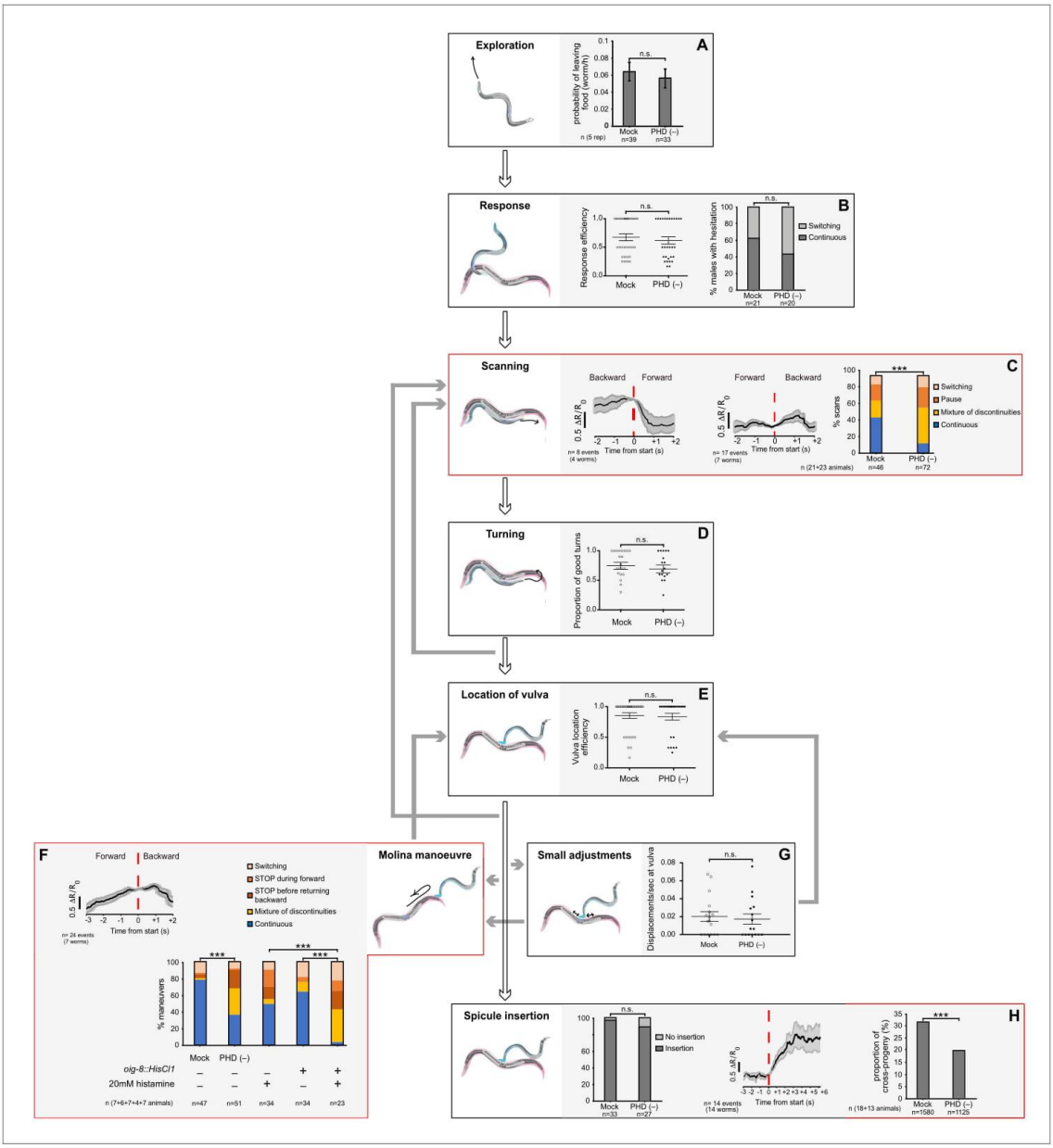

Figure 7. The PHD neurons are required for coordinated backward locomotion and effective intromission during mating. Diagram depicting the steps of reproductive behaviours controlled by the male tail circuits. The steps affected by PHD ablation are highlighted in red. Intact (mock) and ablated males carried either an *oig-8*^{prom}*::gfp* or an *unc-17*^{prom}*::gfp* transgene to identify the PHD neurons for ablation. In F, males carrying an *oig-8*^{prom}*::HisCl1* transgene were used to silence PHD neurons acutely. White arrows indicate the transitions between the mating sequence. Grey arrows indicate the corrective transitions that males perform when they fail to attain the subsequent goal. The corrective transitions that occur upon failure of spicule insertion attempts (between location of vulva and spicule insertion) are always preceded by a displacement from the vulva (not depicted). Behavioural

Figure 7 continued on next page

Figure 7 continued

analysis in intact and PHD-ablated males are shown for each step. Calcium imaging in PHD neurons is shown for steps C, F, and H. The black trace shows PHD activity as normalised GCaMP/RFP fluorescence ratio changes averaged for several events and phase locked (red dotted line) to the switch in the direction of locomotion (**C and F**) or to the start of spicule insertion (**H**). The grey shadow shows S.E.M. (**A**) Male exploratory behaviour measured as P_L values (probability of leaving food per worm per hour). n, number of males tested. Maximum likelihood statistical analysis was used to compare P_L values. n.s., no statistically significant difference, $p \geq 0.05$; error bars, S.E.M. (**B**) Response efficiency, measured as 1/number of contacts with a mate before responding; and hesitation, measured as a switch in direction of locomotion during response. (**C**) Scanning locomotion during vulva search. Categories: switching (change in the direction of locomotion from backward to forward); pause (stopping during backward scanning); mixture (scans with switches and pauses); continuous (uninterrupted backward movement along the mate's body). $p<0.001$ (χ^2 test of continuous and discontinuous scans); n = number of events. (**D**) Turning, measured as proportion of good turns per male. (**E**) Vulva location efficiency measured as 1/number of vulva encounters before stopping. (**F**) Proportion of continuous and discontinuous Molina manoeuvres. Categories: switching (a brief change in the direction of movement either during forward locomotion away from the vulva or during backward locomotion returning to the vulva); STOP during forward (stopping during forward movement away from the vulva and then continuing in the same direction); STOP before returning backward (stopping at the transition between forward movement away from the vulva and returning backwards to the vulva); mixture (manoeuvres that displayed more than one of the discontinuities described above); continuous (smooth movement forward away from the vulva and return backwards to the vulva without stopping or switching in between). $p<0.001$ (χ^2 test of continuous and discontinuous manoeuvres); n = number of events. (**G**) Number of displacements away from the vulva per unit of time spent at vulva. (**H**) Left bar chart, proportion of males able to insert their spicules; n.s., no statistically significant difference, $p \geq 0.05$ (χ^2 test); n = animals tested. Right bar chart, sperm transfer efficiency measured as percentage of cross-progeny; $p<0.001$ (χ^2 test); n = total progeny. For B, D, E, and G, bar and dots represent mean and individual animal values, respectively; error bars, S.E.M. n.s., no statistically significant difference, $p \geq 0.05$ (Mann-Whitney U test). Worm cartoons were modified with permission from original drawings by Rene García.
©2018 Genetics Society of America. Figure 7 contains modified versions of the male and hermaphrodite worm cartoons from ***Barr et al., 2018*** used with permission. They are not covered by the CC-BY 4.0 licence and further reproduction of this panel would need permission from the copyright holder.

The online version of this article includes the following source data and figure supplement(s) for figure 7:

Source data 1. Analysis of mate searching, fertility, and male-mating behaviours and measurements of PHD neuronal activity during mating in *wildtype* and PHD-ablated animals.
Figure supplement 1. PHD neuron ablation control.
Figure supplement 2. Some ectopic prodding occurs during discontinuous Molina manoeuvres and during pauses while scanning.
Figure supplement 2—source data 1. Scoring of ectopic prodding events during mating in *wildtype* and PHD-ablated animals.

intact males (***Figure 7C***). Consistent with this, we observed higher activity (i.e. Ca^{2+} levels) in PHD during backward locomotion than during forward locomotion while scanning (***Figure 7C***). PHD activity also peaked just after the switch to backward locomotion during Molina manoeuvres, when the tail tip displays an acute bent posture, and PHD-ablated males performed defective, discontinuous manoeuvres, often stopping at the transition from forward to backward locomotion to return to the vulva (***Figure 7F*** and ***Video 7***). Importantly, we did not find significant differences between intact and PHD-ablated males in number of events that trigger the initiation of manoeuvres (***Figure 7G***), indicating that PHDs are specifically required for coordinated locomotion during the manoeuvre itself, at the transition point to backward locomotion. Similar locomotion defects resulting in discontinuous manoeuvres were observed when PHD neurons were acutely silenced with an inducible chloride channel transgene (*oig-8^{prom}::HisCl1::sl2::rfp*) (***Figure 7G***). Together, these data demonstrate that without intact PHD neurons, backward movement along the mating partner becomes slightly erratic, often interrupted by a switch in direction (during scanning),

Video 5. Males performing Molina manoeuvres during mating: *wildtype* male performing a Molina manoeuvre during mating with a paralysed *unc-51 (e359)* hermaphrodite. Videos are played at 40 fps (sped up x2).
https://elifesciences.org/articles/48361#video5

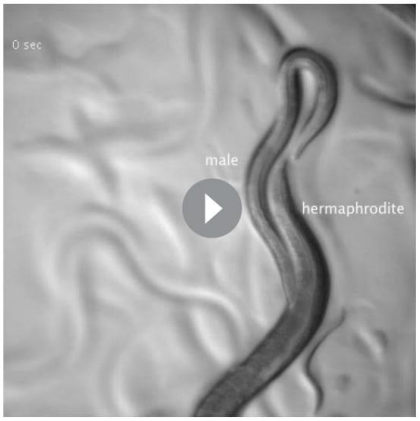

Video 6. Males performing Molina manoeuvres during mating: *wildtype* male performing a Molina manoeuvre during mating with a *wildtype* hermaphrodite. Videos are played at 40 fps (sped up x2).
https://elifesciences.org/articles/48361#video6

Video 7. Males performing Molina manoeuvres during mating: PHD-ablated male performing a defective, discontinuous Molina manoeuvre. Videos are played at 40 fps (sped up x2).
https://elifesciences.org/articles/48361#video7

or its initiation is delayed by a stop (during Molina manoeuvres). The qualitative difference in locomotion defects between these two steps of mating may result from differences in the state of the neural network before and after spicule insertion attempts (***Correa et al., 2015***; ***Correa et al., 2012***; ***Liu et al., 2011***). Sometimes while pausing, particularly during Molina manoeuvres but also during scanning, *wildtype* and PHD-ablated males prodded their spicules at locations other than the vulva (***Figure 7—figure supplement 2***). Ectopic prodding happened rarely but it occurred significantly more often in ablated than in *wildtype* males (***Figure 7—figure supplement 2A***). Because ectopic prodding occurred only during pauses and PHD-ablated males produced many more discontinuous manoeuvres than *wildtype* males, we interpret the increase in ectopic prodding as a secondary consequence of pausing rather than as the main defect of PHD-ablated males. Consistent with this interpretation, there was no statistically significant difference in the occurrence of ectopic prodding events between ablated and *wildtype* males when only discontinuous manoeuvres were considered (***Figure 7—figure supplement 2B***).

In addition to the aforementioned changes in neuronal activity, the highest level of PHD activation was observed during intromission, the penultimate step of the mating sequence, which precedes sperm transfer and involves full insertion of the spicules into the mate's vulva while sustaining backward locomotion. PHD activity increased two-fold upon spicule insertion and remained high for several seconds while the spicules were inserted (***Figure 7H***). PHDs are required for the efficiency of these two last steps of mating since PHD-ablated males that were observed to complete the mating sequence, including intromission and ejaculation, during a single mating with one individual mate, produced fewer cross-progeny than intact males in the same conditions (***Figure 7H***). Intact PHDs may increase the efficiency of sperm transfer by controlling the male's posture during intromission. While the cues and network interactions that activate PHDs during mating are presently not known, the high levels of PHD activity upon spicule insertion are consistent with a putative proprioceptive role for these neurons.

Discussion

The data presented here extend John Sulston's original observations and demonstrate that male PHso1 cells undergo a direct glia-to-neuron transdifferentiation to produce a novel class of bilateral cholinergic, peptidergic, and ciliated sensory neurons, the phasmid D neurons. This updates the anatomy of the adult *C. elegans* male: it now comprises 387 neurons (93 of which are male-specific) and 90 glia (two are lost during the transdifferentiation to the PHDs). This is the second example of neurons arising from glia in *C. elegans*, confirming that glia can act as neural progenitors across metazoan taxa. In both cases we have demonstrated that fully differentiated, functional glia can retain neural progenitor properties during normal development. The complete glia-to-neuron cell fate switches we observe strongly suggest the production of neurons from glia is a process of natural transdifferentiation. In the first case (**Sammut et al., 2015**), this is an indirect transdifferentiation as it occurs via an asymmetric cell division, leading to self-renewal of the glial cell and the production of a neuron. In contrast, the work described here characterises a direct transdifferentiation and as such is the second direct transdifferentiation to be described in *C. elegans*. The first involves the transdifferentiation of the rectal epithelial cell Y into the motor neuron PDA, which occurs in hermaphrodites at earlier larval stages, before sexual maturation (**Jarriault et al., 2008**). Excitingly, most of the key genes that regulate the Y-to-PDA cell fate switch (**Kagias et al., 2012**; **Richard et al., 2011**; **Zuryn et al., 2014**) appear dispensable for PHso1-to-PHD and AMso-to-AMso +MCM transdifferentiation, indicating that independent molecular mechanisms exist that control cell-fate plasticity in a sex-specific, time-specific and/or a cell-specific manner. Intriguingly, direct conversion of glial-like neural stem cells has been observed in the adult zebrafish brain (**Barbosa et al., 2015**), suggesting that this may be a conserved mechanism for post-embryonic generation of neurons. Furthermore, it will be interesting to understand the molecular basis underlying the variability in the low frequency, background-dependent division of PHso1 and whether it has any functional or evolutionary consequence. The fact that a cell's terminal division can be variable is especially surprising in *C. elegans*, as its cell lineage is considered highly stereotyped and invariable. The only other neurons known to be variable in their generation are the post-embryonic and male-specific DX3/4 and EF3/4 interneurons located in the pre-anal ganglion (**Sulston et al., 1983**). It is intriguing that the EF neurons are the main post-synaptic partners of PHD (**Figure 6D**), and as such it is tempting to speculate there may be a possible link between cell division and cell connectivity.

Based on our manipulations and imaging of PHD activity in restrained and freely mating animals, we propose that PHDs may be proprioceptive neurons which become activated by tail-tip deformations and engage the circuits for backward locomotion. The high levels of PHD activity during intromission and upon tail-tip bending during the Molina manoeuvre, steps which require inhibition of forward locomotion and sustained backward movement, are consistent with such a model. PHDs may ensure sustained backward locomotion through excitation of their post-synaptic targets PVY, PVX, and EF interneurons, all of which have been shown to promote backward movement through AVA and AVB during scanning and location of vulva (**Sherlekar and Lints, 2014**; **Sherlekar et al., 2013**). As *wildtype* hermaphrodites are highly uncooperative during mating and actively move away (**Kleemann and Basolo, 2007**), any erratic and uncoordinated movement by the male is likely to result in the loss of its mate.

Sensory input from the mating partner is essential for successful mating and accordingly, many sensory neurons in copulation circuits are dedicated to this purpose (reviewed in **Villella and Hall, 2008** and **Barr et al., 2018**). However, coordinated motor control in all animals also requires proprioception, sensory feedback from internal tissues that inform the individual about its posture and strength exerted during movement (**Sherrington, 1907**; **Tuthill and Azim, 2018**). Several putative proprioceptive neurons have been identified in *C. elegans* (reviewed in **Schafer, 2015**). Within the male copulation circuit, a putative proprioceptive role has been attributed only to the spicule neuron SPC, on the basis of the attachment of its dendrite to the base of the spicules (**Sulston et al., 1980**). The SPC neuron is required for full spicule protraction during intromission (**García et al., 2001**; **Liu and Sternberg, 1995**). The presence of proprioceptive neurons in copulation circuits may be a broadly employed mechanism to regulate behavioural transitions during mating. In this light, it would be interesting to determine whether the mechanosensory neurons found in the mating circuits of several other organisms (**Liu et al., 2007**; **Ng and Kopp, 2008**; **Pavlou et al., 2016**) may play a role in self-sensory feedback.

In summary our results provide new insight into the developmental mechanisms underlying the neural substrates of sexually dimorphic behaviour. The glia-to-neuron transdifferentiation that results in PHD represents an extreme form of sexual dimorphism acquired by differentiated sex-shared glial cells during sexual maturation. The PHD neurons, perhaps through proprioception, enable the smooth and coordinated readjustment of the male's movement along its mate when spicule insertion becomes difficult to attain. This readjustment movement represents an alternative step within the stereotyped mating sequence. These findings reveal the extent to which both cell fate and innate behaviour can be plastic yet developmentally wired.

Materials and methods

Key resources table

Reagent type (species) or resource	Designation	Source or reference	Identifiers	Additional information
Genetic reagent (*C. elegans*)	*C. elegans*: Strain N2	Caenorhabditis Genetics Center	WormBase: N2	
Genetic reagent (*C. elegans*)	AW827	Dr Alison Woollard laboratory		*him-5(e1490), heIs63 [wrt-2p::GFP::PH + wrt-2p::GFP::H2B + lin-48p::mCherry] V*
Genetic reagent (*C. elegans*)	CHL56	This study		*drpIs3 [lin-48p::tdTomato] I; him-5(e1490) V*
Genetic reagent (*C. elegans*)	BAR37	This study		*nsIs198 [mir-228p::GFP + lin-15(+)]; otIs356 [rab-3p::2xNLS::TagRFP], him-5(e1490) V*
Genetic reagent (*C. elegans*)	CHL32	This study		*dpy-5(e907) I; otIs356 [rab-3p::2xNLS::TagRFP], him-5 (e1490) V; drpIs1 [grl-2p::GFP, dpy-5(+)] X*
Genetic reagent (*C. elegans*)	OH13083	Pereira et al. Elife. 2015; Caenorhabditis Genetics Center		*him-5(e1490) V; otIs576 [unc-17fos::GFP + lin-44::YFP]*
Genetic reagent (*C. elegans*)	CHL36	This study		*inIs179 [ida-1p::GFP]; drpIs3 [lin-48p::tdTomato]; him-8(e1489) IV*
genetic reagent (*C. elegans*)	CHL57	This study		*drpIs3 [lin-48::tdTomato] I; mnIs17 [osm-6p::GFP + unc-36(+)]; him-5(e1490) V*
Genetic reagent (*C. elegans*)	CHL58	This study		*drpIs3 [lin-48::tdTomato] I; otIs291 [rab-3p::2xNLS::yfp + rol-6(su1006)], him-5(e1490) V*
Genetic reagent (*C. elegans*)	CHL59	This study		*drpIs3 [lin-48p::tdTomato] I; dpy-17(e164) III; otIs291 [rab-3p::2xNLS::yfp + rol-6(su1006)], him-5(e1490) V*
Genetic reagent (*C. elegans*)	CHL60	This study		*drpIs3 [lin-48p::tdTomato] I; ced-4(n1162), dpy-17(e164) III; otIs291 [rab-3p::2xNLS::YFP + rol-6(su1006)], him-5(e1490) V*
Genetic reagent (*C. elegans*)	CHL61	This study		*drpIs3 [lin-48p::tdTomato] I; him-5(e1490)V; drpIs1 [grl-2p::GFP, dpy-5(+)] X*
Genetic reagent (*C. elegans*)	CHL63	This study		*drpIs3 [lin-48p::tdTomato] I; him-5(e1490) V; vsIs48 [unc-17p::GFP] X*
Genetic reagent (*C. elegans*)	CHL64	This study		*drpIs3 [lin-48p::tdTomato] I; inIs179[ida-1p::GFP] II; him-5(e1490)V*

Continued on next page

Continued

Reagent type (species) or resource	Designation	Source or reference	Identifiers	Additional information
Genetic reagent (*C. elegans*)	CHL67	This study		*drpIs3 [lin-48p::tdTomato] I; drpIs4 [oig-8p::GFP + pha-1(+)]; him-5(e1490) V*
Genetic reagent (*C. elegans*)	CHL65	This study		*drpIs4 [oig-8p::GFP + pha-1(+)]; him-5(e1490) V*
Genetic reagent (*C. elegans*)	BAR77	This study		*oleEx24 [grl-2(1 kb)::fem-3::SL2::mCherry (8 ng)+ elt-2p::GFP (40 ng)]; inIs179 [ida-1p::GFP] II; him-8(e1489) IV*
Genetic reagent (*C. elegans*)	CHL62	This study		*oleEx18 [grl-2(1 kb)::fem-3::SL2::mCherry(20 ng) + elt-2p::GFP (40 ng)]; drpIs3 [lin-48p::tdTomato] I; otIs291 [rab-3p::2xNLS::YFP + rol-6(su1006)], him-5(e1490) V*
Genetic reagent (*C. elegans*)	CHL68	This study		*sem-4(n19719), drpIs3 [lin-48p::tdTomato] I; otIs291 [rab-3p::2xNLS::YFP + rol-6(su1006)], him-5(e1490) V*
Genetic reagent (*C. elegans*)	CHL69	This study		*drpIs3 [lin-48p::tdTomato] I; egl-27(ok1670) II; otIs291 [rab-3p::2xNLS::YFP + rol-6(su1006)], him-5(e1490) V*
Genetic reagent (*C. elegans*)	CHL70	This study		*drpIs3 [lin-48p::tdTomato] I; otIs291 [rab-3p::2xNLS::YFP + rol-6(su1006)], him-5(e1490) V; nre-1(hd20), lin-15B(hd126) X*
Genetic reagent (*C. elegans*)	CHL71	This study		*drpIs3 [lin-48p::tdTomato] I; inIs179 [ida-1p::GFP] II; him-8(e1489) IV*
Genetic reagent (*C. elegans*)	CHL72	This study		*drpIs3 [lin-48p::tdTomato] I; inIs179 [ida-1p::GFP] II; him-8(e1489) IV; otEx4454 [sox-2(fosmid)::mCherry + elt-2p::DsRed]*
Genetic reagent (*C. elegans*)	CHL73	This study		*drpIs3 [lin-48p::tdTomato] I; inIs179 [ida-1p::GFP] II; him-8(e1489) IV; sox-2(ot640[unc-119(+)]) X; otEx4454 [sox-2(fosmid)::mCherry + elt-2p::DsRed]*
Genetic reagent (*C. elegans*)	CHL74	This study		*drpIs3 [lin-48p::tdTomato] I; inIs179 [ida-1p::GFP] II; him-8(e1489) IV; nre-1(hd20), lin-15B(hd126) X*
Genetic reagent (*C. elegans*)	EM1370	Dr Scott Emmons laboratory		*bxEx271 [oig-8p::GFP + oig-8p::mCherry::rab-3]; him-5(e1490) V*
Genetic reagent (*C. elegans*)	EM1371	Dr Scott Emmons laboratory		*bxEx272 [oig-8p::GFP + oig-8p::mCherry::rab-3]; him-5(e1490) V*
Genetic reagent (*C. elegans*)	BAR90	This study		*him-5(e1490) V; oleEx27 [oig-8p::GCaMP6f::SL2::mRFP(30 ng/µl) + cc::GFP(30 ng/µl)]*
Genetic reagent (*C. elegans*)	BAR115	This study		*unc-51(e369), him-5(e1490) V; oleEx27 [oig-8p::GCaMP6f::SL2::mRFP(30 ng/µl) + cc::GFP(30 ng/µl)]*

Continued on next page

Continued

Reagent type (species) or resource	Designation	Source or reference	Identifiers	Additional information
Genetic reagent (*C. elegans*)	BAR115	This study		*unc-51(e369), him-5(e1490) V; oleEx27 [oig-8p::GCaMP6f:: SL2::mRFP(30 ng/µl) + cc::GFP(30 ng/µl)]; oleEx38 [myo-3::HisCL1::SL2::Cherry(20 ng/µl)]*
Genetic reagent (*C. elegans*)	BAR95	This study		*unc-13 (e51) I; him-5 (e1490) V; oleEx27 [oig-8p::GCaMP6f:: SL2::mRFP(30 ng/µl) + cc::GFP(30 ng/µl)]*
Genetic reagent (*C. elegans*)	BAR106	This study		*unc-31(e169) IV; him-5(e1490) V; oleEx27 [oig-8p::GCaMP6f:: SL2::mRFP(30 ng/µl) + cc::GFP(30 ng/µl)]*
Genetic reagent (*C. elegans*)	EM1251	Dr Scott W. Emmons laboratory		*bxEx201[oig-8p::GFP + pha-1(+)]; him-5(e1490) V - line#1*
Genetic reagent (*C. elegans*)	EM1253	Dr Scott W. Emmons laboratory		*bxEx201[oig-8p::GFP + pha-1(+)]; him-5(e1490) V - line#3*
Genetic reagent (*C. elegans*)	BAR94	This study		*him-5(e1490) V; lite-1(ce314) X; oleEx30[oig-8p::GCaMP6f::SL2::mRFP(50 ng/µl)]*
Genetic reagent (*C. elegans*)	CB369	Caenorhabditis Genetics Center		*unc-51(e369) V*
Genetic reagent (*C. elegans*)	BAR160	This study		*him-5(e1490) V; oleEx53 [pAB6(oig-8p::HisCl1::SL2::RFP) (30 ng/uL)+unc-122p::GFP(25 ng/uL)]*
Strain, strain background (*E. coli*)	Strain OP50	Caenorhabditis Genetics Center	OP50	
Strain, strain background (*E. coli*)	Strain MG1693 (Thy-)	*E. coli* stock centre	MG1693	Strain for EdU staining experiments
Strain, strain background (*E. coli*)	Strain: HT115 (DE3)	Caenorhabditis Genetics Center	HT115	
Tecombinant DNA reagent	Plasmid: pPD95.75	Addgene	#1494	See: *DNA constructs and transgenic strains* Used to create *oig-8prom::gfp* and for PCR fusions
Recombinant DNA reagent	Plasmid: *oig-8prom::gfp*	This study		See: *DNA constructs and transgenic strains* 964 bp upstream of the *oig-8* ATG
Recombinant DNA reagent	Plasmid: *pkd-2prom::mCherry::rab-3*	Dr María I. Lázaro-Peña		See: *DNA constructs and transgenic strains* Replaced promoter by *oig-8prom*
Recombinant DNA reagent	Plasmid: *oig-8prom::mCherry::rab-3*	This study		See: *DNA constructs and transgenic strains* Created from *pkd-2prom::mCherry::rab-3*
Recombinant DNA reagent	Plasmid pLR306	Dr Luis Rene García Laboratory		See: *DNA constructs and transgenic strains* Gateway plasmid used to amplify *GCaMP6f::sl2::rfp*
Recombinant DNA reagent	Plasmid: *oig-8prom::GCaMP6f::SL2::RFP*	This study		See: *DNA constructs and transgenic strains* Created by PCR fusion (see primers)
Recombinant DNA reagent	Plasmid: pNP471	Dr Cori Bargmann Laboratory		See: *DNA constructs and transgenic strains* Used to amplify *HisCl1::sl2::mCherry*
Recombinant DNA reagent	Plasmid: *oig-8prom::HisCl1::sl2::rfp*	This study		See: *DNA constructs and transgenic strains* Created by Gibson
Recombinant DNA reagent	Plasmid: *myo-3prom::HisCl1::sl2::mCherry*	This study		See: *DNA constructs and transgenic strains* Created by PCR fusion (see primers)
Recombinant DNA reagent	Plasmid: *lin-48prom::tdTomato*	Dr Mike Boxem Laboratory		See: *DNA constructs and transgenic strains* 6.8 kb upstream of *lin-48* ATG
Recombinant DNA reagent	Plasmid pPD129.36 (L4440)	Dr Andrew Fire Laboratory, Addgene	#1654	Control plasmid for RNAi experiments

Continued on next page

Continued

Reagent type (species) or resource	Designation	Source or reference	Identifiers	Additional information
Recombinant DNA reagent	Plasmid: *sox-2* RNAi clone	Source BioScience		Silence endogenous *sox-2* gene
Sequence-based reagent	primer_oig-8 fusion_F	This study	PCR fusion primers	See: *DNA constructs and transgenic strains* gggagtgacctatgcaaacc
Sequence-based reagent	primer_oig-8 fusion_R	This study	PCR fusion primers	See: *DNA constructs and transgenic strains* CGACGTGATGAGTCGACCAT tgttttacctgaaatctttt
Sequence-based reagent	primer_myo-3 fusion_F	This study	PCR fusion primers	See: *DNA constructs and transgenic strains* cgtgccatagttttacattcc
Sequence-based reagent	primer_myo-3 fusion_R	This study	PCR fusion primers	See: *DNA constructs and transgenic strains* gctagttgggctttgcatGCttctagatggatctagtggtc
Sequence-based reagent	primer_ced-4 (n1162)_F	This study	PCR genotyping primers	See: *C. elegans strains* gatgctctgcgaaatcgaatgc
Sequence-based reagent	primer_ced-4 (n1162)_R	This study	PCR genotyping primers	See: *C. elegans strains* tcacctaaatcacacatctcgtcg
Sequence-based reagent	primer_dpy-17 (e164)_F	This study	PCR genotyping primers	See: *C. elegans strains* aggaggaagcccaatcaacc
Sequence-based reagent	primer_dpy-17 (e164)_R	This study	PCR genotyping primers	See: *C. elegans strains* cagttggtccttcttctccagc
Sequence-based reagent	primer_sem-4 (n1971)_F	This study	PCR genotyping primers	See: *C. elegans strains* aaggtgatgcgatgatgtctcc
Sequence-based reagent	primer_sem-4 (n1971)_R	This study	PCR genotyping primers	See: *C. elegans strains* taatgatcggcttgggtgtgg
Sequence-based reagent	primer_egl-27 (ok1679)_F ext	This study	PCR genotyping primers	See: *C. elegans strains* tcatcgtttccagtctcttcagg
Sequence-based reagent	primer_egl-27 (ok1679)_R ext	This study	PCR genotyping primers	See: *C. elegans strains* cgctggttatcaaatgacgcc
Sequence-based reagent	primer_egl-27 (ok1679)_F int	This study	PCR genotyping primers	See: *C. elegans strains* agacaccagaagctacgaaacc
Sequence-based reagent	primer_egl-27 (ok1679)_R int	This study	PCR genotyping primers	See: *C. elegans strains* gtttgcatcacggtcttcacg
Sequence-based reagent	primer_nre-1(hd20) lin-15B(hd126)_F	This study	PCR genotyping primers	See: *C. elegans strains* catgagagctgcgctgaggc
Sequence-based reagent	primer_nre-1(hd20) lin-15B(hd126)_R	This study	PCR genotyping primers	See: *C. elegans strains* ggttcgggctcgcggtagtc
Chemical compound, drug	Paraformaldehyde	Thermo Fisher Scientific	#28908	Used at 4%
Chemical compound, drug	β-mercapto-ethanol	Sigma Aldrich	M6250	Used at 5%
Chemical compound, drug	Collagenase type IV	Sigma Aldrich	C-5138	Used at 1 mg/ml
Chemical compound, drug	Vectashield antifade	Vector Laboratories	H-1900	
Chemical compound, drug	Isopropyl-β-D-thiogalactopyranoside (IPTG)	Generon	GEN-S-02122	Used at 0.6 mM in plates for RNAi knock-down
Chemical compound, drug	Histamine	Sigma	H7125	Used at 20 mM in plates for behavioural assays
Chemical compound, drug	Wormglu	GluStitch, Delta, Canada		
Antibody	Anti-RFP pAb (Rabbit polyclonal antibody)	MBL International	PM005	(1:500)

Continued on next page

Continued

Reagent type (species) or resource	Designation	Source or reference	Identifiers	Additional information
Antibody	Donkey anti-Rabbit IgG (H+L) Highly Cross-Adsorbed Secondary Antibody, Alexa Fluor 555 (Donkey polyclonal antibody)	Molecular probes	A-31572	(1:200)
Commercial assay or kit	Click-IT EdU Alexa Fluor 594	Invitrogen	C10339	
Software, algorithm	ImageJ	ImageJ (http://imagej.nih.gov/ij/)	RRID:SCR_003070	
Software, algorithm	GraphPad Prism	GraphPad Prism (graphpad.com)	RRID:SCR_002798	
Software, algorithm	Affinity Designer	https://affinity.serif.com/en-us/designer/	RRID:SCR_016952	

C. elegans strains

Nematode culture and genetics were performed following standard procedures (**Brenner, 1974**; **Stiernagle, 2006**). For genetic crosses, all genotypes were confirmed using PCR unless the mutant phenotype was obvious (see Key Resource Table for primer sequences). Animals considered *wild-type* carry *him-5* or *him-8* mutations to facilitate male analysis. All assays were conducted at 20˚C. Strains used in this study are listed in the Key Resource Table.

DNA constructs and transgenic strains

The *oig-8^{prom}::gfp* reporter was built by amplifying a 964 bp promoter fragment upstream of the *oig-8* ATG adding the restriction sites of SphI and XmaI (see Key Resource Table for these and other primer sequences). This promoter drives expression in PHD neurons and two pairs of sensory neurons in the head which we have not identified. The PCR product was digested and ligated into SphI/XmaI-digested pPD95.75 vector. To generate *oig-8^{prom}::mCherry::rab-3*, the same *oig-8* promoter fragment was ligated into SphI/XmaI-digested *pkd-2^{prom}::mCherry::rab-3* (a gift from M. Lázaro-Peña). The *oig-8^{prom}::GCaMP6f::SL2::RFP* construct was created by PCR fusion (**Hobert, 2002**). A ~ 1 kb promoter region of the *oig-8* locus was PCR fused with the GCaMP sequence. The *GCaMP6f::sl2::rfp* fragment was amplified from gateway plasmid pLR306, a kind gift from Luis Rene García. The same promoter region was used to create the *oig-8^{prom}::HisCl1::sl2::rfp* plasmid by Gibson cloning. The *myo-3^{prom}::HisCl1::sl2::mCherry* construct was created as PCR fusion. A 2.2 kb promoter region of the *myo-3* locus was amplified and PCR fused with the *HisCl1* sequence (see Key Resource Table for primer sequences). The *HisCl1::sl2::mCherry* fragment was amplified from plasmid pNP471, a kind gift from the Bargmann lab. The *grl-2 ^{prom}::gfp* reporter was generated by integrating *sEx12852* (**Hao et al., 2006**) to generate *drpIs1*. The *lin-48^{prom}::tdTomato* construct was a kind gift from Mike Boxem and contains a 6.8 kb promoter fragment upstream of the coding sequence of *tdTomato* and the *unc-54* 3' UTR. It was injected into *him-5(e1490)* animals and spontaneously integrated generating *drpIs3*.

PHso1-to-PHD single animal live imaging

Animals containing the *lin-48^{prom}::tdTomato drpIs3* transgene were synchronised via sodium hypochlorite treatment and allowed to develop until the early L3 stage. Next, they were mounted individually on 5% agarose pads in a droplet of the minimum concentration of sodium azide that paralysed the animals (which varied within experimental replicates) and viewed under a compound microscope to determine their developmental time. A total of 10–20 males in which the gonad had just turned to grow posteriorly were imaged. Care was taken to use the lowest fluorescent light intensity and exposure in order to minimise toxicity. After the initial imaging, animals were gently recovered by aspiration, washed in a droplet of M9 buffer, transferred to individual plates and allowed to develop overnight at 15˚C. 12 hr later, animals were gradually shifted to higher temperatures up to 25˚C to reduce the effects of photobleaching on the fluorophore. Each animal was then immobilised and

imaged as described above. In those animals where the leading edge of the gonad had crossed back over to the ventral side, a sequence of time-lapse images was taken every 2–4 hr until PHso1-to-PHD remodelling was complete, 10–12 hr later.

Immunohistochemistry and EdU staining

EdU (5-ethynyl-2′-deoxyuridine) feeding was performed as previously described (**van den Heuvel and Kipreos, 2012**) combined with immunohistochemistry to enhance reporter transgene fluorescence. In short, MG1693 bacteria (Thy-deficient, *E. coli* stock centre: http://cgsc.biology.yale.edu/) were grown in 100 ml of minimal medium containing 20 mM EdU for at least 24 hr, concentrated by centrifugation and seeded on NGM plates with 100 µg/mL ampicillin. A synchronised population of L1 larvae, obtained by hypochlorite treatment and hatching in M9 buffer, was allowed to feed on OP50 *E. coli* until early L3 (24–28 hr at 20˚C). Worms were washed thoroughly in M9, plated onto MG1693 EdU containing plates and allowed to grow until late L4 – early adult stage (22–24 hr). Hard-tube fixation was chosen in order to preserve the male tail morphology (**McIntire et al., 1992**). Worms were washed thoroughly, transferred to DNA LoBind tubes (Eppendorf) and fixed for 12 hr in 4% paraformaldehyde at 4˚C in a rocking nutator, followed by 5% β-mercapto-ethanol for another 12 hr at 37˚C in a rocking nutator. Worms were then incubated for 6 hr in 1 mg/ml collagenase (Sigma Aldrich) at 37˚C and 700 rpm, followed by 24 hr with rabbit anti-RFP antibody (1:500, MBL) to detect the tdTomato fluorescence from the *drpIs3* reporter transgene. Alexa 555-conjugated donkey anti-rabbit (1:200; Molecular probes) was used as secondary antibody. As EdU reaction can interfere with antibody staining, this was performed after the immunohistochemistry. The Click-IT reaction was performed in a total volume of 50 µl per tube, in the dark, according to the manufacturer's instructions (Click-IT EdU Alexa Fluor 594 kit, Invitrogen). Slides were mounted in Vectashield antifade mounting medium (Vector Laboratories). Samples were analysed the same day or the day after mounting, to minimise fading of fluorescence. Only animals where both head and tail were properly stained for tdTomato (cell body) and EdU (nucleus) were scored. Four independent EdU experiments were performed (see Source Data **Figure 3**) and all animals scored were plotted in the same bar chart.

RNAi feeding experiments

The RNAi bacterial clone for *sox-2* was obtained from the Ahringer RNAi Collection (Source BioScience) (**Kamath et al., 2003**). RNAi feeding experiments were performed following standard protocols (**Kamath et al., 2001**). Briefly, isopropyl β-D-1-thiogalactopyranoside (IPTG) was added to a final concentration of 0.6 mM to NGM medium to prepare the RNAi plates. 24 hr later, HT115 bacteria transfected with the *sox-2* RNAi clone was seeded onto RNAi plates. Staged early-L4 larvae were transferred to seeded RNAi plates and 4–5 days later their progeny, which had developed under the embryonic effects of RNAi knock-down (F1 generation), was scored at the stage of young adult. To exclusively analyse post-embryonic effects, a synchronised population of L1 larvae was transferred to RNAi seeded plates and young adult males were scored 2–3 days later (P0 generation).

All experiments were performed at 20˚C. The *nre-1(hd20) lin-15b(hd126)* background was used to sensitise worms to the RNAi effects. One experiment was performed with three replicate plates per condition. L4440 empty vector (pPD129.36, Addgene) was used as negative control and *gfp* RNAi clone as positive control.

Cell-type specific sex transformations

We used two previously described strains each containing an array that drives *fem-3* expression from a *grl-2* promoter fragment (**Sammut et al., 2015**). This *grl-2* promoter is expressed in PHso1 and PHso2 in the tail, and AMso, excretory pore, and excretory duct in the head (**Hao et al., 2006**). In the case of *oleEx24* the presence/absence of the array in PHso1 and PHso2 was monitored by the *mCherry* expression from the array itself and the expression of an *ida-1*^{prom}*::gfp* reporter (*inIs179*), in the background of the strain was used to monitor neuronal fate in PHso1/PHD. In the case of *oleEx18,* we had difficulty visualising the *mCherry* from the array in PHD and crossed a *lin-48*^{prom}*:: tdTomato* transgene (*drpIs3*) into the strain to visualise PHso1/PHD. The presence/absence of the

array in whole animals was assessed using the array co-injection marker *elt-2^{prom}::gfp*. Neuronal fate was monitored using a *rab-3^{prom}::yfp* reporter.

Cell ablations

PHD was ablated with a laser microbeam as previously described (**Bargmann and Avery, 1995**). L4 males were staged and placed on a seeded plate the night before. Ablations were carried out at one-day of adulthood and PHD was identified by *oig-^{prom}::gfp* or *unc-17^{prom}::gfp* reporter expression. Mock-ablated animals underwent the same treatment as ablated males except for laser trigger. Animals were left to recover overnight and behavioural assays were performed the next day. After behavioural assays, animals were checked for lack of GFP expression in the tail-tip region where PHD is normally located to confirm correct cell ablation. The few animals in which PHD had not been efficiently ablated (judged by the presence/return of GFP) were discarded from the data.

Behavioural assays

All behavioural assays were scored blind to the manipulation. Males carried either an *oig-8^{prom}::gfp* or an *unc-17^{prom}::gfp* transgene to identify the PHD neurons for ablation. For the experiments in which PHD was silenced with a HisCl1 transgene, mating assays were performed in 2-day-old adults, as in the ablations. Before the assay, *wildtype* or array-carrying animals with RFP-positive PHD neurons were moved to a 20 mM histamine plate with food for 1 hr. As controls, array-carrying animals not treated with histamine were also tested. Histamine plates were prepared as regular NGM plates adding 20 mM histamine when the agar cooled to a temperature below 56˚C.

Food leaving

Animals were tested as 3-day-old adults (the day after they had been tested for mating). Assays were performed and scored as previously described (**Barrios et al., 2008**).

Mating

Assays were performed and scored as previously described (**Sammut et al., 2015**). Males were tested at two days of adulthood with 1-day-old *unc-51(e369)* hermaphrodites picked the night before as L4s. Each male was tested once for all steps of mating. Those males that were not successful at inserting their spicules with the first hermaphrodite were tested again with a maximum of three hermaphrodites to control for hermaphrodite-specific difficulty in penetration (**Liu and Sternberg, 1995**). Assays were replicated at least three times on different days and with different sets of males. Videos of mating events were recorded and scored blind by two independent observers.

Response

A male was scored as responding to mate contact if it placed its tail ventral down on the mate's body and initiated the mating sequence by backing along the mate's body to make a turn. The response efficiency was calculated by dividing 1 (response) by the total number of contacts made with the mate before responding. If a male did not respond within three minutes, it was scored as having 0 efficiency. As a more sensitive measure of the quality of response, we scored hesitation during response. Hesitation is a switch in direction between forward and backward locomotion from the time the male establishes contact with the mate to the first turn (or to location of vulva if this occurs without the need of a turn).

Scanning

A single scan was scored as the journey around the mate's body away from and returning to the vulva position. The first scan was counted as the journey from the point of first contact to the hermaphrodite vulva position. A scan was considered continuous if locomotion was maintained in the backward direction without switching direction or pausing.

Ectopic prodding

Prodding was scored as a visible protrusion of the spicules out of the gubernaculum and/or visible twitching of the spicule muscles. Prodding was considered ectopic if it occurred at regions of the mate's body other than the vulva.

Molina manoeuvres

A continuous single manoeuvre was scored as the journey away from the vulva in forward locomotion, to a distance bigger than two tail-tips length, and return to the vulva in backward locomotion. Since the transition between the forward and backward steps could take up to 3 s in a *wildtype* male, the category of discontinuous manoeuvre 'stop before backward step' was scored if the pause was longer than 3 s. Any other visible pause during forward or backward locomotion was considered a STOP regardless of its duration. The category of discontinuous manoeuvre 'switching' was scored as a change in direction of locomotion while travelling away or towards the vulva without reaching it.

Displacements from the vulva

Scored as movements of one or two tail-tip lengths away from the vulva.

Fertility assays

Each individual male was monitored for all mating steps during a single mating until it ejaculated. After disengagement from the mate, the hermaphrodite was picked and placed in a fresh plate to lay progeny. The adult hermaphrodite was transferred to a fresh plate each day during three consecutive days. After three days from the eggs being laid, L4 larvae and adult progeny were counted as Unc self-progeny of Wt cross-progeny.

Microscopy and imaging

Worms were anesthetised using 50 mM sodium azide and mounted on 5% agarose pads on glass slides. Images were acquired on a Zeiss AxioImager using a Zeiss Colibri LED fluorescent light source and custom TimeToLive multichannel recording software (Caenotec). Representative images are shown following maximum intensity projections of 2–10 1 µm z-stack slices and was perfumed in ImageJ.

Ca^{2+} imaging

Imaging was performed in an upright Zeiss Axio Imager two microscope with a 470 nm LED and a GYR LED (CoolLED) with a dual-band excitation filter F59-019 and dichroic F58-019 (Chroma) in the microscope turret. Emission filters ET515/30M and ET641/75 and dichroic T565lprx-UF2 were placed in the cube of a Cairn OptoSplit II attached between the microscope and an ORCA-Flash four camera (Hamamatsu). Acquisition was performed at 20 fps. Imaging during mating was performed with a 20x long working distance objective (LD Plan-NEOFLUAR numerical aperture 0.4), placing the male on an agar pad with food and 20 hermaphrodites. The ~50 mm per side agar pad was cut out from a regular, seeded NGM plate and placed on a glass slide. The hermaphrodites were placed in a ~ 100 mm^2 centre region. A fresh pad was used every two recordings.

Imaging in restrained animals was performed for 2.5–3 min with a 63x objective (LD C- apochromat numerical aperture 1.15). Animals were glued with Wormglu along the body to a 5% agarose pad on a glass slide and covered with M9 or 20 mM histamine (Sigma, H7125) and a coverslip.

Ca^{2+} imaging analysis

A moving region of interest in both channels was identified and mean fluorescent ratios (GFP/RFP) were calculated with custom-made Matlab scripts (***Busch et al., 2012***), kindly shared by Zoltan Soltesz and Mario de Bono. For recordings in restrained animals, bleach correction was applied to those traces in which an exponential decay curve fitted with an R square >0.6. Ratios for each recording were smoothened using an 8-frame rolling average. For $\Delta R/R_0$ values, R_0 for each recording period was calculated as the mean of the lowest 10^{th} percentile of ratio values. Traces that were locked to behavioural transitions had their $\Delta R/R_0$ values added or subtracted such that all events had the same value at t = 0.

Peaks were identified manually by an observer blind to the genotype and treatment. Peaks were called as signals above 0.2 $\Delta R/R_{max}$ (where R_{max} was calculated as the highest 5^{th} percentile of ratio values), above 2σ from local basal and a minimum duration of 5 s.

Electron microscopy and serial reconstruction

The samples were fixed by chemical fixation or high-pressure freezing and freeze substitution as previously described (**Hall et al., 2012**). Several archival print series from *wildtype* male tails in the MRC/LMB collection were compared to *wildtype* adult males prepared in the Hall lab, showing the same features overall. Ultrathin sections were cut using an RMC Powertome XL, collected onto grids, and imaged using a Philips CM10 TEM. The PHD cell bodies were identified in the EM sections based on position and morphology. This was followed by serial tracing of the projections to establish their morphology and connectivity. The method of quantitative reconstruction using our custom software is described in detail in **Jarrell et al., 2012** and **Xu et al., 2013**. The connectivity of the PHD neurons was determined from the legacy N2Y EM series (**Sulston et al., 1980**). Circuit diagrams were generated using Cytoscape (**Smoot et al., 2011**). PHD neuronal maps and connectivity tools are available at www.wormwiring.org.

Acknowledgements

We thank Mario de Bono and Zoltan Soltesz for kindly sharing custom-made software for ratiometric analysis of Ca^{2+} imaging in moving animals; Rene Garcia for worm cartoons used in **Figure 7**; Ken Nguyen for help with EM; John G White and Jonathan Hodgkin for their help in transferring archival TEM data from the MRC/LMB to the Hall Lab at the Albert Einstein College of Medicine for long-term curation and study; Shai Shaham for sharing the *mir-228^{prom}::gfp* strain prior to publication; Mike Boxem, María Lázaro-Peña, Alison Woollard and Cori Bargmann for additional strains and reagents; Sheila Poole for edits on the manuscript; Baris Kuru for aid with behavioural experiments. Additional strains were obtained from the CGC, which is supported NIH grant P40 OD010440. Christopher Brittin was influential in designing and creating www.wormwiring.org. This work was supported by a Newton Fellowship from the Royal Society to LMG (NF160914), a Wellcome Trust PhD studentship to RB, Marie Curie CIG grant 618779 and Wellcome Trust Enhancement Funding (095722/Z/11/A) to RJP, Leverhulme Trust grant RPG-2018–287 to AB, NIH R01 GM066897 grant and the G Harold and Leila Y Mathers Charitable Foundation to SWE, NIH OD 010943 to DHH, NIH T32GM007491 and F32 MH115438 01 to SJC; RJP was supported by a Wellcome Trust Research Career Development Fellowship (095722/Z/11/Z) and is currently a Wellcome Senior Fellow in Basic Biomedical Science (207483/Z/17/Z). AB and RJP are members of COST Action BM1408.

Additional information

Funding

Funder	Grant reference number	Author
Royal Society	Newton Fellowship NF160914	Laura Molina-Garcia
Wellcome Trust	PhD Studentship	Rachel C Bonnington
National Institutes of Health	T32 GM007491	Steven J Cook
National Institutes of Health	F32 MH115438	Steven J Cook
National Institutes of Health	OD 010943	David H Hall
National Institutes of Health	R01 GM066897	Scott W Emmons
Mathers Foundation		Scott W Emmons
Wellcome Trust	Research Career Development Fellowship 095722/Z/11/Z	Richard J Poole
Wellcome Trust	Enhancement Funding 095722/Z/11/A	Richard J Poole
Wellcome Trust	Senior Research Fellowship 207483/Z/17/Z	Richard J Poole

The funders had no role in study design, data collection and interpretation, or the decision to submit the work for publication.

Author contributions

Laura Molina-García, Conceptualization, Resources, Formal analysis, Supervision, Funding acquisition, Investigation, Visualization, Writing - review and editing, LMG performed, analysed and interpreted the behavioural experiments; Carla Lloret-Fernández, Conceptualization, Resources, Formal analysis, Supervision, Investigation, Visualization, Writing - review and editing, CLF characterised the direct PHso1-to-PHD transdifferentiation, analysed mutant alleles and performed the Edu experiments; Steven J Cook, Resources, Formal analysis, Supervision, Funding acquisition, Investigation, Visualization, SJC with SWE reconstructed the connectivity; Byunghyuk Kim, Resources, Formal analysis, Funding acquisition, Investigation, Visualization, BK also identified neuronal characteristics in PHD and generated the oig-8 reporter constructs; Rachel C Bonnington, Formal analysis, Supervision, Funding acquisition, Investigation, Visualization, Writing - review and editing, RCB performed the sex-transformation experiments and with MS and with JMO performed the characterisation of the PHso1-to-PHD molecular transdifferentiation; Michele Sammut, Resources, Investigation, Visualization, Writing - review and editing, MS performed single-animal imaging experiments; Jack M O'Shea, Investigation, Visualization; Sophie PR Gilbert, Formal analysis, Investigation, Visualization, SPRG helped characterise lin-48 expression; David J Elliott, Investigation, DJE provided technical assistance; David H Hall, Resources, Data curation, Supervision, Funding acquisition, Investigation, Visualization, DHH provided and analysed the electron micrographs; Scott W Emmons, Resources, Supervision, Funding acquisition, Investigation; Arantza Barrios, Conceptualization, Resources, Formal analysis, Supervision, Funding acquisition, Investigation, Visualization, Writing - original draft, Project administration, Writing - review and editing, AB conceived, performed and interpreted the behavioural and Ca2+ imaging experiments and co-wrote the manuscript; Richard J Poole, Conceptualization, Resources, Formal analysis, Supervision, Funding acquisition, Investigation, Visualization, Writing - original draft, Project administration, Writing - review and editing, RJP conceived and performed the analysis of the PHso1-to-PHD transdifferentiation and co-wrote the manuscript

Author ORCIDs

Laura Molina-García https://orcid.org/0000-0002-1530-4061
Carla Lloret-Fernández https://orcid.org/0000-0002-5370-9318
Steven J Cook https://orcid.org/0000-0002-1345-7566
Byunghyuk Kim https://orcid.org/0000-0002-2220-4173
Rachel C Bonnington https://orcid.org/0000-0002-5652-0297
Michele Sammut https://orcid.org/0000-0002-0281-6121
David H Hall https://orcid.org/0000-0001-8459-9820
Arantza Barrios https://orcid.org/0000-0001-6153-8830
Richard J Poole https://orcid.org/0000-0001-6414-2479

Decision letter and Author response

Decision letter https://doi.org/10.7554/eLife.48361.sa1
Author response https://doi.org/10.7554/eLife.48361.sa2

Additional files

Supplementary files

- Supplementary file 1. PHD connectivity. A table indicating the quantification of pre-synaptic inputs and post-synaptic outputs of the PHD neurons as derived from the electron microscopy serial reconstruction (see Materials and methods). The number of synapses and number of sections over which synapses are observed for each input/output neuron are indicated.
- Transparent reporting form

Data availability

All data generated or analysed during this study are included in the manuscript and supporting files.

References

Abraham MC, Lu Y, Shaham S. 2007. A morphologically conserved nonapoptotic program promotes linker cell death in *Caenorhabditis elegans*. *Developmental Cell* **12**:73–86. DOI: https://doi.org/10.1016/j.devcel.2006.11.012, PMID: 17199042

Alfonso A, Grundahl K, Duerr JS, Han HP, Rand JB. 1993. The *Caenorhabditis elegans* unc-17 gene: a putative vesicular acetylcholine transporter. *Science* **261**:617–619. DOI: https://doi.org/10.1126/science.8342028, PMID: 8342028

Auer TO, Benton R. 2016. Sexual circuitry in *Drosophila*. *Current Opinion in Neurobiology* **38**:18–26. DOI: https://doi.org/10.1016/j.conb.2016.01.004, PMID: 26851712

Barbosa JS, Sanchez-Gonzalez R, Di Giaimo R, Baumgart EV, Theis FJ, Götz M, Ninkovic J. 2015. Neurodevelopment live imaging of adult neural stem cell behavior in the intact and injured zebrafish brain. *Science* **348**:789–793. DOI: https://doi.org/10.1126/science.aaa2729, PMID: 25977550

Bargmann CI, Avery L. 1995. Laser killing of cells in *Caenorhabditis elegans*. *Methods in Cell Biology* **48**:225–250. DOI: https://doi.org/10.1016/s0091-679x(08)61390-4, PMID: 8531727

Barr MM, García LR, Portman DS. 2018. Sexual dimorphism and sex differences in *Caenorhabditis elegans* Neuronal Development and Behavior. *Genetics* **208**:909–935. DOI: https://doi.org/10.1534/genetics.117.300294, PMID: 29487147

Barr MM, Sternberg PW. 1999. A polycystic kidney-disease gene homologue required for male mating behaviour in *C. elegans*. *Nature* **401**:386–389. DOI: https://doi.org/10.1038/43913, PMID: 10517638

Barrios A, Nurrish S, Emmons SW. 2008. Sensory regulation of *C. elegans* male mate-searching behavior. *Current Biology* **18**:1865–1871. DOI: https://doi.org/10.1016/j.cub.2008.10.050, PMID: 19062284

Barrios A, Ghosh R, Fang C, Emmons SW, Barr MM. 2012. PDF-1 neuropeptide signaling modulates a neural circuit for mate-searching behavior in *C. elegans*. *Nature Neuroscience* **15**:1675–1682. DOI: https://doi.org/10.1038/nn.3253, PMID: 23143519

Bird AF, Bird J. 1991. *The Structure of Nematodes*. Academic Press.

Brenner S. 1974. The genetics of Caenorhabditis elegans. *Genetics* **77**:71–94. PMID: 4366476

Busch KE, Laurent P, Soltesz Z, Murphy RJ, Faivre O, Hedwig B, Thomas M, Smith HL, de Bono M. 2012. Tonic signaling from O_2 sensors sets neural circuit activity and behavioral state. *Nature Neuroscience* **15**:581–591. DOI: https://doi.org/10.1038/nn.3061, PMID: 22388961

Collet J, Spike CA, Lundquist EA, Shaw JE, Herman RK. 1998. Analysis of osm-6. a gene that affects sensory cilium structure and sensory neuron function in *Caenorhabditis elegans*. *Genetics* **148**:187–200. PMID: 9475731

Conradt B, Wu YC, Xue D. 2016. Programmed cell death during *Caenorhabditis elegans* Development. *Genetics* **203**:1533–1562. DOI: https://doi.org/10.1534/genetics.115.186247, PMID: 27516615

Cook SJ, Jarrell TA, Brittin CA, Wang Y, Bloniarz AE, Yakovlev MA, Nguyen KCQ, Tang LT, Bayer EA, Duerr JS, Bülow HE, Hobert O, Hall DH, Emmons SW. 2019. Whole-animal connectomes of both *Caenorhabditis elegans* sexes. *Nature* **571**:63–71. DOI: https://doi.org/10.1038/s41586-019-1352-7, PMID: 31270481

Correa P, LeBoeuf B, García LR. 2012. *C. elegans* dopaminergic D2-like receptors delimit recurrent cholinergic-mediated motor programs during a goal-oriented behavior. *PLOS Genetics* **8**:e1003015. DOI: https://doi.org/10.1371/journal.pgen.1003015, PMID: 23166505

Correa PA, Gruninger T, García LR. 2015. DOP-2 D2-Like receptor regulates UNC-7 innexins to attenuate recurrent sensory motor neurons during *C. elegans* Copulation. *Journal of Neuroscience* **35**:9990–10004. DOI: https://doi.org/10.1523/JNEUROSCI.0940-15.2015, PMID: 26156999

Doroquez DB, Berciu C, Anderson JR, Sengupta P, Nicastro D. 2014. A high-resolution morphological and ultrastructural map of anterior sensory cilia and Glia in *Caenorhabditis elegans*. *eLife* **3**:e01948. DOI: https://doi.org/10.7554/eLife.01948, PMID: 24668170

Ellis HM, Horvitz HR. 1986. Genetic control of programmed cell death in the nematode *C. elegans*. *Cell* **44**:817–829. DOI: https://doi.org/10.1016/0092-8674(86)90004-8, PMID: 3955651

Emmons SW. 2018. Neural circuits of sexual behavior in *Caenorhabditis elegans*. *Annual Review of Neuroscience* **41**:349–369. DOI: https://doi.org/10.1146/annurev-neuro-070815-014056, PMID: 29709211

Fagan KA, Luo J, Lagoy RC, Schroeder FC, Albrecht DR, Portman DS. 2018. A Single-Neuron chemosensory switch determines the valence of a sexually dimorphic sensory behavior. *Current Biology* **28**:902–914. DOI: https://doi.org/10.1016/j.cub.2018.02.029, PMID: 29526590

García LR, Mehta P, Sternberg PW. 2001. Regulation of distinct muscle behaviors controls the *C. elegans* male's copulatory spicules during mating. *Cell* **107**:777–788. DOI: https://doi.org/10.1016/S0092-8674(01)00600-6, PMID: 11747813

García LR. 2014. Regulation of sensory motor circuits used in *C. elegans* male intromission behavior. *Seminars in Cell & Developmental Biology* **33**:42–49. DOI: https://doi.org/10.1016/j.semcdb.2014.05.006, PMID: 24887696

Hall DH, Hartwieg E, Nguyen KC. 2012. Modern electron microscopy methods for *C. elegans*. *Methods in Cell Biology* **107**:93–149. DOI: https://doi.org/10.1016/B978-0-12-394620-1.00004-7, PMID: 22226522

Hao L, Johnsen R, Lauter G, Baillie D, Bürglin TR. 2006. Comprehensive analysis of gene expression patterns of hedgehog-related genes. *BMC Genomics* **7**:280. DOI: https://doi.org/10.1186/1471-2164-7-280, PMID: 17076889

Herman MA, Ch'ng Q, Hettenbach SM, Ratliff TM, Kenyon C, Herman RK. 1999. EGL-27 is similar to a metastasis-associated factor and controls cell polarity and cell migration in *C. elegans*. *Development* **126**:1055–1064. PMID: 9927605

Hilbert ZA, Kim DH. 2017. Sexually dimorphic control of gene expression in sensory neurons regulates decision-making behavior in *C. elegans*. *eLife* **6**:e21166. DOI: https://doi.org/10.7554/eLife.21166, PMID: 28117661

Hobert O. 2002. PCR fusion-based approach to create reporter gene constructs for expression analysis in transgenic *C. elegans*. *BioTechniques* **32**:728–730. DOI: https://doi.org/10.2144/02324bm01, PMID: 11962590

Hodgkin J. 1987. A genetic analysis of the sex-determining gene, tra-1, in the nematode *Caenorhabditis elegans*. *Genes and Development* **1**:731–745. DOI: https://doi.org/10.1101/gad.1.7.731, PMID: 3428597

Howell K, Hobert O. 2017. Morphological diversity of *C. elegans* sensory cilia instructed by the differential expression of an immunoglobulin domain protein. *Current Biology* **27**:1782–1790. DOI: https://doi.org/10.1016/j.cub.2017.05.006, PMID: 28578929

Jarrell TA, Wang Y, Bloniarz AE, Brittin CA, Xu M, Thomson JN, Albertson DG, Hall DH, Emmons SW. 2012. The connectome of a decision-making neural network. *Science* **337**:437–444. DOI: https://doi.org/10.1126/science.1221762, PMID: 22837521

Jarriault S, Schwab Y, Greenwald I. 2008. A *Caenorhabditis elegans* model for epithelial-neuronal transdifferentiation. *PNAS* **105**:3790–3795. DOI: https://doi.org/10.1073/pnas.0712159105, PMID: 18308937

Johnson AD, Fitzsimmons D, Hagman J, Chamberlin HM. 2001. EGL-38 Pax regulates the ovo-related gene lin-48 during *Caenorhabditis elegans* organ development. *Development* **128**:2857–2865. PMID: 11532910

Kagias K, Ahier A, Fischer N, Jarriault S. 2012. Members of the NODE (Nanog and Oct4-associated deacetylase) complex and SOX-2 promote the initiation of a natural cellular reprogramming event in vivo. *PNAS* **109**:6596–6601. DOI: https://doi.org/10.1073/pnas.1117031109, PMID: 22493276

Kamath RS, Martinez-Campos M, Zipperlen P, Fraser AG, Ahringer J. 2001. Effectiveness of specific RNA-mediated interference through ingested double-stranded RNA in *Caenorhabditis elegans*. *Genome Biology* **2**:RESEARCH0002. DOI: https://doi.org/10.1186/gb-2000-2-1-research0002, PMID: 11178279

Kamath RS, Fraser AG, Dong Y, Poulin G, Durbin R, Gotta M, Kanapin A, Le Bot N, Moreno S, Sohrmann M, Welchman DP, Zipperlen P, Ahringer J. 2003. Systematic functional analysis of the *Caenorhabditis elegans* genome using RNAi. *Nature* **421**:231–237. DOI: https://doi.org/10.1038/nature01278, PMID: 12529635

Kleemann GA, Basolo AL. 2007. Facultative decrease in mating resistance in hermaphroditic *Caenorhabditis elegans* with self-sperm depletion. *Animal Behaviour* **74**:1339–1347. DOI: https://doi.org/10.1016/j.anbehav.2007.02.031

Koo PK, Bian X, Sherlekar AL, Bunkers MR, Lints R. 2011. The robustness of *Caenorhabditis elegans* male mating behavior depends on the distributed properties of ray sensory neurons and their output through core and male-specific targets. *Journal of Neuroscience* **31**:7497–7510. DOI: https://doi.org/10.1523/JNEUROSCI.6153-10.2011, PMID: 21593334

Lee K, Portman DS. 2007. Neural sex modifies the function of a *C. elegans* sensory circuit. *Current Biology* **17**:1858–1863. DOI: https://doi.org/10.1016/j.cub.2007.10.015, PMID: 17964163

Lipton J, Kleemann G, Ghosh R, Lints R, Emmons SW. 2004. Mate searching in *Caenorhabditis elegans*: a genetic model for sex drive in a simple invertebrate. *Journal of Neuroscience* **24**:7427–7434. DOI: https://doi.org/10.1523/JNEUROSCI.1746-04.2004, PMID: 15329389

Liu T, Kim K, Li C, Barr MM. 2007. FMRFamide-like neuropeptides and mechanosensory touch receptor neurons regulate male sexual turning behavior in *Caenorhabditis elegans*. *Journal of Neuroscience* **27**:7174–7182. DOI: https://doi.org/10.1523/JNEUROSCI.1405-07.2007, PMID: 17611271

Liu Y, LeBeouf B, Guo X, Correa PA, Gualberto DG, Lints R, Garcia LR. 2011. A cholinergic-regulated circuit coordinates the maintenance and bi-stable states of a sensory-motor behavior during *Caenorhabditis elegans* male copulation. *PLOS Genetics* **7**:e1001326. DOI: https://doi.org/10.1371/journal.pgen.1001326, PMID: 21423722

Liu KS, Sternberg PW. 1995. Sensory regulation of male mating behavior in *Caenorhabditis elegans*. *Neuron* **14**:79–89. DOI: https://doi.org/10.1016/0896-6273(95)90242-2, PMID: 7826644

Low IIC, Williams CR, Chong MK, McLachlan IG, Wierbowski BM, Kolotuev I, Heiman MG. 2019. Morphogenesis of neurons and Glia within an epithelium. *Development* **146**:dev171124. DOI: https://doi.org/10.1242/dev.171124, PMID: 30683663

McIntire SL, Garriga G, White J, Jacobson D, Horvitz HR. 1992. Genes necessary for directed axonal elongation or fasciculation in *C. elegans*. *Neuron* **8**:307–322. DOI: https://doi.org/10.1016/0896-6273(92)90297-Q, PMID: 1739461

Miller KG, Alfonso A, Nguyen M, Crowell JA, Johnson CD, Rand JB. 1996. A genetic selection for *Caenorhabditis elegans* synaptic transmission mutants. *PNAS* **93**:12593–12598. DOI: https://doi.org/10.1073/pnas.93.22.12593, PMID: 8901627

Ng CS, Kopp A. 2008. Sex combs are important for male mating success in *Drosophila melanogaster*. *Behavior Genetics* **38**:195–201. DOI: https://doi.org/10.1007/s10519-008-9190-7, PMID: 18213513

Ogura K, Shirakawa M, Barnes TM, Hekimi S, Ohshima Y. 1997. The UNC-14 protein required for axonal elongation and guidance in *Caenorhabditis elegans* interacts with the serine/threonine kinase UNC-51. *Genes & Development* **11**:1801–1811. DOI: https://doi.org/10.1101/gad.11.14.1801, PMID: 9242488

Oren-Suissa M, Bayer EA, Hobert O. 2016. Sex-specific pruning of neuronal synapses in *Caenorhabditis elegans*. *Nature* **533**:206–211. DOI: https://doi.org/10.1038/nature17977, PMID: 27144354

Pavlou HJ, Lin AC, Neville MC, Nojima T, Diao F, Chen BE, White BH, Goodwin SF. 2016. Neural circuitry coordinating male copulation. *eLife* **5**:e20713. DOI: https://doi.org/10.7554/eLife.20713, PMID: 27855059

Pereira L, Kratsios P, Serrano-Saiz E, Sheftel H, Mayo AE, Hall DH, White JG, LeBoeuf B, Garcia LR, Alon U, Hobert O. 2015. A cellular and regulatory map of the cholinergic nervous system of *C. elegans*. *eLife* **4**:e12432. DOI: https://doi.org/10.7554/eLife.12432, PMID: 26705699

Pereira L, Aeschimann F, Wang C, Lawson H, Serrano-Saiz E, Portman DS, Großhans H, Hobert O. 2019. Timing mechanism of sexually dimorphic nervous system differentiation. *eLife* **8**:e42078. DOI: https://doi.org/10.7554/eLife.42078, PMID: 30599092

Perkins LA, Hedgecock EM, Thomson JN, Culotti JG. 1986. Mutant sensory cilia in the nematode *Caenorhabditis elegans*. *Developmental Biology* **117**:456–487. DOI: https://doi.org/10.1016/0012-1606(86)90314-3, PMID: 2428682

Pokala N, Liu Q, Gordus A, Bargmann CI. 2014. Inducible and titratable silencing of *Caenorhabditis elegans* neurons in vivo with histamine-gated chloride channels. *PNAS* **111**:2770–2775. DOI: https://doi.org/10.1073/pnas.1400615111, PMID: 24550306

Richard JP, Zuryn S, Fischer N, Pavet V, Vaucamps N, Jarriault S. 2011. Direct in vivo cellular reprogramming involves transition through discrete, non-pluripotent steps. *Development* **138**:1483–1492. DOI: https://doi.org/10.1242/dev.063115, PMID: 21389048

Ryan DA, Miller RM, Lee K, Neal SJ, Fagan KA, Sengupta P, Portman DS. 2014. Sex, age, and hunger regulate behavioral prioritization through dynamic modulation of chemoreceptor expression. *Current Biology* **24**:2509–2517. DOI: https://doi.org/10.1016/j.cub.2014.09.032, PMID: 25438941

Sammut M, Cook SJ, Nguyen KCQ, Felton T, Hall DH, Emmons SW, Poole RJ, Barrios A. 2015. Glia-derived neurons are required for sex-specific learning in *C. elegans*. *Nature* **526**:385–390. DOI: https://doi.org/10.1038/nature15700, PMID: 26469050

Schafer WR. 2015. Mechanosensory molecules and circuits in *C. elegans*. *Pflügers Archiv - European Journal of Physiology* **467**:39–48. DOI: https://doi.org/10.1007/s00424-014-1574-3

Schmitz C, Kinge P, Hutter H. 2007. Axon guidance genes identified in a large-scale RNAi screen using the RNAi-hypersensitive *Caenorhabditis elegans* strain *nre-1(hd20) lin-15b(hd126)*. *PNAS* **104**:834–839. DOI: https://doi.org/10.1073/pnas.0510527104, PMID: 17213328

Serrano-Saiz E, Oren-Suissa M, Bayer EA, Hobert O. 2017a. Sexually dimorphic differentiation of a *C. elegans* Hub Neuron Is Cell Autonomously Controlled by a Conserved Transcription Factor. *Current Biology* **27**:199–209. DOI: https://doi.org/10.1016/j.cub.2016.11.045, PMID: 28065609

Serrano-Saiz E, Pereira L, Gendrel M, Aghayeva U, Bhattacharya A, Howell K, Garcia LR, Hobert O. 2017b. A neurotransmitter atlas of the *Caenorhabditis elegans* Male Nervous System Reveals Sexually Dimorphic Neurotransmitter Usage. *Genetics* **206**:1251–1269. DOI: https://doi.org/10.1534/genetics.117.202127, PMID: 28684604

Sherlekar AL, Janssen A, Siehr MS, Koo PK, Caflisch L, Boggess M, Lints R. 2013. The *C. elegans* male exercises directional control during mating through cholinergic regulation of sex-shared command interneurons. *PLOS ONE* **8**:e60597. DOI: https://doi.org/10.1371/journal.pone.0060597, PMID: 23577128

Sherlekar AL, Lints R. 2014. Nematode tango milonguero - *the C. elegans* male's search for the hermaphrodite vulva. *Seminars in Cell & Developmental Biology* **33**:34–41. DOI: https://doi.org/10.1016/j.semcdb.2014.05.009, PMID: 24862858

Sherrington CS. 1907. On the proprio-ceptive system, especially in its reflex aspect. *Brain* **29**:467–482. DOI: https://doi.org/10.1093/brain/29.4.467

Smoot ME, Ono K, Ruscheinski J, Wang PL, Ideker T. 2011. Cytoscape 2.8: new features for data integration and network visualization. *Bioinformatics* **27**:431–432. DOI: https://doi.org/10.1093/bioinformatics/btq675, PMID: 21149340

Speese S, Petrie M, Schuske K, Ailion M, Ann K, Iwasaki K, Jorgensen EM, Martin TF. 2007. UNC-31 (CAPS) is required for dense-core vesicle but not synaptic vesicle exocytosis in *Caenorhabditis elegans*. *Journal of Neuroscience* **27**:6150–6162. DOI: https://doi.org/10.1523/JNEUROSCI.1466-07.2007, PMID: 17553987

Stefanakis N, Carrera I, Hobert O. 2015. Regulatory logic of Pan-Neuronal gene expression in *C. elegans*. *Neuron* **87**:733–750. DOI: https://doi.org/10.1016/j.neuron.2015.07.031, PMID: 26291158

Stiernagle T. 2006. Maintenance of C. elegans. *WormBook : The Online Review of C. Elegans Biology* **1**:101. DOI: https://doi.org/10.1895/wormbook.1.101.1

Sulston JE, Albertson DG, Thomson JN. 1980. The *Caenorhabditis elegans* male: Postembryonic development of nongonadal structures. *Developmental Biology* **78**:542–576. DOI: https://doi.org/10.1016/0012-1606(80)90352-8, PMID: 7409314

Sulston JE, Schierenberg E, White JG, Thomson JN. 1983. The embryonic cell lineage of the nematode *Caenorhabditis elegans*. *Developmental Biology* **100**:64–119. DOI: https://doi.org/10.1016/0012-1606(83)90201-4, PMID: 6684600

Sulston JE, Horvitz HR. 1977. Post-embryonic cell lineages of the nematode, *Caenorhabditis elegans*. *Developmental Biology* **56**:110–156. DOI: https://doi.org/10.1016/0012-1606(77)90158-0, PMID: 838129

Tuthill JC, Azim E. 2018. Proprioception. *Current Biology* **28**:R194–R203. DOI: https://doi.org/10.1016/j.cub.2018.01.064, PMID: 29510103

van den Heuvel S, Kipreos ET. 2012. *C. elegans* cell cycle analysis. *Methods in Cell Biology* **107**:265–294. DOI: https://doi.org/10.1016/B978-0-12-394620-1.00009-6, PMID: 22226527

Vidal B, Santella A, Serrano-Saiz E, Bao Z, Chuang CF, Hobert O. 2015. *C. elegans* SoxB genes are dispensable for embryonic neurogenesis but required for terminal differentiation of specific neuron types. *Development* **142**:2464–2477. DOI: https://doi.org/10.1242/dev.125740, PMID: 26153233

Villella A, Hall JC. 2008. Neurogenetics of courtship and mating in *Drosophila*. *Advances in Genetics* **62**:67–184. DOI: https://doi.org/10.1016/S0065-2660(08)00603-2, PMID: 19010254

Wallace SW, Singhvi A, Liang Y, Lu Y, Shaham S. 2016. PROS-1/Prospero is a major regulator of the Glia-Specific secretome controlling Sensory-Neuron shape and function in *C. elegans*. *Cell Reports* **15**:550–562. DOI: https://doi.org/10.1016/j.celrep.2016.03.051, PMID: 27068465

Ward S, Thomson N, White JG, Brenner S. 1975. Electron microscopical reconstruction of the anterior sensory anatomy of the nematode *Caenorhabditis elegans*.?2uu. *The Journal of Comparative Neurology* **160**:313–337. DOI: https://doi.org/10.1002/cne.901600305, PMID: 1112927

Weinberg P, Berkseth M, Zarkower D, Hobert O. 2018. Sexually dimorphic unc-6/Netrin expression controls Sex-Specific maintenance of synaptic connectivity. *Current Biology* **28**:623–629. DOI: https://doi.org/10.1016/j.cub.2018.01.002, PMID: 29429615

White JG, Southgate E, Thomson JN, Brenner S. 1986. The structure of the nervous system of the nematode *Caenorhabditis elegans*. *Philosophical Transactions of the Royal Society of London. Series B, Biological Sciences* **314**:1–340. DOI: https://doi.org/10.1098/rstb.1986.0056, PMID: 22462104

White JQ, Nicholas TJ, Gritton J, Truong L, Davidson ER, Jorgensen EM. 2007. The sensory circuitry for sexual attraction in *C. elegans* males. *Current Biology* **17**:1847–1857. DOI: https://doi.org/10.1016/j.cub.2007.09.011, PMID: 17964166

White JQ, Jorgensen EM. 2012. Sensation in a single neuron pair represses male behavior in hermaphrodites. *Neuron* **75**:593–600. DOI: https://doi.org/10.1016/j.neuron.2012.03.044, PMID: 22920252

Wildwater M, Sander N, de Vreede G, van den Heuvel S. 2011. Cell shape and wnt signaling redundantly control the division Axis of *C. elegans* epithelial stem cells. *Development* **138**:4375–4385. DOI: https://doi.org/10.1242/dev.066431, PMID: 21937595

Xu M, Jarrell TA, Wang Y, Cook SJ, Hall DH, Emmons SW. 2013. Computer assisted assembly of connectomes from electron micrographs: application to *Caenorhabditis elegans*. *PLOS ONE* **8**:e54050. DOI: https://doi.org/10.1371/journal.pone.0054050, PMID: 23342070

Yang CF, Shah NM. 2014. Representing sex in the brain, one module at a time. *Neuron* **82**:261–278. DOI: https://doi.org/10.1016/j.neuron.2014.03.029, PMID: 24742456

Yuan J, Horvitz HR. 1992. The *Caenorhabditis elegans* cell death gene ced-4 encodes a novel protein and is expressed during the period of extensive programmed cell death. *Development* **116**:309–320. PMID: 1286611

Zahn TR, Macmorris MA, Dong W, Day R, Hutton JC. 2001. IDA-1, *a Caenorhabditis elegans* homolog of the diabetic autoantigens IA-2 and Phogrin, is expressed in Peptidergic neurons in the worm. *The Journal of Comparative Neurology* **429**:127–143. DOI: https://doi.org/10.1002/1096-9861(20000101)429:1<127::AID-CNE10>3.0.CO;2-H, PMID: 11086294

Zarkower D. 2006. Somatic sex determination. *WormBook* **1**:1–12. DOI: https://doi.org/10.1895/wormbook.1.84.1

Zuryn S, Ahier A, Portoso M, White ER, Morin MC, Margueron R, Jarriault S. 2014. Transdifferentiation sequential histone-modifying activities determine the robustness of transdifferentiation. *Science* **345**:826–829. DOI: https://doi.org/10.1126/science.1255885, PMID: 25124442

References

Ali, F., Hindley, C., McDowell, G., Deibler, R., Jones, A., Kirschner, M., Guillemot, F., & Philpott, A. (2011). Cell cycle-regulated multi-site phosphorylation of neurogenin 2 coordinates cell cycling with differentiation during neurogenesis. *Development*, *138*(19), 4267–4277.

Altmann, C. R., Chow, R. L., Lang, R. A., & Hemmati-Brivanlou, A. (1997). Lens Induction by Pax-6 inXenopus laevis. *Developmental Biology*, *185*(1), 119–123.

Alvarez-Buylla, A., Theelen, M., & Nottebohm, F. (1990). Proliferation hot spots in adult avian ventricular zone reveal radial cell division. *Neuron*, *5*(1), 101–109.

Ambros, V., & Horvitz, H. R. (1987). The lin-14 locus of *Caenorhabditis elegans* controls the time of expression of specific postembryonic developmental events. *Genes & Development*, *1*(4), 398–414.

Anders, L., Ke, N., Hydbring, P., Choi, Y. J., Widlund, H. R., Chick, J. M., Zhai, H., Vidal, M., Gygi, S. P., Braun, P., & Sicinski, P. (2011). A Systematic Screen for CDK4/6 Substrates Links FOXM1 Phosphorylation to Senescence Suppression in Cancer Cells. *Cancer Cell*, *20*(5), 620–634.

Andreu, Z., Khan, M. A., González-Gõmez, P., Negueruela, S., Hortigüela, R., San Emeterio, J., Ferrõn, S. R., Martínez, G., Vidal, A., Fariñas, I., Lie, D. C., & Mira, H. (2015). The cyclin-dependent kinase inhibitor p27kip1 regulates radial stem cell quiescence and neurogenesis in the adult hippocampus. *Stem Cells*, *33*(1), 219–229.

Artavanis-Tsakonas, S., Rand, M. D., & Lake, R. J. (1999). Notch signaling: Cell fate control and signal integration in development. In *Science* (Vol. 284, Issue 5415, pp. 770–776).

Ashery-Padan, R., & Gruss, P. (2001). Pax6 lights-up the way for eye development. *Current Opinion in Cell Biology*, *13*(6), 706–714.

Avilion, A. A. (2003). Multipotent cell lineages in early mouse development depend on SOX2 function. *Genes & Development*, *17*(1), 126–140.

Avvakumov, N., Nourani, A., & Côté, J. (2011). Histone Chaperones: Modulators of Chromatin Marks. In *Molecular Cell* (Vol. 41, Issue 5, pp. 502–514). Cell Press.

Aze, A., & Maiorano, D. (2018). Recent advances in understanding DNA

replication: Cell type–specific adaptation of the DNA replication program. In *F1000Research* (Vol. 7). F1000 Research Ltd.

Bacaj, T., Tevlin, M., Lu, Y., & Shaham, S. (2008). Glia are essential for sensory organ function in *C. elegans*. *Science (New York, N.Y.)*, *322*(5902), 744–747.

Bakkers, J., Verhoeven, M. C., & Abdelilah-Seyfried, S. (2009). Shaping the zebrafish heart: From left–right axis specification to epithelial tissue morphogenesis. *Developmental Biology*, *330*(2), 213–220.

Bao, Z., Zhao, Z., Boyle, T. J., Murray, J. I., & Waterston, R. H. (2008). Control of cell cycle timing during *C. elegans* embryogenesis. *Developmental Biology*, *318*(1), 65–72.

Barbosa, J. S., Sanchez-Gonzalez, R., Di Giaimo, R., Baumgart, E. V., Theis, F. J., Götz, M., & Ninkovic, J. (2015). Live imaging of adult neural stem cell behavior in the intact and injured zebrafish brain. *Science*, *348*(6236), 789–793.

Bargmann, C. I., & Horvitz, H. R. (1991). Chemosensory neurons with overlapping functions direct chemotaxis to multiple chemicals in *C. elegans*. *Neuron*, *7*(5), 729–742.

Barrios, A., Nurrish, S., & Emmons, S. W. (2008). Sensory regulation of *C. elegans* male mate-searching behavior. *Current Biology : CB*, *18*(23), 1865–1871.

Bate, C. M. (1976). Embryogenesis of an insect nervous system. I. A map of the thoracic and abdominal neuroblasts in Locusta migratoria. *Journal of Embryology and Experimental Morphology*, *35*(1), 107–123.

Batzoglou, S., Jaffe, D. B., Stanley, K., Butler, J., Gnerre, S., Mauceli, E., Berger, B., Mesirov, J. P., & Lander, E. S. (2002). ARACHNE: A whole-genome shotgun assembler. *Genome Research*, *12*(1), 177–189.

Bavestrello, G., Sommer, C., & Sara, M. (1992). Bi-directional conversion in *Turritopsis nutricula*. *Aspects of Hydrozoan Biology*, *56*, 137–140.

Béby, F., Housset, M., Fossat, N., Le Greneur, C., Flamant, F., Godement, P., & Lamonerie, T. (2010). Otx2 gene deletion in adult mouse retina induces rapid RPE dystrophy and slow photoreceptor degeneration. *PLoS ONE*, *5*(7), 1–8.

Bertoli, C., Skotheim, J. M., & de Bruin, R. A. M. (2013). Control of cell cycle transcription during G1 and S phases. *Nature Reviews Molecular Cell*

Biology, *14*(8), 518–528.

Bertrand, N., Castro, D. S., & Guillemot, F. (2002). Proneural genes and the specification of neural cell types. *Nature Reviews Neuroscience*, *3*(7), 517–530.

Besson, A., Gurian-West, M., Chen, X., Kelly-Spratt, K. S., Kemp, C. J., & Roberts, J. M. (2006). A pathway in quiescent cells that controls p27Kip1 stability, subcellular localization, and tumor suppression. *Genes and Development*, *20*(1), 47–64.

Bisteau, X., Paternot, S., Colleoni, B., Ecker, K., Coulonval, K., de Groote, P., Declercq, W., Hengst, L., & Roger, P. P. (2013). CDK4 T172 Phosphorylation Is Central in a CDK7-Dependent Bidirectional CDK4/CDK2 Interplay Mediated by p21 Phosphorylation at the Restriction Point. *PLoS Genetics*, *9*(5), 1–21.

Bjornson, C. R. R., Cheung, T. H., Liu, L., Tripathi, P. V., Steeper, K. M., & Rando, T. A. (2012). Notch signaling is necessary to maintain quiescence in adult muscle stem cells. *Stem Cells*, *30*(2), 232–242.

Blain, S. (2008). Switching cyclin D-Cdk4 kinase activity on and off. In *Cell Cycle* (Vol. 7, Issue 7).

Blau, H. M., Chiu, C.-P., & Webster, C. (1983). Cytoplasmic Activation of Human Nuclear Genes in Stable Heterocaryons. In *Cell* (Vol. 32).

Bockstaele, L., Kooken, H., Libert, F., Paternot, S., Dumont, J. E., de Launoit, Y., Roger, P. P., & Coulonval, K. (2006). Regulated Activating Thr172 Phosphorylation of Cyclin-Dependent Kinase 4(CDK4): Its Relationship with Cyclins and CDK “Inhibitors.” *Molecular and Cellular Biology*, *26*(13), 5070–5085.

Boxem, M., Srinivasan, D. G., & van den Heuvel, S. (1999). *C. elegans ncc-1* is required for M phase. *Development*, *126*, 2227–2239.

Boxem, M., & van den Heuvel, S. (2001). *lin-35* Rb and *cki-1* Cip/Kip cooperate in developmental regulation of G1 progression in *C. elegans. Development*, *128*(21), 4349–4359.

Boxem, M., & van den Heuvel, S. (2002). *C. elegans* class B synthetic multivulva genes act in G(1) regulation. *Current Biology*, *12*(11), 906–911.

Boyl, P. P., Signore, M., Annino, A., Barbera, J. P. M., Acampora, D., & Simeone, A. (2001). Otx genes in the development and evolution of the vertebrate brain. *International Journal of Developmental Neuroscience*,

19(4), 353–363.

Brenner, S. (1973). The genetics of behaviour. *British Medical Bulletin, 29*(3), Pages 269–271.

Brenner, S. (1974). The genetics of *Caenorhabditis elegans*. *Genetlcs*, *77*, 71–94.

Briggs, R., & King, T. J. (1952). Transplantation of Living Nuclei From Blastula Cells into Enucleated Frogs' Eggs. *Proceedings of the National Academy of Sciences of the United States of America*, *38*(5), 455–463.

Britten, R. J., & Davidson, E. H. (1969). Gene regulation for higher cells: a theory. *Science (New York, N.Y.)*, *165*(3891), 349–357.

Buck, S. H., Chiu, D., & Saito, M. R. (2009). The cyclin-dependent kinase inhibitors, *cki-1* and *cki-2*, act in overlapping but distinct pathways to control cell-cycle quiescence during *C. elegans* development. *Cell Cycle*, *8*(16), 2613–2620.

Budhavarapu, V. N., Chavez, M., & Tyler, J. K. (2013). How is epigenetic information maintained through DNA replication? *Epigenetics and Chromatin*, *6*(1), 32.

Busanello, A., Battistelli, C., Carbone, M., Mostocotto, C., & Maione, R. (2012). MyoD regulates p57kip2 expression by interacting with a distant cis-element and modifying a higher order chromatin structure. *Nucleic Acids Research*, *40*(17), 8266–8275.

***C. elegans* Sequencing Consortium**. (1998). Genome sequence of the nematode *C. elegans*: A platform for investigating biology. In *Science* (Vol. 282, Issue 5396, pp. 2012–2018).

Calvi, B. R., Lilly, M. A., & Spradling, A. C. (1998). Cell cycle control of chorion gene amplification. *Genes and Development*, *12*(5), 734–744.

Casarosa, S., Fode, C., & Guillemot, F. (1999). Mash1 regulates neurogenesis in the ventral telencephalon. *Development*, *126*, 525–534.

Castro, D. S., Martynoga, B., Parras, C., Ramesh, V., Pacary, E., Johnston, C., Drechsel, D., Lebel-Potter, M., Garcia, L. G., Hunt, C., Dolle, D., Bithell, A., Ettwiller, L., Buckley, N., & Guillemot, F. (2011). A novel function of the proneural factor Ascl1 in progenitor proliferation identified by genome-wide characterization of its targets. *Genes and Development*, *25*(9), 930–945.

Cavallaro, M., Mariani, J., Lancini, C., Latorre, E., Caccia, R., Gullo, F., Valotta, M., DeBiasi, S., Spinardi, L., Ronchi, A., Wanke, E., Brunelli, S., Favaro, R., Ottolenghi, S., & Nicolis, S. K. (2008). Impaired generation of mature neurons by neural stem cells from hypomorphic Sox2 mutants. *Development*, *135*(3), 541–557.

Cen, L., Carlson, B. L., Schroeder, M. A., Ostrem, J. L., Kitange, G. J., Mladek, A. C., Fink, S. R., Decker, P. A., Wu, W., Kim, J. S., Waldman, T., Jenkins, R. B., & Sarkaria, J. N. (2012). P16-Cdk4-Rb axis controls sensitivity to a cyclin-dependent kinase inhibitor PD0332991 in glioblastoma xenograft cells. *Neuro-Oncology*, *14*(7), 870–881.

Cenciarelli, C., De Santa, F., Puri, P. L., Mattei, E., Ricci, L., Bucci, F., Felsani, A., & Caruso, M. (1999). Critical role played by cyclin D3 in the MyoD-mediated arrest of cell cycle during myoblast differentiation. *Molecular and Cellular Biology*, *19*(7), 5203–5217.

Chalfie, M., Tu, Y., Euskirchen, G., Ward, W., Prasher, D., & M Chalfie, Y Tu, G Euskirchen, WW Ward, D. P. (1994). Green fluorescent protein as a marker for gene expression. *Science*, *263*(5148).

Chambers, I., Colby, D., Robertson, M., Nichols, J., Lee, S., Tweedie, S., & Smith, A. (2003). Functional expression cloning of Nanog, a pluripotency sustaining factor in embryonic stem cells. *Cell*, *113*(5), 643–655.

Chanda, S., Ang, C. E., Davila, J., Pak, C., Mall, M., Lee, Q. Y., Ahlenius, H., Jung, S. W., Südhof, T. C., & Wernig, M. (2014). Generation of Induced Neuronal Cells by the Single Reprogramming Factor ASCL1. *Stem Cell Reports*, *3*(2), 282–296.

Chandramohan, V., Mineva, N. D., Burke, B., Jeay, S., Wu, M., Shen, J., Yang, W., Hann, S. R., & Sonenshein, G. E. (2008). c-Myc Represses FOXO3a-Mediated Transcription of the Gene Encoding the p27 Kip1 Cyclin Dependent Kinase Inhibitor. *Journal of Cellular Biochemistry*, *104*, 2091–2106.

Chen, H., Xu, X., Wang, G. G., Zhang, B., Wang, G. G., Xin, G., Liu, J., Jiang, Q., Zhang, H., & Zhang, C. (2017). CDK4 protein is degraded by anaphase-promoting complex/cyclosome in mitosis and reaccumulates in early G1 phase to initiate a new cell cycle in HeLa cells. *The Journal of Biological Chemistry*, *292*(24), 10131–10141.

Chen, M. J., Ng, J. M. J., Peng, Z. F., Manikandan, J., Yap, Y. W., Llanos, R. M., Beart, P. M., & Cheung, N. S. (2013). Gene profiling identifies commonalities in neuronal pathways in excitotoxicity: Evidence favouring cell cycle re-activation in concert with oxidative stress. *Neurochemistry*

International, *62*(5), 719–730.

Chen, M., Takano-Maruyama, M., Pereira-Smith, O. M., Gaufo, G. O., & Tominaga, K. (2009). MRG15, a component of HAT and HDAC complexes, is essential for proliferation and differentiation of neural precursor cells. *Journal of Neuroscience Research*, *87*(7), 1522–1531.

Chen, T., & Dent, S. Y. R. (2014). Chromatin modifiers and remodellers: Regulators of cellular differentiation. In *Nature Reviews Genetics* (Vol. 15, Issue 2, pp. 93–106). Nature Publishing Group.

Cheng, M., Olivier, P., Diehl, J. A., Fero, M., Roussel, M. F., Roberts, J. M., & Sherr, C. J. (1999). The p21 Cip1 and p27 Kip1 CDK "inhibitors" are essential activators of cyclin D-depretrieveendent kinases in murine fibroblasts. In *The EMBO Journal* (Vol. 18, Issue 6).

Cirillo, L. A., Lin, F. R., Cuesta, I., Friedman, D., Jarnik, M., & Zaret, K. S. (2002). Opening of Compacted Chromatin by Early Developmental Transcription Factors HNF3 (FoxA) and GATA-4. In *Molecular Cell* (Vol. 9).

Cirillo, L. A., & Zaret, K. S. (1999). An Early Developmental Transcription Factor Complex that Is More Stable on Nucleosome Core Particles Than on Free DNA The results also address the more general issue of how. In *Molecular Cell* (Vol. 4). Sasaki and Hogan.

Cobaleda, C., Jochum, W., & Busslinger, M. (2007). Conversion of mature B cells into T cells by dedifferentiation to uncommitted progenitors. *Nature*, *449*(7161), 473–477.

Colleoni, B., Paternot, S., Pita, J. M., Bisteau, X., Coulonval, K., Davis, R. J., Raspé, E., & Roger, P. P. (2017). JNKs function as CDK4-activating kinases by phosphorylating CDK4 and p21. *Oncogene*, *36*(30), 4349–4361.

Collignon, J., Sockanathan, S., Hacker, A., Cohen-Tannoudji, M., Norris, D., Rastan, S., Stevanovic, M., Goodfellow, P. N., & Lovell-Badge, R. (1996). A comparison of the properties of Sox-3 with Sry and two related genes, Sox-1 and Sox-2. *Development*, *122*(2).

Conradt, B., & Horvitz, H. R. (1999). The TRA-1A sex determination protein of *C. elegans* regulates sexually dimorphic cell deaths by repressing the egl-1 cell death activator gene. *Cell*, *98*(3), 317–327.

Cook, S. J., Jarrell, T. A., Brittin, C. A., Wang, Y., Bloniarz, A. E., Yakovlev, M. A., Nguyen, K. C. Q., Tang, L. T. H., Bayer, E. A., Duerr, J. S., Bülow, H. E., Hobert, O., Hall, D. H., & Emmons, S. W. (2019). Whole-animal connectomes of both *Caenorhabditis elegans* sexes. *Nature*, *571*(7763),

63–71.

Cowan, C. A., Atienza, J., Melton, D. A., & Eggan, K. (2005). Nuclear Reprogramming of Somatic Cells After Fusion with Human Embryonic Stem Cells. *Science*, *300*(5621), 913–916.

Das, M., Singh, S., Pradhan, S., & Narayan, G. (2014). MCM Paradox: Abundance of Eukaryotic Replicative Helicases and Genomic Integrity. *Molecular Biology International*, *2014*, 574850.

Davis, G., Haas, M., & Pocock, R. (2015). MicroRNAs: Not “Fine-Tuners” but Key Regulators of Neuronal Development and Function. *Frontiers in Neurology*, *6*, 245.

Davis, R. L., Weintraub, H., & Lassar, A. B. (1987). Expression of a single transfected cDNA converts fibroblasts to myoblasts. *Cell*, *51*(6), 987–1000.

Day, P. J., Cleasby, A., Tickle, I. J., O’Reilly, M., Coyle, J. E., Holding, F. P., McMenamin, R. L., Yon, J., Chopra, R., Lengauer, C., & Jhoti, H. (2009). Crystal structure of human CDK4 in complex with a D-type cyclin. *Proceedings of the National Academy of Sciences of the United States of America*, *106*(11), 4166–4170.

de Nooij, J. C., Letendre, M. A., & Hariharan, I. K. (1996). A cyclin-dependent kinase inhibitor, Dacapo, is necessary for timely exit from the cell cycle during *Drosophila* embryogenesis. *Cell*, *87*(7), 1237–1247.

De Robertis, E. M., Wessely, O., Oelgeschläger, M., Brizuela, B., Pera, E., Larraín, J., Abreu, J., & Bachiller, D. (2001). Molecular mechanisms of cell-cell signaling by the Spemann-Mangold organizer. *The International Journal of Developmental Biology*, *45*(1), 189–197.

Del Bene, F., Wehman, A. M., Link, B. A., & Baier, H. (2008). Regulation of Neurogenesis by Interkinetic Nuclear Migration through an Apical-Basal Notch Gradient. *Cell*, *134*(6), 1055–1065.

Dennis, D. J., Han, S., & Schuurmans, C. (2018). bHLH transcription factors in neural development, disease, and reprogramming. *Brain Research*, *1705*, 48–65.

Di Berardino, M. A., & King, T. J. (1967). Development and cellular differentiation of neural nuclear-transplants of known karyotype. *Developmental Biology*, *15*(2), 102–128.

Di Salvio, M., Di Giovannantonio, L. G., Acampora, D., Prosperi, R., Omodei, D., Prakash, N., Wurst, W., & Simeone, A. (2010). Otx2 controls

neuron subtype identity in ventral tegmental area and antagonizes vulnerability to MPTP. *Nature Neuroscience*, *13*(12), 1481–1488.

Doe, C. Q. (1992). Molecular markers for identified neuroblasts and ganglion mother cells in the *Drosophila* central nervous system. *Development (Cambridge, England)*, *116*(4), 855–863.

Doetsch, F., Caille, I., Lim, D. A., Garcia-Verdugo, J. M., & Alvarez-Buylla, A. (1999). Subventricular zone astrocytes are neural stem cells in the adult mammalian brain. *Cell*, *97*(6), 703–716.

Doitsidou, M., Jarriault, S., & Poole, R. J. (2016). Next-Generation Sequencing-Based Approaches for Mutation Mapping and Identification in *Caenorhabditis elegans*. *Genetics*, *204*(2), 451–474.

Doroquez, D. B., Berciu, C., Anderson, J. R., Sengupta, P., & Nicastro, D. (2014). A high-resolution morphological and ultrastructural map of anterior sensory cilia and glia in *Caenorhabditis elegans*. *ELife*, *3*(3), e01948.

Ebrahimi, B. (2015). Reprogramming barriers and enhancers: strategies to enhance the efficiency and kinetics of induced pluripotency. *Cell Regeneration (London, England)*, *4*, 10.

Echeverri, K., & Tanaka, E. M. (2002). Ectoderm to mesoderm lineage switching during axolotl tail regeneration. *Science (New York, N.Y.)*, *298*(5600), 1993–1996.

Edel, M. J., Menchon, C., Menendez, S., Consiglio, A., Raya, A., & Izpisua Belmonte, J. C. (2010). Rem2 GTPase maintains survival of human embryonic stem cells as well as enhancing reprogramming by regulating p53 and cyclin D1. *Genes & Development*, *24*(6), 561–573.

Efroni, S., Duttagupta, R., Cheng, J., Dehghani, H., Hoeppner, D. J., Dash, C., Bazett-Jones, D. P., Le Grice, S., McKay, R. D. G., Buetow, K. H., Gingeras, T. R., Misteli, T., & Meshorer, E. (2008). Global Transcription in Pluripotent Embryonic Stem Cells. *Cell Stem Cell*, *2*(5), 437–447.

Eguchi, G., & Kodama, R. (1993). Transdifferentiation. *Current Opinion in Cell Biology*, *5*(6), 1023–1028.

Eguchi, G., & Okada, T. S. (1973). Differentiation of Lens Tissue from the Progeny of Chick Retinal Pigment Cells Cultured In Vitro: A Demonstration of a Switch of Cell Types in Clonal Cell Culture. *Proceedings of the National Academy of Sciences of the United States of America*, *70*(5), 1495–1499.

Engler, A., Rolando, C., Giachino, C., Saotome, I., Erni, A., Brien, C., Zhang, R., Zimber-Strobl, U., Radtke, F., Artavanis-Tsakonas, S., Louvi, A., & Taylor, V. (2018). Notch2 Signaling Maintains NSC Quiescence in the Murine Ventricular-Subventricular Zone. *Cell Reports*, *22*(4), 992–1002.

Eriksson, P. S., Perfilieva, E., Björk-Eriksson, T., Alborn, A.-M., Nordborg, C., Peterson, D. A., & Gage, F. H. (1998). Neurogenesis in the adult human hippocampus. *Nature Medicine*, *4*(11), 1313–1317.

Etchberger, J. F., Lorch, A., Sleumer, M. C., Zapf, R., Jones, S. J., Marra, M. A., Holt, R. A., Moerman, D. G., & Hobert, O. (2007). The molecular signature and cis-regulatory architecture of a *C. elegans* gustatory neuron. *Genes & Development*, *21*(13), 1653–1674.

Euling, S., & Ambros, V. (1996). Heterochronic genes control cell cycle progress and developmental competence of *C. elegans* vulva precursor cells. *Cell*, *84*(5), 667–676.

Evans, T., Rosenthal, E. T., Youngblom, J., Distel, D., & Hunt, T. (1983). Cyclin: A Protein Specified by Maternal mRNA in Sea Urchin Eggs That Is Destroyed at Each Cleavage Division. In *Cell* (Vol. 33).

Farrell, J. A., & O'Farrell, P. H. (2014). From Egg to Gastrula: How the Cell Cycle Is Remodeled During the *Drosophila* Mid-Blastula Transition. *Annual Review of Genetics*, *48*(1), 269–294.

Fay, D. S., Keenan, S., & Han, M. (2002). *fzr-1* and *lin-35*/Rb function redundantly to control cell proliferation in *C. elegans* as revealed by a nonbiased synthetic screen. *Genes & Development*, *16*(4), 503–517.

Ferguson, E. L., & Horvitz, H. R. (1989). The multivulva phenotype of certain *Caenorhabditis elegans* mutants results from defects in two functionally redundant pathways. *Genetics*, *123*(1), 109–121.

Fire, A., Xu, S., Montgomery, M. K., Kostas, S. A., Driver, S. E., & Mello, C. C. (1998). Potent and specific genetic interference by double-stranded RNA in *Caenorhabditis elegans*. *Nature*, *391*(6669), 806–811.

Fisher, R. P., & Morgan, D. O. (1994). A novel cyclin associates with M015/CDK7 to form the CDK-activating kinase. *Cell*, *78*(4), 713–724.

Flemington, E. K., Speck, S. H., & Kaelin, W. G. (1993). E2F-1-mediated transactivation is inhibited by complex formation with the retinoblastoma susceptibility gene product. *Proceedings of the National Academy of Sciences of the United States of America*, *90*(15), 6914–6918.

Flemming, W. (1882). *Zellsubstanz, kern und zelltheilung*.

Fox, P. M., Vought, V. E., Hanazawa, M., Lee, M.-H., Maine, E. M., & Schedl, T. (2011). Cyclin E and CDK-2 regulate proliferative cell fate and cell cycle progression in the *C. elegans* germline. *Development*, *138*(11), 2223–2234.

Frank, C. A., Baum, P. D., & Garriga, G. (2003). HLH-14 is a *C. elegans* achaete-scute protein that promotes neurogenesis through asymmetric cell division. *Development (Cambridge, England)*, *130*(26), 6507–6518.

Fujita, S. (1963). The matrix cell and cytogenesis in the developing central nervous system. *The Journal of Comparative Neurology*, *120*(1), 37–42.

Fukuyama, M., Gendreau, S. B., Derry, W. B., & Rothman, J. H. (2003). Essential embryonic roles of the CKI-1 cyclin-dependent kinase inhibitor in cell-cycle exit and morphogenesis in *C. elegans*. *Developmental Biology*, *260*(1), 273–286.

Fukuyama, M., Sakuma, K., Park, R., Kasuga, H., Nagaya, R., Atsumi, Y., Shimomura, Y., Takahashi, S., Kajiho, H., Rougvie, A., Kontani, K., & Katada, T. (2012). *C. elegans* AMPKs promote survival and arrest germline development during nutrient stress. *Biology Open*, *1*(10), 929–936.

Gaiano, N., Nye, J. S., & Fishell, G. (2000). Radial glial identity is promoted by Notch1 signaling in the murine forebrain. *Neuron*, *26*(2), 395–404.

García-Bellido, A. (1975). Genetic control of wing disc development in *Drosophila*. *Ciba Foundation Symposium*, *29*, 161–182.

García-Bellido, A. (1979). Genetic Analysis of the Achaete-Scute System of *DROSOPHILA MELANOGASTER*. *Genetics*, *91*(3), 491.

Garcia, L. R., Mehta, P., & Sternberg, P. W. (2001). Regulation of distinct muscle behaviors controls the *C. elegans* male's copulatory spicules during mating. *Cell*, *107*(6), 777–788.

Gebara, E., Bonaguidi, M. A., Beckervordersandforth, R., Sultan, S., Udry, F., Gijs, P.-J., Lie, D. C., Ming, G.-L., Song, H., & Toni, N. (2016). Heterogeneity of Radial Glia-Like Cells in the Adult Hippocampus. *Stem Cells (Dayton, Ohio)*, *34*(4), 997–1010.

Gemberling, M., Bailey, T. J., Hyde, D. R., & Poss, K. D. (2013). The zebrafish as a model for complex tissue regeneration. *Trends in Genetics : TIG*, *29*(11), 611–620.

Georgia, S., & Bhushan, A. (2006). p27 regulates the transition of β-cells from quiescence to proliferation. *Diabetes*, *55*(11), 2950–2956.

Gifford, C. A., Ziller, M. J., Gu, H., Trapnell, C., Donaghey, J., Tsankov, A., Shalek, A. K., Kelley, D. R., Shishkin, A. A., Issner, R., Zhang, X., Coyne, M., Fostel, J. L., Holmes, L., Meldrim, J., Guttman, M., Epstein, C., Park, H., Kohlbacher, O., … Meissner, A. (2013). Transcriptional and epigenetic dynamics during specification of human embryonic stem cells. *Cell*, *153*(5), 1149–1163.

Goel, S., Decristo, M. J., Mcallister, S. S., & Zhao, J. J. (2018). *CDK4/6 Inhibition in Cancer: Beyond Cell Cycle Arrest*.

Graham, V., Khudyakov, J., Ellis, P., & Pevny, L. (2003). SOX2 functions to maintain neural progenitor identity. *Neuron*, *39*(5), 749–765.

Greenwald, I. S., Sternberg, P. W., & Horvitz, H. R. (1983). The lin-12 Locus Specifies Cell Fates in *Caenorhabditis elegans*. *Cell*, *34*(2), 435–444.

Gurdon, J. B. (1960a). Factors Responsible for the Abnormal Development of Embryos Obtained by Nuclear Transplantation in Xenopus laevis. *J Embryol Exp Morphol*, *8*(3), 327–340.

Gurdon, J. B. (1960b). The Developmental Capacity of Nuclei Taken from Differentiating Endoderm Cells of Xenopus Laevis. *Journal of Embryology and Experimental Morphology*, *8*(4), 505–526.

Gurdon, J. B. (1962). The Developmental Capacity of Nuclei taken from Intestinal Epithelium Cells of Feeding Tadpoles. *Journal of Embryology and Experimental Morphology*, *10*, 622–640.

Gurdon, J. B., & Brown, D. D. (1965). Cytoplasmic regulation of RNA synthesis and nucleolus formation in developing embryos of Xenopus laevis. *Journal of Molecular Biology*, *12*(1), 27–35.

Gurdon, J. B., & Uehlinger, V. (1966). “Fertile” Intestine Nuclei. *Nature*, *210*(5042), 1240–1241.

Hadorn, E. (1976). Initial Ttransdetermination in the First Leg Discs of Different *Drosophila* Species. *Technical Methods, 25*(1964), 1966–1968.

Hadorn, E. (1965). Problems of determination and transdetermination. *Brookhaven Symposia in Biology*, 18:148–161.

Hagey, D. W., & Muhr, J. (2014). Sox2 Acts in a Dose-Dependent Fashion to Regulate Proliferation of Cortical Progenitors. *Cell Reports*, *9*(5), 1908–

1920.

Hajduskova, M., Baytek, G., Kolundzic, E., Gosdschan, A., Kazmierczak, M., Ofenbauer, A., Del Rosal, M. L. B., Herzog, S., Ul Fatima, N., Mertins, P., Seelk-Müthel, S., & Tursun, B. (2019). MRG-1/MRG15 is a barrier for germ cell to neuron reprogramming in *Caenorhabditis elegans*. *Genetics*, *211*(1), 121–139.

Halder, G., Callaerts, P., & Gehring, W. (1995). Induction of ectopic eyes by targeted expression of the eyeless gene in *Drosophila*. *Science*, *267*(5205), 1788–1792.

Halevy, O., Novitch, B. G., Spicer, D. B., Skapek, S. X., Rhee, J., Hannon, G. J., Beach, D., & Lassar, A. B. (1995). Correlation of terminal cell cycle arrest of skeletal muscle with induction of p21 by MyoD. *Science*, *267*(5200), 1018–1021.

Hall, D. H., & Russell, R. L. (1991). The posterior nervous system of the nematode *Caenorhabditis elegans*: Serial reconstruction of identified neurons and complete pattern of synaptic interactions. *Journal of Neuroscience*, *11*(1), 1–22.

Hamilton, E., & Infante, J. R. (2016). Targeting CDK4/6 in patients with cancer. In *Cancer Treatment Reviews* (Vol. 45, pp. 129–138).

Harland, R., & Gerhart, J. (1997). Formation and function of Spemann's organizer. *Annual Review of Cell and Developmental Biology*, *13*(1), 611–667.

Hartwell, L. H., Mortimer, R. K., Culotti, J., & Culotti, M. (1973). Genetic control of the cell division cycle in yeast: V. Genetic analysis of cdc mutants. *Genetics*, *74*(2), 267–286.

Hartwell, Leland H, Culotti, J., Pringle, J. R., & Reid, B. J. (1974). Genetic control of the cell division cycle in yeast. In *Science* (Vol. 183, Issue 4120, pp. 46–51). American Association for the Advancement of Science.

Hazelrigg, T., & Kaufman, T. C. (1983). Revertants of Dominant Mutations Associated with the Antennapedia Gene Complex of *Drosophila melanogaster*: Cytology and Genetics. *Genetics*, *105*(3), 581–600.

Hedgecock, E. M., & Russell, R. L. (1975). Normal and mutant thermotaxis in the nematode *Caenorhabditis elegans*. *Proceedings of the National Academy of Sciences of the United States of America*, *72*(10), 4061–4065.

Helin, K., Harlow, E., & Fattaey, A. (1993). Inhibition of E2F-1 transactivation

by direct binding of the retinoblastoma protein. *Molecular and Cellular Biology*, *13*(10), 6501–6508.

Helm, C., Karl, A., Beckers, P., Kaul-Strehlow, S., Ulbricht, E., Kourtesis, I., Kuhrt, H., Hausen, H., Bartolomaeus, T., Reichenbach, A., & Bleidorn, C. (2017). Early evolution of radial glial cells in Bilateria. *Proceedings of the Royal Society B: Biological Sciences*, *284*(1859).

Hilbert, Z. A., & Kim, D. H. (2017). Sexually dimorphic control of gene expression in sensory neurons regulates decision-making behavior in *C. elegans*. *ELife*, *6*.

Hindley, C., Ali, F., McDowell, G., Cheng, K., Jones, A., Guillemot, F., & Philpott, A. (2012). Post-translational modification of Ngn2 differentially affects transcription of distinct targets to regulate the balance between progenitor maintenance and differentiation. *Development*, *139*(10), 1718–1723.

Hirata, H., Yoshiura, S., Ohtsuka, T., Bessho, Y., Harada, T., Yoshikawa, K., & Kageyama, R. (2002). Oscillatory expression of the BHLH factor Hes1 regulated by a negative feedback loop. *Science*, *298*(5594), 840–843.

Hirschhorn, J. N., Brown, S. A., Clark, C. D., & Winston, F. (1992). Evidence that SNF2/SWI2 and SNF5 activate transcription in yeast by altering chromatin structure. *Genes & Development*, *6*(12A), 2288–2298.

His, W. (1889). *Die neuroblasten und deren entstehung im embryonalen mark* (15th ed.). Bandes der Abhandlungen der mathematisch-physischen Classe der Königl. Sächische Gesellschafl der Wissenschaften.

Hobert, O. (2008). Regulatory logic of neuronal diversity: Terminal selector genes and selector motifs. *Proceedings of the National Academy of Sciences*, *105*(51), 20067–20071.

Hobert, O. (2011). Regulation of Terminal Differentiation Programs in the Nervous System. *Annu. Rev. Cell Dev. Biol*, *27*, 681–696.

Hobert, O. (2016). Terminal Selectors of Neuronal Identity. In *Current Topics in Developmental Biology* (Vol. 116, pp. 455–475).

Hodgkin, J. (1987). A genetic analysis of the sex-determining gene, tra-1, in the nematode *Caenorhabditis elegans*. *Genes & Development*, *1*(7), 731–745.

Hodgkin, J. (1988). *Sexual Dimorphism and Sex Determination*. *240*(4858), 243–279.

Hodgkin, J., Horvitz, H. R., & Brenner, S. (1979). Nondisjunction Mutants of the Nematode *Caenorhabditis elegans*. *Genetics*, *91*(1), 67–94.

Holliday, R., & Pugh, J. E. (1975). DNA modification mechanisms and gene activity during development. *Science*, *187*(4173), 226–232.

Hong, H., Takahashi, K., Ichisaka, T., Aoi, T., Kanagawa, O., Nakagawa, M., Okita, K., & Yamanaka, S. (2009). Suppression of induced pluripotent stem cell generation by the p53-p21 pathway. *Nature*, *460*(7259), 1132–1135.

Hong, Y., Roy, R., & Ambros, V. (1998). Developmental regulation of a cyclin-dependent kinase inhibitor controls postembryonic cell cycle progression in *Caenorhabditis elegans*. *Development*, *125*(18), 3585–3597.

Horton, S., Meredith, A., Richardson, J. A., & Johnson, J. E. (1999). *Correct Coordination of Neuronal Differentiation Events in Ventral Forebrain Requires the bHLH Factor MASH1*. *4–5*, 355–369.

Housset, M., Samuel, A., Ettaiche, M., Bemelmans, A., Beby, F., Billon, N., & Lamonerie, T. (2013). Loss of Otx2 in the Adult Retina Disrupts Retinal Pigment Epithelium Function, Causing Photoreceptor Degeneration. *Journal of Neuroscience*, *33*(24), 9890–9904.

Hufnagel, R. B., Riesenberg, A. N., Quinn, M., Brzezinski, J. A., Glaser, T., & Brown, N. L. (2013). Heterochronic misexpression of Ascl1 in the Atoh7 retinal cell lineage blocks cell cycle exit. *Molecular and Cellular Neuroscience*, *54*, 108–120.

Hydbring, P., Malumbres, M., & Sicinski, P. (2016). Non-canonical functions of cell cycle cyclins and cyclin-dependent kinases. *Nature Reviews. Molecular Cell Biology*, *17*(5), 280–292.

Ikawa, T., Masuda, K., Endo, T. A., Endo, M., Isono, K., Koseki, Y., Nakagawa, R., Kometani, K., Takano, J., Agata, Y., Katsura, Y., Kurosaki, T., Vidal, M., Koseki, H., & Kawamoto, H. (2016). Conversion of T cells to B cells by inactivation of polycomb-mediated epigenetic suppression of the B-lineage program. *Genes & Development*, *30*(22), 2475–2485.

Imayoshi, I., Sakamoto, M., Yamaguchi, M., Mori, K., & Kageyama, R. (2010). Essential roles of Notch signaling in maintenance of neural stem cells in developing and adult brains. *Journal of Neuroscience*, *30*(9), 3489–3498.

Iso, T., Kedes, L., & Hamamori, Y. (2003). HES and HERP families: Multiple

effectors of the notch signaling pathway. *Journal of Cellular Physiology*, *194*(3), 237–255.

James, M. K., Ray, A., Leznova, D., & Blain, S. W. (2008). Differential modification of p27Kip1 controls its cyclin D-cdk4 inhibitory activity. *Molecular and Cellular Biology*, *28*(1), 498–510.

Jan, Y. N., & Jan, L. Y. (1994). Genetic Control of Cell Fate Specification in *Drosophila* Peripheral Nervous System. *Annual Review of Genetics*, *28*(1), 373–393.

Jarrell, T. A., Wang, Y., Bloniarz, A. E., Brittin, C. A., Xu, M., Thomson, J. N., Albertson, D. G., Hall, D. H., & Emmons, S. W. (2012). The Connectome of a Decision-Making Neural Network. *Science*, *337*(6093).

Jarriault, S., Schwab, Y., & Greenwald, I. (2008). A *Caenorhabditis elegans* model for epithelial-neuronal transdifferentiation. *Proceedings of the National Academy of Sciences of the United States of America*, *105*(10), 3790–3795.

Jeffrey, P. D., Russo, A. A., Polyak, K., Gibbs, E., Hurwitz, J., Massagué, J., & Pavletich, N. P. (1995). Mechanism of CDK activation revealed by the structure of a cyclinA-CDK2 complex. *Nature*, *376*(6538), 313–320.

Jeffrey, P. D., Tong, L., & Pavletich, N. P. (2000). Structural basis of inhibition of CDK-cyclin complexes by INK4 inhibitors. *Genes and Development*, *14*(24), 3115–3125.

Jessen, K. R., Mirsky, R., & Burnett, Allison, L. (1973). *Biology of Hydra* (1st ed., Vol. 56, Issue 14). Academic Press, New York.

Jiménez, F., & Modolell, J. (1993). Neural fate specification in *Drosophila*. *Current Opinion in Genetics & Development*, *3*(4), 626–632.

Johnson, A. D., Fitzsimmons, D., Hagman, J., & Chamberlin, H. M. (2001). EGL-38 Pax regulates the ovo-related gene lin-48 during *Caenorhabditis elegans* organ development. *Development*, *128*(15).

Johnson, R. T., & Rao, P. N. (1970). Mammalian cell fusion: Induction of premature chromosome condensation in interphase nuclei. *Nature*, *226*(5247), 717–722.

Jorgensen, E. M., & Mango, S. E. (2002). The art and design of genetic screens: *Caenorhabditis elegans*. *Nature Reviews. Genetics*, *3*(5), 356–369.

Kafatos, F. C. (1968). The labial gland: a salt secreting organ of saturniid moths. *Journal of Experimental Biology*, *48*, 435–453.

Kafatos, F. C., & Williams, C. M. (1964). Enzymatic Mechanism for the Escape of Certain Moths from Their Cocoons. *Science*, *146*(3643), 538–540.

Kafatos, F. C., & Williams, C. M. (1968). Cytodifferentiation during Insect Metamorphosis: The Galea of Silkmoths. *Science*, *161*(3643), 470–472.

Kagias, K., Ahier, A., Fischer, N., & Jarriault, S. (2012). Members of the NODE (Nanog and Oct4-associated deacetylase) complex and SOX-2 promote the initiation of a natural cellular reprogramming event in vivo. *Proceedings of the National Academy of Sciences of the United States of America*, *109*(17), 6596–6601.

Kaldis, P., Sutton, A., & Solomon, M. J. (1996). The Cdk-activating kinase (CAK) from budding yeast. *Cell*, *86*(4), 553–564.

Kato, J. Y., Matsuoka, M., Strom, D. K., & Sherr, C. J. (1994). Regulation of cyclin D-dependent kinase 4 (cdk4) by cdk4-activating kinase. *Molecular and Cellular Biology*, *14*(4), 2713–2721.

Kawamura, T., Suzuki, J., Wang, Y. V., Menendez, S., Morera, L. B., Raya, A., Wahl, G. M., & Belmonte, J. C. I. (2009). Linking the p53 tumour suppressor pathway to somatic cell reprogramming. *Nature*, *460*(7259), 1140–1144.

Kempermann, G., Jessberger, S., Steiner, B., & Kronenberg, G. (2004). Milestones of neuronal development in the adult hippocampus. *Trends in Neurosciences*, *27*(8), 447–452.

Kikuchi, K., Holdway, J. E., Werdich, A. A., Anderson, R. M., Fang, Y., Egnaczyk, G. F., Evans, T., MacRae, C. A., Stainier, D. Y. R., & Poss, K. D. (2010). Primary contribution to zebrafish heart regeneration by gata4 + cardiomyocytes. *Nature*, *464*(7288), 601–605.

King, T. J., & Briggs, R. (1956). Serial Transplantation of Embryonic Nuclei. *Cold Spring Harbor Symposia on Quantitative Biology*, *21*(0), 271–290.

Kingston, R. E., & Narlikar, G. J. (1999). ATP-dependent remodeling and acetylation as regulators of chromatin fluidity. In *Genes and Development* (Vol. 13, Issue 18, pp. 2339–2352).

Kishimoto, N., Shimizu, K., & Sawamoto, K. (2012). Neuronal regeneration in a zebrafish model of adult brain injury. *Disease Models & Mechanisms*, *5*(2), 200–209.

Kitzmann, M., Vandromme, M., Schaeffer, V., Carnac, G., Labbé, J. C., Lamb, N., & Fernandez, A. (1999). cdk1- and cdk2-mediated phosphorylation of MyoD Ser200 in growing C2 myoblasts: role in modulating MyoD half-life and myogenic activity. *Molecular and Cellular Biology*, *19*(4), 3167–3176.

Knudsen, E. S., & Witkiewicz, A. K. (2017). The Strange Case of CDK4/6 Inhibitors: Mechanisms, Resistance, and Combination Strategies. In *Trends in Cancer* (Vol. 3, Issue 1, pp. 39–55). Cell Press.

Koch, R., Van Luenen, H. G. A. M., Van Der Horst, M., Thijssen, K. L., & Plasterk, R. H. A. (2000). Single nucleotide polymorphisms in wild isolates of *Caenorhabditis elegans*. *Genome Research*, *10*(11), 1690–1696.

Koche, R. P., Smith, Z. D., Adli, M., Gu, H., Ku, M., Gnirke, A., Bernstein, B. E., & Meissner, A. (2011). Reprogramming factor expression initiates widespread targeted chromatin remodeling. *Cell Stem Cell*, *8*(1), 96–105.

Koizumi, O., & Bode, H. R. (1986). Plasticity in the nervous system of adult hydra: I. The position-dependent expression of FMRFamide-like immunoreactivity. *Developmental Biology*, *116*(2), 407–421.

Kolundzic, E., Ofenbauer, A., Bulut, S. I., Uyar, B., Baytek, G., Sommermeier, A., Seelk, S., He, M., Hirsekorn, A., Vucicevic, D., Akalin, A., Diecke, S., Lacadie, S. A., & Tursun, B. (2018). FACT Sets a Barrier for Cell Fate Reprogramming in *Caenorhabditis elegans* and Human Cells. *Developmental Cell*, *46*(5), 611-626.e12.

Kornev, A. P., Haste, N. M., Taylor, S. S., & Ten Eyck, L. F. (2006). Surface comparison of active and inactive protein kinases identifies a conserved activation mechanism. *Proceedings of the National Academy of Sciences*, *103*(47), 17783–17788.

Korzelius, J., The, I., Ruijtenberg, S., Portegijs, V., Xu, H., Horvitz, H. R., & van den Heuvel, S. (2011). *C. elegans* MCM-4 is a general DNA replication and checkpoint component with an epidermis-specific requirement for growth and viability. *Developmental Biology*, *350*(2), 358–369.

Kragl, M., Knapp, D., Nacu, E., Khattak, S., Maden, M., Epperlein, H. H., & Tanaka, E. M. (2009). Cells keep a memory of their tissue origin during axolotl limb regeneration. *Nature*, *460*(7251), 60–65.

Kratsios, P., Stolfi, A., Levine, M., & Hobert, O. (2012). Coordinated regulation of cholinergic motor neuron traits through a conserved terminal selector gene. *Nature Neuroscience*, *15*(2), 205–214.

Kriegstein, A., & Alvarez-Buylla, A. (2009). The Glial Nature of Embryonic and Adult Neural Stem Cells. *Annual Review of Neuroscience*, *32*(1), 149–184.

Kroehne, V., Freudenreich, D., Hans, S., Kaslin, J., & Brand, M. (2011). Regeneration of the adult zebrafish brain from neurogenic radial glia-type progenitors. *Development*, *138*(22), 4831–4841.

Kruesi, W. S., Core, L. J., Waters, C. T., Lis, J. T., & Meyer, B. J. (2013). Condensin controls recruitment of RNA polymerase II to achieve nematode X-chromosome dosage compensation. *ELife*, *2*, e00808.

Kubota, S. (2011). Repeating rejuvenation in *Turritopsis*, an immortal hydrozoan (Cnidaria, Hydrozoa). *Biogeography*, *13*, 101–103.

Lacomme, M., Liaubet, L., Pituello, F., & Bel-Vialar, S. (2012). NEUROG2 drives cell cycle exit of neuronal precursors by specifically repressing a subset of cyclins acting at the G1 and S phases of the cell cycle. *Molecular and Cellular Biology*, *32*(13), 2596–2607.

Laguna, A., Schintu, N., Nobre, A., Alvarsson, A., Volakakis, N., Jacobsen, J. K., Gómez-Galán, M., Sopova, E., Joodmardi, E., Yoshitake, T., Deng, Q., Kehr, J., Ericson, J., Svenningsson, P., Shupliakov, O., & Perlmann, T. (2015). Dopaminergic control of autophagic-lysosomal function implicates Lmx1b in Parkinson's disease. *Nature Neuroscience*, *18*(6), 826–835.

Lane, M. E., Sauer, K., Wallace, K., Jan, Y. N., Lehner, C. F., & Vaessin, H. (1996). Dacapo, a cyclin-dependent kinase inhibitor, stops cell proliferation during *Drosophila* development. *Cell*, *87*(7), 1225–1235.

Lange, C., Huttner, W. B., & Calegari, F. (2009). Cdk4/CyclinD1 Overexpression in Neural Stem Cells Shortens G1, Delays Neurogenesis, and Promotes the Generation and Expansion of Basal Progenitors. *Cell Stem Cell*, *5*(3), 320–331.

Lau, A. C., & Csankovszki, G. (2015). Balancing up and downregulation of the *C. elegans* X chromosomes. *Current Opinion in Genetics & Development*, *31*, 50–56.

Lee, J. H., Protze, S. I., Laksman, Z., Backx, P. H., & Keller, G. M. (2017). Human Pluripotent Stem Cell-Derived Atrial and Ventricular Cardiomyocytes Develop from Distinct Mesoderm Populations. *Cell Stem Cell*, *21*(2), 179-194.e4.

Lee, M. G., & Nurse, P. (1987). Complementation used to clone a human

homologue of the fission yeast cell cycle control gene cdc2. *Nature*, *327*(6117), 31–35.

Lee, & Orr-Weaver, T. (2003). Regulation of Cell Cycles in *Drosophila* Development: Intrinsic and Extrinsic Cues. *Annual Review of Genetics*, *37*(1), 545–578.

Lee, R. C., Feinbaum, R. L., & Ambros, V. (1993). The *C. elegans* heterochronic gene lin-4 encodes small RNAs with antisense complementarity to lin-14. *Cell*, *75*(5), 843–854.

Lees, A. D., & Waddington, C. H. (1942). The Development of the Bristles in Normal and some Mutant Types of *Drosophila melanogaster*. *Proceedings of the Royal Society B: Biological Sciences*, *131*(862), 87–110.

Lemons, J. M. S., Feng, X.-J., Bennett, B. D., Legesse-Miller, A., Johnson, E. L., Raitman, I., Pollina, E. A., Rabitz, H. A., Rabinowitz, J. D., & Coller, H. A. (2010). Quiescent Fibroblasts Exhibit High Metabolic Activity. *PLoS Biology*, *8*(10), e1000514.

Leung, B., Hermann, G. J., & Priess, J. R. (1999). Organogenesis of the *Caenorhabditis elegans* intestine. *Developmental Biology*, *216*(1), 114–134.

Levitt, P., Cooper, M. L., & Rakic, P. (1981). Coexistence of neuronal and glial precursor cells in the cerebral ventricular zone of the fetal monkey: An ultrastructural immunoperoxidase analysis. *Journal of Neuroscience*, *1*(1), 27–39.

Lewis, J. A., & Hodgkin, J. A. (1977). Specific neuroanatomical changes in chemosensory mutants of the nematode *Caenorhabditis elegans*. *Journal of Comparative Neurology*, *172*(3), 489–510.

Li, Barbash, O., & Diehl, J. A. (2015). Regulation of the Cell Cycle. In *The Molecular Basis of Cancer* (pp. 165-178.e2). Content Repository Only!

Li, H., Collado, M., Villasante, A., Strati, K., Ortega, S., Cañamero, M., Blasco, M. A., & Serrano, M. (2009). The Ink4/Arf locus is a barrier for iPS cell reprogramming. *Nature*, *460*(7259), 1136–1139.

Li, W., Nakanishi, M., Zumsteg, A., Shear, M., Wright, C., Melton, D. A., & Zhou, Q. (2014). In vivo reprogramming of pancreatic acinar cells to three islet endocrine subtypes. *ELife*, *3*, e01846.

Liang, G., & Zhang, Y. (2013). Embryonic stem cell and induced pluripotent stem cell: an epigenetic perspective. *Cell Research*, *23*(1), 49–69.

Lim, S., Bhinge, A., Bragado Alonso, S., Aksoy, I., Aprea, J., Cheok, C. F., Calegari, F., Stanton, L. W., & Kaldis, P. (2017). Cyclin-Dependent Kinase-Dependent Phosphorylation of Sox2 at Serine 39 Regulates Neurogenesis. *Molecular and Cellular Biology*, *37*(16), e00201-17.

Lim, S., & Kaldis, P. (2012). Loss of Cdk2 and Cdk4 induces a switch from proliferation to differentiation in neural stem cells. *Stem Cells*, *30*(7), 1509–1520.

Lin, C. Y., Lovén, J., Rahl, P. B., Paranal, R. M., Burge, C. B., Bradner, J. E., Lee, T. I., & Young, R. A. (2012). Transcriptional amplification in tumor cells with elevated c-Myc. *Cell*, *151*(1), 56–67.

Lipton, J., Kleemann, G., Ghosh, R., Lints, R., & Emmons, S. W. (2004). Mate Searching in *Caenorhabditis elegans*: A Genetic Model for Sex Drive in a Simple Invertebrate. *Journal of Neuroscience*, *24*(34), 7427–7434.

Liu, K. S., & Sternberg, P. W. (1995). Sensory Regulation of Male Mating Behavior in *Caenorhabditis elegans*. In *Neuron* (Vol. 14).

Lorson, M. A., Horvitz, H. R., & Van Den Heuvel, S. (2000). LIN-5 is a novel component of the spindle apparatus required for chromosome segregation and cleavage plane specification in *Caenorhabditis elegans*. *Journal of Cell Biology*, *148*(1), 73–86.

Lowell, R. D., & Burnett, A. L. (1969). Regeneration of Complete Hydra from Isolated Epidermal Explants. In *Source: Biological Bulletin* (Vol. 137, Issue 2).

Lu, X., & Horvitz, H. R. (1998). *lin-35* and *lin-53*, Two Genes that Antagonize a *C. elegans* Ras Pathway, Encode Proteins Similar to Rb and Its Binding Protein RbAp48. *Cell*, *95*(7), 981–991.

Luger, K., Mäder, A. W., Richmond, R. K., Sargent, D. F., & Richmond, T. J. (1997). Crystal structure of the nucleosome core particle at 2.8 Å resolution. *Nature*, *389*(6648), 251–260.

Lugert, S., Basak, O., Knuckles, P., Haussler, U., Fabel, K., Götz, M., Haas, C. A., Kempermann, G., Taylor, V., & Giachino, C. (2010). Quiescent and active hippocampal neural stem cells with distinct morphologies respond selectively to physiological and pathological stimuli and aging. *Cell Stem Cell*, *6*(5), 445–456.

Madhavan, M., Haynes, T. L., Frisch, N. C., Call, M. K., Minich, C. M., Tsonis, P. A., & Del Rio-Tsonis, K. (2006). The role of Pax-6 in lens regeneration. *Proceedings of the National Academy of Sciences of the*

United States of America, *103*(40), 14848–14853.

Magnaghi-Jaulin, L., Groisman, R., Naguibneva, I., Robin, P., Lorain, S., Le Villain, J. P., Troalen, F., Trouche, D., & Harel-Bellan, A. (1998). Retinoblastoma protein represses transcription by recruiting a histone deacetylase. *Nature*, *391*(6667), 601–605.

Malatesta, P., Hartfuss, E., & Götz, M. (2000). Isolation of radial glial cells by fluorescent-activated cell sorting reveals a neuronal lineage. *Development*, *127*(24), 5253–5263.

Malumbres, M. (2014). Cyclin-dependent kinases. *Genome Biology*, *15*(6), 122.

Marro, S., Pang, Z. P., Yang, N., Tsai, M.-C. C., Qu, K., Chang, H. Y., Südhof, T. C., Wernig, M., Sü, T. C., & Wernig, M. (2011). Direct lineage conversion of terminally differentiated hepatocytes to functional neurons. *Cell Stem Cell*, *9*(4), 374–382.

McLenachan, S., Menchón, C., Raya, A., Consiglio, A., & Edel, M. J. (2012). Cyclin A1 is essential for setting the pluripotent state and reducing tumorigenicity of induced pluripotent stem cells. *Stem Cells and Development*, *21*(15), 2891–2899.

Meharena, H. S., Chang, P., Keshwani, M. M., Oruganty, K., Nene, A. K., Kannan, N., Taylor, S. S., & Kornev, A. P. (2013). Deciphering the Structural Basis of Eukaryotic Protein Kinase Regulation. *PLoS Biology*, *11*(10), e1001680.

Meister, P., Towbin, B. D., Pike, B. L., Ponti, A., & Gasser, S. M. (2010). The spatial dynamics of tissue-specific promoters during *C. elegans* development. *Genes and Development*, *24*(8), 766–782.

Mello, C., & Fire, A. (1995). Chapter 19 DNA Transformation. *Methods in Cell Biology*, *48*, 451–482.

Mello, C., Kramer, J., Stinchcomb, D., & Ambros, V. (1991). Efficient gene transfer in *C.elegans*: extrachromosomal maintenance and integration of transforming sequences. *The EMBO Journal*, *10*(1), 3959–3970.

Meyer, B. J. (2005). X-Chromosome dosage compensation. *WormBook*.

Minevich, G., Park, D. S., Blankenberg, D., Poole, R. J., & Hobert, O. (2012). CloudMap: a cloud-based pipeline for analysis of mutant genome sequences. *Genetics*, *192*(4), 1249–1269.

Mitsui, K., Tokuzawa, Y., Itoh, H., Segawa, K., Murakami, M., Takahashi, K., Maruyama, M., Maeda, M., & Yamanaka, S. (2003). The homeoprotein Nanog is required for maintenance of pluripotency in mouse epiblast and ES cells. *Cell*, *113*(5), 631–642.

Morgan, D. O. (2007). The Cell Cycle: Principles of Control. In *New Science Press*.

Morgan, T. H. (1900). Regeneration in teleosts. *Archiv Fur Entwicklungsmechanik Der Organismen*, *10*(1), 120–134.

Morgan, T. H. (1901). Regeneration in the egg, embryo, and adult. *The American Naturalist*, *35*(420), 949–973.

Morgan, T. H., Hendee, J. R., Muller, T. J., & Bridges, C. B. (1915). *The Mechanism of Mendelian Heredity*. Henry Holt and Company.

Mori, I., & Ohshima, Y. (1995). Neural regulation of thermotaxis in *Caenorhabditis elegans*. *Nature*, *376*(6538), 344–348.

Moss, E. G., Lee, R. C., & Ambros, V. (1997). The cold shock domain protein LIN-28 controls developmental timing in *C. elegans* and is regulated by the lin-4 RNA. *Cell*, *88*(5), 637–646.

Mukherjee, P., Winter, S. L., & Alexandrow, M. G. (2010). Cell Cycle Arrest by Transforming Growth Factor 1 near G1/S Is Mediated by Acute Abrogation of Prereplication Complex Activation Involving an Rb-MCM Interaction. *Molecular and Cellular Biology*, *30*(3), 845–856.

Müller, P., Yanze, N., Schmid, V., & Spring, J. (1999). The homeobox gene Otx of the jellyfish Podocoryne carnea: Role of a head gene in striated muscle and evolution. *Developmental Biology*, *216*(2), 582–594.

Muneoka, K., Fox, W. F., & Bryant, S. V. (1986). Cellular contribution from dermis and cartilage to the regenerating limb blastema in axolotls. *Developmental Biology*, *116*(1), 256–260.

Murre, C., McCaw, P. S., & Baltimore, D. (1989). A new DNA binding and dimerization motif in immunoglobulin enhancer binding, daughterless, MyoD, and myc proteins. *Cell*, *56*(5), 777–783.

Nagel, G., Szellas, T., Kateriya, S., Adeishvili, N., Hegemann, P., & Bamberg, E. (2005). Channelrhodopsins: directly light-gated cation channels. *Biochemical Society Transactions*, *33*(Pt 4), 863–866.

Nakagawa, M., Koyanagi, M., Tanabe, K., Takahashi, K., Ichisaka, T., Aoi,

T., Okita, K., Mochiduki, Y., Takizawa, N., & Yamanaka, S. (2008). Generation of induced pluripotent stem cells without Myc from mouse and human fibroblasts. *Nature Biotechnology*, *26*(1), 101–106.

Nallamshetty, S., Crook, M., Boehm, M., Yoshimoto, T., Olive, M., & Nabel, E. G. (2005). The cell cycle regulator p27Kip1 interacts with MCM7, a DNA replication licensing factor, to inhibit initiation of DNA replication. *FEBS Letters*, *579*(29), 6529–6536.

Ng, S. Y., Wong, C. K., & Tsang, S. Y. (2010). Differential gene expressions in atrial and ventricular myocytes: insights into the road of applying embryonic stem cell-derived cardiomyocytes for future therapies. *American Journal of Physiology-Cell Physiology*, *299*(6), C1234–C1249.

Nguyen, L., Besson, A., Heng, J. I. T., Schuurmans, C., Teboul, L., Parras, C., Philpott, A., Roberts, J. M., & Guillemot, F. (2006). p27kip1 independently promotes neuronal differentiation and migration in the cerebral cortex. *Genes & Development*, *20*(11), 1511–1524.

Niu, W., Zang, T., Smith, D. K., Vue, T. Y., Zou, Y., Bachoo, R., Johnson, J. E., & Zhang, C. L. (2015). SOX2 reprograms resident astrocytes into neural progenitors in the adult brain. *Stem Cell Reports*, *4*(5), 780–794.

Noctor, S. C., Martínez-Cerdeño, V., Ivic, L., & Kriegstein, A. R. (2004). Cortical neurons arise in symmetric and asymmetric division zones and migrate through specific phases. *Nature Neuroscience*, *7*(2).

Nutt, S. L., Heavey, B., Rolink, A. G., & Busslinger, M. (1999). Commitment to the B-lymphoid lineage depends on the transcription factor Pax5. *Nature*, *401*(6753), 556–562.

O'Farrell, P. H. (2015). Growing an Embryo from a Single Cell: A Hurdle in Animal Life. *Cold Spring Harbor Perspectives in Biology*, *7*(11), a019042.

Obernier, K., Cebrian-Silla, A., Thomson, M., Parraguez, J. I., Anderson, R., Guinto, C., Rodas Rodriguez, J., Garcia-Verdugo, J.-M., & Alvarez-Buylla, A. (2018). Adult Neurogenesis Is Sustained by Symmetric Self-Renewal and Differentiation. *Cell Stem Cell*, *22*(2), 221-234.e8.

Oesterle, E. C., Chien, W. M., Campbell, S., Nellimarla, P., & Fero, M. L. (2011). p27Kip1 is required to maintain proliferative quiescence in the adult cochlea and pituitary. *Cell Cycle*, *10*(8), 1237–1248.

Oikonomou, C., & Cross, F. R. (2011). Rising cyclin-CDK levels order cell cycle events. *PLoS ONE*, *6*(6).

Oikonomou, G., & Shaham, S. (2011). The glia of *Caenorhabditis elegans*. *Glia*, *59*(9), 1253–1263.

Okumura-Nakanishi, S., Saito, M., Niwa, H., & Ishikawa, F. (2005). Oct-3/4 and Sox2 regulate Oct-3/4 gene in embryonic stem cells. *The Journal of Biological Chemistry*, *280*(7), 5307–5317.

Olanich, M. E., Sun, W., Hewitt, S. M., Abdullaev, Z., Pack, S. D., & Barr, F. G. (2015). CDK4 amplification reduces sensitivity to CDK4/6 inhibition in fusion-positive rhabdomyosarcoma. *Clinical Cancer Research*, *21*(21), 4947–4959.

Oren-Suissa, M., Bayer, E. A., & Hobert, O. (2016). Sex-specific pruning of neuronal synapses in *Caenorhabditis elegans*. *Nature*, *533*(7602), 206–211.

Orphanides, G., LeRoy, G., Chang, C.-H., Luse, D. S., & Reinberg, D. (1998). FACT, a Factor that Facilitates Transcript Elongation through Nucleosomes. *Cell*, *92*(1), 105–116.

Otsuki, L., & Brand, A. H. (2018). Cell cycle heterogeneity directs the timing of neural stem cell activation from quiescence. *Science*, *360*(6384), 99–102.

Ouyang, J., Yu, W., Liu, J., Zhang, N., Florens, L., Chen, J., Liu, H., Washburn, M., Pei, D., & Xie, T. (2015). Cyclin-dependent kinase-mediated Sox2 phosphorylation enhances the ability of Sox2 to establish the pluripotent state. *The Journal of Biological Chemistry*, *290*(37), 22782–22794.

Pandey, K., An, H., Kim, S. K., Lee, S. A., Kim, S., Lim, S. M., Kim, G. M., Sohn, J., & Moon, Y. W. (2019). Molecular mechanisms of resistance to CDK4/6 inhibitors in breast cancer: A review. *International Journal of Cancer*, *145*(5), 1179–1188.

Papanayotou, C., Mey, A., Birot, A. M., Saka, Y., Boast, S., Smith, J. C., Samarut, J., & Stern, C. D. (2008). A mechanism regulating the onset of Sox2 expression in the embryonic neural plate. *PLoS Biology*, *6*(1), 0109–0123.

Park, D. S., Morris, E. J., Padmanabhan, J., Shelanski, M. L., Geller, H. M., & Greene, L. A. (1998). Cyclin-dependent kinases participate in death of neurons evoked by DNA-damaging agents. *The Journal of Cell Biology*, *143*(2), 457–467.

Park, & Krause, M. (1999). Regulation of post-embryonic G1 cell cycle progression by a cyclin D/cyclin dependent kinase-like complex in

C. elegans. *Development*, *126*, 4849–4860.

Park, S. H., Park, S. H., Kook, M. C., Kim, E. Y., Park, S., & Lim, J. H. (2004). Ultrastructure of human embryonic stem cells and spontaneous and retinoic acid-induced differentiating cells. *Ultrastructural Pathology*, *28*(4), 229–238.

Parnavelas, J. G. (1999). Glial Cell Lineages in the Rat Cerebral Cortex. *Experimental Neurology*, *156*(2), 418–429.

Pasque, V., Gillich, A., Garrett, N., & Gurdon, J. B. (2011). Histone variant macroH2A confers resistance to nuclear reprogramming. *The EMBO Journal*, *30*, 2373–2387.

Pasque, V., Radzisheuskaya, A., Gillich, A., Halley-Stott, R. P., Panamarova, M., Zernicka-Goetz, M., Surani, M. A., & Silva, J. C. R. (2012). Histone variant macroH2A marks embryonic differentiation in vivo and acts as an epigenetic barrier to induced pluripotency. *Journal of Cell Science*, *125*(Pt 24), 6094–6104.

Patel, T., & Hobert, O. (2017). Coordinated control of terminal differentiation and restriction of cellular plasticity. *ELife*, *6*.

Pawlak, M., & Jaenisch, R. (2011). De novo DNA methylation by Dnmt3a and Dnmt3b is dispensable for nuclear reprogramming of somatic cells to a pluripotent state. *Genes & Development*, *25*(10), 1035–1040.

Pereira, L., Kratsios, P., Serrano-Saiz, E., Sheftel, H., Mayo, A. E., Hall, D. H., White, J. G., LeBoeuf, B., Garcia, L. R., Alon, U., & Hobert, O. (2015). A cellular and regulatory map of the cholinergic nervous system of *C. elegans*. *ELife*, *4*.

Perkins, L. A., Hedgecock, E. M., Thomson, J. N., & Culotti, J. G. (1986). Mutant sensory cilia in the nematode *Caenorhabditis elegans*. *Developmental Biology*, *117*(2), 456–487.

Philippos, M., Sambasivan, R., Castel, D., Rocheteau, P., Bizzarro, V., & Tajbakhsh, S. (2012). A critical requirement for notch signaling in maintenance of the quiescent skeletal muscle stem cell state. *Stem Cells*, *30*(2), 243–252.

Pilz, G. A., Bottes, S., Betizeau, M., Jörg, D. J., Carta, S., Simons, B. D., Helmchen, F., & Jessberger, S. (2018). Live imaging of neurogenesis in the adult mouse hippocampus. *Science*, *359*(6376), 658–662.

Piraino, S., Boero, F., Aeschbach, B., & Schmid, V. (1996). Reversing the life

cycle: Medusae transforming into polyps and cell transdifferentiation in *Turritopsis nutricula* (Cnidaria, Hydrozoa). *Biological Bulletin*, *190*(3), 302–312.

Polach, K. J., & Widom, J. (1996). A Model for the Cooperative Binding of Eukaryotic Regulatory Proteins to Nucleosomal Target Sites. *Journal of Molecular Biology*, *258*(5), 800–812.

Poss, K. D., Wilson, L. G., & Keating, M. T. (2002). Heart regeneration in zebrafish. *Science (New York, N.Y.)*, *298*(5601), 2188–2190.

Priess, J., & Nichol Thomson, J. (1987). Cellular Interactions in Early *C. elegans* Embryos. *Cell*, *48*(0), 241–250.

Rakic, P. (1972). Mode of cell migration to the superficial layers of fetal monkey neocortex. *The Journal of Comparative Neurology*, *145*(1), 61–83.

Rao, P. N., & Johnson, R. T. (1970). Mammalian cell fusion: Studies on the regulation of DNA synthesis and mitosis. *Nature*, *225*(5228), 159–164.

Ray, A., James, M. K., Larochelle, S., Fisher, R. P., & Blain, S. W. (2009). p27Kip1 inhibits cyclin D-cyclin-dependent kinase 4 by two independent modes. *Molecular and Cellular Biology*, *29*(4), 986–999.

Reed, M. F., Liu, V. F., Ladha, M. H., Ando, K., Griffin, J. D., Weaver, D. T., & Ewen, M. E. (1998). Enforced CDK4 expression in a hematopoietic cell line confers resistance to the G1 arrest induced by ionizing radiation. *Oncogene*, *17*(23), 2961–2971.

Reynaud, E. G., Leibovitch, M. P., Tintignac, L. A., Pelpel, K., Guillier, M., & Leibovitch, S. A. (2000). Stabilization of MyoD by direct binding to p57(Kip2). *The Journal of Biological Chemistry*, *275*(25), 18767–18776.

Richard, J. P., Zuryn, S., Fischer, N., Pavet, V., Vaucamps, N., Jarriault, S., & Jai Prakash Richard*, Steven Zuryn*, Nadine Fischer, Valeria Pavet, N. V. and S. J. (2011). Direct in vivo cellular reprogramming involves transition through discrete, non-pluripotent steps. *Development*, *138*(8).

Ring, K. L., Tong, L. M., Balestra, M. E., Javier, R., Andrews-Zwilling, Y., Li, G., Walker, D., Zhang, W. R., Kreitzer, A. C., & Huang, Y. (2012). Direct reprogramming of mouse and human fibroblasts into multipotent neural stem cells with a single factor. *Cell Stem Cell*, *11*(1), 100–109.

Rodda, D. J., Chew, J.-L., Lim, L.-H., Loh, Y.-H., Wang, B., Ng, H.-H., & Robson, P. (2005). Transcriptional regulation of Nanog by OCT4 and SOX2. *The Journal of Biological Chemistry*, *280*(26), 24731–24737.

Rogers, C. D., Harafuji, N., Archer, T., Cunningham, D. D., & Casey, E. S. (2009). Xenopus Sox3 activates sox2 and geminin and indirectly represses Xvent2 expression to induce neural progenitor formation at the expense of non-neural ectodermal derivatives. *Mechanisms of Development*, *126*(1–2), 42–55.

Ross, S. E., Greenberg, M. E., & Stiles, C. D. (2003). Basic helix-loop-helix factors in cortical development. In *Neuron* (Vol. 39, Issue 1, pp. 13–25). Cell Press.

Ruiz, S., Panopoulos, A. D., Herrerías, A., Bissig, K.-D., Lutz, M., Berggren, W. T., Verma, I. M., & Izpisua Belmonte, J. C. (2011). A high proliferation rate is required for cell reprogramming and maintenance of human embryonic stem cell identity. *Current Biology : CB*, *21*(1), 45–52.

Russo, A. A., Jeffrey, P. D., Patten, A. K., Massagué, J., & Pavletich, N. P. (1996). Crystal structure of the p27Kip1 cyclin-dependent-kinase inibitor bound to the cyclin A–Cdk2 complex. *Nature*, *382*(6589), 325–331.

Russo, A. A., Tong, L., Lee, J. O., Jeffrey, P. D., & Pavletich, N. P. (1998). Structural basis for inhibition of the cyclin-dependent kinase Cdk6 by the tumour suppressor p16(INK4a). *Nature*, *395*(6699), 237–243.

Ryan, D. A., Miller, R. M., Lee, K., Neal, S. J., Fagan, K. A., Sengupta, P., & Portman, D. S. (2014). Sex, age, and hunger regulate behavioral prioritization through dynamic modulation of chemoreceptor expression. *Current Biology : CB*, *24*(21), 2509–2517.

Saito, R. M., Perreault, A., Peach, B., Satterlee, J. S., & van den Heuvel, S. (2004). The CDC-14 phosphatase controls developmental cell-cycle arrest in *C. elegans*. *Nature Cell Biology*, *6*(8), 777–783.

Sammut, M., Cook, S. J., Nguyen, K. C. Q., Felton, T., Hall, D. H., Emmons, S. W., Poole, R. J., & Barrios, A. (2015). Glia-derived neurons are required for sex-specific learning in *C. elegans. Nature*, *526*(7573), 385–390.

Sarkar, A., & Hochedlinger, K. (2013). The sox family of transcription factors: versatile regulators of stem and progenitor cell fate. *Cell Stem Cell*, *12*(1), 15–30.

Satterlee, J. S., Sasakura, H., Kuhara, A., Berkeley, M., Mori, I., & Sengupta, P. (2001). Specification of Thermosensory Neuron Fate in *C. elegans* Requires *ttx-1*, a Homolog of otd/Otx. *Neuron*, *31*(6), 943–956.

Schachter, M. M., Merrick, K. A., Larochelle, S., Hirschi, A., Zhang, C.,

Shokat, K. M., Rubin, S. M., & Fisher, R. P. (2013). A Cdk7-Cdk4 T-Loop Phosphorylation Cascade Promotes G1 Progression. *Molecular Cell*, *50*(2), 250–260.

Schaper, A. A. (1897). The Earliest Differentiation in the Central Nervous System of Vertebrates. *Science*, *5*(115), 430–431.

Schettini, F., De Santo, I., Rea, C. G., De Placido, P., Formisano, L., Giuliano, M., Arpino, G., De Laurentiis, M., Puglisi, F., De Placido, S., & Del Mastro, L. (2018). CDK 4/6 Inhibitors as Single Agent in Advanced Solid Tumors. *Frontiers in Oncology*, *8*.

Schmid, V. (1992). Transdifferentiation in Medusae. *International Review of Cytology*, *142*(C), 213–261.

Schmidt, R., & Plath, K. (2012). The roles of the reprogramming factors Oct4, Sox2 and Klf4 in resetting the somatic cell epigenome during induced pluripotent stem cell generation. *Genome Biology*, *13*(10), 251.

Schneider, C. A., Rasband, W. S., & Eliceiri, K. W. (2012). NIH Image to ImageJ: 25 years of image analysis. *Nature Methods*, *9*(7), 671–675.

Schneuwly, S., Klemenz, R., & Gehring, W. J. (1987). Redesigning the body plan of *Drosophila* by ectopic expression of the homoeotic gene Antennapedia. *Nature*, *325*(6107), 816–818.

Schöler, H. R., Balling, R., Hatzopoulos, A. K., Suzuki, N., & Gruss, P. (1989). Octamer binding proteins confer transcriptional activity in early mouse embryogenesis. *The EMBO Journal*, *8*(9), 2551–2557.

Schubiger, G., & Hadorn, E. (1968). Auto- and allotypical differentiations of in vivo cultivated blastemas of the front leg of *Drosophila melanogaster*. *Developmental Biology*, *17*, 584–586.

Schuettengruber, B., Chourrout, D., Vervoort, M., Leblanc, B., & Cavalli, G. (2007). Genome Regulation by Polycomb and Trithorax Proteins. In *Cell* (Vol. 128, Issue 4, pp. 735–745).

Schulenburg, H., & Félix, M. A. (2017). The natural biotic environment of *Caenorhabditis elegans*. *Genetics*, *206*(1), 55–86.

Scott, M. P., Weiner, A. J., Hazelrigg, T. I., Polisky, B. A., Pirrotta, V., Scalenghe, F., & Kaufman, T. C. (1983). The molecular organization of the Antennapedia locus of *Drosophila*. *Cell*, *35*(3 Pt 2), 763–776.

Selman, K., & Kafatos, F. C. (1974). Transdifferentiation in the labial gland of

silk moths: is DNA required for cellular metamorphosis? *Cell Differentiation*, *3*(2), 81–94.

Seri, B., García-Verdugo, J. M., McEwen, B. S., & Alvarez-Buylla, A. (2001). Astrocytes give rise to new neurons in the adult mammalian hippocampus. *The Journal of Neuroscience : The Official Journal of the Society for Neuroscience*, *21*(18), 7153–7160.

Serra-Cardona, A., & Zhang, Z. (2018). Replication-Coupled Nucleosome Assembly in the Passage of Epigenetic Information and Cell Identity. In *Trends in Biochemical Sciences* (Vol. 43, Issue 2, pp. 136–148). Elsevier Ltd.

Serrano-Saiz, E., Oren-Suissa, M., Bayer, E. A., & Hobert, O. (2017). Sexually Dimorphic Differentiation of a *C. elegans* Hub Neuron Is Cell Autonomously Controlled by a Conserved Transcription Factor. *Current Biology : CB*, *27*(2), 199–209.

Serrano-Saiz, E., Pereira, L., Gendrel, M., Aghayeva, U., Battacharya, A., Howell, K., Garcia, L. R., & Hobert, O. (2017). A neurotransmitter atlas of the *Caenorhabditis elegans* male nervous system reveals sexually dimorphic neurotransmitter usage. *Genetics*, *206*(3), 1251–1269.

Shaham, S. (2005). Glia–Neuron Interactions in Nervous System Function and Development. In *Current topics in developmental biology* (Vol. 69, pp. 39–66).

Shaham, S. (2006). Glia–neuron interactions in the nervous system of *Caenorhabditis elegans*. *Current Opinion in Neurobiology*, *16*(5), 522–528.

Shaye, D. D., & Greenwald, I. (2011). OrthoList: a compendium of *C. elegans* genes with human orthologs. *PloS One*, *6*(5), e20085.

Sherr, C. J., & Roberts, J. M. (1999). CDK inhibitors: positive and negative regulators of G1-phase progression. *Genes & Development*, *13*(12), 1501–1512.

Siebert, S., Anton-Erxleben, F., & Bosch, T. C. G. (2008). Cell type complexity in the basal metazoan Hydra is maintained by both stem cell based mechanisms and transdifferentiation. *Developmental Biology*, *313*(1), 13–24.

Siegfried, K. R., Kidd, A. R., Chesney, M. A., Kimble, J., & Kimble, J. (2004). The *sys-1* and *sys-3* genes cooperate with Wnt signaling to establish the proximal-distal axis of the *Caenorhabditis elegans* gonad. *Genetics*, *166*(1), 171–186.

Sievers, F., & Higgins, D. (2018). Clustal Omega for making accurate alignments of many protein sequences. *Protein Science*, *27*(1), 135–145.

Snyder, M., Huang, X.-Y., & Zhang, J. J. (2009). The minichromosome maintenance proteins 2-7 (MCM2-7) are necessary for RNA polymerase II (Pol II)-mediated transcription. *The Journal of Biological Chemistry*, *284*(20), 13466–13472.

Song, A., Wang, Q., Goebl, M. G., & Harrington, M. A. (1998). Phosphorylation of nuclear MyoD is required for its rapid degradation. *Molecular and Cellular Biology*, *18*(9), 4994–4999.

Soufi, A., & Dalton, S. (2016). Cycling through developmental decisions: how cell cycle dynamics control pluripotency, differentiation and reprogramming. *Development*, *143*(23), 4301–4311.

Southall, T. D., & Brand, A. H. (2009). Neural stem cell transcriptional networks highlight genes essential for nervous system development. *The EMBO Journal*, *28*(24), 3799–3807.

Spallanzani, L. (1768). *Prodromo di un' opera da imprimersi sopra le riproduzioni animali*. Nella Stamperia di Giovanni Montanari.

Spemann, H., & Mangold, H. (1924). Über Induktion von Embryonalanlagen durch Implantation artfremder Organisatoren. *Archiv Für Mikroskopische Anatomie Und Entwicklungsmechanik*, *100: 599-638*.

Srinivasan, D. G., Fisk, R. M., Xu, H., & Van den Heuvel, S. (2003). A complex of LIN-5 and GPR proteins regulates G protein signaling and spindle function in *C. elegans*. *Genes and Development*, *17*(10), 1225–1239.

Starich, T. A., Herman, R. K., Kari, C. K., Yeh, W. H., Schackwitz, W. S., Schuyler, M. W., Collet, J., Thomas, J. H., & Riddle, D. L. (1995). Mutations affecting in chemosensory neurons of *Caenorhabditis elegans*. *Genetics*, *139*(1), 171–188.

Stefanakis, N., Carrera, I., & Hobert, O. (2015). Regulatory Logic of Pan-Neuronal Gene Expression in *C. elegans*. *Neuron*, *87*(4), 733–750.

Sterner, J. M., Dew-Knight, S., Musahl, C., Kornbluth, S., & Horowitz, J. M. (1998). Negative Regulation of DNA Replication by the Retinoblastoma Protein Is Mediated by Its Association with MCM7. *Molecular and Cellular Biology*, *18*(5), 2748–2757.

Steward, F. C., Mapes, M. O., & Mears, K. (1958). Growth and Organized

Development of Cultured Cells. II. Organization in Cultures Grown from Freely Suspended Cells. In *Source: American Journal of Botany* (Vol. 45, Issue 10).

Strahl, B. D., & Allis, C. D. (2000). The language of covalent histone modifications. *Nature*, *403*(6765), 41–45.

Strausfeld, N. J., & Hirth, F. (2016). Introduction to 'Homology and convergence in nervous system evolution.' *Philosophical Transactions of the Royal Society B: Biological Sciences*, *371*(1685).

Streit, A., Berliner, A. J., Papanayotou, C., Slrulnik, A., & Stern, C. D. (2000). Initiation of neural induction by FGF signalling before gastrulation. *Nature*, *406*(6791), 74–78.

Sueda, R., Imayoshi, I., Harima, Y., & Kageyama, R. (2019). High Hes1 expression and resultant Ascl1 suppression regulate quiescent vs. active neural stem cells in the adult mouse brain. *Genes and Development*, *33*(9–10), 511–523.

Sulston, J. E. (1983). Neuronal Cell Lineages in the Nematode *Caenorhabditis elegans*. *Cold Spring Harbor Symposia on Quantitative Biology*, *48*(0), 443–452.

Sulston, J. E., Albertson, D. G., & Thomson, J. N. (1980). The *Caenorhabditis elegans* male: Postembryonic development of nongonadal structures. *Developmental Biology*, *78*(2), 542–576.

Sulston, J. E., & Horvitz, H. R. (1977). Post-embryonic cell lineages of the nematode, *Caenorhabditis elegans*. *Developmental Biology*, *56*(1), 110–156.

Sulston, J. E., Schierenberg, E., White, J. G., & Thomson, J. N. (1983). The embryonic cell lineage of the nematode *Caenorhabditis elegans*. *Developmental Biology*, *100*(1), 64–119.

Sulston, J. E., & White, J. G. (1980). Regulation and cell autonomy during postembryonic development of *Caenorhabditis elegans*. *Developmental Biology*, *78*(2), 577–597.

Sun, A., Bagella, L., Tutton, S., Romano, G., & Giordano, A. (2007). From G0 to S phase: A view of the roles played by the retinoblastoma (Rb) family members in the Rb-E2F pathway. *Journal of Cellular Biochemistry*, *102*(6), 1400–1404.

Swaffer, M. P., Jones, A. W., Flynn, H. R., Snijders, A. P., & Nurse, P.

(2016). CDK Substrate Phosphorylation and Ordering the Cell Cycle. *Cell*, *167*(7), 1750-1761.e16.

Tada, M., Takahama, Y., Abe, K., Nakatsuji, N., & Tada, T. (2001). Nuclear reprogramming of somatic cells by in vitro hybridization with ES cells. *Current Biology : CB*, *11*(19), 1553–1558.

Takahashi, K., Tanabe, K., Ohnuki, M., Narita, M., Ichisaka, T., Tomoda, K., & Yamanaka, S. (2007). Induction of Pluripotent Stem Cells from Adult Human Fibroblasts by Defined Factors. *Cell*, *131*(5), 861–872.

Takahashi, K., & Yamanaka, S. (2006). Induction of Pluripotent Stem Cells from Mouse Embryonic and Adult Fibroblast Cultures by Defined Factors. *Cell*, *126*(4), 663–676.

Tapia, N., & Schöler, H. R. (2016). Molecular Obstacles to Clinical Translation of iPSCs. *Cell Stem Cell*, *19*(3), 298–309.

The, I., Ruijtenberg, S., Bouchet, B. P., Cristobal, A., Prinsen, M. B. W. W., Van Mourik, T., Koreth, J., Xu, H., Heck, A. J. R. R., Akhmanova, A., Cuppen, E., Boxem, M., Muñoz, J., & Van Den Heuvel, S. (2015). Rb and FZR1/Cdh1 determine CDK4/6-cyclin D requirement in *C. elegans* and human cancer cells. *Nature Communications*, *6*, 5906.

Thomson, M., Liu, S. J., Zou, L.-N., Smith, Z., Meissner, A., & Ramanathan, S. (2011). Pluripotency factors in embryonic stem cells regulate differentiation into germ layers. *Cell*, *145*(6), 875–889.

Tilmann, C., & Kimble, J. (2005). Cyclin D Regulation of a Sexually Dimorphic Asymmetric Cell Division. *Developmental Cell*, *9*(4), 489–499.

Tintignac, L. A., Leibovitch, M. P., Kitzmann, M., Fernandez, A., Ducommun, B., Meijer, L., & Leibovitch, S. A. (2000). Cyclin E–Cdk2 Phosphorylation Promotes Late G1-Phase Degradation of MyoD in Muscle Cells. *Experimental Cell Research*, *259*(1), 300–307.

Trembley, A. (1744). *Mémoires pour servir à l'histoire d'un genre de polypes d'eau douce, à bras en forme de cornes*. Chez Jean & Herman Verbeek,.

Trounson, A., & DeWitt, N. D. (2016). Pluripotent stem cells progressing to the clinic. *Nature Reviews Molecular Cell Biology*, *17*(3), 194–200.

Truman, J. W., & Ball, E. E. (1998). Patterns of embryonic neurogenesis in a primitive wingless insect, the silverfish, Ctenolepisma longicaudata: comparison with those seen in flying insects. *Development Genes and Evolution*, *208*(7), 357–368.

Tucker, M., Sieber, M., Morphew, M., & Han, M. (2005). The *Caenorhabditis elegans* aristaless orthologue, alr-1, is required for maintaining the functional and structural integrity of the amphid sensory organs. *Molecular Biology of the Cell*, *16*(10), 4695–4704.

Tursun, B., Patel, T., Kratsios, P., & Hobert, O. (2011). Direct conversion of *C. elegans* germ cells into specific neuron types. *Science*, *331*(6015), 304–308.

Uchida, O., Nakano, H., Koga, M., & Ohshima, Y. (2003). The *C. elegans* che-1 gene encodes a zinc finger transcription factor required for specification of the ASE chemosensory neurons. *Development*, *130*(7), 1215–1224.

Urbán, N., Van Den Berg, D. L. C., Forget, A., Andersen, J., Demmers, J. A. A., Hunt, C., Ayrault, O., & Guillemot, F. (2016). Return to Quiescence of mouse neural stem cells by degradation of a proactivation protein. *Science*, *353*(6296), 292–295.

Van Rijnberk, L. M., Van Der Horst, S. E. M., Van Den Heuvel, S., & Ruijtenberg, S. (2017). A dual transcriptional reporter and CDK-activity sensor marks cell cycle entry and progression in *C. elegans*. *PLoS ONE*, *12*(2).

Vasil, I. K., Hildebrandt, A. C., & Riker, A. J. (1964). Endive Plantlets from Freely Suspended Cells and Cell Groups Grown in vitro. *Science*, *146*(3640), 76–77.

Vasil, Indra K, & Vasil, V. (1972). Totipotency and embryogenesis in plant cell and tissue cultures. In *IN VITRO* (Vol. 8, Issue 3).

Vasil, V., & Hildebrandt, A. C. (1965). Differentiation of Tobacco Plants from Single, Isolated Cells in Microcultures. *Science (New York, N.Y.)*, *150*(3698), 889–892.

Vernon, A. E., Devine, C., & Philpott, A. (2003). The cdk inhibitor p27Xic1 is required for differentiation of primary neurones in Xenopus. *Development (Cambridge, England)*, *130*(1), 85–92.

Vidal, S. E., Amlani, B., Chen, T., Tsirigos, A., & Stadtfeld, M. (2014). Combinatorial modulation of signaling pathways reveals cell-type-specific requirements for highly efficient and synchronous iPSC reprogramming. *Stem Cell Reports*, *3*(4), 574–584.

Vierbuchen, T., Ostermeier, A., Pang, Z. P., Kokubu, Y., Südhof, T. C., & Wernig, M. (2010). Direct conversion of fibroblasts to functional neurons by

defined factors. *Nature*, *463*(7284).

Waddington, C. H. (1936). *How animals develop*. W.W. Norton & Company,.

Waddington, C. H. (1942). Canalization of Development and the Inheritance of Acquired Characters. *Nature*, *150*(3811), 563–565.

Waddington, C. H. (1957). The strategy of the genes. In *Journal of Chemical Information and Modeling* (Vol. 53, Issue 9). George Allen & Unwin Ltd.

Waddington, Conrad H. (1932). Experiments on the development of chick and duck embryos, cultivated in vitro. *Philosophical Transactions of the Royal Society of London. Series B, Containing Papers of a Biological Character*, *221*(474–482), 179–230.

Wallace, K., Liu, T.-H., & Vaessin, H. (2000). The pan-neural bHLH proteins DEADPAN and ASENSE regulate mitotic activity and cdk inhibitordacapo expression in the*Drosophila* larval optic lobes. *Genesis*, *26*(1), 77–85.

Wallenfang, M. R., & Seydoux, G. (2002). *cdk-7* Is required for mRNA transcription and cell cycle progression in *Caenorhabditis elegans* embryos. *Proceedings of the National Academy of Sciences of the United States of America*, *99*(8), 5527–5532.

Wapinski, O. L., Lee, Q. Y., Chen, A. C., Li, R., Corces, M. R., Ang, C. E., Treutlein, B., Xiang, C., Baubet, V., Suchy, F. P., Sankar, V., Sim, S., Quake, S. R., Dahmane, N., Wernig, M., & Chang, H. Y. (2017). Rapid Chromatin Switch in the Direct Reprogramming of Fibroblasts to Neurons. *Cell Reports*, *20*(13), 3236–3247.

Wapinski, O. L., Vierbuchen, T., Qu, K., Lee, Q. Y., Chanda, S., Fuentes, D. R., Giresi, P. G., Ng, Y. H., Marro, S., Neff, N. F., Drechsel, D., Martynoga, B., Castro, D. S., Webb, A. E., Südhof, T. C., Brunet, A., Guillemot, F., Chang, H. Y., Wernig, M., … Wernig, M. (2013). Hierarchical Mechanisms for Direct Reprogramming of Fibroblasts to Neurons. *Cell*, *155*(3), 621–635.

Ward, S., Thomson, N., White, J. G., & Brenner, S. (1975). Electron microscopical reconstruction of the anterior sensory anatomy of the nematode *Caenorhabditis elegans*. *The Journal of Comparative Neurology*, *160*(3), 313–337.

Wei, Z., Angerer, R. C., & Angerer, L. M. (2011). Direct development of neurons within foregut endoderm of sea urchin embryos. *Proceedings of the National Academy of Sciences of the United States of America*, *108*(22), 9143–9147.

Weinberg, P., Berkseth, M., Zarkower, D., & Hobert, O. (2018). Sexually Dimorphic unc-6/Netrin Expression Controls Sex-Specific Maintenance of Synaptic Connectivity. *Current Biology*, *28*(4), 623-629.e3.

Weintraub, H., Tapscott, S. J., Davis, R. L., Thayer, M. J., Adam, M. A., Lassar, A. B., & Miller, A. D. (1989). Activation of muscle-specific genes in pigment, nerve, fat, liver, and fibroblast cell lines by forced expression of MyoD. *Proceedings of the National Academy of Sciences of the United States of America*, *86*(14), 5434–5438.

White, J, Southgate, E., Thomson, J. N., & Brenner, S. (1976). The Structure of the Ventral Nerve Cord of *Caenorhabditis elegans*. *Philosophical Transactions of the Royal Society B: Biological Sciences*, *275*(938), 327–348.

White, JG. (1986). The structure of the nervous system of the nematode *Caenorhabditis elegans*. *Philosophical Transactions of the Royal Society of London B: Biological Sciences*, *314*(1165).

Wicks, S. R., Yeh, R. T., Gish, W. R., Waterston, R. H., & Plasterk, R. H. A. (2001). Rapid gene mapping in *Caenorhabditis elegans* using a high density polymorphism map. *Nature Genetics*, *28*(2), 160–164.

Wildermuth, H. (1970). *Determination and transdetermination in cells of the fruitfly* (Vol. 58, Issue 231).

Wood, D. J., & Endicott, J. A. (2018). Structural insights into the functional diversity of the CDK–cyclin family. In *Open Biology* (Vol. 8, Issue 9).

Wood, H. B., & Episkopou, V. (1999). Comparative expression of the mouse Sox1, Sox2 and Sox3 genes from pre-gastrulation to early somite stages. *Mechanisms of Development*, *86*(1–2), 197–201.

Wu, A., Wu, B., Guo, J., Luo, W., Wu, D., Yang, H., Zhen, Y., Yu, X., Wang, H., Zhou, Y., Liu, Z., Fang, W., & Yang, Z. (2011). Elevated expression of CDK4 in lung cancer. *Journal of Translational Medicine*, *9*(1), 38.

Wu, J., Huang, B., Chen, H., Yin, Q., Liu, Y., Xiang, Y., Zhang, B., Liu, B., Wang, Q., Xia, W., Li, W., Li, Y., Ma, J., Peng, X., Zheng, H., Ming, J., Zhang, W., Zhang, J., Tian, G., … Xie, W. (2016). The landscape of accessible chromatin in mammalian preimplantation embryos. *Nature*, *534*(7609), 652–657.

Xie, W., Schultz, M. D., Lister, R., Hou, Z., Rajagopal, N., Ray, P., Whitaker, J. W., Tian, S., Hawkins, R. D., Leung, D., Yang, H., Wang, T., Lee, A. Y., Swanson, S. A., Zhang, J., Zhu, Y., Kim, A., Nery, J. R., Urich, M. A.,

… Ren, B. (2013). Epigenomic analysis of multilineage differentiation of human embryonic stem cells. *Cell*, *153*(5), 1134–1148.

Xu, J., Du, Y., & Deng, H. (2015). Direct lineage reprogramming: Strategies, mechanisms, and applications. In *Cell Stem Cell* (Vol. 16, Issue 2, pp. 119–134). Cell Press.

Yang, W., Warrington, N. M., Taylor, S. J., Whitmire, P., Carrasco, E., Singleton, K. W., Wu, N., Lathia, J. D., Berens, M. E., Kim, A. H., Barnholtz-Sloan, J. S., Swanson, K. R., Luo, J., & Rubin, J. B. (2019). Sex differences in GBM revealed by analysis of patient imaging, transcriptome, and survival data. *Science Translational Medicine*, *11*(473).

Yankulov, K., Todorov, I., Romanowski, P., Licatalosi, D., Cilli, K., McCracken, S., Laskey, R., & Bentley, D. L. (1999). MCM proteins are associated with RNA polymerase II holoenzyme. *Molecular and Cellular Biology*, *19*(9), 6154–6163.

Yanowitz, J., & Fire, A. (2005). Cyclin D involvement demarcates a late transition in *C. elegans* embryogenesis. *Developmental Biology*, *279*(1), 244–251.

Yeh, A. C., & Ramaswamy, S. (2015). Mechanisms of cancer cell dormancy-another hallmark of cancer? In *Cancer Research* (Vol. 75, Issue 23, pp. 5014–5022). American Association for Cancer Research Inc.

Yong Wan, Otsuna, H., Chi-Bin Chien, & Hansen, C. (2009). An interactive visualization tool for multi-channel confocal microscopy data in neurobiology research. *IEEE Transactions on Visualization and Computer Graphics*, *15*(6), 1489–1496.

Yuzyuk, T., Fakhouri, T. H. I., Kiefer, J., & Mango, S. E. (2009). The Polycomb Complex Protein mes-2/E(z) Promotes the Transition from Developmental Plasticity to Differentiation in *C. elegans* Embryos. *Developmental Cell*, *16*(5), 699–710.

Zahn, T. R., Macmorris, M. A., Dong, W., Day, R., & Hutton, J. C. (2001). IDA-1, a *Caenorhabditis elegans* homolog of the diabetic autoantigens IA-2 and phogrin, is expressed in peptidergic neurons in the worm. *Journal of Comparative Neurology*, *429*(1), 127–143.

Zaret, K. S., & Carroll, J. S. (2011). Pioneer transcription factors: establishing competence for gene expression. *Genes & Development*, *25*(21), 2227–2241.

Zarkower, D. (2005). Somatic sex determination. *WormBook The C. elegans*

Research Community, *841*(101).

Zaveri, L., & Dhawan, J. (2018). Cycling to Meet Fate: Connecting Pluripotency to the Cell Cycle. *Frontiers in Cell and Developmental Biology*, *6*, 57.

Zeineddine, D., Hammoud, A. A., Mortada, M., & Boeuf, H. (2014). The Oct4 protein: more than a magic stemness marker. *American Journal of Stem Cells*, *3*(2), 74–82.

Zhang, J. J., Zhao, Y., Chait, B. T., Lathem, W. W., Ritzi, M., Knippers, R., & Darnell, J. E. (1998). Ser727-dependent recruitment of MCM5 by Stat1α in IFN-γ-induced transcriptional activation. *The EMBO Journal*, *17*(23), 6963–6971.

Zhang, R., Han, P., Yang, H., Ouyang, K., Lee, D., Lin, Y. F., Ocorr, K., Kang, G., Chen, J., Stainier, D. Y. R., Yelon, D., & Chi, N. C. (2013). In vivo cardiac reprogramming contributes to zebrafish heart regeneration. *Nature*, *498*(7455), 497–501.

Zhang, Wei, Q., Zhao, X., & Paterson, B. M. (1999). Coupling of the cell cycle and myogenesis through the cyclin D1-dependent interaction of MyoD with cdk4. *EMBO Journal*, *18*(4), 926–933.

Zhao, C., & Emmons, S. W. (1995). A transcription factor controlling development of peripheral sense organs in *C. elegans*. *Nature*, *373*(6509), 74–78.

Zhou, Q., Brown, J., Kanarek, A., Rajagopal, J., & Melton, D. A. (2008). In vivo reprogramming of adult pancreatic exocrine cells to β-cells. *Nature*, *455*(7213), 627–632.

Zhu, J., Adli, M., Zou, J. Y., Verstappen, G., Coyne, M., Zhang, X., Durham, T., Miri, M., Deshpande, V., De Jager, P. L., Bennett, D. A., Houmard, J. A., Muoio, D. M., Onder, T. T., Camahort, R., Cowan, C. A., Meissner, A., Epstein, C. B., Shoresh, N., & Bernstein, B. E. (2013). Genome-wide chromatin state transitions associated with developmental and environmental cues. *Cell*, *152*(3), 642–654.

Zuryn, S., Ahier, A., Portoso, M., White, E. R., Morin, M. C., Margueron, R., & Jarriault, S. (2014). Sequential histone-modifying activities determine the robustness of transdifferentiation. *Science*, *345*(6198), 826–829.

Zuryn, S., Le Gras, S., Jamet, K., & Jarriault, S. (2010). A strategy for direct mapping and identification of mutations by whole-genome sequencing. *Genetics*, *186*(1), 427–430.